THE THERMAL ANALYSIS OF RED AMORPHOUS SELENIUM

Kathryn Grace Bennett

A DISSERATION

in

Chemistry

Presented in Partial Fulfillment of the Requirements for the
Degree of Master of Science at
Sir George Williams University

May, 1970

M.Sc. Chemistry

Kathryn Grace Bennett

THE THERMAL ANALYSIS OF RED AMORPHOUS SELENIUM

ABSTRACT

Red amorphous selenium has been investigated experimentally by differential thermal analysis (DTA) and differential scanning calorimetry (DSC).

The storage temperature has been found to affect the stability of this allotrope. Thermally stable red amorphous selenium (stored at 273°K) transforms irreversibly to black amorphous selenium at a temperature of 327.2 ± 0.5°K; crystallization to trigonal selenium occurs at 361.3 ± 0.7°K. The enthalpy values of these transitions have been determined. No transitions were observed at sub-ambient temperatures; a glass transition point is believed to be present near 303°K.

Storage at 297°K reduces the thermal stability, and red amorphous selenium has been found to transform slowly to another amorphous form of selenium, in which an endothermic peak is visible at 316-319°K, and crystallization to trigonal selenium occurs at 386-397°K; preliminary investigations show that this other form may possibly be black vitreous amorphous selenium. Hypotheses are formulated to explain the observed transitions at the molecular level.

Moist red amorphous selenium exhibits highly-distorted thermograms, but prolonged storage at 273°K or 297°K results in a gradual disappearance of these effects.

Internally-consistent values are reported for the heats of fusion of a set of four temperature calibration standards (Fisher TherMetrics).

The nature of an "amorphous allotrope" is discussed.

ACKNOWLEDGEMENTS

The author wishes to express her gratitude to the members of her research committee, and most especially to Dr. R. A. Westbury, whose guidance, interest and consideration throughout all the phases of this investigation were deeply appreciated.

In addition, the author is indebted to Mrs. C. Ferreira and to Mr. W. Reisinger for proofreading the manuscript, and also to the latter for translating services.

The financial support of the Chemistry Department is also gratefully acknowledged.

TABLE OF CONTENTS

LIST OF TABLES

LIST OF FIGURES

INTRODUCTION

Although the element selenium was discovered in 1817 (1), the chemical literature pertaining to the structure, physical properties and transitions of the various selenium allotropes is still characterized by a considerable degree of confusion. Indeed, reviewers rarely agree even on so basic a question as the number of existing allotropes.

Under normal pressure conditions, selenium has been reported to exist in the following distinct allotropic forms: grey trigonal (formerly called hexagonal) selenium (1-8), α - and β - red monoclinic selenium (2,5,6,8), red powdery amorphous selenium (3,5,6,8), black amorphous selenium (2), black vitreous selenium (2,4,5,8), red vitreous selenium (5), a glassy modification (5), and more recently, two cubic modifications called α - and β - cubic selenium (8), as well as a new monoclinic form named β' - monoclinic (9).

On the other hand, black amorphous, vitreous and glassy selenium are sometimes regarded as but a single selenium modification (1,6,7). Also, it has been claimed that either red amorphous selenium and black amorphous selenium (4), or red amorphous selenium and vitreous selenium (3) differ only in their degree of subdivision. This type of confusion leads to obvious difficulties in attempting to correlate physical properties, especially thermal behavior, with the appropriate allotropic form. Moreover, this list does not include any unconfirmed allotropic modifications reported in the literature prior to 1940, as it is only within the last few years that high purity selenium has been available;

impurities have a marked effect on the physical properties of selenium (10). For the sake of completeness, it should also be mentioned that selenium can be obtained in the colloidal state (1,2,8). However, as this form of selenium has no bearing on the results in this thesis, it will not be discussed further.

Even though the actual number of crystalline allotropes of selenium is still in doubt, at least these allotropes do have an advantage over the amorphous forms, by virtue of being differentiable on the basis of their crystal structures, whereas a somewhat arbitrary basis must be chosen to describe the various amorphous forms of selenium. Thus, by way of an introduction to the allotropes of selenium, the crystalline allotropes will be discussed first, on the basis of their crystal structure as well as their preparation methods, followed by the amorphous modifications, defined on the basis of the methods by which they are commonly prepared.

Since some of the thermal transitions reported for the various selenium allotropes have not been confirmed, nor the transition processes clearly defined, the chemical literature on this subject is often rather inconsistent. This investigation was originally intended to constitute a thermal study of one of the amorphous forms of selenium, red amorphous selenium, at sub-ambient temperatures. In time, the investigation was extended to include higher temperatures as well.

THE CRYSTALLINE MODIFICATIONS OF SELENIUM

Structure. Of the various crystalline modifications of selenium, the structures of the trigonal, α- monoclinic and β- monoclinic allotropes are known; the existence of the two cubic modifications is questionable.

The crystal lattice of trigonal selenium consists of parallel helical chains located at the corners and center of a regular hexagon (11-13). Every fourth atom in a chain begins a new period of the helix (14). The c- axis of the crystal falls along the helical axis (11,12). The lattice constants, as recently determined by Cherin and Unger (15), are given as: a = 4.3662 A° and c = 4.9536 A°. There are three atoms per unit cell; a projection of the atoms onto a plane perpendicular to the c- axis forms equilateral triangles.(12) Each selenium atom has two nearest neighbors at 2.32 A° (3,16) in its own chain, and four next nearest neighbors at 3.46 A° (16) in adjacent chains. Next nearest neighbors in the same chain are at 3.69 A° (3). Cherin and Unger give the values 2.373 A°, 3.436 A° and 3.716 A° respectively for these bond lengths (17). Bonding within the helical chains is covalent (4), while bonding between adjacent chains is of the van der Waal's type (4). However, absolute values of the bonding anisotropy of selenium and tellurium (18,19) suggest that inter-chain bonding does not consist solely of van der Waal's bonding, but perhaps also of weak overlap of wave functions (20), particularly in the case of tellurium.

The two non-metallic forms of selenium, the α- monoclinic and β - monoclinic allotropes, are molecular crystals composed of eight-membered ring molecules puckered into the shape of a crown (17,21,22). There are four molecules per unit cell. The difference between the

α - and β - monoclinic allotropes results from different stacking patterns of the Se_8 ring molecules (17). In β - monoclinic selenium the ring molecules are packed together in such a way that their axes are aligned parallel to one another, but all in the same direction. In α - monoclinic selenium there are two stacking directions. Bonding in the rings is covalent, while between the rings the weaker van der Waal's type of bond prevails (23). The average bond length in α - monoclinic selenium is 2.32 A° (24), and that in β - monoclinic is 2.34 A° (24), although this difference may be insignificant as it is just at the borderline of being within experimental error. According to Cherin and Unger, the intermolecular distances begin at 3.58 A° and 3.44 A° for these two allotropes respectively (24); Abdullayev et al. quote 3.53 A° and 3.48 A° respectively (23). In either case, the value given for β - monoclinic selenium is quite close to the value 3.46 A°, reported as the nearest neighbor distance between adjacent chains of trigonal selenium. And indeed, in the structure of β - monoclinic selenium proposed by Cherin and Unger, a five-atom configuration does occur which is very similar to that found in trigonal selenium.

Cherin and Unger also mentioned the discovery of a new crystal form which they called β' - monoclinic selenium (9). The b- lattice constant was three times the size of that for β - monoclinic selenium. They derived a base-centered cell. However no symmetry was observed, and therefore the unit cell was triclinic. This discovery has yet to be confirmed.

The existence of two cubic modifications of selenium has been proposed by Andrievsky et al. in a series of papers dealing with the crystallization of thin films of selenium (25,26). They reported that

films of red amorphous selenium, obtained by subliming chemically pure vitreous or red amorphous selenium in a vacuum and then dissolving away the bases, developed four rings in their electron diffraction patterns when held at 298 °K for five hours. These rings were not present in the freshly prepared substance. With gradual heating to 303 °K, these rings are increased somewhat, and weak lines indicative of crystallization begin to occur. An electron diffraction pattern characteristic of polycrystalline α - monoclinic selenium appears at 308–313 °K. If the temperature is gradually increased to 328–333 °K over a period of two hours, the central rings begin to erode at 323 °K, lines of β - monoclinic selenium appearing simultaneously and becoming distinct at 338 K. Subsequent heating to 423–433 °K resulted in gradual recrystallization into a new face-centered cubic modification, called β - cubic selenium, provided the samples are held at 433 °K for some time. The lattice constant was given as a = 5.755 Å. A second new form, α - cubic selenium, with a primitive cubic lattice, is obtained by heating red amorphous selenium films. The films were mounted on zapon varnish films this time, but details of the heating treatment were not stated. Trigonal selenium was evidently also formed. The α - cubic lattice constant was a = 2.970 Å. Both forms were reported stable at room temperature. However, the specimen holder was made of copper wire netting, and as Similetov pointed out, the β - cubic modification could be actually Cu_2Se (27). Therefore Andrievsky and Nabitovich reexamined some thin selenium films in the absence of copper. The selenium was vaporized in a vacuum at 293 °K, and then heated rapidly to 333 °K. When held at this temperature for one hour, the amorphous selenium films were converted to either trigonal or β - cubic selenium, depending on the heating rate (28). Electron diffraction

studies showed that the face-centered β - cubic form has a diamond lattice, with a new value of 6.04 ± 0.01 °A being given for the lattice constant. On heating β - cubic selenium above 403 °K, trigonal selenium was formed. No mention was made of the α - cubic form.

In contrast to these results, Griffiths and Sang (29) state that they observed no evidence of any selenium modification other than the monoclinic and trigonal forms, even when they crystallized the amorphous phase by heating or through electron bombardment. When copper specimen support grids were used, they did observe copper diffusion (30), which resulted in the formation of $Cu_{1.8}Se$, a stable copper selenide with a structure and lattice constant identical to those of the β - cubic modification proposed by Andrievsky et al. (26,28). This appears to be the latest word in the controversy.

Preparation. Trigonal selenium can be prepared by cooling molten selenium to 453 °K, and then maintaining the selenium at this temperature for quite some time (8), or by condensing selenium vapor on a substrate whose temperature is just slightly below 493 °K (7). Once prepared, the grey trigonal selenium, formerly called hexagonal selenium, is stable at all temperatures below the melting point of selenium (31). Under normal pressure conditions, the various other forms of selenium convert monotropically to this stable allotrope at rates which are highly temperature dependent. Trigonal selenium is the densest of the selenium allotropes, with a specific gravity of 4.82 g/cc (1) (presumably at 293 °K). Trigonal selenium is insoluble in carbon disulfide (1,7) and melts at about 490-3 °K.

Crystals of monoclinic selenium are obtained by the controlled evaporation, usually at room temperature, of carbon disulfide solutions

saturated with red amorphous (2,32) or vitreous (1) selenium; slow evaporation is supposed to give α - monoclinic selenium, and rapid evaporation the β - monoclinic variety. Both forms are appreciably soluble in carbon disulfide (1,7). The density of α - monoclinic selenium is reported as being 4.47 g/cc (8) and that of β - monoclinic selenium as 4.50 g/cc (8) (presumably at 293 °K). According to Bagnall's review, both monoclinic forms melt at about 473 °K if heating is rapid (1). Values of 423 °K and 453 °K are also quoted as the melting point of these two forms (3,6). In addition, Chizhikov and Schastlivyi (8) quote a melting point of 443 °K for α - monoclinic selenium and a range from 417-453 °K for the melting point of β - monoclinic selenium.

THE AMORPHOUS MODIFICATIONS OF SELENIUM

Preparation. The term amorphous selenium is meant to refer to all the non-crystalline forms of selenium in general. A specific amorphous modification will be distinguished by a qualifying adjective, such as red amorphous, black amorphous, black vitreous amorphous selenium, etc.

There are two reported methods of preparing red amorphous selenium. The more common of these methods is to chemically reduce an aqueous solution of some selenium compound at a temperature usually less than 293 °K (1-3,6-8). As an example of the method, the element selenium is recovered from the flue dust of roasted ores which contain selenium in their natural state, or from lead chamber sludge (3), by bringing it into solution with sulfuric acid and sodium nitrate to form mainly selenious acid and selenic acid. The latter is reduced to selenious acid by warming with hydrochloric acid. A precipitate of red amorphous selenium is then obtained by passing sulfur dioxide through the solution as a reducing agent. Hydrazine hydrate also serves as a good reducing agent (3). The equations for these reactions are as follows:

$$H_2SeO_3 + 2SO_2 + H_2O \longrightarrow Se\downarrow + 2H_2SeO_4 \qquad (1)$$

$$H_2SeO_3 + N_2H_4 \longrightarrow Se\downarrow + 3H_2O + N_2\uparrow \qquad (2)$$

Gattow and Heinrich (33) dissolved solid sublimed selenium dioxide in an aqueous hydrochloric acid solution, obtaining selenious acid which they subsequently reduced to the red amorphous form. With hydrazine hydrate, which they used as the reducing agent, the reduction step had to be carried out very slowly in order to prevent the heat which is generated from raising the solution temperature above 293 K. The reaction was performed in the dark, with constant stirring for a period

of twenty-four hours. There was also provision for water cooling of the solution. The product was kept cool during the filtration stage, then dried at a temperature of less than 293°K.

If selenium is leached from lead chamber sludge by digestion with a warm potassium cyanide solution, potassium selenocyanate, $K[SeCN]$, is formed (3). This product can be decomposed with hydrochloric acid to yield red amorphous selenium (1,3,6):

$$SeCN^- + H_3O^+ \longrightarrow Se\downarrow + HCN + H_2O \qquad (3)$$

Other chemical methods for the formation of red amorphous selenium have been given by Ato and Ichioka (34), and by Tarayan and Arstamyan (35).

The second general method of preparing red amorphous selenium is by the rapid condensation of selenium vapor (1,3,8). Thus, Gobrecht (36) passed selenium vapor through a temperature region of about 1273°K, and then into liquid nitrogen. However, neither how long the selenium vapor was maintained in the 1273°K region prior to quenching, nor its actual temperature, were mentioned. (Evidence will be presented in the discussion to the effect that red amorphous selenium, as produced by these two general methods, exhibits different properties.)

Red amorphous selenium is said to be soluble in carbon disulfide (6,37). It has a specific gravity of 4.26 g/cc (6), (presumably at 293°K), and is the least dense allotrope of selenium. One source states that it is stable at room temperature (2), another that it is stable for at least three to five years if kept cool and dry (38), which would seem to imply that room temperature is too warm, and a third conflicting reference that red amorphous selenium slowly crystallizes on aging, even at 273°K (39).

In the case of black amorphous selenium, there appears to be

some doubt as to its constituting a valid allotropic form of selenium. As mentioned previously, several authors make no distinction at all between black amorphous and black vitreous amorphous selenium. Even those authors who do separate these two modifications still do not refer to black amorphous selenium as a definite allotrope. For example, Feher (2) differentiates between vitreous amorphous selenium prepared by rapid cooling of molten selenium, and amorphous selenium which is prepared by the reduction of selenium compounds at moderate temperatures. The latter form is supposedly either red or black, depending on its state of aggregation. Feher also states that a dark amorphous modification of selenium can be obtained by heating red amorphous selenium with boiling water, or by reducing heated selenious acid with hydrazine hydrate. The greyish-black powder obtained by the above methods is stable at room temperature.

Gattow and Heinrich (33) distinguish between vitreous (glassy) amorphous selenium prepared by quenching molten selenium in ice-water, and black amorphous selenium, obtained by heating the chemically reduced form of red amorphous selenium to temperatures higher than 303°K, where the red amorphous form undergoes an irreversible transition to give black amorphous selenium. They state however, that because black amorphous selenium does not exhibit any definite phase transition temperature, it therefore represents only a transitional modification between red amorphous selenium and the grey trigonal form.

Vitreous amorphous selenium is prepared by three methods essentially. The first method is to heat any solid modification of selenium to 493°K or higher, and then to quench the resultant molten selenium in either ice-water (1,2,33) or in liquid nitrogen (36). As a result

of supercooling, the vitreous amorphous selenium is obtained in the glassy state (8). These terms, vitreous and glassy, are really synonymous, since they represent the English equivalents of the German word "glasig". Vitreous amorphous selenium obtained in this manner can appear either red or black in color. Feher states that thin layers are translucent and red, while thick layers are greyish-black (2). It is also claimed that ground-up vitreous amorphous selenium shows a red tint on cooling below 193°K, and is distinctly red at 77°K, with the original color being restored on heating (40).

The second way of preparing vitreous amorphous selenium is to condense selenium vapor onto a substrate whose temperature is maintained somewhat lower than the melting point of selenium (7); room temperature is often found convenient for this purpose. Although Addison (7) places no restriction on the substrate temperature other than that it be far enough below the melting point of selenium to avoid crystallization to the trigonal form, work by Griffiths and Sang (41) on the growth of thin films of selenium suggests that the substrate temperature should be held at 313°K or lower to prevent crystallization in these films.

The third method of preparation is to allow molten selenium to slowly cool down to room temperature (5,42).

Agreement concerning the stability of vitreous amorphous selenium is lacking. There are claims that it is stable for a long time at room temperature (2), that it tends to crystallize imperfectly after two to three weeks storage at room temperature (5), and rather ambiguously, that it is sufficiently stable at room temperature (8). Bagnall reports that vitreous amorphous selenium undergoes a slow transformation at room temperature, there being no clearly defined transition temperature (1).

Sato and Kaneko also claim that there is no definite crystallization temperature (43), since vitreous amorphous selenium is essentially a supercooled liquid. They state that the rate of crystallization begins to decline to zero below 333 °K, although they do not mention whether this rate is zero or not at a temperature of approximately 297 °K.

It is generally agreed that vitreous amorphous selenium is soluble in carbon disulfide (5-8), though to a lesser degree than red amorphous selenium (8). The specific gravity of vitreous selenium has been reported as 4.28 g/cc (1) or as 4.30 g/cc (5) (presumably at 293 °K).

Apart from the previously mentioned fact that thin layers of quench-prepared vitreous amorphous selenium may appear red in color, there is one other instance of a red form of vitreous amorphous selenium being cited. Thus, Brasted refers to a red vitreous form which converts to the grey trigonal allotrope with prolonged heating at 423 °K (5).

Structure. Because the structure of the amorphous forms of selenium can not be determined directly, several authors have resorted to inferring possible structures for these forms by relating the physical behavior of the amorphous modifications to that of the structurally-defined crystalline allotropes.

The prevalent opinion as to the structure of amorphous selenium modifications now centers around the idea that there exists a dynamic equilibrium in liquid selenium (44,45) between at least two molecular species, an eight-membered cyclic monomer (Se_8) and a chain-like polymer (Se_x), and that this equilibrium is "frozen in" when the molten element is quenched to form vitreous amorphous selenium. Abdullayev et al. have represented this equilibrium by the equations shown on the following page:

$$Se_x^* + Se_8 \longrightarrow Se_{x+8}^* \qquad (4)$$

$$Se_x \longrightarrow Se_{x-n8} + nSe_8 \qquad (5)$$

where * represents a diradical (31).

The historical origin of the idea of a composite ring-chain molecular model for the amorphous forms of selenium can be traced back to Briegleb's work (46,47). He concluded from solubility measurements that vitreous amorphous selenium consisted of two molecular forms, one of which dissolved faster in carbon disulfide than the other. Since monoclinic selenium, composed exclusively of eight-membered puckered ring molecules, dissolves in carbon disulfide, whereas trigonal selenium, composed of parallel helical chains, is insoluble in carbon disulfide, most selenium chemists have interpreted these results as being indicative of the presence of ring and chain molecules in vitreous amorphous selenium --the monomeric ring molecules dissolving more easily than the polymeric chains. In addition, cryoscopic measurements by Beckmann and Pfeiffer indicate that selenium dissolved in carbon disulfide has a molecular weight corresponding to the formula Se_8 (3,48).

By analogy, red amorphous selenium, which shows a higher degree of solubility in carbon disulfide than does vitreous amorphous selenium, should therefore contain a higher proportion of ring molecules (37).

Briegleb's results also showed that the higher the temperature from which the vitreous amorphous selenium was quenched, with respect to the melting point, the smaller was the amount of fast-dissolving component.

The presence of chain-like polymeric molecules in amorphous selenium is inferred mainly from viscosity measurements. From a theory by Andrade (49), the viscosity of a hypothetical monatomic liquid selenium should be about 0.01 poise at the melting point. However, measurements

by Keezer and Bailey (50) have shown that the actual viscosity of liquid selenium is several thousand times larger at this temperature. Thus it is concluded that a complex molecular structure must be present in molten selenium and that this unusually high viscosity (51) can be explained by assuming the presence of a long-chain species (52) in the melt.

There seems to be only one voice of dissention with regard to this interpretation, which is that of Krebs. In a paper with Marsh (53), the presence of very large high-molecular-weight rings, $Se_{500-1000}$, is suggested, rather than polymeric chains, because he feels that the presence of selenium chains with free-radical ends is not plausible. However the general consensus among selenium chemists is that the melt must contain diradical chains, because only this can explain all the manifold data collected on liquid selenium; consequently, this suggestion by Krebs has been generally disregarded.

Clearly the most exciting results concerning the structure of vitreous amorphous selenium are those of Lucovsky et al. (54,55). Using infrared and laser Raman spectroscopy, they studied first the eight-membered puckered ring structure of α - monoclinic selenium and the parallel helical chain structure of trigonal selenium. They then determined the absorption spectra of both cast and evaporated samples of vitreous amorphous selenium. Lucovsky has reported that the latter spectra bore a much closer resemblance to the spectrum of Se_8 ring molecules than to the spectrum of Se_x chain molecules (56), after the frequencies and symmetry characteristics of the fundamental vibration modes had been identified. Apart from one band which was quite close in frequency to an E mode of trigonal selenium whose effective charge and restoring force

are derived solely from atoms within a single helix, almost the entire spectrum could be explained on the basis of the vibrations of an eight-membered puckered ring molecule.

Srb and Vasko (57) had previously concluded that Se_8 rings existed in vitreous amorphous selenium, though by a slightly more indirect method. They reported that the dominant bands of amorphous selenium in the middle infrared region are due to the vibrations of Se_8 rings, having observed a quantitative similarity between the absorption spectrum of vitreous amorphous selenium and that of rhombic sulfur, which is composed of eight-membered sulfur rings. In addition, they also noted that the spectrum of liquid selenium is identical to that of solid amorphous selenium in the temperature range 523-673°K, with only a small shift of the bands towards longer wavelengths (58).

It had been previously postulated, by Richter et al. (59-61), that the internal structure of amorphous selenium could be considered as a package structure of layers of Se_6 molecules, having a folded ring structure. But Lucovsky has observed (62) that higher frequencies should have been observed if six-membered were present. Moreover, he considers Richter et al.'s interpretation as being somewhat questionable, in view of the fact that their structural model relies heavily on higher order (5,6,7,8 etc.) next nearest neighbor distances.

Therefore it would appear that the favored structural model of vitreous amorphous selenium at the present time is a model consisting of a mixture of Se_8 rings and Se_x polymeric chains with possibly 10^4 to 10^6 atoms per chain at the melting point.(51)

Although long range order is completely broken down in solid vitreous amorphous selenium, the results of inelastic neutron scattering

experiments (63) have been interpreted on the basis that there still exists some short range order. Mande and Patil (64) have arrived at the same conclusion from K absorption-edge discontinuity studies.

Bonding in vitreous amorphous selenium is said to be of the van der Waal's type (65), perhaps by analogy to monoclinic and trigonal selenium (66).

While both Axmann et al. (63) and Vasko (58) have concluded that the internal structures of liquid and solid amorphous selenium are very similar, it has also been suggested that a correlation may well exist between the internal structure of molten selenium at various quench temperatures and the observed values of some physical properties of vitreous amorphous selenium (68).

Thus, viscosity measurements (45,69) have been made on liquid selenium at various temperatures above the melting point to determine the average number of atoms per chain as a function of temperature. In this way it is hoped to gain a rough estimate of the chain length in solid vitreous amorphous selenium. It has been found that the viscosity of liquid selenium decreases uniformly with increasing temperature. Some average chain lengths which were calculated from viscosity measurements are shown in Table I.

Although this type of measurement can not be used to determine the chain length in red amorphous selenium, Karal'nik et al. (67) have shown that there is a difference between the K absorption-edge in red amorphous selenium and vitreous amorphous selenium.

There have also been a limited number of investigations as to what are the molecular forms which are present in the vapor phase of selenium as a function of temperature.

Table I

Chain Length in Liquid Selenium as a Function of Temperature

Reference	Temperature (°K)	Number of Atoms per Chain
Eisenberg, Tobolsky (45)	500	8000
	550	3040
	600	1360
	650	664
Harrison (69)	509	4800
	531	3200
	568	1600
	623	800
	649	640
	685	480

Bagnall (1) quotes results to the effect that in the temperature range 493-823°K, selenium vapor is composed of Se_8 molecules, which decompose above 823°K to give Se_6 molecules up to 1073°K. Above 1173°K, Se_2 molecules are observed, and these eventually break down to Se at temperatures greater than 1273°K. The boiling point of selenium is 958°K.

These results do not agree well with the more recent results of Fugisaki et al. (70) who detected all possible Se_n^+ ions (n = 1-8) in the mass spectrum of the vapor from trigonal selenium subliming at 375-460°K. They believe that the ions Se_5^+, Se_6^+, Se_7^+, and Se_8^+ arise mainly from the ionization of the corresponding cyclic parent molecules, and state that the vapor composition at 448°K is as follows: $Se_5 < 29.0\%$, $Se_6 > 57.5\%$, $Se_7 > 11.4\%$ and $Se_8 > 2.0\%$. Small amounts of Se_9^+ and Se_{10}^+

were also detected.

Results by Yamdagni and Porter (71) indicate that at 625°K, Se_2, Se_5, Se_6, Se_7 and Se_8 were present in the vapor phase of selenium. They also mention having detected Se_n (n = 1-8) in the vapor in general.

TRANSITIONS AMONG THE SELENIUM ALLOTROPES

Not only is there disagreement over the actual number of allotropic forms of selenium, but also , the conditions favoring the presence of a particular allotrope and the nature of the transformations from one form to another are likewise uncertain in some cases.

Although all forms of selenium are eventually converted to the stable trigonal form on heating, the temperatures at which this transition is reported to occur vary over a wide range. Thus, the transformation from monoclinic to trigonal selenium has been observed over the temperature range 298-403°K, as shown in Table II.

Table II

Reported Transformation Temperature: Monoclinic to Trigonal Selenium

Reference and Instrumental Technique	Temperature (°K)	Monoclinic Modification
Costy (72)	278-280.5	not stated
Mondain-Monval (73)	>393	not stated
Das Gupta et al. (74) (Debye-Scherrer diagrams)	393 (12 hr) 353 (15 days) 338 (17 days)	not stated
Muthmann (75)	383-393 398-403	α - monoclinic β - monoclinic
Semiletov (76) (X-ray diffraction)	363-373	not stated
Asadov (77) (Optical; Laue photogr.)	398	α - monoclinic
Abdullayev et al. (78) (X-ray diffraction)	388-403	α-, β - monoclinic
Nekrasov (79)	393 (1 hr) 353 (15 days) 338 (70 days)	not stated
Melckerson (80)	353 (as solids) 298 (in quinoline)	α-, β - monoclinic

There is a similar degree of variance in the reported temperatures of the transformations of the amorphous modifications of selenium to the trigonal form, as can be seen in Table III.

Table III

Reported Transition Temperature: Amorphous Forms to Trigonal Selenium

Reference and Instrumental Technique	Temperature (°K)	Amorphous Modification
Mondain-Monval (81)	403	"amorphous"
Tanaka (82)	347 (2 hr)	vitreous, quench.
Prins, Dekeyser (83) (X-ray refl'n photogr.)	> 346	vitreous
Isikawa, Sato (84) (Different'l gas dilatometer)	348 (33 hr, 60% cryst'n)	vitreous
Morinaga et al. (85) (Metallurgical tests)	393-398	vitreous
Sato, Kaneko (43)	398 (max. nuclei form'n) > 373 (high cryst'n rate)	vitreous
Hirahara (86) (Heat capacity meas'ts)	373	vitreous
Semiletov (76) (X-ray diffraction)	363-373 (slow change)	vitreous
Nasledov et al. (87) (X-ray study)	403	vitreous
Hashimoto et al. (88) (X-ray study)	363 (max. nuclei form'n)	vitreous
Dorabialska et al. (89) (Dynam. calorimetry)	343-353	vitreous, water quenched
Fourie et al. (90) (Resistance vs. temp.)	363 (max. cryst'n)	vitreous
Andrievsky et al. (28) (X-ray study)	333 (1 hr; proport'l to heating rate)	vitreous
Abdullayev et al. (91) (X-ray analysis)	353 (pure selenium) 333 (I or Br impurity)	"amorphous"

Table III (con't)

Reference and Instrumental Technique	Temperature (°K)	Amorphous Modification
Goffe, Givens (92)	348 (1 hr)	vitreous
Mamedov, Nurieva (93) (X-ray line intensity; var'n elect. resistance)	343-490 490 (max. deg. cryst'n)	vitreous
Gattow, Heinrich (94) (Spec. heat meas'ts)	>348 >353	vitreous, H_2O quen. black amorphous
Hamada et al. (39) (X-ray study)	273 (very slowly) 353 (sev. hr) 373 (sev. min)	red amorphous
Mamedov et al. (95) (Diff. thermal anal.)	398	"amorphous"
Gobrecht (36) (Diff. enthalpic anal.)	363-368 (from his graph)	vitreous, quench. in liq. N_2
Griffiths, Sang (41) (X-ray study)	>313 (cryst'n thin films) >343 (epitaxial growth) >368 (single cry. growth)	vitreous, vapor condensed
Lanyon (97) (Diff. thermal anal.)	416	vitreous

The amorphous forms of selenium have also been reported to undergo other transitions. The results of Gattow and Heinrich (33,94), obtained from plots of the temperature dependence of the heat content of vitreous (quenched) and red amorphous (chemically reduced) selenium in the temperature range 93-373°K, are illustrated in Table IV. To explain their results, they assumed that vitreous amorphous selenium (quenched) is a mixture of high-molecular-weight rings, of chains and of low-molecular-weight rings, most probably Se_8 rings. They state that red amorphous selenium contains chains which are probably shorter than the chains in vitreous amorphous selenium, and which can close to form large rings, and that it also contains low-molecular weight Seg rings. They

Table IV

Results of Gattow and Heinrich's Investigation of

Amorphous Forms of Selenium

Amorphous Modification	Temperature (°K)	Description of Transition
Vitreous amorphous	128±2	reversible endotherm $\Delta H = 0.04 \pm 0.02$ kcal/g-atom
	284±1	reversible endotherm $\Delta H = 0.03 \pm 0.02$ kcal/g-atom
	303	glass transition point $\Delta H = 0 \pm 0.02$ kcal/g-atom
	>348	irreversible exotherm, crystallization to trigonal selenium
Red amorphous	139±2	reversible endotherm $\Delta H = 0.16 \pm 0.02$ kcal/g-atom
	283±1	reversible endotherm $\Delta H = 0.06 \pm 0.02$ kcal/g-atom
	>303	irreversible transition to black amorphous selenium
Black amorphous	>353	irreversible exotherm, crystallization to trigonal selenium

ascribed the transitions at 128±2 °K and 139±2 °K to the beginning of vibrations in the high-molecular-weight constituents, and the transitions at 284±1 °K and 283±1 °K to the ring vibrations of the Se_8 molecules. Gattow suggested that above 303 °K, the large rings cleave and the chains

gradually move into a parallel orientation. With continued heating, enough energy is eventually absorbed to split the Se_8 rings, at which point crystallization to the trigonal form of selenium occurs.

However, because Mamedov et al. (98) observed no irregularities in the specific heat versus temperature curve of amorphous (probably vitreous amorphous) selenium in the temperature range 56-332 °K, such as had led Gattow and Heinrich to suggest the presence of transitions at 128±2 °K and 284±1 °K, Gattow and Buss (99) decided to reinvestigate vitreous amorphous selenium at low temperatures. Purifying their selenium very carefully, they repeated the work in question and this time observed no transitions at 128±2 °K or 284±1 °K. Hence they have suggested that possibly some red amorphous selenium was present in the vitreous selenium used by Gattow and Heinrich.

The value of the glass transition temperature determined by Buss and Gattow (110) using vitreous amorphous selenium agrees very well with other values in the literature. These glass transition temperatures are tabulated in Table V.

In a differential enthalpy analysis study of both freshly prepared vitreous amorphous (quenched in liquid nitrogen from the melt) and red amorphous (quenched from the vapor, in liquid nitrogen) selenium, in the temperature range 273-503 °K, Gobrecht observed only crystallization, beginning at about 363 °K, and fusion at roughly 495 °K, in either case (36). However, after these selenium samples had been stored at 297 °K for a few days, a new endothermic peak appeared in both samples in the region 308-318 °K. (The temperatures reported are apparently those temperatures at which the peak began to break away from the baseline.) This new peak grew larger with time. After seven weeks annealing time at 297 °K,

Table V

Selenium Glass Transition Temperature

Reference and Detection Method	Temperature (°K)	Amorphous Modification
Mondain-Monval (100) (Dilatometry)	305	vitreous
Orthmann et al. (101) (Thermal conductivity)	303	vitreous(glassy)
Sekiguchi (102)	~303	"amorphous"
Eisenberg et al. (103) (Viscosity)	304	"amorphous"
Abdinov, Aliev (104) (Thermal conductivity)	303.9	vitreous, 99.9999%
Chang (105) (Elect. conductivity)	~303	vitreous
Mamedov et al. (98) (Specific heat)	303.4	"amorphous" (probably vitreous)
Abdullayev et al. (106) (Thermal conductivity)	~304 307 (Cd impurity) 300 (Mn impurity)	"amorphous"
Chaudhari et al. (107) (Heat capacity)	301 (T_g^* proport'l to quench temp.)	vitreous(glassy)
Dzhalilov, Orudzheva (108) (Viscosity)	--- (Sb increases T_g^*)	"amorphous"
Dzhalilov, Rzaev (109) (Viscosity, specific heats, volumetric meas'ts)	291-309 (Te decreases T_g^*, cooling rate affects T_g^*)	"amorphous"
Gattow, Buss (110) (Density)	303.4±0.1	vitreous

a new endotherm was observed in the red amorphous form at 343°K, and was suggested to be due to the dehydration of H_2SeO_3, which could possibly have been formed according to the reaction:

$$Se + H_2O + O_2 \rightleftharpoons H_2SeO_3 \qquad (6)$$

* T_g represents temperature of the glass transition

Selenious acid, known to decompose at about 343 °K, could have been formed by the selenium reacting with the water and oxygen in the atmosphere.

As an illustration of the acceptance of the ring-chain equilibrium theory in explaining transitions in amorphous selenium, Andrievsky et al. (111) have concluded from electron diffraction data on thin layers (~1000 Å) of amorphous selenium, prepared by vacuum sublimation, that there are two forms of amorphous selenium. The first form occurs at 293 °K and the second at 343 °K . Supposedly the form at 293 °K gradually transforms to the second type through the decay of ringlike structural units with the simultaneous formation of chainlike units. The two forms are said to be present in equal quantities between 303 °K and 313 °K .

As a second example, Cherkasov and Ionov (112) classify amorphous selenium layers, obtained by vacuum sublimation at 293-323 °K, into three types: i) low-molecular-weight layers containing rings and linear molecules with $\leq$ 8 atoms, observed at 293 °K, ii) high-molecular-weight layers containing linear molecules with $\geq$ 1000 atoms, observed at 323 °K, and iii) amorphous layers which include the trigonal crystalline phase as a result of heat treatment at 343 °K in air.

There is some evidence in the literature that vitreous amorphous selenium crystallizes into monoclinic as well as trigonal selenium. Das Gupta et al. (74) claim that this occurs slowly at room temperature, and that at this temperature the monoclinic modification is the preferred form. Yamamori (113) maintains that both vitreous amorphous and red amorphous selenium behave in this manner. Andrievsky and Nabitovich (25) have reported that vitreous selenium is converted to α - monoclinic selenium at 308-313 °K and to β - monoclinic selenium at 338 °K if heating was continued. Similetov states that vitreous selenium heated to 333-343 °K

for thirty to forty minutes changes to the monoclinic form (76). However, Andrievsky and Nabitovich (28) claim that if amorphous selenium is heated rapidly from 293 °K to 333 °K, and held at this temperature for one hour, it will then convert to the trigonal or β - cubic modification, depending on the heating rate.

There is also one instance of a reported transition, endothermic in nature, having been observed in vitreous selenium at 318 °K (114).

The enthalpy values of some of the transitions observed in the various amorphous allotropes have been listed in Table VI.

Table VI

Enthalpy Values of Some Transitions in Selenium Allotropes

Reference and Detection Method	Enthalpy Values (kcal/g-atom)	Amorphous Modification
Mondain-Monval (81)	1.07	"amorphous" to trigonal selenium
Dorabialska et al. (89) (Calorimetry)	1.1-1.3	vitreous amorphous to trigonal selenium
Mamedov et al. (95) (Differential thermal anal.)	1.07	"amorphous" to trigonal selenium
Gattow, Draeger (115) (Thermodynamical calc'ns)	-0.09*	red amorphous to black amorphous
	3.06	black amorphous to trigonal selenium
	1.24	vitreous amorphous to trigonal selenium
	-1.82*	vitreous amorphous to black amorphous
Chaudhari et al. (107) (Heat capacity)	-0.04*	transition obs'd in vitreous amorphous selenium; attributed to glass transition

* A negative sign represents an endothermic transition

THERMAL ANALYSIS TECHNIQUES

In this thesis, two thermal analysis techniques have been used to study transitions in red amorphous selenium: differential thermal analysis (DTA) and differential scanning calorimetry (DSC).

Differential thermal analysis is the technique of recording the difference in temperature between a substance and a reference material, against either time or temperature, as the two specimens are subjected to identical temperature regimes in an environment heated or cooled at a controlled rate (116). The temperature difference between the sample and the reference material is measured by two thermocouples wired in opposition (117). When the temperature of the sample equals the temperature of the reference material, the two thermocouples produce identical voltages and the net differential signal is zero, which produces a steady baseline signal. When a temperature is reached where a physical or chemical change occurs in the sample, and there is no concomitant change in the thermally inert reference material, the voltages produced by the two thermocouples are no longer identical and a positive or negative differential signal results, depending on whether the transition which occurs in the sample is exothermic or endothermic in nature respectively. As an example, in an endothermic transition, the reference temperature continues to rise while the sample remains at the transition temperature until the transition is complete. The sample temperature then recovers until it catches up with the reference temperature and the differential output voltage of the thermocouples is again equal to zero (118). Thus when the temperature difference between the sample and reference is plotted on the ordinate against the temperature of the sample material on the abscissa, a peak is obtained corresponding to each thermal transi-

tion occurring in the sample.

Differential scanning calorimetry is the technique of recording the energy necessary to establish zero temperature difference between a substance and a reference material, against either time or temperature, as the two specimens are subjected to identical temperature regimes in an environment heated or cooled at a constant rate. The temperature of the sample and reference material is continually monitored by platinum-resistance thermometers permanently embedded in the bases of the specimen holders. The sample and reference material are maintained at identical temperatures by feeding a variable amount of heat to the sample or reference, as the situation requires. The amount of heat necessary to maintain this balance is commonly plotted on the ordinate against the programmed temperature on the abscissa. Thus when an exothermic or endothermic transition occurs in the sample, and not in the thermally inert reference material, the resultant excess flow of heat produces a peak, similar to a DTA peak, although in this case the area under the peak is directly proportional to the heat energy absorbed or liberated during the sample transition. Such an arrangement is especially convenient when the enthalpy change resulting from such a transition is to be measured.

There are two types of changes of state, first-order transitions and second-order transitions. At the transition temperature T_t of a first-order transition, the free energies G of the two forms present are equal, but there is a discontinuous change in the slope of the G versus T curve of whatever substance is transforming. Since $(\partial G/\partial T)_p = -S$, where S is the entropy, there is therefore a break in the S versus T curve at T_t, the value of ΔS at T_t being related to the observed latent heat for the

transition by the equation $\Delta\bar{S} = \lambda/T_t$, where λ is the latent heat. In first-order transitions there is also a discontinuous change in the volume, since the densities of the two forms are not the same. However there are some transitions in which no latent heat or density change can be detected. Examples of second-order transitions, as these latter are called, are the transformations of certain metals from ferromagnetic to paramagnetic solids at their Curie points, the transitions of some metals at low temperatures to a condition of electrical superconductivity, and the glass transitions in polymers. In these cases, there is a change in the slope, but no discontinuity, of the S versus T curve at T_t. As a result, there is a break in the heat capacity curve though, since $C_p = T(\partial S/\partial T)_p$, (119).

These two types of transitions give rise to peaks of different appearances, when studied by differential thermal analysis or by differential scanning calorimetry.

For a first-order transition, whether an endotherm or an exotherm, a pure substance will exhibit a sharp, almost symmetrical peak, the low temperature side of which is relatively straight and almost vertical, assuming the substance is being heated, with the recovery to the original baseline assuming an exponential-type appearance. Crystallization or fusion of a sample are represented by peaks of this nature. For an amorphous polymer-like substance, these peaks can appear broader than for a monomeric-type substance, in accordance with the gradualness of the transition in the polymer due to the varying rates of reaction of the different polymer constituents.

In discussing a particular second-order transition, the glass transition, there appears to be some discrepancy in the literature

concerning the expected appearance of a glass transition point. One source (120) suggests that the glass transition point may appear either as a sudden shift in the baseline, imparting to the latter a stepped or sigmoidal appearance, or as simply a sharp change in the slope of the baseline. According to Billmeyer, the glass transition peak of amorphous poly(ethylene terephthalate), detected by Ke (122) using differential thermal analysis, appears quite similar to a first-order transition peak, except that the baseline is not fully recovered, that is, the new baseline is somewhat lower than the pre-transition baseline (121). Another source (123) shows that poly(ethylene terephthalate), scanned by differential thermal analysis at 10°K/min, registers a sharp jump downwards in the baseline at the glass transition point followed by a minute upward movement prior to establishment of the new baseline. A fourth reference (124) states that either a sigmoidal jump in the baseline or else an apparent peak, but with a non-totally recovered baseline, represents the typical glass transition point appearance as observed by differential scanning calorimetry.

Wendlandt (125) has shown some differential thermal analysis curves, originally obtained by Ke and Sisko (126), on a series of polyadipamides and polysebacamides, in which the glass transition point appears sometimes as a very small dip in the baseline and sometimes as a small step in the baseline.

On the other hand, Lambert (127), using differential scanning calorimetry with very high heating rates, has scanned some quenched polymer samples and observed apparent first-order peaks in some cases and sigmoidal baseline changes in others. Using a theory developed by Wunderlich and Bodily (128), Lambert has explained his apparent first-

order peaks on the basis that his fast heating rates caused an overshoot of the equilibrium number of holes in the polymer, which then returned to the equilibrium condition via a path that appeared to be endothermic. It is also of interest that Lambert noticed a correlation between increasing sample size and higher values of the glass transition temperature. From his curve of glass transition temperatures versus scanning rates, it would appear that the value of the glass transition temperature observed when the scanning rate was 20°K/min was 5°K higher than the value observed with a rate of 5°K/min, and that this value in turn was 1°K higher than the glass transition temperature corresponding to a heating rate of 0°K/min .

With respect to selenium, Fyans (129) has published a differential scanning calorimeter trace of "amorphous" selenium, scanned at 20°K/min on a Perkin-Elmer DSC-1 instrument. He observed a distinct peak at 330°K, with first-order characteristics, and ascribed this peak to the glass transition in selenium. He used a sample weight of approximately 20 mg. and a sensitivity of range 16, that is, 1/16 of the total sensitivity of the instrument.

MATERIALS

Potassium nitrate, described as certified primary standard, was purchased from Fisher Scientific Company. It was used either without further treatment, or after having been ground into fine particles and stored in a stoppered erlenmeyer flask. A separate quantity of each of these potassium nitrate samples was dried for seven days on a vacuum line and stored in a screw-top glass bottle within a dessicator, over drierite (anhydrous calcium sulfate). Similar experimental results were obtained from each of these variously treated samples of potassium nitrate.

Indium powder, 325 mesh, described as being of 99.999% purity, was purchased from Alfa Inorganics. It was stored in a small screw-top container within a dessicator, over drierite.

A set of four high-purity homogeneous TherMetric standards, comprised of samples of p-nitrotoluene, naphthalene, benzoic acid and adipic acid, was purchased from Fisher Scientific Company.

Selenium dioxide of highest purity, described as 99.999% (Canadian Copper Refineries, lot 547-A), was obtained from Noranda Mines Ltd.[1] Selenious acid, 96.4% pure, was purchased from Fisher Scientific Company. Both substances were stored in their original containers in a dessicator over drierite.

Hydrazine hydrate was purchased from Fisher Scientific Company as an 85% solution.

Demineralized water, obtained by passing tap water through a standard Barnstead column, was used in the preparation of all solutions.

---

[1]Through the courtesy of Dr. W. C. Cooper, Director of Research at Noranda Research Center, Pointe Claire, Quebec.

PREPARATION OF RED AMORPHOUS SELENIUM

In order to differentiate between two or more samples of red amorphous selenium, numbers have been assigned to these samples. These numbers are intended to reflect solely the sequence in which the red amorphous selenium samples were prepared.

Precipitation. The apparatus for precipitating red amorphous selenium, shown assembled in Figure 1, was set up in a darkened fume hood, in order to minimize the possibility of crystallization due to the effect of light (130).

A 700 ml five-neck reaction kettle, C, was placed in a one gallon container, B, which was so packed with crushed ice that the reaction kettle was completely surrounded by a mixture of ice and water. The kettle and its jacket vessel were positioned within an ice chest, A, of 44 l capacity, which was then filled with crushed ice to a level just below the lip of the jacket vessel, B. This arrangement proved very effective in ensuring that the temperature within the reaction kettle remained almost constant throughout the entire precipitation procedure. During the entire precipitation period the temperature, as indicated on thermometer F, never rose above 274°K.

Two hundred ml. of demineralized water and 20 ml of reagent hydrochloric acid were poured into the reaction kettle. After the temperature of the solution was constant at 273°K, 0.027 moles of selenium dioxide were dissolved into the solution. A glass double-bladed stirring rod, G, was then fixed into position, and the upper and lower halves of the reaction kettle sealed firmly together by means of a flange clamp, H. To prevent inadvertant contamination of the precipitating red amorphous

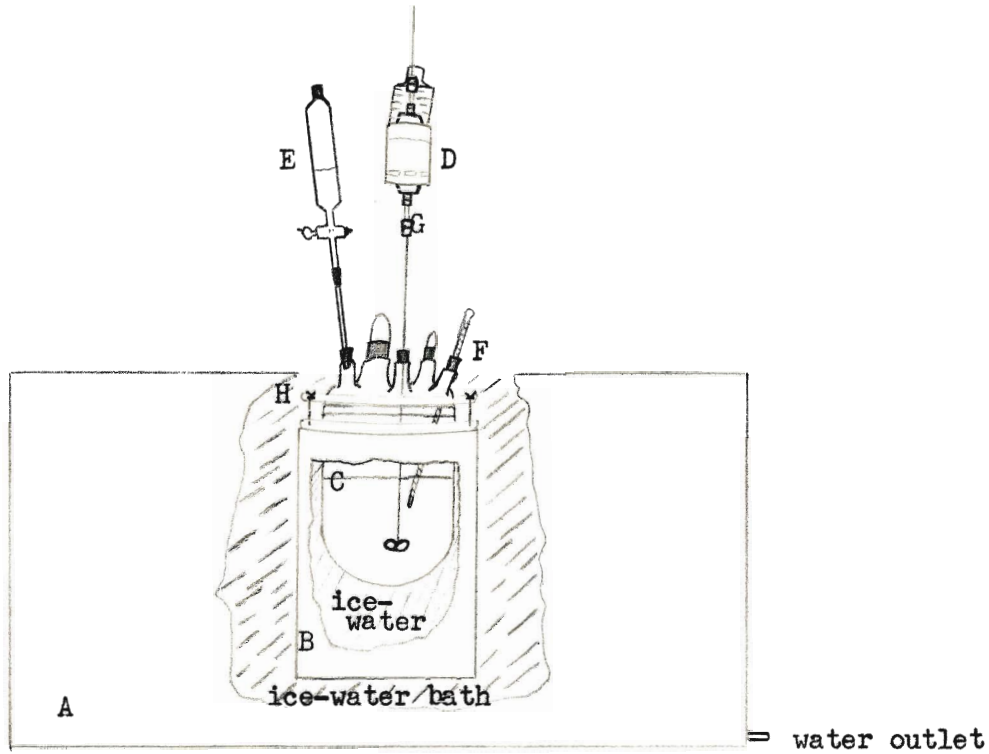

Figure 1

Diagram of Precipitation Apparatus

selenium, no lubricant or grease was used on the ground glass joints of the reaction kettle. The stirrer motor, D, was adjusted to a rate which provided smooth and even stirring of the solution.

When the temperature of the solution in the reaction kettle was again at 273°K, 34 ml of an 8.5% refrigerated solution of hydrazine hydrate were introduced into the mixture via the dropping funnel E. The rate of addition was approximately one drop every ten to fifteen seconds, corresponding to a total addition time of about ninety minutes. A slow addition rate was deliberately chosen in order that the solution temperature would not rise above 274°K, and to permit the maximum degree of coagulation.

After addition of the hydrazine hydrate solution was proceeding smoothly, the reaction kettle lid was covered with aluminium foil and more ice was added until the ice chest had been completely filled. As the ice melted, the resultant water was drained off steadily at the bottom of the ice chest, and additional ice added as required. The red amorphous selenium began to precipitate out during the period when hydrazine hydrate was being added to the solution. When this addition step had been completed, the solution was stirred for another twenty-four hours prior to filtration.

Before the particular apparatus design described above was adopted, some other variations were tested. In one instance, the reaction kettle was placed directly into a large plastic vessel filled with crushed ice, and the water in the vessel circulated by means of a small circulatory pump. With this arrangement however, the temperature in the reaction kettle varied over the range 273-6°K, and the design was therefore considered unsuitable. An attempt to keep the temperature below 274°K

by reducing the amount of heat being transferred from the circulatory pump with the insertion of a second ice-water bath between the pump outlet and the reaction kettle also failed.

As the whole arrangement was tending towards greater complexity and less efficiency, it seemed expedient to consider the elimination of the circulatory pump altogether. Subsequent tests showed that an ice-water jacket could be maintained around the reaction kettle for a period of at least twenty-four hours if the reaction kettle were placed inside a one-gallon metal container. The temperature would then remain between 273-274°K.

In another instance, an attempt was made to replace the mechanical stirrer, which tended to speed up or slow down unpredictably, by a magnetic stirring arrangement. However, the experimental setup was such that the resultant interaction of the stirrer bar with the magnetic field was extremely weak. Therefore the idea of magnetic stirring had to be rejected.

Filtration. After removing the metal jacket-vessel from the ice chest, the reaction kettle was opened and the red amorphous selenium precipitate filtered as quickly as possible. It was necessary to keep the base of the reaction kettle in an ice-water bath between those periods when the precipitate was actually being transferred to the filtration funnel. The complete time for filtration was at least thirty minutes, or two hours if the precipitate was filtered by gravity.

Choosing the filtration apparatus meant balancing several design factors. The loss of precipitate to the filter paper after suction filtration could be minimized by the use of a funnel with a small plate area. However, if a very small funnel was used, the time required for

filtration became extreme, and maintaining the precipitate temperature close to 273°K became a problem, since a funnel of very small dimensions could only be surrounded by an equally small ice-water bath. Also, the faster the red amorphous selenium could be filtered, the less the amount of light to which it had to be exposed. For this reason it was necessary to rule out filtration by gravity, even though this method permitted easier removal of the precipitate from the filter paper. Also to be considered was the fact that the red amorphous selenium tended to creep up the walls of the funnel, and thus these had to be of moderate height.

Of the apparatuses tried, a jacketed Buchner funnel, jacketed Gooch crucibles with or without suction, as well as ordinary glass funnels, also jacketed, the filtration apparatus finally resolved upon was a Buchner funnel with a plate diameter of 80 mm, surrounded by an ice-water bath contained in a vessel of 500 ml capacity. A water aspirator was used to provide the suction needed for rapid filtration. Using this method, a small amount of red amorphous selenium was unavoidably lost to the filter paper, but this loss was considered tolerable because of the faster filtration, and the better temperature control that could be achieved with a moderate-sized ice-water bath.

The precipitate was washed with demineralized water, approximately 275°K in temperature, until no chlorine ions were detectable in the filtrate when the latter was tested with a 0.025 M silver nitrate solution. Five hundred ml. of demineralized water were usually sufficient for washing the precipitate.

Drying. When the filtration process had been completed, the red amorphous selenium was immediately transferred to porcelain combustion boats, 100 mm long by 20 mm wide. These were placed into a drying tube on a

vacuum line. The drying apparatus is illustrated in Figure 2.

The entire apparatus was constructed of pyrex glass tubing, except for the Nonex glass in the Pyrani gauges. From the manifold A, 28 mm in diameter, there branched out: a piece of 20 mm tubing B, which led to the pump trap and vacuum pump; a matched pair of Pyrani gauges C; a stopcock D, which served for bleeding air into the system at a slow rate; and two stopcocks E and F, which led to the drying tubes containing the porcelain boats. During drying, a vacuum was maintained within the system by means of a Welch Duo-Seal pump. It was customary to run the pump continuously for three to five days prior to the actual drying. The pressure in the system was approximately 0.001 mm-Hg. This pressure increased somewhat during the initial drying period, then gradually fell back to 0.001 mm-Hg after three to four days of drying. Pressure readings were obtained from the pair of Pyrani gauges C, whose electrical circuit is shown in Figure 3.

The design of each drying tube was identical. The tube for use at 273°K was constructed starting with a ♂45/50 ground glass joint as a basis. The female side was sealed off, and an additional length of 35 mm wide glass tubing was added to the male side. The end of this latter tubing was also sealed, and the male end of a ♂24/40 ground glass joint blown into the drying tube to provide a means of attachment to the main vacuum line, through stopcock F. The drying tube intended for use at 297°K differed only in that it was based on a ♂34/45 ground glass joint, instead of a ♂45/50. Attachment to the main line was through stopcock E.

All stopcocks and ground glass joints were lubricated with Silicon high-vacuum grease. The sealed drying tube(s) containing the red amorphous selenium in porcelain boats was(were) wrapped in heavy alumin-

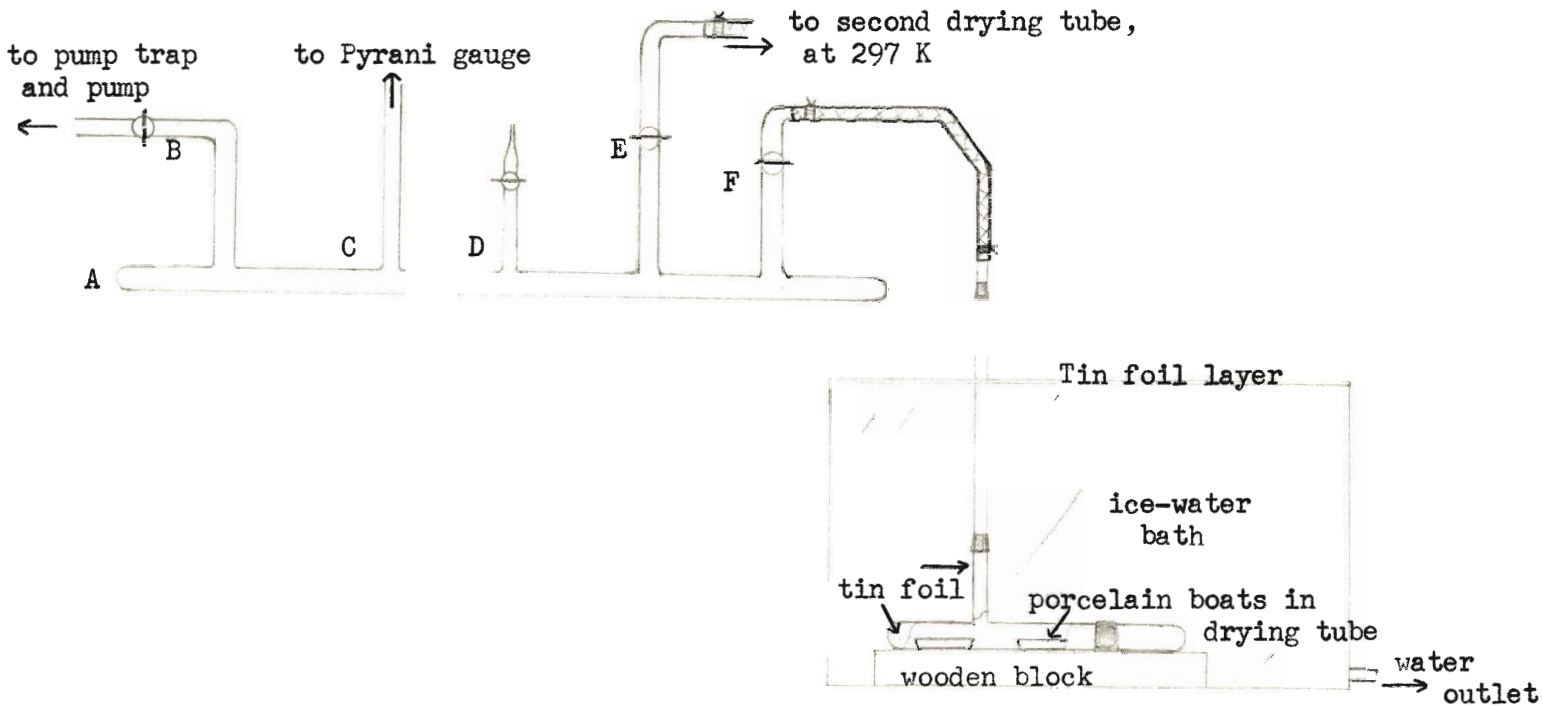

Figure 2

Diagram of Drying Apparatus

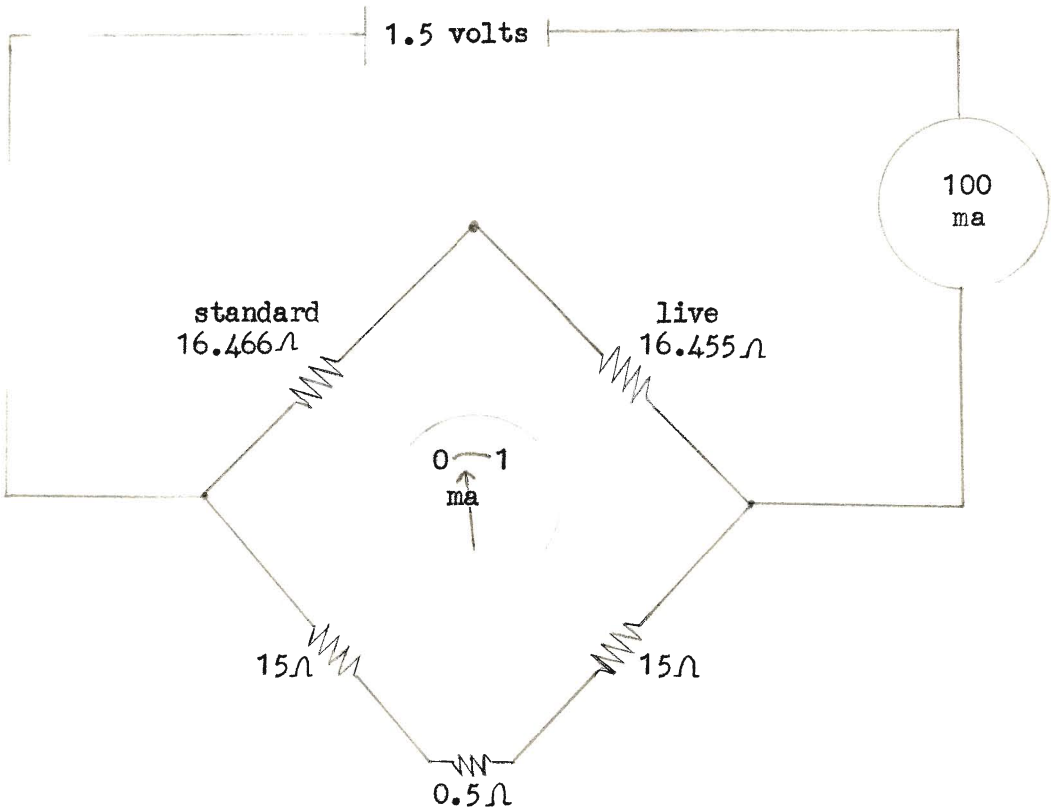

Figure 3

Electrical Circuit of the Pyrani Gauges

ium foil to reduce light exposure, and then attached to the appropriate stopcock via a length of steel-reinforced tygon tubing. The drying tube used at 273°K was mounted on a wooden block which rested on the bottom of the ice chest, and the ice chest was then filled with crushed ice. To retard melting of the ice, the entire chest top was then covered with aluminium foil. The wooden block provided stability and raised the drying tube above the water-outlet level.

Drying normally lasted for a period of seven to eight days, after which air was bled slowly into the system, to prevent the red amorphous selenium from being scattered all over the walls of the drying tube. The drying tube was then opened and the red amorphous selenium transferred to small screw-topped glass bottles for storage in a dessicator at whatever temperature it was dried.

An attempt was originally made to use the reaction kettle as a drying vessel. The filter paper on which the red amorphous selenium had been collected was placed in the base of the reaction kettle, which was then sealed and attached to the drying line. But a problem arose when it was attempted to open the reaction kettle upon completion of drying. The ground glass joint between the upper and lower halves of this vessel had "frozen", and because of the large surface area, a fair degree of force was neccessary to break the seal. The arrangement was awkward, since it was essential that the precipitate on the filter paper not be disturbed, and yet at the same time, the red amorphous selenium could not be allowed to warm up to room temperature. Hence it was decided to construct the special drying tubes, as these could be manipulated more easily.

EXPERIMENTAL PROCEDURES

Two instruments were used to study the thermal behavior pattern of red amorphous selenium: a Du Pont 900 differential thermal analyzer, hereafter referred to as the DTA apparatus, and a Perkin-Elmer DSC-1B differential scanning calorimeter, hereafter referred to as the DSC apparatus.

The DTA apparatus. Two different temperature cells were used with the DTA apparatus: a standard cell for the temperature range 297-773 °K, and a quick-cool cell for the temperature range 77-363 °K. Samples varying in weight from 5 to 30 mg were analyzed using the "macro" heating block and sample tubes. The thermocouples were standard Chromel-Alumel types, obtained from Du Pont. Glass beads, oven-dried before being used, served as the reference material. Whereas the standard temperature cell could be used with an air atmosphere, an atmosphere of dry nitrogen was necessary inside the quick-cool cell during an experiment.

The standard heating rate adopted for all thermograms, both calibration and experimental, was 5 °K/min. The usual range chosen for the ΔT scale was 0.1 °K/in. The four TherMetric standards, p-nitrotoluene, naphthalene, benzoic acid and adipic acid, were used to calibrate the temperature scale between 273 °K and 453 °K.

Assembly of the quick-cool cell, when necessary, was the first step in a typical low temperature DTA experiment on red amorphous selenium. Glass beads and red amorphous selenium were weighed out into separate macro-size glass tubes which were then positioned appropriately in the heating block. Thermocouples were carefully embedded into the centers of the sample and reference materials, all electrical connections

inspected to ensure good contacts, and finally, the bell jar was clamped down over the cell and its atmosphere adjusted so that dry nitrogen gas was flowing through the interior of the bell jar at a rate of two to three standard cubic feet per hour. For the next thirty to forty-five minutes, while water vapor was being purged from the cell, the sample temperature was held below 297°K. Upon completion of this preparatory step, the sample was cooled rapidly by pouring liquid nitrogen into the small Dewar flask surrounding the heating block, through the appropriate tube in the bell jar roof. When the sample had been cooled to the desired initial temperature of the experiment, usually 77°K, any excess liquid nitrogen was allowed to boil off and then the reaction started. An X-Y recorder was used to record all thermograms. During the experiments, appropriate ΔT shifts and baseline-slope corrections were made, when necessary, as the sample temperature gradually approached the desired final temperature. At the end of the experiment the heater was switched off and the bell jar opened to permit faster cooling to the initial temperature of the next experiment.

In a few instances, a cyclic procedure was followed. The sample was heated from an initial temperature of approximately 77°K up to 273°K, and then cooled to 253°K and purged with dry nitrogen gas for twenty minutes, followed by cooling again to 77°K. This cycle was sometimes repeated as often as six times, allowing the temperature to rise to 333°K in the final cycle.

The low temperature cell was also convenient for obtaining thermograms over the temperature range 283-373°K.

The procedure for using the standard temperature cell was identical to that described above, up to the point when the bell jar was

clamped down over the cell. As the sample atmosphere was to be air, the experiment could be started immediately. The cyclic procedure was inapplicable with this cell, since irreversible changes occurred in the sample during heating. Thermograms were usually obtained over the temperature range 295-373 °K.

In the results from this thesis, peak temperatures from DTA thermograms have been converted to degrees Kelvin from degrees centigrade, in order to have these values consistent with those from the DSC, which is calibrated in degrees Kelvin.

The DSC apparatus. The DSC apparatus was used in combination with a 10 mv full-scale Leeds and Northrup Speedomax W recorder. The sample weight varied between 5 and 30 mg for red amorphous selenium, to less than 1 mg for some of the temperature calibration standards. The reference material consisted of an empty sealed sample pan, similar to those in which the samples were placed. During all DSC experiments, a stream of dry nitrogen gas was passed through the cell at a rate of 20 ml/min . The heating rate for all experiments was 5 °K/min .

The differential and average temperature controls were carefully calibrated, according to the instructions given in the Perkin-Elmer instrument manual (131). Powdered indium and Wood's metal alloy were used to determine the correct differential temperature setting. It was found to be 356.9 °K, and the value 625.0 °K was chosen as the optimum average temperature setting for investigating a peak expected to occur at 326 °K. The temperature scale of the DSC instrument was calibrated with the four TherMetric standards mentioned previously.

The procedure for obtaining a thermogram of red amorphous selenium was as follows: in the first place, nitrogen gas was passed

through the standard temperature cell. Red amorphous selenium was placed into a weighed standard sample pan, a top crimped down over the sample, and the sample pan reweighed. The cell was opened while the sample and reference pans were placed in their respective holders, and then covered with the sample holder covers. The cell lid was twisted down again over its bearing pins, and the range and slope dials adjusted to values appropriate for the particular weight of red amorphous selenium being investigated.

After allowing a few minutes for the sample and reference to heat up to the temperature of the cell, usually 311°K, the experiment was started. As the sample temperature increased, the slope and range controls were adjusted whenever necessary. Range 1 was found to be suitable for red amorphous selenium in the temperature range 311-350°K, while range 4 was used from 360-400°K, which was the usual upper temperature limit of red amorphous selenium thermograms. When the experiment had been completed, the heater was set on standby, and the cell opened to allow faster cooling to the initial temperature of the next experiment. Sample holder covers were cleaned in acetone after each usage, and the sample holders when necessary.

Data collection techniques. Peak temperatures were measured by the (132) extrapolated onset technique, since this particular measurement has been reported to give the most consistent set of values for a peak temperature. In this method, the intersection point of the extrapolated pre-transition baseline and a line drawn through the steepest section of the onset side of a peak is chosen as representing the equilibrium peak temperature. Both DTA and DSC thermograms have been treated by this technique.

Peak areas were determined as the average of two to four manual

planimeter readings. The peak area is defined as that area outlined by the peak trace itself and enclosed by a line which is composed of the thermogram baselines extrapolated inwards from each side of the peak and joined below the center of the peak by a small perpendicular bridging section of line.

Since the baseline is a function of heat capacity, among other things, and since the substance formed as a result of whatever transition gave rise to the peak is very likely to have a different heat capacity from that of the substance present at the start of the transition, the baseline on the post-transition side of the peak is usually offset to a small degree from the pre-transition baseline. This implies that by defining the area of a peak in the above manner one is thus measuring the "increase in enthalpy over the extrapolated heat capacity of the two phases" (133). Figure 4 consists of a typical thermogram in which the outlines of an endothermic peak area are indicated.

All the reported peak area/mg values were measured from DSC thermograms.

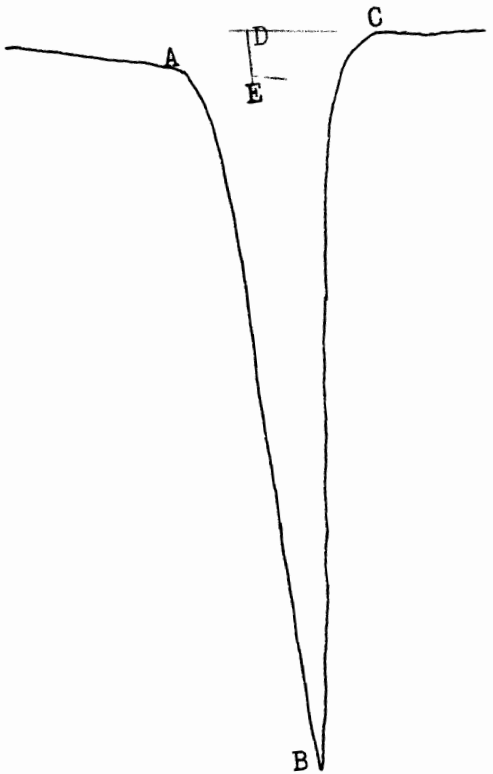

Legend

ABCDE = peak area

Figure 4

Outline of Peak Area

EXPERIMENTAL RESULTS

In order to avoid the presence of an unwieldy number of tables and figures in the main body of the text, experimental thermograms, tables of raw data and a few other miscellaneous items have been relegated to various appendices. A special nomenclature system was thus devised to enable the reader to distinguish readily between tabular or figurative material which is to be found in the main text proper, and that which has been set aside in an appendix. Therefore, a reference to Figure A.1 indicates that this figure will be located in an appendix, in particular, Appendix A; on the other hand, the phrase, Figure 1, refers to a figure in the main body of the text.

Instrument calibration. A set of four Fisher TherMetric standards whose fusion temperatures are accurately known, p-nitrotoluene, naphthalene, benzoic acid and adipic acid, was used to calibrate the temperature scale of the DSC instrument. The heats of fusion of indium and potassium nitrate, as well as the heat of the rhombic to rhombohedral (II→I) transition in potassium nitrate, were adopted as primary enthalpy standards.

In Tables A.I to A.VII, the weight, peak area/mg and observed peak temperatures have been recorded for the DSC thermograms of each of these seven calibration standards. The division of the results into distinct groups, which are determined by the date on which the thermogram was obtained, was necessary for calibration purposes. The dates corresponding to each group are listed in Table A.VIII, and the average temperature of each group of the standards is shown in Table A.IX.

In Figures A.1 to A.6, the average temperatures from Table A.IX

have been plotted, per group, against the literature values of the temperatures of the standard peaks, as listed in Table VII. The linear plots obtained in Figures A.2 to A.5 justify the extrapolations in Figures A.1 and A.6. A mathematical representation of these plots, derived from a least squares analysis of the coordinates of the four TherMetric standards, is given in Table VIII.

It must be emphasized at this point, that the use of roman numerals together with the word group refers to the division of experimental results with respect to the dates on which they were obtained; the word group together with arabic numerals specifies the various specially treated portions of red amorphous selenium samples #10 and #11.

Typical DSC thermograms for the seven standard peaks have been reproduced in Figures A.7 to A.13 . Some corresponding DTA thermograms are shown in Figures A.14 to A.19 . Experimental data relevant to these latter figures is given in Table A.X . The DTA instrument was used in this investigation of the thermal behavior of red amorphous selenium mainly to obtain qualitative information about the general behavior pattern of a substance, while the DSC instrument was used to obtain quantitative values of the enthalpy change associated with a given peak.

Table IX consists of the average of all the peak area/mg values of each standard peak, calculated in each case at the 95% confidence level from a minimum of at least twenty experiments.

The Perkin-Elmer corporation (134) suggests two methods of calculating the enthalpy change associated with a peak recorded by differential scanning calorimetry.

The first of these methods uses the following equation, where standard ΔH represents the known value for the enthalpy of transition

Table VII

Literature Values of the Standardization Peak Temperatures

Reference and Transition Type	Standard Substance	Peak Temperature (°K)
Fisher Sci. Co. (135) (Triple point)	p-Nitrotoluene	324.70±0.05
McCullough et al. (136) (Fusion point)	Naphthalene	353.44±0.05
Goton, Whalley (137) (Fusion point)	Benzoic Acid	395.52
Fisher Sci. Co. (135) (Triple point)	Adipic Acid	424.58±0.05
McLaren, Murdock (138) (Fusion point)	Indium	429.76
Sokolov, Schmidt (139) (II→I transition)	Potassium Nitrate	401.1±0.1
Sokolov, Schmidt (139) (Fusion point)	Potassium Nitrate	607.5±0.1

Table VIII

Mathematical Equations from Least Squares Analysis

of the TherMetric Standards' Coordinates in Figures A.1 to A.6

Figure	Equation
A.1	$y = 0.863x + 44.7$*
A.2	$y = 0.873x + 41.9$
A.3	$y = 0.879x + 40.5$
A.4	$y = 0.873x + 42.6$
A.5	$y = 0.886x + 39.5$
A.6	$y = 0.898x + 36.9$**

* Based on coordinates of p-nitrotoluene and naphthalene only

** The equations obtained from the coordinates of indium and potassium nitrate in Figures A.2, A.3 and A.4 were corrected to give those shown above, and the average correction factor used to obtain the above equation for Figure A.6.

Table IX

Average Area/mg of the Calibration Peaks

Calibration Standard	Number of Experiments	Experiments Rejected*	Average Area/mg	Standard Dev'n(σ)	Coeff. of Variation
p-Nitrotoluene	22	#238	$105.^{6}$	3	3
Naphthalene	28	#246	$123.^{7}$	4	3
Benzoic Acid	28	#143	$121.^{0}$	4	4
Adipic Acid	25	#157	$227.^{1}$	7	3
Indium	25	#24,#25	25.7^{1}	0.6^{1}	2
Potassium Nitrate (II→I Trans'n)	28	#14,#17	43.5^{0}	0.8^{0}	2
Potassium Nitrate (Fusion)	29	#7,#13	41.5^{4}	0.8^{7}	2

* Rejected at the 95% confidence level (1.96σ)

of a calibration standard in kcal/mole, and range refers to a multi-position selector switch whose settings determine the degree of peak attenuation:

$$\Delta H_{sample} = \Delta H_{standard} \times \frac{(\text{area/mg x range x molecular wt.})_{sample}}{(\text{area/mg x range x molecular wt.})_{standard}} \quad (7)$$

The second of these two methods is expressed mathematically in the following equation:

$$\Delta H_{sample} = \frac{60 \times (\text{area/mg x range x molecular wt.})_{sample}}{2 \times 1000 \times \text{standard rectangular area}} \quad (8)$$

The term standard rectangular area refers to the area of a rectangle whose width is equal to one-half the width of the chart paper strip, and whose length equals the amount of chart paper, in inches, traversed by the recorder pen during one minute of travel at a speed identical to the speed which is to be used according to the intended experimental conditions of investigation. The other terms are employed similarly to equation (7).

The chart paper speed used was 1.0 in/min and the ordinate sensitivity is rated as one millicalorie/sec , full scale. Therefore, an area of chart paper one inch long by one-half scale in width should represent 0.03 calories. If equation (8) is rearranged to read as follows:

$$\Delta H_{sample} = \frac{0.03 \times (\text{area/mg x range x molecular wt.})_{sample}}{\text{standard rectangular area}} \quad (9)$$

it becomes obvious that whereas in equation (7) the denominator term referred back to the heat of transition of an actual substance, in equation

(9) the term standard rectangular area refers to a theoretical "heat of transition" for a specified area of chart paper.

A complete list of the reported enthalpy values of the seven standards is given in Table X; of these values, those shown in Table XI have been selected as best representing the enthalpy values of the seven calibration standards.

The values of the heats of transition of the seven calibration peaks as calculated by the method of equation (9), using the area/mg values given in Table IX, are listed in Table XII. This table also includes the heat of transition values for these calibration standards calculated by the method in equation (7), in the columns under the heading "Normalized". This latter method of calculation was used to determine all of the enthalpy values reported in this thesis.

Selenium allotropic investigation. The results of various sets of thermal analysis experiments on red amorphous selenium which are presented in this thesis were obtained from eight presumably equivalent samples of this allotrope prepared under close to identical reaction conditions on the dates shown in Table XIII.

Red amorphous selenium samples #10 and #11 were each divided into several groups, to permit studies on the effects of varying the length of drying time and/or the storage temperature. These groups are defined in Table XIV; group 5 of sample #10 and group 7 of sample #11 correspond to the usual conditions of drying and storage and were maintained as controls for the other groups listed in Table XIV.

The contents of each appendix reflect a different approach in the investigation of red amorphous selenium. Appendix B is a collection of data and thermograms obtained from DTA and DSC experiments on those

Table X

Literature Values of the Heats of Transition

of the Calibration Standards

Reference and Transition Type	Standard Substance	ΔH (kcal/mole)
Rastogi et al. (140) (Fusion)	p-Nitrotoluene	4.47±0.05
McCullough et al. (136) (Fusion)	Naphthalene	4.537±0.001
van Hest, Diepen (141) (Fusion)	Naphthalene	4.540
Dodé, Hagège (142) (Fusion) (143)	Naphthalene	4.540 4.550
Driesbach (144) (Fusion)	Naphthalene*	4.315
Handbk. Chem., Phys. (145) (Fusion)	Naphthalene	4.494
Sklyankin et al. (146) (Fusion)	Benzoic Acid	4.254±0.009
Sekiguchi et al. (147) (Fusion)	Benzoic Acid	4.14
Vassallo et al. (148) (Fusion)	Benzoic Acid	4.14
Handbk. Chem., Phys. (145) (Fusion)	Benzoic Acid	4.139
-------- (Fusion)	Adipic Acid	-----
Oelsen et al. (149) (Fusion)	Indium	0.781±0.004
David (150) (Fusion)	Indium	0.79[2]
Kelley (151) (Fusion)	Indium	0.78

* Of 99.4% purity

Table X (con't)

Reference and Transition Type	Standard Substance	ΔH (kcal/mole)
Kubaschewski (152) (Fusion)	Indium	0.78±0.02
Schneider et al. (153) (Fusion)	Indium	0.79±0.01
Roth et al. (154) (Fusion)	Indium	0.780
Handbk. Chem., Phys. (155) (Fusion)	Indium	0.78[1]
Sokolov, Schmidt (139) (II→I Trans'n)	Potassium Nitrate	1.218±0.005
Sekiguchi et al. (147) (II→I Trans'n)	Potassium Nitrate	1.20±0.03
Kracek (156) (II→I Trans'n)	Potassium Nitrate	1.060
Rao, Rao (157) (II→I Trans'n)	Potassium Nitrate	1.20
Kelley (158) (II→I Trans'n)	Potassium Nitrate	1.30
Am. Inst. Phys. Handbk. (159) (II→I Trans'n)	Potassium Nitrate	1.22
Sokolov, Schmidt (139) (Fusion)	Potassium Nitrate	2.300±0.005
Ko, Hu et al. (160) (Fusion)	Potassium Nitrate	3.080
Kelley (161) (Fusion) (158)	Potassium Nitrate	2.98±0.07 2.8
Kleppa et al. (162) (Fusion)	Potassium Nitrate	2.41±0.03*
Franzosini et al. (163) (Fusion)	Potassium Nitrate	2.40

* Value given at 297°K

Table X (con't)

Reference and Transition Type	Standard Substance	Δ H (kcal/mole)
Doucet, Vallet (164) (Fusion)	Potassium Nitrate	2.357
Goodwin, Kalmus (165) (Fusion)	Potassium Nitrate	2.57[2]
Am. Inst. Phys. Handbk. (159) (Fusion)	Potassium Nitrate	2.30

Table XI

Values Selected as Best Representing the Heats of Transition of the Calibration Standards

Reference and Transition Type	Standard Substance	ΔH (kcal/mole)	Molecular Wt. (g)
Rastogi et al. (140) (Fusion)	p-Nitrotoluene	4.47±0.05	137.142
McCullough et al. (136) (Fusion)	Naphthalene	4.537±0.001	128.175
Sklyankin et al. (146) (Fusion)	Benzoic Acid	4.254±0.009	122.117
-------- (Fusion)	Adipic Acid	---------	146.146
Oelsen et al. (149) (Fusion)	Indium	0.781±0.004	114.82
Sokolov, Schmidt (139) (II→I Trans'n)	Potassium Nitrate	1.218±0.005	101.102
Sokolov, Schmidt (139) (Fusion)	Potassium Nitrate	2.300±0.005	101.102

Table XII

Heats of Transition of the Calibration standards

as Calculated from Equations (7) and (9)

Calibration Standard	ΔH_{sample} in (kcal/mole) (equation (9)) "Un-normalized"	(equation (7)) "Normalized" to: Indium	KNO_3 (Trans'n)	KNO_3 (Fusion)	"Normalized" Average
p-Nitrotoluene	3.7^5	$3.8^3 \pm 0.1$	$4.0^1 \pm 0.1$	$3.9^7 \pm 0.1$	3.9 ± 0.2
Naphthalene	4.1^0	$4.1^9 \pm 0.1$	$4.3^9 \pm 0.1$	$4.3^4 \pm 0.1$	4.3 ± 0.2
Benzoic Acid	3.8^1	$3.9^1 \pm 0.1$	$4.0^9 \pm 0.1$	$4.0^5 \pm 0.1$	4.0 ± 0.2
Adipic Acid	8.5^5	$8.7^8 \pm 0.3$	$9.1^9 \pm 0.3$	$9.0^9 \pm 0.3$	9.0 ± 0.5
Indium	0.7^57	(0.781)	$0.8^18 \pm 0.02$	$0.8^08 \pm 0.03$	0.81 ± 0.04
Potassium Nitrate (II→I Trans'n)	1.1^33	$1.1^63 \pm 0.04$	(1.218)	$1.2^04 \pm 0.03$	1.18 ± 0.05
Potassium Nitrate (Fusion)	2.1^68	$2.2^22 \pm 0.07$	$2.3^26 \pm 0.07$	(2.300)	2.3 ± 0.1

Table XIII

Preparation Dates of the Red Amorphous Selenium Samples

Selenium Sample	Preparation Date	Sample Age on Aug.5, 1969
#4	July 20, 1967	747 days
#5	Aug. 2, 1967	734 days
#6	Dec. 20, 1967	593 days
#7	Jan. 2, 1968	580 days
#8	June 6, 1968	425 days
#9	July 11, 1968	389 days
#10	July 29, 1968	372 days
#11	Aug. 12, 1968	358 days

Table XIV

Identification of the Various Groups of

Red Amorphous Selenium #10 and #11

Selenium Sample	Group No.	Time Dried	Temperature in (°K) of Drying and Storage
#10	1	------	273
	2	------	297
	3	43 hr.	273
	4	43 hr.	297
	5	7 days	273
	6	7 days	297
#11	1	1 hr.	273
	2	1 hr.	297
	3	3 hr.	273
	4	3 hr.	297
	5	24 hr.	273
	6	24 hr.	297
	7	$8\frac{1}{2}$ days	273
	8	$8\frac{1}{2}$ days	297

red amorphous selenium samples which were dried for a period of eight days at 273°K and subsequently stored at this temperature. Both the DTA and DSC instruments were run under standard operating conditions; that is, standard temperature cells were used. Appendix C consists of a set of DTA thermograms which resulted from the investigation of red amorphous selenium over the temperature range 77°K to 333°K, using the DTA low temperature cell. Appendix D contains several DSC thermograms obtained during a qualitative study of the thermal behavior of the various groups of red amorphous selenium samples #10 and #11. Appendix E is a collection of some miscellaneous DSC thermograms on red amorphous selenium, as well as a few DSC traces obtained as the result of a very cursory investigation of black vitreous amorphous selenium.

The peak temperature and area/mg values which were observed for each DSC experiment on red amorphous selenium samples #4 to #11 are presented in Tables B.I to B.VIII respectively. Representative DSC thermograms of these eight samples of red amorphous selenium have been reproduced in Figures B.9 to B.16, in order that it may be possible to compare the appearance of the observed peaks among the various red amorphous selenium samples. For the same reason, typical DTA thermograms of red amorphous selenium are shown in Figures B.1 to B.8. Experimental data pertinent to these latter figures is given in Table B.IX.

In Table XV the average temperature is shown, per group of results, for the endothermic peak exhibited by samples of red amorphous selenium stored at 273°K. The same criterion was employed in grouping these results as was used in Table A.VIII, in connection with the calibration standards. The corrected temperature values given in Table XV were obtained from the equations in Table VIII. Table XVI contains the

Table XV

Average Endotherm Temperature per Group of Results

on Samples of Red Amorphous Selenium

Selenium Sample	Temperature in (°K)					
	Observed			Corrected		
	Group I	Group II	Group VI	Group I	Group II	Group VI
#4	327.1	327.6	324.5	326.9	327.7	328.2
#5	326.4	325.3	323.8	326.3	325.7	327.6
#6	326.5	326.7	325.8	326.4	327.0	329.3
#7	326.0	325.7	326.1	325.9	326.1	329.6
#8	327.1	326.8	326.1	326.9	327.0	329.6
#9	326.4	327.1	325.4	326.3	327.3	329.0
#10 (group 3)*	326.1	-----	-----	326.1	-----	-----
#10 (group 5)	325.9	326.9	324.8	325.9	327.1	328.4
#11 (group 7)	325.6	326.2	323.4	325.6	326.5	327.2

* Experimental data located in Table D.II

Table XVI

Average Exotherm Temperature per Group of Results

on Samples of Red Amorphous Selenium

Selenium Sample	Temperature in (°K)					
	Observed			Corrected		
	Group I	Group II	Group VI	Group I	Group II	Group VI
#4	368.3	368.8	368.3	362.4	363.7	367.5
#5	365.6	365.0	364.1	360.1	360.4	363.7
#6	365.9	365.3	364.2	360.4	360.6	363.8
#7	365.3	364.4	364.3	359.9	359.8	363.9
#8	365.8	365.4	364.6	360.3	360.7	364.2
#9	365.3	365.2	363.2	359.9	360.5	362.9
#10 (group 3)*	365.5	-----	-----	360.0	-----	-----
#10 (group 5)	367.0	366.2	364.0	361.3	361.4	363.6
#10 (group 6)**	367.5	367.5	-----	361.8	362.5	-----
#11 (group 7)	364.0	364.0	361.2	358.7	359.5	361.1
#11 (group 8)***	363.2	364.1	-----	358.0	359.6	-----

* Experimental data located in Table D.II

** Experimental data located in Table D.III

*** Experimental data located in Table D.IV

equivalent data for the exothermic transition peak; results were obtained from red amorphous selenium samples stored at 297 °K, as well as from samples stored at 273 °K.

The average values of the corrected endothermic and exothermic peak temperatures shown in Tables XV and XVI respectively have been listed in Table XVII, per sample of red amorphous selenium. Tables XVIII and XIX are comprised of the average area/mg values of the endothermic and exothermic transition peaks respectively, also listed per sample of red amorphous selenium.

Table XX contains the cumulative average values of the temperature, area/mg and enthalpy of the endothermic and exothermic peaks observed in red amorphous selenium prepared, dried and stored at 273 °K. The values of the temperature and area/mg shown in Table XX for each transition were calculated from the data given in Tables XVII and XVIII to XIX respectively. These cumulative area/mg values were used in equation (7), together with the heats of transition and area/mg values of the primary enthalpy standards, to calculate the "normalized" enthalpies of transition given in Table XX. The average of these "normalized" values represents the experimentally determined enthalpy values of the two transition peaks observed in red amorphous selenium.

The information in this table, especially that concerning the endothermic peak, comprises an important part of the original results which were obtained in this research project.

The results contained in Appendix C consist of typical low temperature thermograms of red amorphous selenium samples #4, #5, #6, #7 and #11; these results were obtained with the DTA instrument. The expression "low temperature" applied to a DTA thermogram usually indicates

Table XVII

Average Transition Temperatures of

Red Amorphous Selenium Samples

Selenium Sample	Endotherm Temp. (°K)	Exotherm Temp. (°K)
#4	327.6	364.5*
#5	326.5	361.4
#6	327.6	361.6
#7	327.2	361.2
#8	327.8	361.7
#9	327.5	361.1
#10 (group 3)	326.1	360.0
#10 (group 5)	327.1	362.1
#10 (group 6)	-----	362.2
#11 (group 7)	326.4	359.8
#11 (group 8)	-----	358.8

* Rejected at the 95% confidence level (1.96σ)

Table XVIII

Average Area/mg of the Endothermic Peak Observed

in Red Amorphous Selenium

Selenium Sample	Number of Experiments	Experiments Rejected*	Average Area/mg	Standard Dev'n(σ)	Coeff. of Variation
#4	7	---	$20.^{22}$	$1.^{4}$	7
#5	8	#8	$20.^{36}$	$1.^{1}$	5
#6	12	#9	19.7^{4}	0.8^{8}	4
#7	13	#7	18.7^{7}	0.6^{8}	4
#8	13	---	20.4^{7}	0.4^{9}	2
#9	10	---	19.8^{1}	0.8^{0}	4
#10 (group 3)	6	---	$19.^{98}$	$1.^{1}$	5
#10 (group 5)	8	#69	20.9^{3}	0.7^{5}	4
#11 (group 7)	7	#44	18.6^{4}	0.5^{6}	3

* Rejected at the 95% confidence level

Table XIX

Average Area/mg of the Exothermic Peak Observed

in Red Amorphous Selenium

Selenium Sample	Number of Experiments	Experiments Rejected	Average Area/mg	Standard Dev'n(σ)	Coeff. of Variation
#4	7	---	$42.^{55}$	$1.^{6}$	4
#5	6	#7	41.1^{4}	0.4^{7}	1
#6	12	---	$42.^{38}$	$1.^{3}$	3
#7	10	---	41.7^{5}	0.9^{3}	2
#8	11	---	$41.^{62}$	$1.^{2}$	3
#9	8	---	42.1^{4}	0.9^{6}	2
#10 (group 3)	6	---	$41.^{58}$	$1.^{3}$	3
#10 (group 5)	10	---	$39.^{25}$	$1.^{9}$	5
#10 (group 6)	6	---	$39.^{52}$	$2.^{9}$	7
#11 (group 7)	7	#26	38.9^{3}	0.5^{4}	1
#11 (group 8)	3	---	$40.^{13}$	$1.^{5}$	4

* Rejected at the 95% confidence level

Table XX

The Cumulative Average Area/mg and Temperature Values, and the Enthalpy Values, of the Transitions Observed in Red Amorphous Selenium*

	Endothermic Peak	Exothermic Peak
Number of Experiments	73	69
Peak Area/mg ± Standard Deviation	$19.8^{7} \pm 0.8^{1}$	$41.^{2} \pm 1.^{4}$
Coefficient of Variation	4	3
Peak Temperature ± Standard Deviation (°K)	327.2 ± 0.5	361.3 ± 0.7
Coefficient of Variation	0.2	0.2
Δ H of Transition: (kcal/g-atom)		
"Normalized" to In	$0.103^{8} \pm 0.005^{1}$	$0.86^{1} \pm 0.03^{7}$
"Normalized" to KNO_3 (II→I Transition)	$0.108^{6} \pm 0.004^{8}$	$0.90^{1} \pm 0.03^{4}$
"Normalized" to KNO_3 (Fusion)	$0.107^{4} \pm 0.004^{9}$	$0.89^{1} \pm 0.03^{5}$
Average ΔH of Transition (kcal/g-atom)	0.107 ± 0.009	0.88 ± 0.06

* The results in this table have been obtained from those samples of red amorphous selenium which were dried and stored at 273°K.

that the initial temperature of the experiment was 77°K, although in some cases the initial temperature was greater than 77°K but less than room temperature (297°K). The final temperature of these experiments was most often 273°K, but in some cases 333°K. Table XXI is a list of the thermograms in Appendix C. Table C.I contains some of the experimental data pertinent to these figures, and corrected values (166) of the low temperature readings obtained from the Chromel-Alumel thermocouples are given in Table C.II.

Appendix D is a collection of thermograms obtained from the various groups of red amorphous selenium samples #10 and #11. The contents of these thermograms, which are summarized in Table XXII, were gathered over a period of days and weeks immediately following drying of the samples. In addition to permitting one to watch for possible aging effects in samples of red amorphous selenium stored at 297°K, with respect to those stored at 273°K, this division of the samples into several groups also made possible simultaneous qualitative observations of the effects of varying the length of sample drying time. Table D.I contains some of the experimental conditions necessary to determine the significance of the thermograms in Appendix D. The area/mg and peak temperature values of groups three and six of red amorphous selenium #10 and of group eight of red amorphous selenium #11 are reported in Tables D.II to D.IV respectively.

Appendix E is composed of a few miscellaneous thermograms. Figure E.1 shows the effect of keeping a sample of red amorphous selenium at 313°K for various lengths of time prior to the start of a normal DSC experiment. Figures E.2 and E.3 represent the results of a study to determine whether the endothermic peak observed at 327°K in red amorphous

Table XXI

Contents of the Figures in Appendix C

Figure Number	Selenium Sample	Experiment Number
C.1A,1B	#4	19
C.2A,2B	#4	18
C.3A	#5	12
C.4A	#5	13
C.5A,5B	#5	16
C.6A,6B	#5	19
C.7A,7B	#6	6
C.8A	#6	8
C.9A,9B	#7	6
C.10A	#7	9A
C.10B	#7	9D
C.10C	#7	9F
C.10D	#7	9G
C.10E	#7	9I
C.11A	#7	10
C.12A	#11, group 8	3

Table XXII

Contents of the Figures in Appendix D

Figure Number	Selenium Sample	Experiment Number
D.1-D.5	#10, group 2	5,10,19,49,66
D.6-D.9	#10, group 1	17,31,50,62
D.10-D.14	#10, group 4	14,20,28,39,65
D.15-D.19	#10, group 3	12,13,29,41,61
D.20-D.22	#10, group 6	40,47,64
D.23-D.26	#10, group 5	37,52,60,69
D.27-D.31	#11, group 2	1,7,13,25,39
D.32-D.34	#11, group 1	3,29,34
D.35-D.38	#11, group 4	6,14,23,40
D.39-D.42	#11, group 3	4,18,28,33
D.43-D.45	#11, group 6	9,22,37
D.46-D.49	#11, group 5	8,17,27,32
D.50-D.52	#11, group 8	20,21,35
D.53-D.56	#11, group 7	16,26,31,43

selenium is reversible or irreversible. Each figure consists of the traces of two consecutive experiments performed on a sample of red amorphous selenium, the upper trace representing the first run in each instance.

A thermogram of poly(ethylene terephthalate) has been reproduced in Figure E.4 in order to show the general appearance of a glass transition process, as detected by the DSC instrument when the heating rate is 5°K/min.

Figures E.5 to E.8 constitute a cursory study of vitreous amorphous selenium; this study was undertaken because of a similarity noted between results obtained in this thesis and those obtained by Gobrecht (36) on vitreous amorphous selenium quenched from the melt and red amorphous selenium quenched from the vapor phase when these samples are stored at 297°K. Figures E.5 and E.6 are thermograms of vitreous amorphous selenium, and Figure E.8 is the thermogram which results from a mixture of red amorphous selenium, stored at 273°K, and vitreous amorphous selenium stored at 297°K. A trace of a red amorphous selenium sample which had been allowed to age for a considerable length of time at 297°K is shown in Figure E.7, for comparison with Figure E.8.

DISCUSSION OF RESULTS

Instrument calibration. As indicated previously, four Fisher TherMetric standards were used to calibrate the temperature scale of the DSC instrument. Originally, it had been anticipated that two of these standards, p-nitrotoluene and naphthalene, could also be used as enthalpy standards. However when the heats of fusion reported in the literature for these substances were inserted in equation (7) in order to calculate the enthalpy values of a transition, the results obtained using p-nitrotoluene as the enthalpy standard were incompatible with those determined using naphthalene as the standard substance. As it was not known which reported heat of fusion value was in error, if not the two values, and because it would be both useful and convenient if there were to exist in future a set of easily-obtainable substances which could serve simultaneously as both enthalpy and temperature calibration standards, it was decided to determine experimentally the heats of fusion of the four Fisher TherMetric standards.

Thus it became necessary to choose a set of primary enthalpy standards, in order that equation (7) might be used to calculate the heats of fusion of the TherMetric standards.

The heat of fusion of indium was chosen as one of the primary enthalpy standards for several reasons: it is a stable reproducible transition with a well-verified enthalpy value; the fusion temperature falls within the temperature range of interest in this project; and no after-effects are exhibited upon fusion (167). Because of these properties, as well as the fact that indium is readily obtainable as a highly purified powder (99.999%), it has often been used as an enthalpy

standard (150,168,169).

Since red amorphous selenium had been observed to undergo a solid-solid transition, it was only appropriate that at least one of the primary enthalpy standards behave similarly. Therefore, potassium nitrate was chosen as the second primary enthalpy standard, since it not only underwent a solid-solid transition from the rhombic to the rhombohedral form, but also melted at a temperature low enough to be usable in this project. In addition, potassium nitrate is being tested to learn whether it is suitable for inclusion in a series of proposed internationally-acceptable thermal analysis standards (170). If it is adopted as a member of this series, results in this thesis will then be more easily compared with those results to be obtained by future workers.

A comparison of Figures A.7 to A.13 with Figures A.14 to A.18 indicates that the results obtained by DTA and DSC methods are qualitatively similar, as would be expected from the nature of these instruments. The peaks onset sharply over a narrow temperature range and are seen to be very well-defined. With the exception of potassium nitrate, the shape of each peak is typical of that observed for the fusion of a pure substance (171). The greater width of the potassium nitrate peaks reflects the granular nature of this substance (172). These peaks also onset sharply, in a manner comparable to the other standard peaks.

The individual peak area/mg values for each of the standard substances have been recorded in Tables A.I to A.VII . The standard deviation (σ) of these area/mg values was calculated for each of the sample transitions. Any values lying outside the 95% confidence level (average area/mg $\pm$ 1.96σ) were rejected. On this basis, an average of one result out of twenty-five was rejected in the case of the TherMetric

standards, and approximately one result out of fifteen for the primary enthalpy standards. The data has been summarized in Table IX. As is evident from the coefficients of variation in this table, the above rejection ratios reflect the higher precision of the average area/mg values of the primary enthalpy standards. The lower precision of the organic TherMetric standards might be due in part to their higher volatility, but a more probable reason is that their average sample weights were much smaller than those of the enthalpy standards. Since the precision of the Mettler micro-balance was estimated to be $\pm$ 0.005 mg, errors of this magnitude would be much more significant in obtaining accurate weights for the smaller-sized samples of the TherMetric standards than for those of the primary enthalpy standards. Larger-sized samples were not used because it was desirable to calibrate the DSC instrument at the same attenuation range, if possible, as would be employed in the thermal investigation of red amorphous selenium.

A complete list of the enthalpy values reported in the literature for the seven calibration peaks, back to at least 1950, is presented in Table X. The enthalpy values in Table XI are believed to represent the best choice for the enthalpies of the transitions occurring within the standard substances, from the values given in Table X.

The value of 0.781 $\pm$ 0.004 kcal/mole, chosen as the heat of fusion of indium, is the most precise of all the values reported for indium, and in view of the good agreement of the data in Table X, it would appear to be reasonably accurate.

In the case of potassium nitrate however, it is not so obvious which value should be selected, eapecially with respect to the fusion peak, where the data in Table X is split into two sets of values, one

higher than the other. By relying on the accuracy of the heat of fusion of indium, and using this value to calculate a theoretical heat of fusion value for potassium nitrate, it was discovered that the set of lower values was the more probable of the two. Among the workers represented in the lower values' group, Sokolov and Schmidt (139) were unique in that they had determined the enthalpy value of the II→I transition as well as the fusion process. On the basis of the relative area/mg values obtained in this project for these two peaks, Sokolov and Schmidt's values can be shown to be self-consistent; and in addition, their values were also the most precise of the several reported. Thus it is believed that these values represent the most suitable choice of enthalpy values for the potassium nitrate peaks.

Table XII lists the enthalpy values determined for the heats of transition of the seven calibration peaks. The "normalized" columns contain the values calculated from equation (7), using the enthalpy values of the primary standards listed in Table XI. The average of the values in these three columns is taken as the heat of transition in the case of the standard substances. The "un-normalized" column represents the enthalpy values as calculated using the method of equation (9). These latter values are seen to be consistently low with respect to the reported values of the enthalpy of transition of the standard substances. If these calculated enthalpies were to be normalized to the values of the primary standards which are given in Table XI, an instrument calibration factor could be determined.

That the enthalpy values reported by Sokolov and Schmidt for the two potassium nitrate peaks are self-consistent is obvious from the fact that the ratio of their values is 0.529, while the ratio of the peak

area/mg values is 0.524. However, it can be seen that the heat of fusion value for indium is not consistent with the enthalpy values for the potassium nitrate peaks, and thus it would be advisable in future to obtain a consistent set of enthalpy values for the primary standards by means of direct calorimetric measurements.

In general, a comparison of the heats of fusion of the TherMetric standards reported in the literature with the calculated values in Table XII indicates that this work has yielded acceptable agreement for the heats of fusion of naphthalene and benzoic acid, but that the discrepancy in the case of p-nitrotoluene is considerable. As the heat of fusion of adipic acid is believed to represent original data, it cannot be compared .

In particular, it can be seen from Tables XII and XI that the calculated enthalpy of fusion of naphthalene is about 0.2 kcal/mole less than the value reported by McCullough et al.;Driesbach has quoted the value 4.315 kcal/mole (or 4.350 kcal/mole for 100% sample) from the Dow Chemical Co. literature on 99.4% pure naphthalene, which agrees excellently with the presently determined enthalpy value, but no similar value has been reported, whereas the value given by McCullough's group is supported by several other workers (cf. Table X).

For benzoic acid the degree of accuracy is similar; the value calculated in this thesis being about 0.1 kcal/mole less than Vassallo and Harden's reported value, and slightly greater than 0.2 kcal/mole below the value determined by Sklyankin and Strelkov, which could be shown to be self-consistant with the value determined by McCullough et al. for naphthalene.

In view of the above differences between the calculated and

reported heat of fusion values, it seems unlikely that one should obtain a discrepancy of 0.6 kcal/mole in the case of p-nitrotoluene. Thus, it may be suggested that the single previously-reported value of the heat of fusion of p-nitrotoluene is in error, and should be replaced, even if only on an interim basis, by the value in this thesis.

In conclusion to this section on instrument calibration, it has been shown that the four TherMetric standards can now be used as secondary enthalpy calibration standards, in addition to their original role as temperature calibration standards. The set of secondary enthalpy values reported in this thesis has the advantage of being based on an internally-consistent group of area/mg values. Should a correction be made in future to bring the enthalpy values of the primary enthalpy standards into better agreement with each other, it would then be a simple matter to revise the values given in this thesis for the heats of fusion of these four TherMetric standards.

Thermal behavior of red amorphous selenium stored at 273 °K. When thermal investigations were carried out within the temperature range 311-393 °K, samples of red amorphous selenium which had been dried and then stored at 273 °K in a dessicator were all observed to undergo an endothermic transition at 327.2 ± 0.5 °K. On continued heating of the sample, an exothermic transition was noted at 361.3 ± 0.7 °K. Fusion occurred at approximately 493 °K.

The endotherm at 327.2 ± 0.5 °K was invariably observed in these samples of red amorphous selenium, whether the DSC experiment was begun at 311 °K or lower, down to as far as 77 °K. This fact itself implies that red amorphous selenium does not undergo any irreversible transitions between 311 °K and 77 °K.

During the transition at 327.2 ± 0.5°K, the selenium gradually changed from a bright red to a black color. Debye-Schirrer X-ray powder patterns[1] obtained on this black substance revealed that it was amorphous in nature.

Representative DTA traces of this transition, obtained from red amorphous selenium samples dried under vacuum for seven to eight days at 273°K, and then stored at this same temperature in a dessicator in the dark, are shown in Figures B.1 to B.8. The age of the samples in these particular thermograms varied from 14 to 199 days. It can be seen that the endothermic transition at 327.2 ± 0.5°K was quite reproducible among the various red amorphous selenium samples. Moreover, if allowances are made for the different sample weights and degrees of sensitivity in these figures, as listed in Table B.IX, it would appear that the peaks representing this transition are exhibiting a constant area/mg value. Qualitatively, this would imply that no correlation exists between the age of the samples and the area of the endothermic peak.

The corresponding DSC traces, shown in the upper halves of Figures B.9 to B.16, again illustrate the reproducible nature of this transition. Furthermore, the data given in Tables B.I to B.VIII, the individual area/mg values obtained from each DSC thermogram of red amorphous selenium, quantitatively confirms the non-dependence of the endothermic peak area on the age of the sample.

From Figures E.2 and E.3, it can be seen that this endothermic transition is irreversible in nature. In each of these figures the upper trace represents a typical DSC experiment on a sample of red amorphous

---

[1]The author is indebted to Dr. P. H. Bird for his assistance both in obtaining and evaluating the Debye-Schirrer X-ray films.

selenium dried and stored at 273°K. On completion of the endothermic transition, the samples were cooled to 316°K. After allowing a few minutes for the temperature to equilibrate, a second experiment was performed on each sample, as shown in the lower trace of each figure. The absence of any peak in these latter traces indicates that cooling the sample to below 327°K does not reverse the effects of this endothermic transition. Identical results are obtained if the sample is cooled rapidly to 77°K rather than to 316°K.

The only reference in the literature to an endothermic transition in amorphous selenium in the region of 327°K is that due to Fyans (129). Although he does not state from which particular amorphous form of selenium his results were obtained, he does report having seen a first-order endothermic transition at 330°K, on heating a sample of amorphous selenium in a Perkin-Elmer DSC-1B instrument, at a rate of 20°K/min. It has been reported in the literature by Lambert (127), and noticed by the author of this thesis, that the temperature at which a peak is observed on a DTA or DSC thermogram will increase as the heating rate is increased. Lambert published a temperature correction scale for determining a peak temperature relative to various heating rates. According to his scale, Fyans' peak at 330°K would be expected to occur at 325°K, if the heating rate were 5°K/min, as was used in this project. This latter temperature would agree quite well with the temperature reported in this thesis.

However, from general experience in operating a DSC instrument of this type, the author of this thesis feels that the deviation between peak temperatures observed at 20°K/min and 5°K/min is probably closer to 10°K. In this case, Fyans' peak would be expected at 320°K, relative to a heating rate of 5°K/min, which is somewhat nearer to the 308-318°K

endothermic region observed by Gobrecht (36) in both quenched vitreous amorphous selenium and red amorphous selenium, than to the endothermic transition at 327°K reported in this thesis for chemically-reduced red amorphous selenium.

Fyans attributed the peak which he observed to the glass transition process in amorphous selenium. However, there is such a large difference between his observed temperature of 330°K and the reported glass transition point, 303°K (cf. Table V), that this explanation seems very unlikely. It is suggested that quite possibly Fyans has observed either the endothermic transition reported by Gobrecht (36), or else the transition described in this thesis, and failed to recognize the significance of his results because he was concerned with proving the applicability of the DSC instrument as a device for detecting glass transition points. Also, since he was only using 1/16 of the instrument's maximum sensitivity, it is possible that there was just not sufficient sensitivity to detect the glass transition point of selenium at 303°K.

As was mentioned in the introduction, one of the characteristics of the glass transition point, as observed by DTA or DSC methods, is that the baselines recorded before and after this transition are usually shifted apart. This effect is shown quite clearly in Figure E.4, which is a thermogram of poly(ethylene terephthalate)[1] containing a glass transition point at 353°K. The irregular nature of the thermogram of this glass transition point contrasts sharply with the well-defined outline of the endothermic transition at 327°K in the red amorphous selenium

---

[1]The author is pleased to acknowledge the assistance of Dr. R. Townshend in providing several polymer samples, as well as his useful comments on the theory of polymer behavior at the glass transition point.

thermograms of Appendix B. It may also be noted in these thermograms that the baseline is fully recovered. This latter fact, together with the aforementioned irreversibility of the endothermic transition, is believed sufficient to eliminate the possibility that the observed peak could represent the glass transition point in selenium.

Gobrecht (36) tentatively suggested that the endotherm which he observed in vitreous amorphous selenium at 308-318 °K may be due to the breakdown of a partially-ordered state which forms near 303 °K, the glass transition point; but at the time of publication his investigations were still incomplete, and he was unable to make a definite comment.

Gattow and Heinrich (33) have observed that red amorphous selenium transforms irreversibly to the black amorphous form above 303 °K, suggesting as the mechanism by which this process can occur the cleavage of high-molecular-weight rings (cf. Krebs--Introduction).

Considering the color change from red to black during the endothermic transition at 327.2 ± 0.5 °K, as well as the retention of the amorphous character of the sample, it may be suggested that this transition be ascribed to the transformation of red amorphous selenium into black amorphous selenium. In view of the fact that red amorphous selenium prepared by precipitation from a selenious acid solution at 273 °K is considered to be composed of a mixture of eight-membered ring molecules and short (with respect to vitreous amorphous selenium) chains, this endothermic transition could then represent the point at which the ring molecules break open to yield short Seg chain segments which subsequently polymerize into longer chain molecules.

Each sample of red amorphous selenium which exhibited an endothermic peak at 327.2 ± 0.5 °K also gave rise to an exothermic peak at

361.3 ± 0.7°K. The sample color changed from black to grey during this transition, and Debye-Schirrer X-ray powder patterns indicated that the sample was crystalline on completion of this transition.

Representative DSC traces of this exothermic transition are shown in the lower halves of Figures B.9 to B.16. The peak is observed to be reproducible among the various selenium samples, and the individual area/mg values in Tables B.I to B.VIII are seen to be independent of the age of the samples, which were all dried in a vacuum at 273°K and afterwards stored in a dessicator at this same temperature.

This exothermic peak at 361.3 ± 0.7°K is ascribed to the crystallization of black amorphous selenium, formed from red amorphous selenium at 327.2 ± 0.5°K, into the grey trigonal allotrope of selenium. It can be seen from Table III that crystallization from the vitreous amorphous modification is usually reported in the temperature range 373 ± 20°K and that the sole mention of crystallization from the black amorphous form is quoted as occurring at a temperature greater than 353°K. These values are given here simply to show that the exothermic peak at 361.3 ± 0.7°K is occurring within the general temperature range which has been reported for the formation of trigonal selenium.

During the transition at 361.3 ± 0.7°K the long tangled chains of the black amorphous form of selenium must realign into the infinitely-long parallel helical chains of grey trigonal selenium.

Thermal behavior of red amorphous selenium stored at 297°K. As mentioned before, the area/mg value of the endothermic peak at 327°K in red amorphous selenium has been shown to be independent of the sample age. In a sense, these results imply that red amorphous selenium, prepared, dried and stored at 273°K, is stable (for at least 748 days, according to the

data in Tables B.I to B.VIII), on the basis that if the red amorphous selenium were undergoing a spontaneous transition at 273°K into another form of selenium, then the area/mg value of the endothermic peak at 327°K would be expected to diminish gradually, as the sample aged. However, if the transition at 327°K involves only the Se_8 ring molecules of red amorphous selenium, then it is conceivable that the chain molecules might slowly increase in length without affecting the area/mg value of this endothermic transition to any appreciable degree.

Contrary to the results of Hamada, Sasaki and Negita (39)--that red amorphous selenium slowly crystallizes even at a temperature as low as 273°K--Debye-Schirrer X-ray films indicate the absence of crystallinity in samples of red amorphous selenium stored at 273°K for up to approximately two years.

Kharlamov and Golubeva (38) state that amorphous selenium is stable over a three- to five-year period, but only if kept cool and dry. They observed the occurrence of noticeable qualitative changes in selenium samples stored for a long time (up to five years) at temperatures greater than 303°K. It is unfortunate that neither the value of the temperature referred to as "cool", nor the specific amorphous selenium modification, were mentioned in the abstract of this particular reference.

In view of these results however, together with those of Gobrecht (36), who noticed the gradual appearance of an endothermic transition at 308-318°K in vitreous amorphous selenium and red amorphous selenium annealed at 297°K, it seemed wise to determine whether storage at 297°K would affect the thermal stability of the red amorphous selenium samples which were prepared at 273°K.

Taken as a unit, Figures D.23 to D.26 constitute a miniature time study of the thermal stability of red amorphous selenium #10, showing thermograms obtained from samples aged 260 hours to 372 days at 273°K, after having been dried seven days at 273°K under a vacuum. The various groupings of red amorphous selenium samples #10 and #11 have been defined in Table XIV. Experimental data relevant to these figures is listed in Table D.I . It can be seen that there was no change in the appearance of the endotherm at 327.2 ± 0.5°K, nor did any new thermal effects develop within this period of time. Thus it is felt that red amorphous selenium can be considered as a thermally-stable allotropic form of selenium under the storage conditions mentioned.

When the temperature at which the red amorphous selenium was dried and stored was increased to 297°K, and all other variables maintained constant, the thermograms in Figures D.20 to D.22 were obtained. Within 10 days of preparation, a new endothermic peak became visible at approximately 316-319°K, and gradually increased in size at the expense of the endotherm at 327°K.

These results, which were duplicated with red amorphous selenium #11 as shown in Figures D.53 to D.56 and D.50 to D.52 respectively, indicate that red amorphous selenium is definitely not thermally stable at 297°K, and is slowly undergoing a transition to another form of selenium.

If one continued to heat the samples which had been stored at 297°K, an exothermic peak was observed at about 361°K, similar in all respects to the exotherm observed in samples of red amorphous selenium stored at 273°K prior to a DSC experiment. Eventually however, a second exothermic peak became visible at about 397°K, in addition to the one

at 361°K. A typical example of such a thermogram is shown in Figure D.63. This new exotherm was only observed when the endotherm at 316-319°K had almost completely replaced the endotherm at 327°K.

Thermal stability of red amorphous selenium. Because the appearance of the endotherm at 316-319°K in chemically-reduced red amorphous selenium stored at 297°K was reminiscent of the results obtained by Gobrecht (36) when both red amorphous (quenched from the vapor phase) and vitreous amorphous (quenched from the melt) selenium were annealed at 297°K, it was decided to perform a few DSC experiments on black vitreous amorphous selenium. This work must be considered as being merely cursory though, for the following reasons: i) an adequate thermal history of the vitreous amorphous selenium was lacking, ii) the exact degree of purity of the sample was unknown, although it was high, and iii) only a limited number of DSC experiments were performed.

With respect to its thermal history, the vitreous amorphous selenium had obviously been prepared by quenching, as it was obtained in the form of small pellets, but neither the temperature of the melt, which would influence the structure of the resultant vitreous amorphous selenium, nor the quenching technique, were known. In addition, although the vitreous amorphous selenium pellets were stored at 297°K during the course of this research project, their previous storage temperature was unknown.

Experimental results were obtained not only from these pellets of vitreous amorphous selenium, but also from a sample prepared by melting some of the pellets and then allowing the molten sample to cool naturally to room temperature (297°K), the temperature at which the sample was to be stored. Although the thermal history was quite as indefinite

from the point of view that the temperature of the melt was not known accurately, at least the storage conditions were such that the sample had definitely not been heated above 297°K after its preparation.

Figures E.5 and E.6 represent typical DSC thermograms obtained from these two types of vitreous amorphous selenium samples respectively. Both of these thermograms exhibit an endothermic peak at about 316°K, and an exothermic peak at about 389-392°K. Whereas the endotherm occurs within the temperature region reported by Gobrecht (36), 308-318°K, the exotherm is roughly twenty-five degrees higher than the exothermic peak temperature which he observed. Although it is possible that this latter deviation may reflect differences in the quench temperatures of Gobrecht's vitreous amorphous selenium samples and those of the samples used in this thesis, the lack of adequate thermal data makes it impossible to conclude anything definite on this point.

However, the temperatures of these two peaks do agree very well with the temperatures observed for the endotherm and exotherm which gradually appear in red amorphous selenium prepared by chemical reduction at 273°K, and subsequently stored at 297°K. Figure E.7 represents a thermogram of red amorphous selenium sufficiently aged at 297°K to exhibit not only the two endotherm peaks, but both crystallization peaks as well. If red amorphous (chemically-reduced) selenium were slowly undergoing a transition to the vitreous amorphous form at 297°K, then one would expect to be able to reproduce Figure E.7 by mixing together some red amorphous selenium stored at 273°K with some vitreous amorphous selenium. This was done, and the resulting thermogram is shown in Figure E.8. A comparison of the various peak temperatures observed in Figures E.5 to E.8 is shown in Table XXIII.

Table XXIII

A Comparison of the Observed Peak Temperature in

Red Amorphous Selenium and Black Vitreous Amorphous Selenium*

Selenium Sample Type	Temperature in (°K)			
	Endotherm #1	Endotherm #2	Exotherm #1	Exotherm #2
Black Vitreous Amorphous Selenium, Figure E.5	316.2	-----	-----	392
Black Vitreous Amorphous Selenium, Figure E.6	316.4	-----	-----	389
Red Amorphous Selenium #11, Group 8, Figure E.7	319.0	328	363.6	397
Red Amorphous Selenium #11, Group 7, Average temp.	-----	323.2	361.2	-----
Red Amorphous Selenium #9, Black Vitreous Amorphous Selenium, Figure E.8	315.3	325.6	364.3	392.1
Red Amorphous Selenium #9, Average temp.	-----	325.4	363.2	-----

* Peaks were numbered in the order of their appearance as a sample was heated.

Judging from the peak shapes and observed temperatures of the transitions in red amorphous selenium #9, the particular selenium sample used to obtain Figure E.8, it would appear that the endotherm and exotherm at 325.6°K and 364.3°K respectively, in Figure E.8, are undoubtedly due to the influence of red amorphous selenium in the sample mixture. Similarly, based on the temperature values observed for the transitions in black vitreous amorphous selenium in Figures E.5 and E.6, the endotherm and exotherm at 315.3°K and 392.1°K respectively, can with equal certainty be ascribed to the presence of black vitreous amorphous selenium.

A comparison of the temperatures in Figures E.7 and E.8 indicates comparative agreement, with the values in Figure E.8 mainly about three to four degrees higher than those of Figure E.7. However, since this amount of variation was previously observed in the transition temperature values of red amorphous selenium samples, it is probably not significant. The cursory nature of these investigations with black vitreous amorphous selenium prohibits a more definite comment on this temperature difference other than to say, that in the limited number of thermograms that were obtained, the endotherm in vitreous amorphous selenium occurred between 316-319°K, and the exotherm between 386-392°K (or slightly higher in some samples which were heated to the melting point, then quenched and rerun after various time intervals).

Gobrecht (36) reported the appearance of the endotherm in his samples as occurring within a ten-degree range, 308-318°K. That he was observing the growth of this endotherm in both vitreous amorphous selenium (quenched from the melt) and red amorphous selenium (quenched from the vapor phase) may explain why he observed such a wide variation in

temperature, although he did not mention that either of these samples was occurring consistently high or low in this ten-degree interval.

About all that can be indicated at this stage, from the brief investigation undertaken on vitreous amorphous selenium, is that it would appear that red amorphous selenium, initially prepared at 273°K, gradually transforms to vitreous amorphous selenium during storage at 297°K.

To explain the peaks observed in a sample of chemically-reduced red amorphous selenium stored at 297°K, the following tentative hypothesis is advanced. On the basis of their relative solubilities in carbon disulfide (cf. Briegleb--Introduction), it would seem logical to accept that the proportion of Se_8 rings in red amorphous selenium is considerably higher than the corresponding proportion in vitreous amorphous selenium. Indeed, Krebs (173) has suggested that red amorphous selenium is composed solely of small ring molecules, predominantly Se_8, although the conditions of the chemical reduction technique would seem to rule out this particular utopia.

A further consequence of Briegleb's work (46,47) is that it can be inferred, on an equal mass basis, that the average chain length in vitreous amorphous selenium is somewhat longer than the corresponding chain length in red amorphous selenium.

It has been suggested by Gattow and Heinrich (33) that the presence of Se_8 rings should tend to promote rigidity in the internal structure of amorphous selenium. Accepting this statement, it might then be inferred that the molecular motion in vitreous amorphous selenium is less constrained relative to that in red amorphous selenium, and hence the Se_8 rings present in the former structure are capable of vibrating

more freely at a given temperature. This greater ease of vibration might well result in cleavage of the Se_8 rings at about 316-319°K, rather than at 327°K, as in the more rigidly bound structure of red amorphous selenium. If some of the rings in red amorphous selenium were being cleaved, one by one in a somewhat random manner, a portion of the sample might eventually be transformed into the higher-chain-length, lower-Se_8-ring-content situation which is characteristic of vitreous amorphous selenium.

The endothermic peak at about 316-319°K would then represent the transition of vitreous amorphous selenium to black amorphous selenium, the mechanism being cleavage of the Se_8 rings, as was similarly suggested for the endotherm at 327°K in red amorphous selenium. It might also be expected that when the amount of red amorphous selenium which underwent ring cleavage was sufficient to ensure an overall decrease in the structural rigidity of the sample, the average length of the resultant selenium chains would be greater in black amorphous selenium formed from vitreous amorphous selenium, than in that formed from red amorphous selenium, because of the greater opportunity for extended polymerization in the less rigid vitreous amorphous selenium structure. This greater chain length in areas of the sample would explain the appearance of the second exothermic peak at roughly 390-400°K in aged red amorphous selenium, since those areas which had converted into the longer chains characteristic of black amorphous selenium formed from vitreous amorphous selenium probably require more energy to eventually settle into the lattice pattern representative of trigonal selenium.

In connection with this hypothesis, it is of interest to note that Dorabialska and Swiatlowski, using microcalorimetric methods (174),

have recently reported a hitherto unknown fact--that freshly-melted selenium pellets release heat spontaneously at room temperature, but that this effect is not due to crystallization. These authors suggest that a process may be occurring wherein a Se_6 ring (cf. Richter--Introduction) reacts with a chain-end free radical, resulting in fission of the ring and an increase in the chain length. The description of their sample implies that these observations were made on vitreous amorphous selenium, but it would be interesting to determine if an analogous process were occurring in red amorphous selenium.

It must be emphasized though, that the above hypothesis can only be regarded as tentative and premature, until further studies are made on vitreous amorphous selenium with an adequately known thermal history. It should also be noted that the hypothesis implies that the peaks observed at 316-319°K and 327°K simply represent the temperatures at which the rate of ring cleavage is a maximum, but not the only temperatures at which cleavage may occur, just as crystallization of an amorphous substance can be observed over a fairly broad temperature range, although there is usually a rather specific temperature region in which the rate of formation of crystal nuclei is a maximum (cf. Table III--Introduction).

In support of this hypothesis, it may be said that Debye-Schirrer X-ray films reveal that a sample of vitreous amorphous selenium is still in an amorphous state after the endothermic transition at 316-319°K. In addition, vitreous amorphous selenium has often been reported to crystallize to the trigonal form of selenium in the region of 397°K (cf. Table III--Introduction).

A series of time studies was made on red amorphous selenium samples stored at 273°K, but dried for different lengths of time, to deter-

mine what effects the presence of moisture would have on the thermal stability of such samples. It may be remembered that Kharlamov and Golubeva stated that amorphous selenium is stable only if kept cool and dry (38).

Figures D.15 to D.18, D.46 to D.49 and D.39 to D.42, corresponding to drying times of 43 hours, 24 hours and 3 hours respectively, indicate that the thermal stability of red amorphous selenium remains unaffected compared to the normal drying time of seven to eight days. Therefore, the effects observed in Figures D.10 to D.14, D.43 to D.45, and D.35 to D.38 on portions of the same samples stored at 297°K rather than 273°K, can be attributed solely to the difference in storage temperatures, as no other variables were changed. In each case a new endotherm developed in the region 316-319°K after about seven days storage at 297°K, and grew steadily at the expense of the endotherm at 327°K. Since this behavior was also observed if these samples were dried for seven to eight days, these results indicate that a reduction of the drying time to three hours seems to have no influence on the stability of red amorphous selenium.

The effect of not drying a sample of red amorphous selenium was also studied. The results are shown in Figures D.6 to D.9 for a storage temperature of 273°K. The presence of water in the sample obviously distorts the usual red amorphous selenium thermogram appearance. In Figures D.6 and D.7 the endotherm at 327°K is barely distinguishable. As the sample ages however, the distortion effects gradually diminish. Thus in Figure D.9, for a sample aged 102 days, the thermogram appears completely normal, while Figure D.8 represents an intermediate stage of 24 days aging. Similar behavior is noted in Figures D.1 to D.5, for a

storage temperature of 297°K, although the gradual reduction of the thermogram distortion was accelerated at this temperature, and appeared to be complete after 21 days. In these latter thermograms the slow evolution of the endotherm at 316–319°K is also visible.

A similar trend was observed in the thermograms of red amorphous selenium dried for one hour. Samples stored at 297°K appeared dry by 31 hours after preparation, as shown in Figure D.27, and judging from Figures D.28 to D.31, their thermal stability seemed unimpaired afterwards. In red amorphous selenium stored at 273°K, this loss of water again occurred, though much more slowly, taking about 23 days on the basis of Figures D.32 to D.34.

These results imply that while the temporary presence of water in red amorphous selenium may cause severe distortional effects in the sample thermograms, it does not seem to destroy the thermal stability of the sample. One may perhaps conclude that the water is merely physically adsorbed at the surface of the sample, and that it is slowly drawn off and absorbed by the dessicant.

The thermal behavior of freshly-prepared vitreous amorphous selenium. Another interesting point which should be mentioned is the difference in behavior between the chemically-reduced red amorphous selenium described in this thesis, and Gobrecht's sample of red amorphous selenium which was quenched from the vapor. Although both varieties exhibit an endotherm in the region of 316–319°K (actually 308–318°K for Gobrecht's samples) when stored at 297°K for a period of at least seven days, the freshly-prepared chemically-reduced form also undergoes an endothermic transition at 327.2°K, while no such endothermic transition is evident in the vapor-quenched form.

Therefore it might be suggested that one is dealing here with two different allotropes. If this is the case, the name red amorphous selenium should be reserved for the chemically-reduced variety of amorphous selenium which is prepared at 273°K, while the term red vitreous amorphous selenium should be used to designate that form of amorphous selenium which is prepared by quenching from the vapor. This latter designation is arrived at by virtue of the similarity in behavior exhibited by the vapor-quenched and melt-quenched forms of amorphous selenium.

The general trend in selenium literature has not been to give a specific name to each form of amorphous selenium which exists under certain definite conditions, but rather to use simply the terms "red amorphous", "vitreous" or "amorphous" selenium. This practice however, tends to fill the literature with apparently conflicting reports; witness the difference in thermal behavior just described between Gobrecht's sample of selenium which is red and amorphous, and the red amorphous sample prepared in this project by chemical reduction.

The author of this thesis feels that it would simplify the interpretation of the literature on selenium if each amorphous form of selenium that exhibits distinct physical properties, for which reproducible values can be obtained, were to be given a specific designation.

In accordance with this suggestion, it is felt that both freshly-prepared black vitreous amorphous selenium, and freshly-prepared red vitreous amorphous selenium, should have specific and distinct names assigned to them, because each of these substances undergoes a transition when stored at 297°K, as evidenced by the appearance of the endotherm in the 308-318°K temperature region. Since most of the previous

results in the literature on vitreous amorphous selenium were probably obtained from samples which had been quenched from the melt and subsequently stored at room temperature, the logical procedure would be to rename the freshly-prepared form of quenched vitreous amorphous selenium, rather than the aged form. It is suggested that the former be called either red or black, as the case may warrant, nova (L. fresh, recent) vitreous amorphous selenium.

Allotropy in amorphous substances. The question of nomenclature brings to mind another somewhat related point. In view of the fact that allotropy is defined (175) as "the existence of an element in two or more different crystalline forms", it seems rather a misnomer to refer to an amorphous substance as an allotrope; but the usage of this term is now so firmly entrenched in the literature, especially in relation to the numerous amorphous forms of the chalcogen group elements, that it must now be accepted.

This is an unfortunate practice in a sense, because referring to an amorphous substance as an allotrope is misleading when this practice tends to make one expect some properties in an amorphous substance which are really characteristic only of a crystalline substance, as for example, the existence of a definite equilibrium transition temperature. Thus it would perhaps be wise to devote a few words to an attempt to describe just what does constitute an allotrope when one is dealing with a substance which lacks a long-range ordered internal structure, and how the amorphousness of this sample will affect its thermal transitions.

Therefore, to be considered as an allotrope, it is suggested that an amorphous modification of a substance should exhibit reproducible physico-chemical properties within a certain temperature region. Since

these properties are dependent on the internal structure of a substance, which is a function of temperature, this amounts to saying that the internal configuration of the amorphous substance should be sufficiently stable as to be capable of existing over a definite temperature range, and sufficiently distinct as to exhibit characteristic physico-chemical properties relative to the other amorphous forms of the same substance.

As long-range order is absent in amorphous substances, their lattice structure (short-range order (176) is thought to exist) is non-homogeneous, and it would be expected that some regions in the sample are more susceptible to undergoing molecular transformations than others. Therefore it is considered that a transition process will occur gradually in these substances over a given temperature range, rather than at a specific temperature. When the sample is held at a constant temperature within this given transition region, the transformation process will proceed at a set rate; if the temperature is held constant at a higher temperature in this region, not only will a greater proportion of the sample be predisposed to transform, but more energy will also be absorbed, and consequently the transition will proceed at a faster rate. However, if the substance is heated at a constant rate, and the sample temperature monitored by a dynamic detection method, such as DSC, then a peak will be obtained which is representative of the maximum rate of transition of the sample, and of course, a definite transition temperature will be observed.

Another quality of an amorphous allotrope should be that the method by which it is prepared gives rise to an equivalent internal structural pattern in each batch of the sample produced. Since the sample is amorphous, small variations in the proportions of the component molecules

can be expected, but these variations should be minor, and limited to a degree such that they do not destroy the reproducibility of the physicochemical properties representative of the allotrope.

If this definition is applied to red amorphous selenium for the purpose of illustration, perhaps a clearer understanding of the whole matter may be gained. Thus, it has been observed that this form of selenium can be readily obtained by the chemical reduction of an aqueous selenious acid solution at 273°K. When a sample so prepared is stored at 273°K, it has been shown to have a stable existence, insofar as the endotherm at 327.2 ± 0.5°K remains unchanged with time, and exhibits a constant area/mg value, as observed by DTA and DSC methods. The small differences between the average area/mg values of the various red amorphous selenium samples probably reflect slight variations in the ratio of the ring to the chain components of this particular form of selenium.

Storage at 297°K for a period of weeks results in a continual slow conversion of the red amorphous form into black vitreous amorphous selenium; obviously then, 297°K belongs to the temperature region wherein the internal structure of red amorphous selenium gradually transforms to that of black vitreous amorphous selenium, which is characterized by a lower proportion of ring molecules. Dynamically the peak is at 316-319°K.

Storage at 313°K for a period of hours results in the conversion of red amorphous selenium into black amorphous selenium, as evidenced by the disappearance altogether of the endotherm at 327.2°K. This transition also occurs gradually, as shown in Figure E.1. From these results it may be gathered that vitreous amorphous selenium is not a necessary intermediate stage in the transition from red amorphous selenium to black amorphous selenium. A dynamic method, such as DSC, shows that the

maximum rate of this transition occurs at 327.2°K.

In addition, the fact that two crystallization exotherms are observed in red amorphous selenium samples,which have aged at 297°K, implies that one portion of the sample may undergo a thermal transition without affecting the rest of the sample, which may be deduced from the fact that this behavioral pattern of the sample is reproducible.

With respect to black amorphous selenium, which has been said to consist entirely of chain molecules, it is felt that this structure differs sufficiently from that of the ring-chain mixture in red amorphous selenium or vitreous amorphous selenium, to merit being called a distinct allotropic form. Gattow and Heinrich (37) have preferred to call black amorphous selenium a "transition type" rather than an allotropic form of selenium, but the author of this thesis feels that this objection is logically invalid, in view of the fact that all the amorphous modifications of selenium can be regarded in this light, since they all convert monotropically to the trigonal allotrope; and whether one refers to several "transition types" or to several amorphous "allotropes" seems to be simply a question of semantics.

Enthalpy values of the transitions in red amorphous selenium stored at 273°K. To obtain the enthalpy values of the heat of transition and the heat of crystallization, the procedure followed was identical to that for determining the heats of fusion of the TherMetric standards.

The data in Tables B.I to B.VIII was first analyzed to reject any area/mg values or peak temperature values lying outside the 95% confidence level, and then inspected to determine if any correlation existed between higher transition area/mg values of a red amorphous selenium sample with either higher or lower crystallization area/mg values, and

vice versa. As no correlations were observed, the average area/mg values for each peak were then calculated and listed in Tables XVIII and XIX, for the endothermic and exothermic transition respectively. These average area/mg values show approximately the same degree of precision as was seen in Table IX for the TherMetric standards; some of the average crystallization area/mg values even exhibited a degree of precision equivalent to that of the primary enthalpy standards. Therefore, in view of the fact that fairly large sample weights were used, and that the sizes of the peaks were large enough to reduce to a minimum the errors inherent in the determination of their areas by the use of a planimeter, this would seem to be the highest precision that one may hope for, while still performing a reasonably small (about 10) number of experiments.

The results in Tables XVIII and XIX were then carefully checked to determine if there existed any trends within the results, particularly with respect to the age of the samples, and again no such relationships were apparent. Thus, these average area/mg values in Tables XVIII and XIX of the individual selenium samples were used to calculate a final cumulative area/mg value for the transition of red amorphous selenium to black amorphous selenium, and the latter's subsequent crystallization to grey trigonal selenium, respectively. These values are recorded in Table XX, together with the cumulative average temperatures of these two peaks.

It may be noted in passing that the system of grouping the individual peak temperatures in accordance with the dates on which they were obtained was carried over as well from the treatment of the TherMetric standards. The individual group averages are given in Tables XV and XVI together with their corrected values, the latter of which formed the

basis of the average peak temperatures for each individual selenium sample, as listed in Table XVII. The cumulative average temperatures in Table XX were calculated from the values in Table XVII.

The enthalpy values in Table XX were determined by means of equation (7), using the appropriate cumulative area/mg value from the same table, with both indium and potassium nitrate serving as primary enthalpy standards. The average of the three enthalpy values thus obtained for each peak observed in red amorphous selenium stored at 273°K is shown in Table XX as the enthalpy of transition. By this means, the heat absorbed during the endothermic transition of red amorphous selenium to black amorphous selenium at 327.2 ± 0.5°K, and the heat evolved during the subsequent exothermic crystallization of the sample at 361.3 ± 0.7°K to form trigonal selenium, have been determined to be -0.107 ± 0.009 kcal/g-atom and +0.88 ± 0.06 kcal/g-atom respectively.

There is no previously-determined experimental value in the literature with which the enthalpy value reported in this thesis for the transition from red amorphous selenium to black amorphous selenium may be compared. Gattow and Draeger (115) have published a value of -0.09 kcal/g-atom, based on thermodynamical calculations--they determined the relative contributions of various selenium allotropes to the heat of formation of selenium dioxide--which certainly agrees well with the value obtained in this thesis. However, a few of their values do not seem to be in very good agreement with others reported in the literature; especially the value for the transition of black amorphous selenium to trigonal selenium. Therefore it is not felt that their value of -0.09 kcal/g-atom can be looked upon as confirming the value in this thesis, and future experimental results are awaited for this purpose.

In view of the enthalpies of crystallization which are shown in Table VI, an enthalpy value of +0.88 ± 0.06 kcal/g-atom appears quite reasonable for the transition whereby the proposed black amorphous selenium transforms to trigonal selenium. Moreover, it is thought that the value determined in this thesis may represent a more positive contribution to the literature, since both the thermal history and purity of the sample are known.

Investigation of red amorphous selenium at low (77-323°K) temperatures. It will be recalled that Gattow and Heinrich (33) had reported the existence of two low-temperature transitions in red amorphous selenium. These transitions were said to be reversible, and to occur at 139±2°K and at 283±1°K. The initial purpose of this research project had been to verify the existence of these two transitions using the low-temperature cell of the DTA apparatus, and then if possible, to determine the enthalpies of transition.

However, the experimental evidence proved to be negative in quality--neither transition could be detected by DTA. Thus it was concluded that Gattow and Heinrich's original observations might have been due to the presence of impurities in their sample.

As mentioned in the introduction, in the same reference Gattow and Heinrich also reported similar transitions in vitreous amorphous selenium, at 128±2°K and 284±1°K. But when Gattow and Buss (99) attempted to reproduce these results with carefully purified vitreous amorphous selenium, they were unable to do so. However, no retraction was made of the work done on red amorphous selenium; in fact it was implied that the results obtained by Gattow and Heinrich were probably caused by the presence of red amorphous selenium as an impurity in the vitreous

amorphous selenium. But perhaps the most enlightening statement on the question of these transitions in red amorphous selenium, in view of the negative results obtained in this thesis and by Mamedov et al. (98), was made by Gattow and Buss themselves (99), when they admitted that the original experimental technique appeared to have been somewhat unreliable.

Therefore the figures in Appendix C have been included in this thesis with a triple purpose: i) to substantiate the non-existence of transitions at 139°K and 283°K in red amorphous selenium, ii) to show what is believed to be the glass transition point in the region of 303°K, and iii) to pass on some useful observations to future users of the low-temperature DTA cell, since information on low-temperature operational techniques is rather scant, and the literature is concerned predominantly with the design of low-temperature calorimeters, as for example (177).

Figure C.1A represents a typical low-temperature thermogram of red amorphous selenium. Although the initial portion of the trace is sharply curved due to the rapid change of the sample heat capacity, there is clearly no evidence of any transition at 139°K, which from Table C.II would be expected to appear at 162°K on a thermogram. The break in the DTA curve at 273°K resulted from some necessary adjustments to the instrument recorder controls as the experiment proceeded into the higher temperature range. The small endothermic effect in the baseline at about 303°K is believed to be due to the glass transition in red amorphous selenium. Wendlandt (125) has published traces of the glass transition points in polymers which appear very similar, and the temperature agrees well with reported values of the glass transition

point listed in Table V for vitreous amorphous selenium. It would seem likely that the glass transition point should not differ significantly in these two allotropes of selenium. The transition observed at 331°K represents the endothermic transformation of red amorphous selenium to black amorphous selenium.

The sample was then cooled down and rerun twice, the resulting traces being shown in Figure C.1B. It can be seen that the endothermic effect at 331°K has vanished, and a new and as yet unexplained endothermic peak is noted at about 310°K. In addition, trace III of this figure exhibited a small endothermic-type effect at approximately 286°K, which was somewhat reminiscent of a glass transition point in its appearance. At present there is no information in the literature which may be said to refer with certainty to the thermal behavior of black amorphous selenium formed by a transition from the red amorphous form at 327.2°K; and it was decided that an investigation of said black amorphous selenium would have to be left to the future.

Figure C.2A contains the low-temperature portion of another thermogram on red amorphous selenium. In contrast to Figure C.1A, a baseline shift occurs between 155-163°K, and a small endothermic irregularity is seen at 269°K. Had not the higher temperature portion of this thermogram also exhibited anomalous regions at 314°K and 340-350°K, as shown in Figure C.2B, relative to those DTA or DSC thermograms contained in Appendix B, it might have been assumed that Gattow and Heinrich's transition at 139°K was being observed. However, the endothermic effect at 269°K also led one to consider the possibility that some water might have condensed onto the sample, even in spite of the fact that nitrogen gas was being passed through the bell jar.

Figures C.3A and C.4A lend credence to this idea. Trace I of Figure C.3A is a normal low-temperature thermogram of red amorphous selenium, which was obtained in an air atmosphere. When the temperature reached 273°K, the sample was quickly cooled to 77°K with liquid nitrogen, virtually ensuring the condensation of some water vapor on the sample. Trace II is the thermogram which was obtained when the sample was rerun. Anomalous regions were found at 98-123°K, at 140-164°K and at 247-260°K . In Figure C.4A a second sample of red amorphous selenium was investigated under the same experimental conditions, except that this time dry nitrogen gas was passed over the sample. After completion of the experiment represented by trace I, the dry nitrogen gas was allowed to flow through the bell jar for roughly twenty-five minutes, and then the sample was recooled to 77°K and the experiment repeated. This time no anomalous regions were observed, as shown in trace II of Figure C.4A, and thus it would seem that this treatment was sufficient to eliminate the possibility of water vapor being condensed on the sample.

Again, the thermograms in Figure C.5A and C.5B, obtained under flowing nitrogen, appear normal while those in Figures C.6A and C.6B, obtained in air, showed a baseline shift at about 152-161°K and a small endotherm at 276°K.

It should be emphasized however, that the baseline shift observed in Figures C.2A and C.6A was only seen very infrequently, and has been mentioned mainly to show the need to have a dry sample atmosphere during low-temperature investigations. Figures C.10A to C.10E illustrate the absence of any spurious effects in a sample recycled four times, when the system underwent intermittent purging with dry nitrogen gas.

That the various red amorphous selenium samples exhibited the

same type of sub-ambient thermograms is shown by Figures C.1A, C.5A, C.5B, C.7A, C.7B, C.9A, C.9B and C.11A, as was expected. It was also assumed that some sort of thermal effect would be noted in the region of 303°K, due to the glass transition, if such a phenomenon existed in red amorphous selenium prepared by chemical reduction. As mentioned previously, Figure C.1A contains what appears to be a very small endotherm at 303°K. Figure C.10E also shows a similar endothermic effect at 303°K. Although there do appear to be baseline shifts in Figures C.5B and C.7B, they occur at about 290°K and 293°K respectively. Also, in Figure C.12A there is a gradual step upwards in the baseline at 295°K. In Figures C.8B and C.9B extremely shallow dips in the baseline are shown at 300°K and 303°K respectively, rather than an actual baseline shift. In Figure C.6B a change occurs in the slope of the baseline at approximately 303°K, although this trace should perhaps be ignored, because of the suspected presence of water vapor in the red amorphous selenium. Therefore, while the reproducibility of these thermal effects is rather poor, both with respect to their temperatures and to their shapes, it does at least seem certain that some type of thermal transition is occurring in roughly the temperature region reported for the glass transition point in vitreous amorphous selenium. In addition, the general shapes of the observed effects are not inconsistent with the expected appearance of a glass transformation point as detected by differential thermal analysis.

SUMMARY AND CONTRIBUTIONS TO KNOWLEDGE

1. Red amorphous selenium, prepared by the chemical reduction of a selenious acid solution at 273°K, and then dried at 273°K for 7 to 8 days, and stored at this temperature in a dessicator, in the dark, exhibits thermal stability for a period of at least two years. The length of drying time of the sample can be reduced to as little as three hours, without affecting the stability of the material.

2. When heated from room temperature at a constant rate of 5°K/min, in a differential scanning calorimeter (DSC) apparatus, red amorphous selenium, prepared and stored as above, undergoes an irreversible endothermic transition at 327.2 ± 0.5°K, with an enthalpy of transition of -0.107 ± 0.009 kcal/g-atom. Continued heating of the sample produces an irreversible exothermic transition at 361.3 ± 0.7°K, with an enthalpy of transition of +0.88 ± 0.06 kcal/g-atom. Further heating results in the fusion of the selenium at about 493°K.

3. The endothermic transition at 327.2°K in red amorphous selenium stored at 273°K is thought to represent the transition from red amorphous selenium to black amorphous selenium. This transition is suggested to occur via the cleavage of Se_8 rings into short chain segments, which subsequently polymerize into the longer chain molecules representative of black amorphous selenium. At 361.3°K, these chain molecules orient themselves into the trigonal selenium lattice pattern. These two temperatures represent the maximum rates of ring cleavage and crystallization respectively.

4. If drying and storage of the red amorphous selenium were carried out at 297°K, rather than at 273°K, a gradual change in the thermal behavior of the material was observed. The endotherm at 327.2°K is slowly replaced (over a period of weeks) by an irreversible endothermic peak in the 316–319°K temperature region. Tentatively this transition is attributed to the process whereby black vitreous amorphous selenium, formed as the result of gradual structural rearrangements in red amorphous selenium stored at 297°K, is transformed to black amorphous selenium.

5. Until such time as the endotherm at 327.2°K has almost completely disappeared, crystallization to the trigonal form of selenium occurs only at 361.3°K, in red amorphous selenium stored at 297°K. Samples aged at this temperature eventually developed a second exotherm, in the 386–400°K temperature region. This latter exotherm is also attributed to crystallization into the trigonal allotrope of selenium.

6. No thermal transitions were observed in red amorphous selenium (prepared and stored at 273°K) in the temperature range 77–273°K, contrary to a previous report in the literature.

7. A glass transition point for red amorphous selenium is believed to have been observed at 295–305°K, by differential thermal analysis (DTA).

8. Cursory studies on black vitreous amorphous selenium revealed the presence of an endothermic transition in the 316–319°K temperature region, and an exothermic transition at 390–400°K. The latter transition is attributed to crystallization to trigonal selenium.

9. A hypothesis has been advanced to explain the various observations which are apparently dependent upon the storage temperature. The hypothesis suggests that the original internal structural rigidity of the red amorphous selenium gradually relaxes at 297°K; and this relaxation permits several processes to occur at temperatures lower than would normally be expected.

10. By consideration of the relevant literature, the author has been led to suggest that freshly-prepared vitreous amorphous selenium, whether black (as when quenched from the melt) or red (as when quenched from the vapor), constitutes a separate amorphous selenium modification and as such, should be renamed. The name nova black, or red, vitreous amorphous selenium is suggested as a possible future designation.

11. It has been pointed out that red amorphous selenium (prepared by the chemical reduction of an aqueous selenious acid solution) and red amorphous selenium (prepared by quenching from the vapor) do not exhibit the same thermal behavior in their DSC thermograms. It is suggested that the latter form be called red vitreous amorphous selenium.

12. The nature of "amorphous allotropes" is discussed, in the light of some of the amorphous selenium forms mentioned in this thesis together with their thermal behavior.

13. A set of internally-consistent heat of fusion values has been obtained for four Fisher TherMetric standards suitable for instrument temperature calibration purposes in the temperature region 323-423°K. The heat of fusion of adipic acid, previously unknown, has been determined to be 9.0 ± 0.5 kcal/mole .

SUGGESTIONS FOR FUTURE WORK

It is obvious that a good deal of future work could evolve from this thesis, and in more than one direction. Some of the more obvious paths that such work might take are as follows:

1. Prepare red amorphous selenium at 297°K by the method described in this thesis, to determine whether red amorphous selenium or vitreous amorphous selenium will be obtained. Similarly, prepare red amorphous selenium at some temperature in the range 273-297°K, to learn if red amorphous selenium transforms to vitreous amorphous selenium below 297°K.

2. Determine if black amorphous selenium can be directly prepared by the chemical reduction of selenious acid at some temperature in the range 327-361°K.

3. Prepare vitreous amorphous selenium with a known thermal history, and study this allotrope by DTA and DSC methods in the temperature region 77-493°K.

4. If possible, repeat Gobrecht's work (36) on vitreous amorphous selenium forms.

5. Determine if the temperature at which black vitreous amorphous selenium crystallizes is proportional to the temperature from which the selenium is quenched.

6. Investigate the appearance of a glass transition point, as seen by DTA and DSC methods, and check Lambert's data (127) for interpolating the value of a glass transition point at various scanning speeds.

7. Obtain DSC and DTA thermograms of the glass transition

point in the various amorphous forms of selenium.

8. Obtain IR spectra of the various forms of selenium.

9. Determine the relative solubilities of the various forms of selenium in carbon disulfide, using the purest materials obtainable.

10. Obtain internally-consistent enthalpy values for the primary enthalpy standard transitions used in this project, by a direct calorimetric method.

APPENDIX A

Instrument Calibration Data

Table A.I

Peak Area/mg and Observed Fusion Temperature of p-Nitrotoluene

	Run No.	Sample Wt. (mg)	Area/mg	Peak Temp. (°K)
I	220	2.832	106	325.0
	221	3.193	107	325.0
	224	2.790	104	324.8
	225	3.601	110	324.9
	230	1.810	106	324.7
	231	2.882	107	324.8
	232	1.021	104	324.6
	233	1.605	103	324.7
	236	1.086	102	324.7
	237	1.108	102	324.7
II	238*	0.945	97	322.2
	239	1.155	104	322.4
	240	1.097	100	324.3
	241	0.650	101	324.8
	242	0.635	106	324.7
III	243	0.765	110	320.8
	244	0.705	105	322.1
	245	1.043	110	323.9

* Rejected at the 95% confidence level

Table A.I (con't)

	Run No.	Sample Wt. (mg)	Area/mg	Peak Temp. (°K)
IV	246	1.043	107	322.9
	247	0.541	110	323.0
V	248	0.710	106	321.4
	249	1.077	108	321.4

Table A.II

Peak Area/mg and Observed Fusion Temperature of Naphthalene

	Run No.	Sample Wt. (mg)	Area/mg	Peak Temp. (°K)
I	219	1.966	131	358.2
	226	2.280	126	358.3
	227	6.104	130	358.2
	228	1.836	118	358.2
	229	1.730	116	358.2
	234	1.122	124	357.8
	235	1.046	124	358.0
	238	1.438	122	358.1
	239	1.904	127	358.0
II	241	0.705	123	355.2
	242	0.714	120	358.4
	243	0.921	123	358.3
	244	0.820	126	357.9
III	245	0.867	126	356.6
	246*	0.564	114	356.7
	247	0.539	123	356.7

* Rejected at the 95% confidence level

Table A.II (con't)

	Run No.	Sample Wt. (mg)	Area/mg	Peak Temp. (°K)
IV	248	0.534	124	356.0
	249	0.530	116	355.9
	250	0.805	122	355.8
	252	1.037	132	356.0
V	253	0.608	126	354.8
	254	1.053	119	354.6
	255	1.122	122	354.5
	256	1.096	124	354.2
	257	1.285	128	355.0
	258	1.164	127	355.0
	259	1.035	120	355.2
	260	1.306	123	355.0

Table A.III

Peak Area/mg and Observed Fusion Temperature of Benzoic Acid

	Run No.	Sample Wt. (mg)	Area/mg	Peak Temp. (°K)
II	130	0.440	117	402.4
	131	0.569	116	405.9
	132	0.763	126	405.6
	133	0.562	121	405.4
III	134	0.465	118	404.3
	135	0.750	123	404.3
	136	0.381	116	404.2
	137	0.649	116	404.4
	138	0.924	125	404.3
	139	0.295	115	404.5
IV	140	0.958	125	405.1
	141	0.833	126	405.1
	142	0.617	125	406.0
	143*	0.592	105	404.7
	144	0.300	115	404.8
	145	0.456	119	405.2
	146	0.340	118	405.2
	147	0.841	126	405.0
	148	0.645	127	405.0
	149	0.628	115	405.1

* Rejected at the 95% confidence level

Table A.III (con't)

	Run No.	Sample Wt. (mg)	Area/mg	Peak Temp. (°K)
V	150	0.766	125	401.4
	151	0.997	124	401.5
	152	1.184	121	402.1
	153	0.821	121	402.7
	154	0.743	127	403.1
	155	1.117	123	403.2
	156	0.946	115	403.5
	157	0.875	123	402.7

Table A.IV

Peak Area/mg and Observed Fusion Temperature of Adipic Acid

	Run No.	Sample Wt. (mg)	Area/mg	Peak Temp. (°K)
II	148	0.298	225	438.0
	149	0.210	218	438.7
	150	0.486	228	438.0
	151	0.421	224	438.1
III	152	0.510	231	436.8
	153	0.362	218	437.0
	154	0.379	237	436.8
	155	0.297	226	436.8
	156	0.466	228	436.8
	157*	0.253	198	435.5
IV	158	0.134	241	436.8
	159	0.218	218	437.3
	160	0.238	213	437.1
	161	0.354	230	437.2
	162	0.151	232	437.0
	163	0.326	226	436.5
	164	0.371	228	436.9
	165	0.178	222	436.9
	166	0.169	223	437.0
	167	0.268	218	436.9

* Rejection at the 95% confidence level

Table A.IV (con't)

	Run No.	Sample Wt. (mg)	Area/mg	Peak Temp. (°K)
V	168	0.361	237	433.8
	169	0.536	230	433.5
	170	0.560	240	433.6
	171	0.362	236	433.5
	172	0.327	224	435.5

Table A.V

Peak Area/mg and Observed Fusion Temperature of Indium

	Run No.	Sample Wt. (mg)	Area/mg	Peak Temp. (°K)
II	1	6.427	25.2	443.6
	2	2.880	25.7	444.0
	3	3.435	25.9	443.8
	4	5.719	25.2	443.8
	5	3.600	25.3	443.6
	6	1.703	25.0	443.4
	7	2.356	26.2	442.9
III	8	2.623	25.5	441.2
	9	4.221	25.1	441.8
	10	4.195	26.0	441.0
	11	1.894	25.6	440.7
	12	1.414	25.5	442.3
IV	13	3.362	25.8	443.5
	14	3.183	25.8	442.8
	15	2.277	26.4	442.2
	16	3.440	26.2	442.1
	17	2.861	26.8	441.8
	18	3.480	25.7	442.2

Table A.V (con't)

	Run No.	Sample Wt. (mg)	Area/mg	Peak Temp. (°K)
V	19	2.957	24.8	441.3
	20	3.250	24.6	441.3
	21	2.991	25.6	440.8
	22	3.316	26.8	440.9
VI	23	5.039	26.7	439.3
	24*	7.413	27.5	439.4
	25*	4.329	27.7	438.6

* Rejected at the 95% confidence level

Table A.VI

Peak Area/mg and Observed Transition Temperature of Potassium Nitrate

	Run No.	Sample Wt. (mg)	Area/mg	Peak Temp. (°K)
II	2	19.472	45.3	410.8
	3	13.634	43.6	411.1
	4	5.298	42.5	412.8
	5	4.422	43.4	414.2
	6	3.275	43.0	413.7
	8	5.788	44.2	413.8
	9	4.921	43.8	413.8
	10	4.133	43.3	414.2
	11	4.190	43.8	413.6
	12	1.831	43.7	413.2
IV	13	3.123	44.8	412.4
	14*	0.818	41.2	413.2
	15	3.569	42.9	414.4
	16	4.875	43.0	411.0
	17*	2.147	45.5	411.0
	18	3.693	43.0	411.3
	19	5.449	45.1	410.6
	20	2.225	42.2	411.2
	21	2.799	42.2	411.3
	22	2.837	43.3	411.1

* Rejected at the 95% confidence level

Table A.VI (con't)

	Run No.	Sample Wt. (mg)	Area/mg	Peak Temp. (°K)
V	23	3.171	43.4	411.1
	24	4.185	42.9	412.5
	25	2.871	43.0	411.8
	26	4.013	43.5	411.1
	28	7.209	44.1	410.0
VI	29	1.751	44.5	409.8
	30	5.496	43.8	410.5
	31	4.526	42.8	410.6

Table A.VII

Peak Area/mg and Observed Fusion Temperature of Potassium Nitrate

	Run No.	Sample Wt. (mg)	Area/mg	Peak Temp. (°K)
II	2	19.472	42.9	622.8
	3	13.634	41.7	622.6
	5	4.422	42.1	626.0
	6	3.275	42.0	626.0
	7*	5.822	44.0	626.0
	8	5.778	42.2	626.1
	9	4.921	42.4	625.8
	10	4.133	41.9	625.7
	11	4.190	42.8	626.1
	12	1.831	40.8	625.8
IV	13*	3.123	39.4	622.4
	14	0.818	39.7	622.6
	15	3.569	41.4	622.0
	16	4.875	41.5	622.2
	17	2.147	41.0	620.7
	18	3.693	41.1	622.0
	19	5.449	40.0	621.9
	20	2.225	41.6	621.4
	21	2.799	42.8	622.3
	22	2.837	40.9	622.3

* Rejected at the 95% confidence level

Table A.VII (con't)

	Run No.	Sample Wt. (mg)	Area/mg	Peak Temp. (°K)
V	23	3.171	41.5	621.5
	24	4.185	40.5	622.7
	25	2.871	40.6	621.8
	26	4.013	41.9	622.8
	27	4.774	41.9	622.6
	28	7.209	43.0	621.0
VI	29	1.751	40.5	618.8
	30	5.496	41.2	620.7
	31	4.526	41.8	621.2

Table A.VIII

Criterion for Grouping Results Prior to Temperature Calibration of the Apparatus

Group No.	Data Collection Date
I	May 29 - July 4, 1968
II	Oct. 13 - Nov. 8, 1968
III	Dec. 19 - Dec. 24, 1968
IV	Mar. 17 - Mar. 23, 1969
V	Apr. 16 - May 4, 1969
VI	Aug. 5 - Aug. 6, 1969

Table A.IX

Average Observed Peak Temperatures of the Calibration Standards

Arranged by Groups

Calibration Standard	Temperature - °K					
	Group I	Group II	Group III	Group IV	Group V	Group VI
p-Nitrotoluene	324.8	323.7	323.0	323.0	321.4	------
Naphthalene	358.1	357.5	356.7	355.9	354.8	------
Benzoic Acid	------	405.6	404.3	405.0	402.5	------
Adipic Acid	------	438.2	436.8	437.0	434.0	------
Potassium Nitrate (Transition)	------	413.4	------	411.5	411.3	410.3
Potassium Nitrate (Fusion)	------	625.3	------	622.0	622.1	620.2
Indium	------	443.6	441.4	442.6	441.1	439.3

Table A.X

Some Experimental Data Accompanying Figures A.14 to A.18

Figure No.	Sample Wt. (mg)	Reference Wt. (mg)	ΔT (°K/in)	Temperature (°K)	Rate (°K/min)
A.14	-------	-------	1.0	327.6	10
A.15	-------	-------	1.0	355.9	10
A.16	-------	-------	1.0	402.0	10
A.17	-------	-------	2.0	433.0	20
A.18 Left	13.634	41.213	1.0	407.2	5
A.18 Right	13.634	41.213	2.0	611.6	10

FIGURE A.1

TEMPERATURE CALIBRATION GRAPH, GROUP I RESULTS

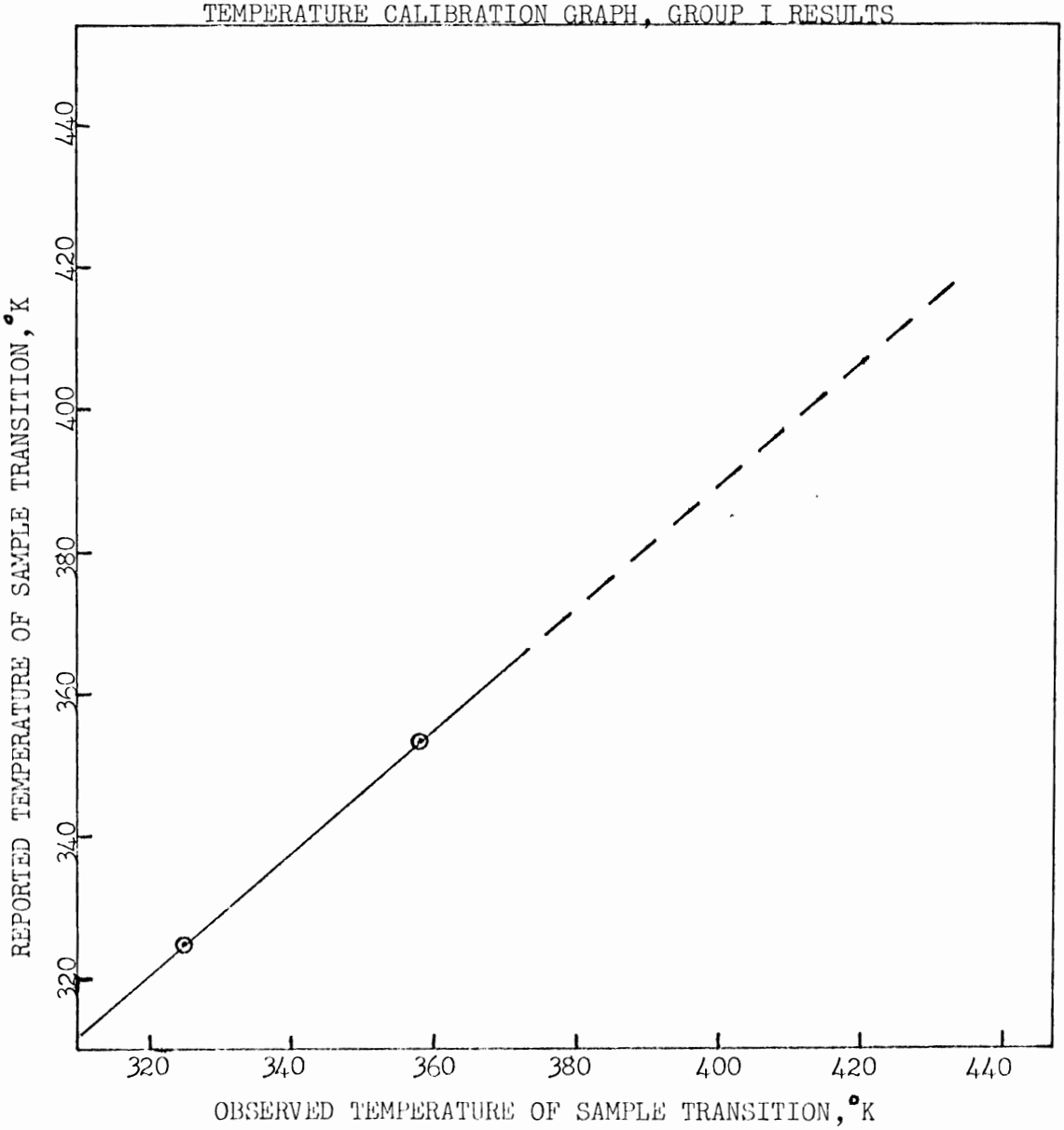

FIGURE A.2

TEMPERATURE CALIBRATION GRAPH, GROUP II RESULTS

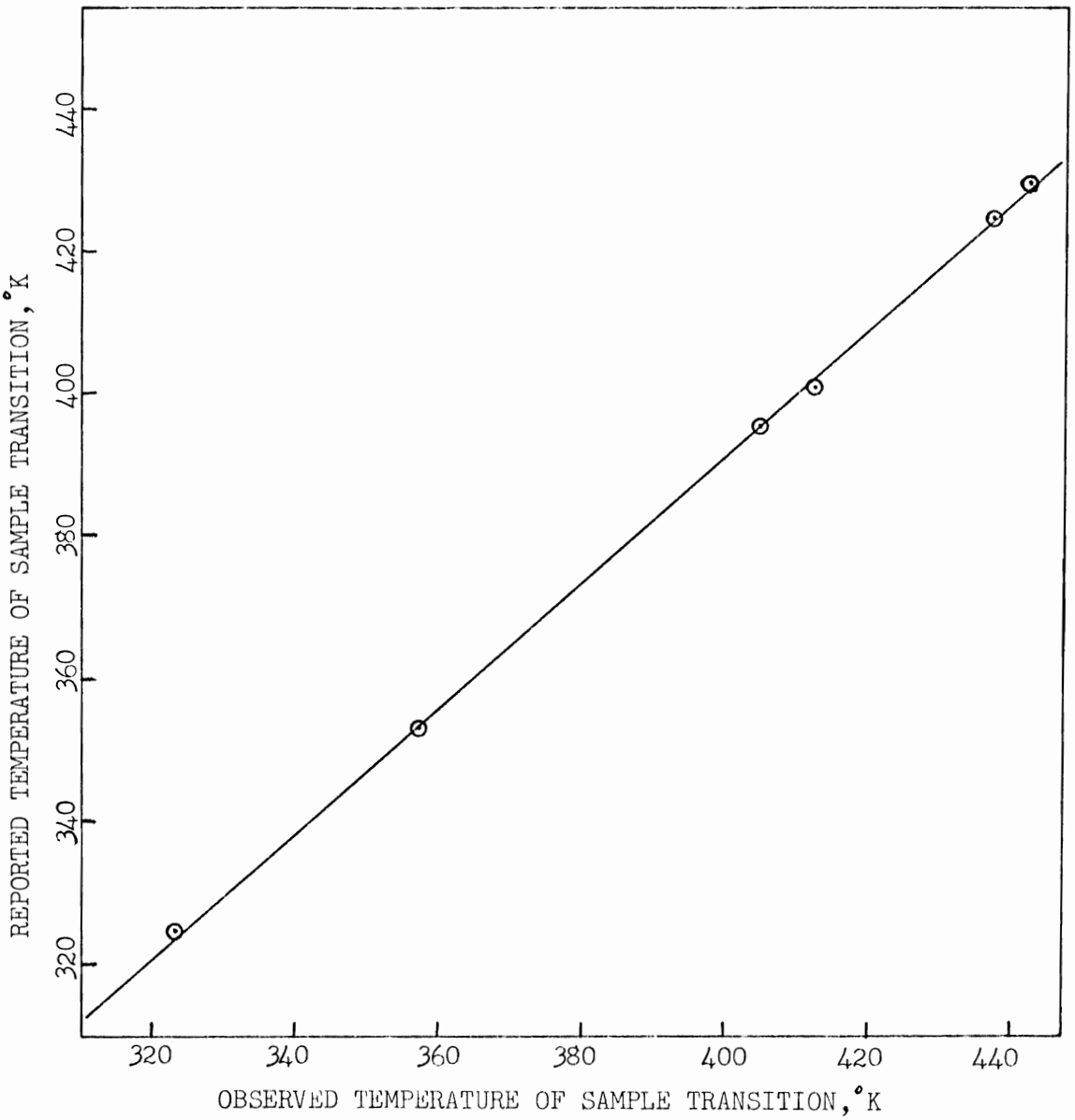

FIGURE A.3

TEMPERATURE CALIBRATION GRAPH, GROUP III RESULTS

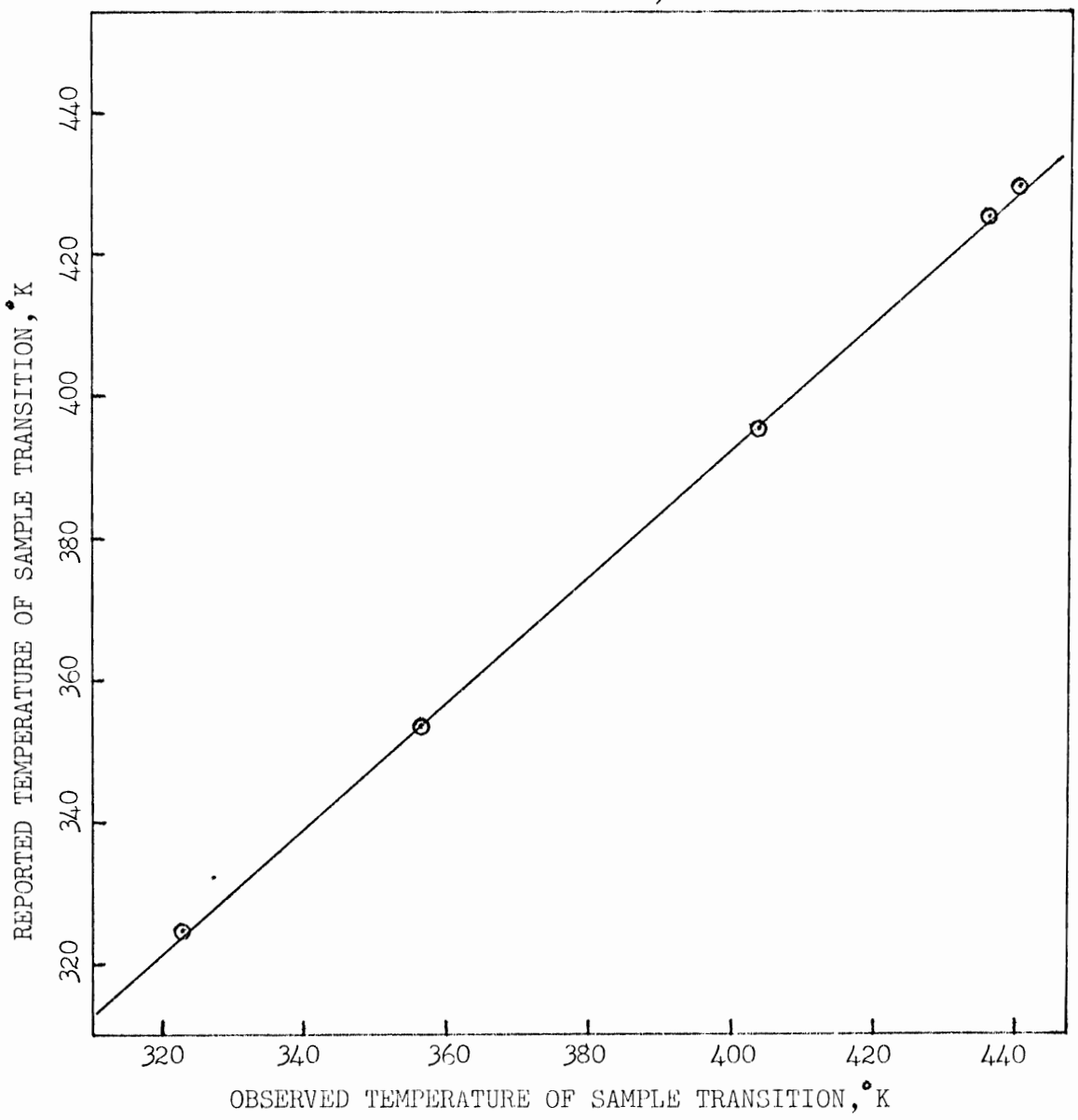

FIGURE A.4

TEMPERATURE CALIBRATION GRAPH, GROUP IV RESULTS

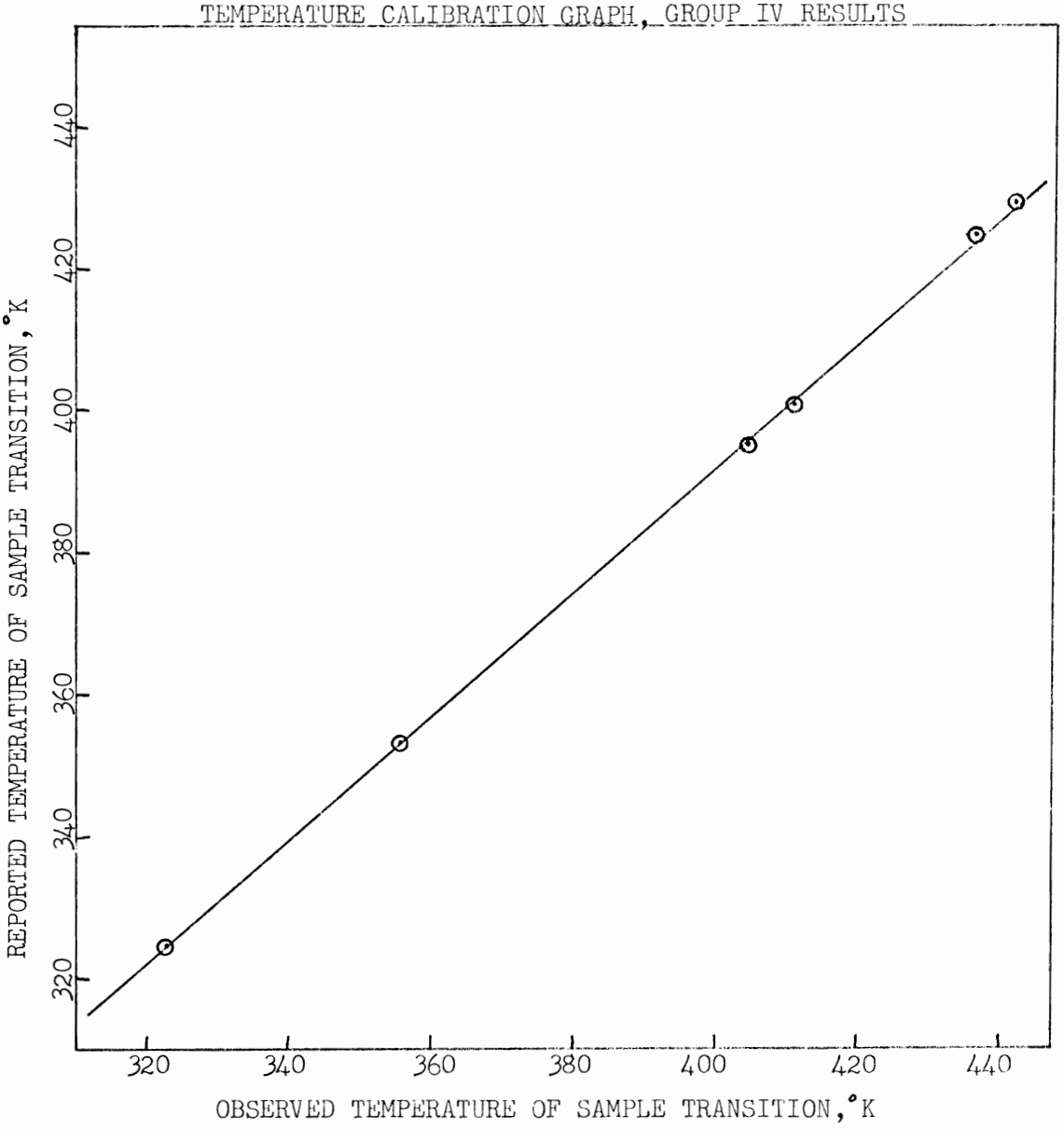

FIGURE A.5

TEMPERATURE CALIBRATION GRAPH, GROUP V RESULTS

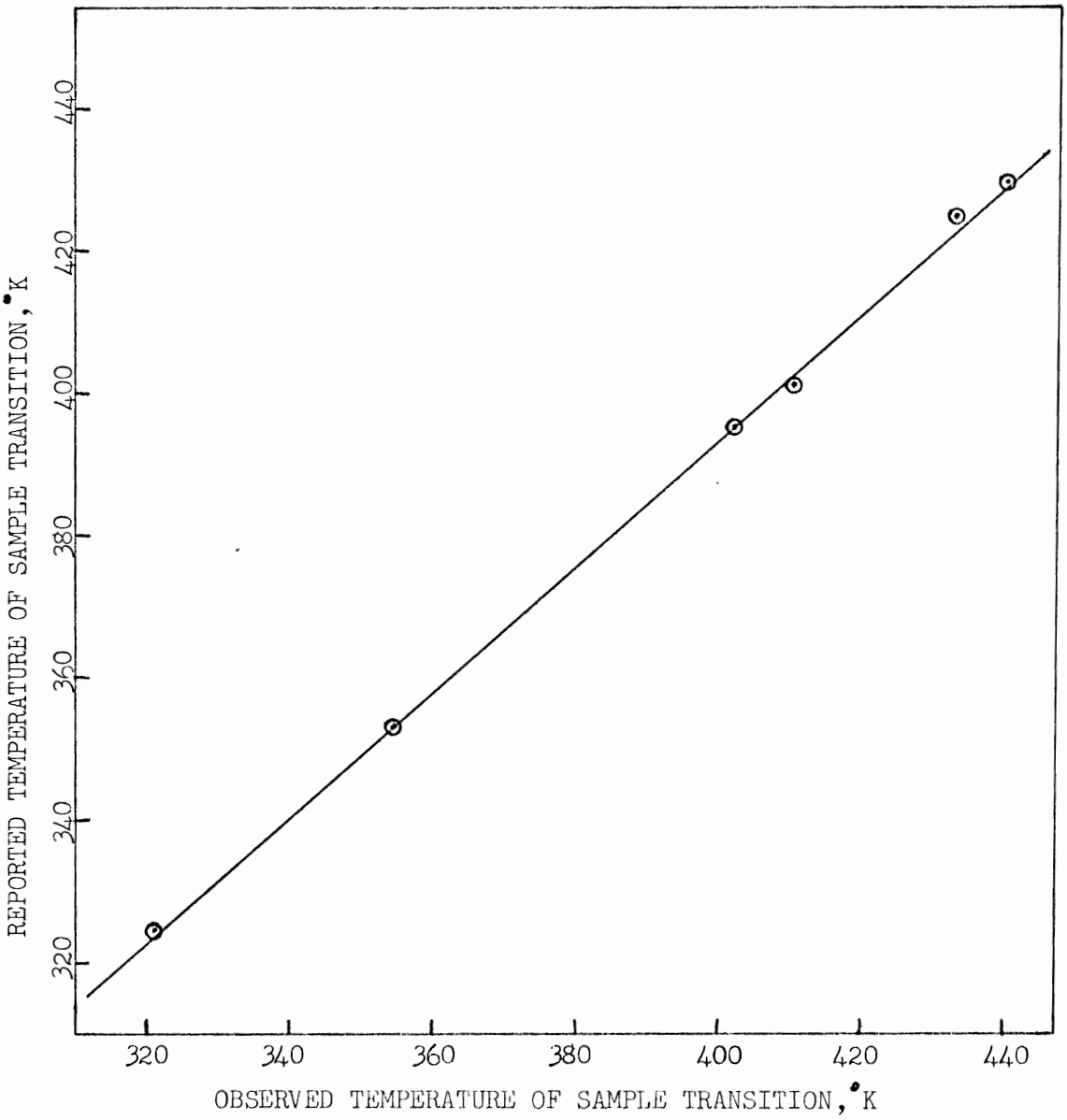

FIGURE A.6

TEMPERATURE CALIBRATION GRAPH, GROUP VI RESULTS

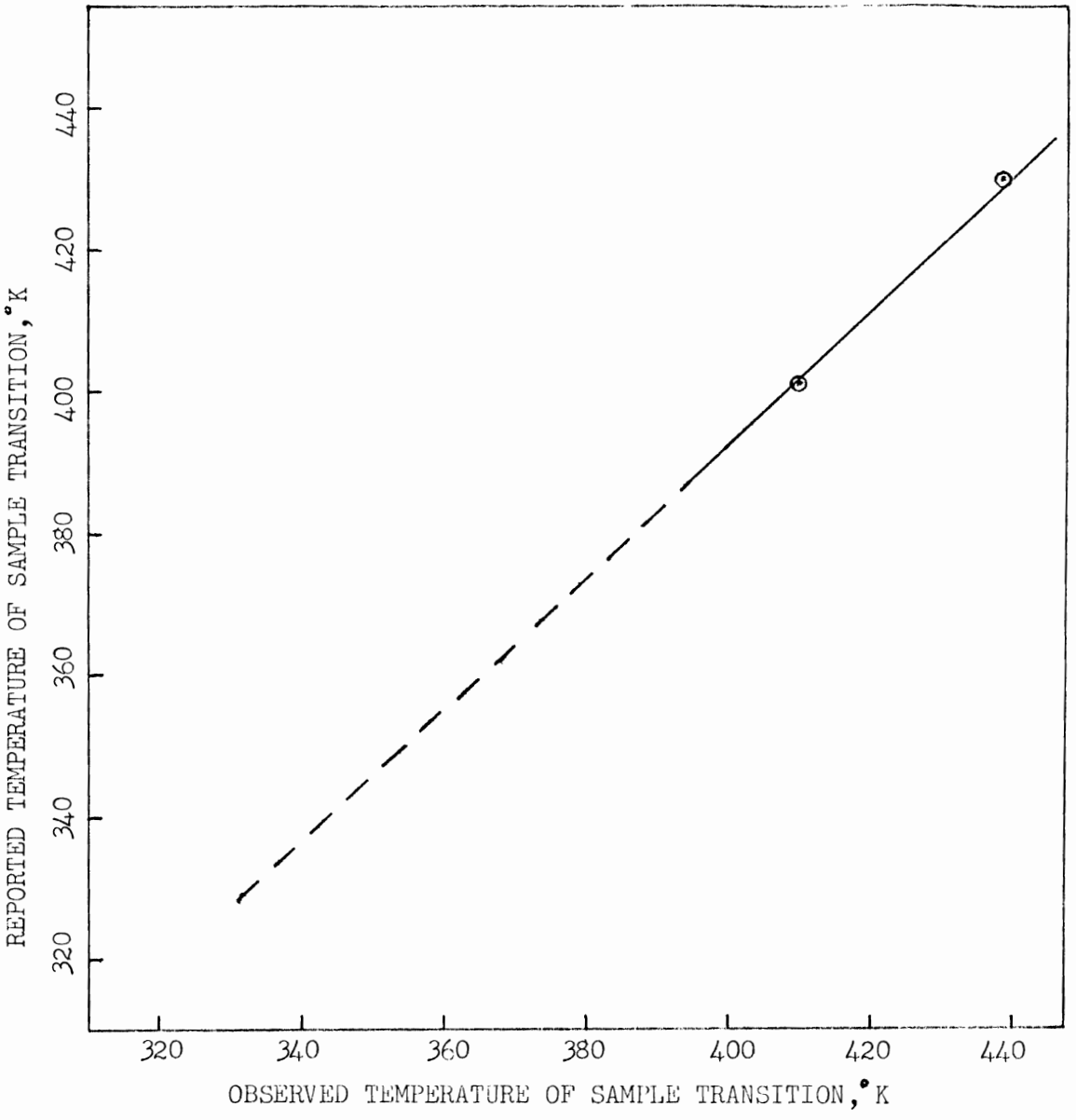

FIGURE A.7

DSC THERMOGRAM of p-NITROTOLUENE, RUN 247

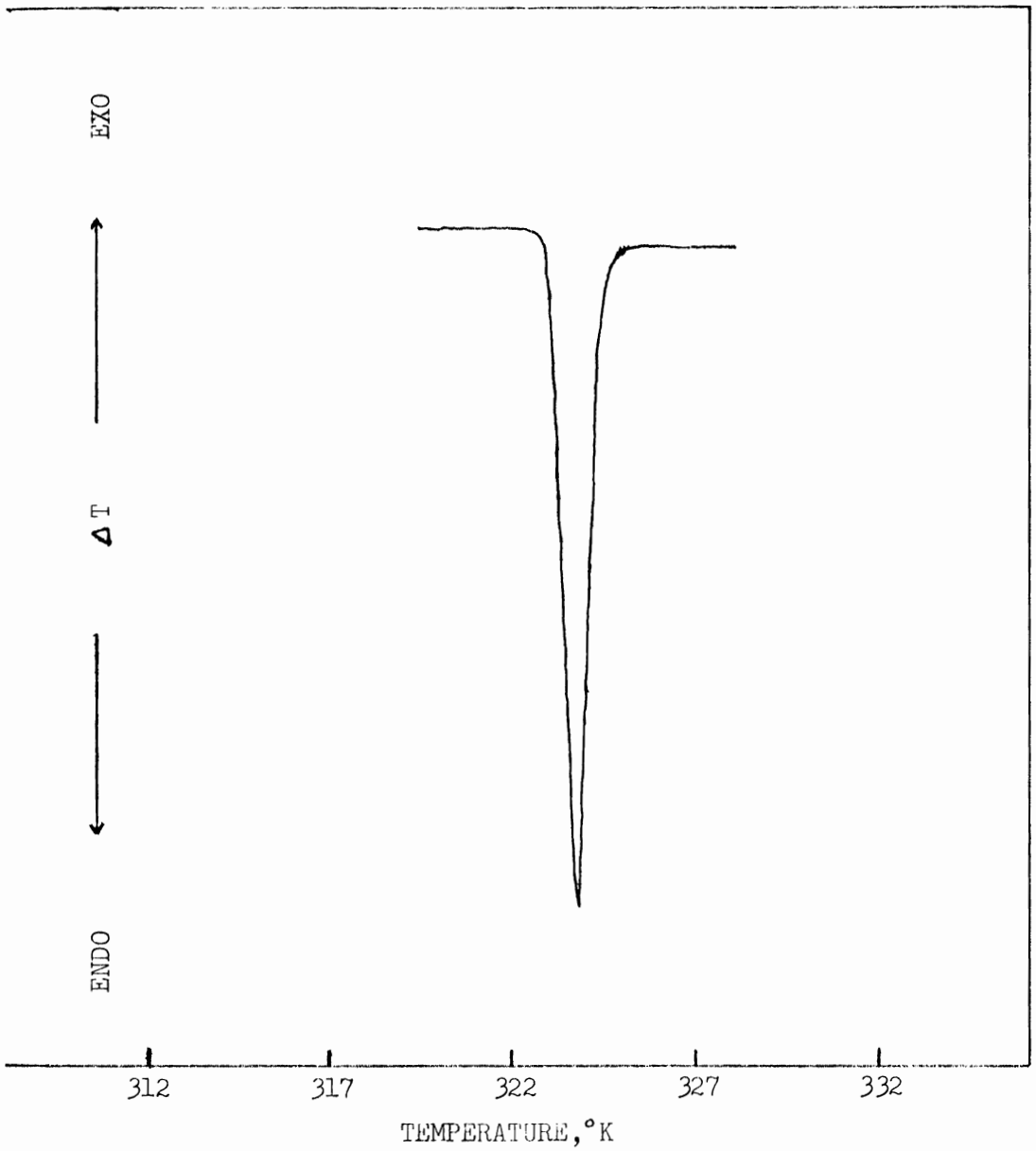

FIGURE A.8

DSC THERMOGRAM of NAPHTHALENE, RUN 248

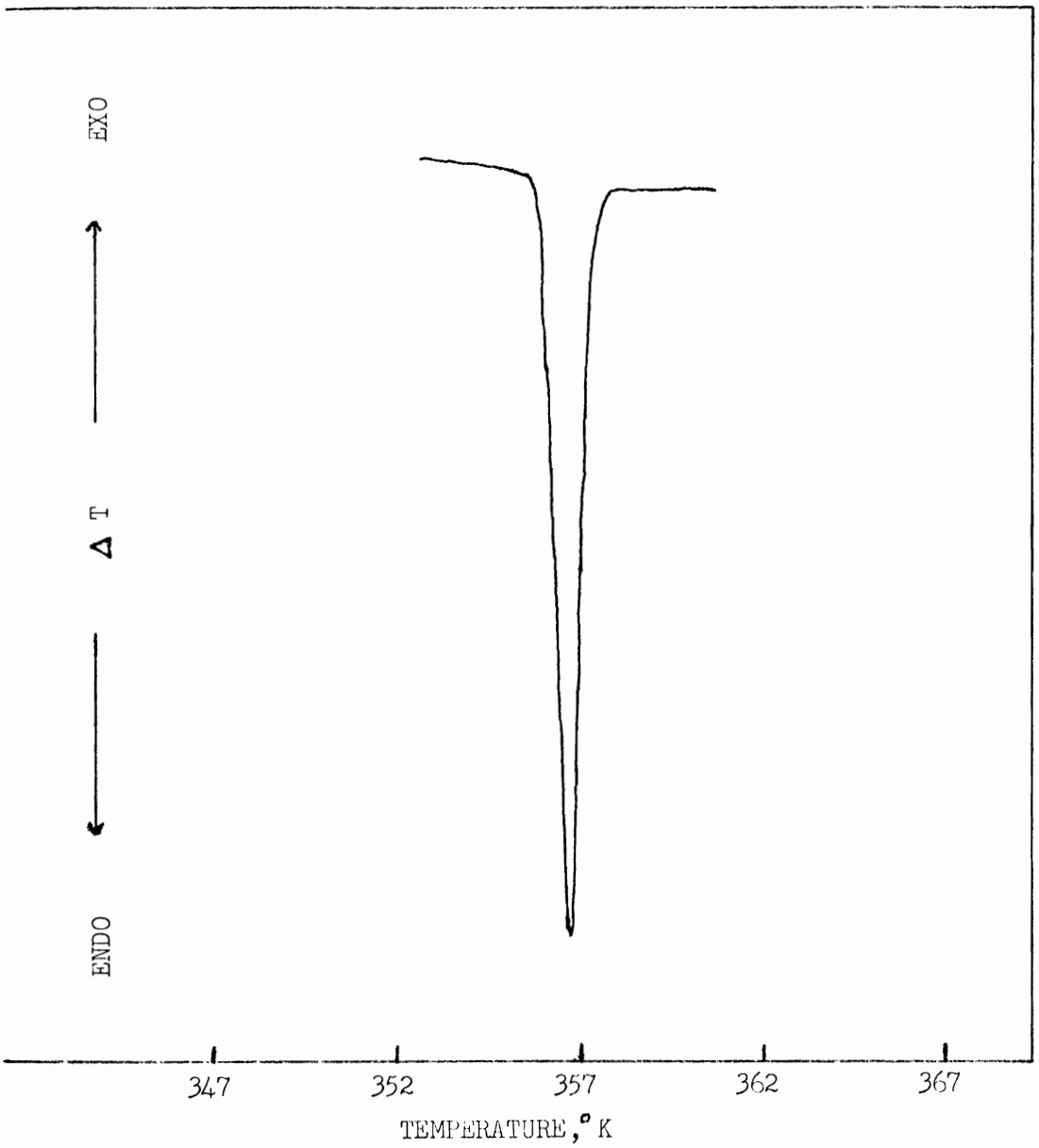

FIGURE A.9

DSC THERMOGRAM of BENZOIC ACID, RUN 149

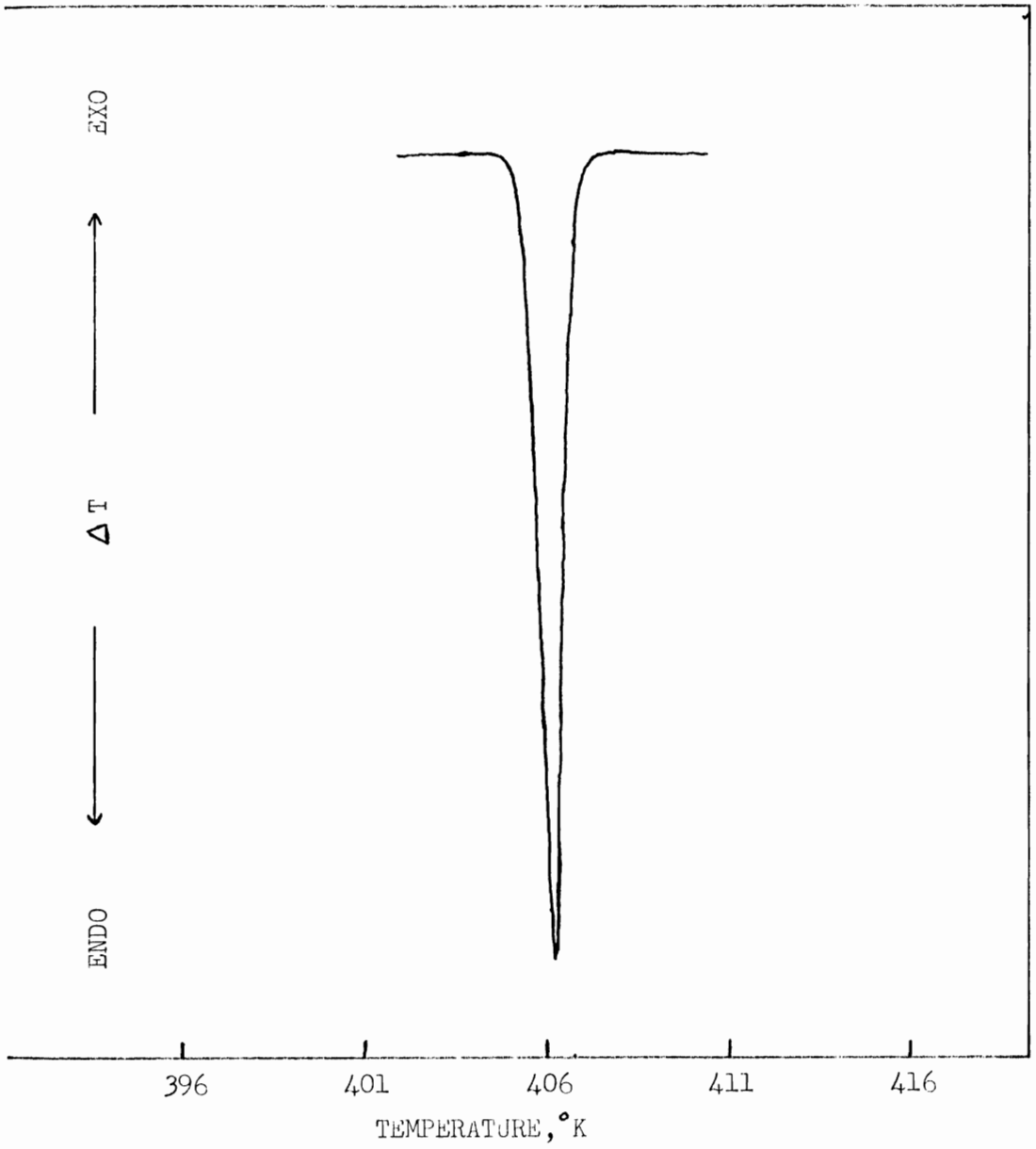

FIGURE A.10

DSC THERMOGRAM of ADIPIC ACID, RUN 157

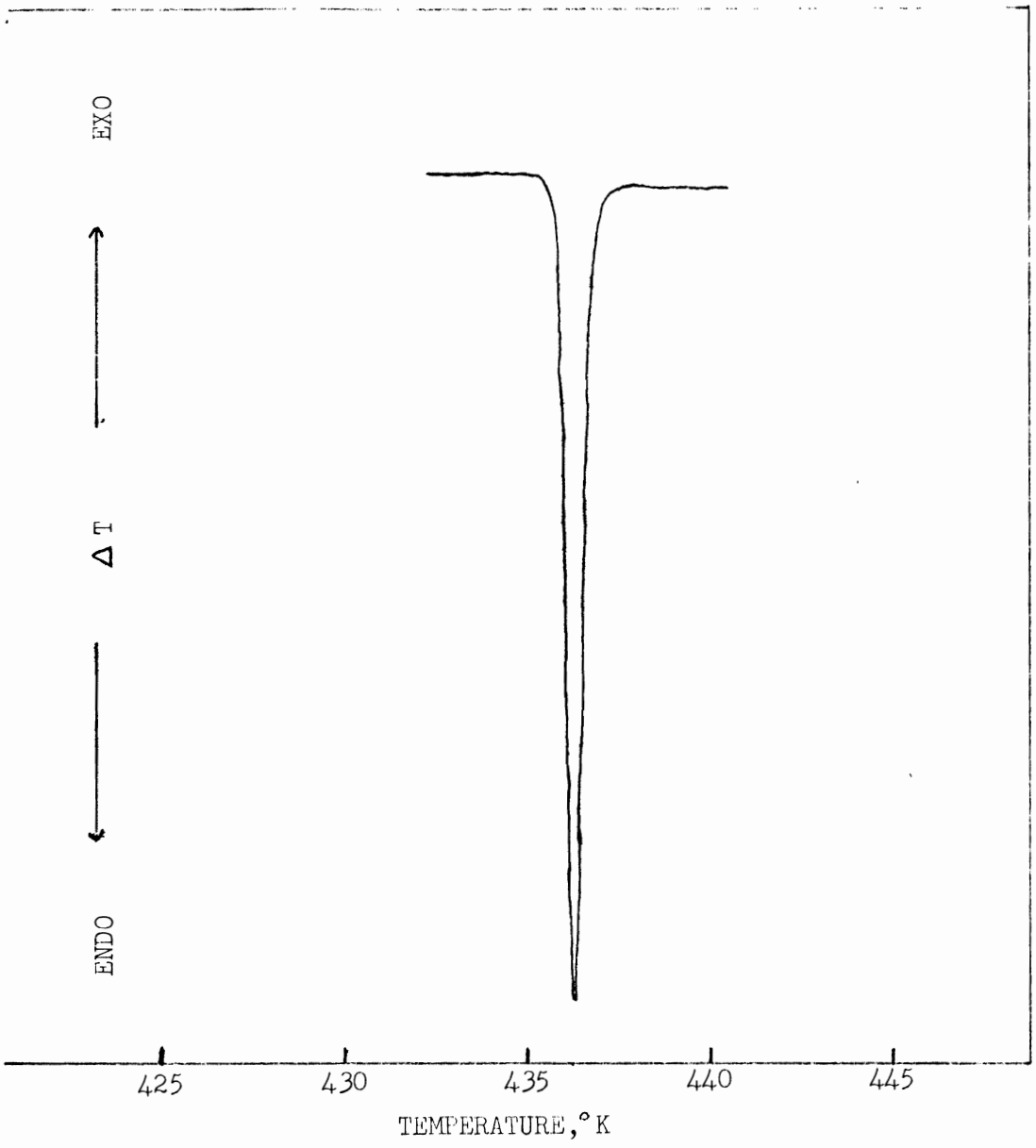

FIGURE A.11

DSC THERMOGRAM of INDIUM, RUN 4

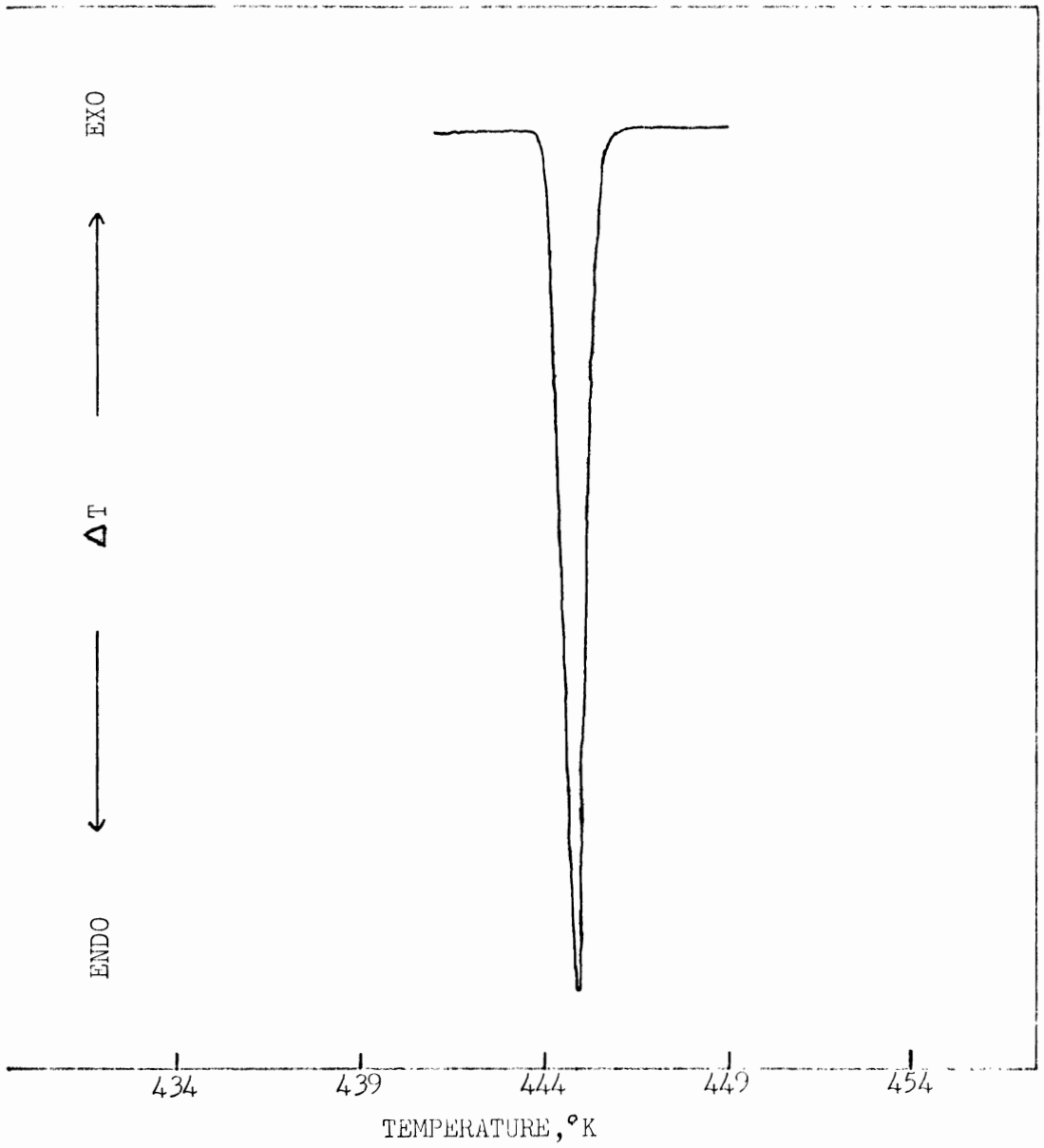

FIGURE A.12

DSC THERMOGRAM of POTASSIUM NITRATE, II→I TRANSITION, RUN 26

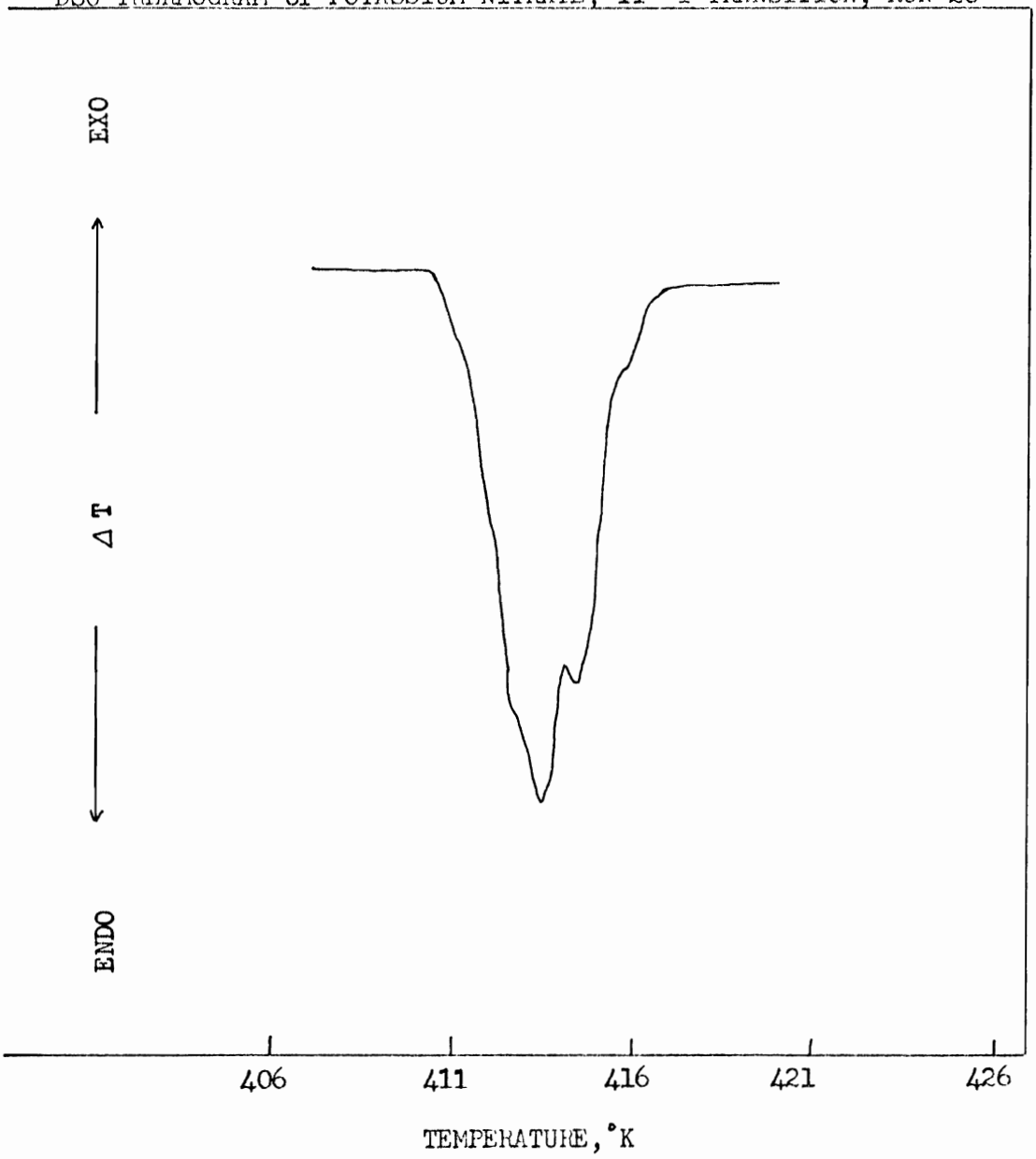

FIGURE A.13

DSC THERMOGRAM of POTASSIUM NITRATE, FUSION, RUN 26

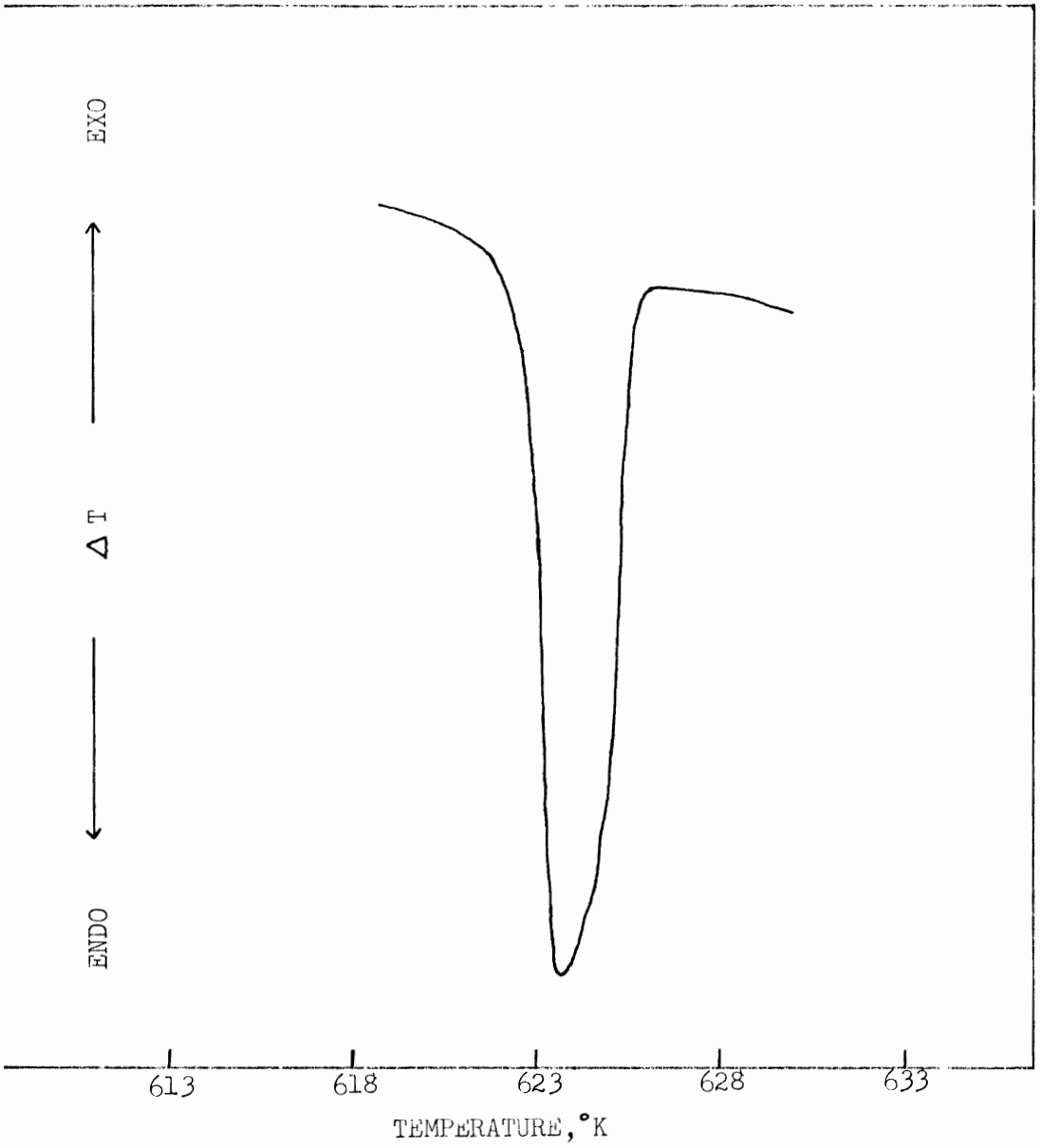

FIGURE A.14

DTA THERMOGRAM of p-NITROTOLUENE, RUN 11

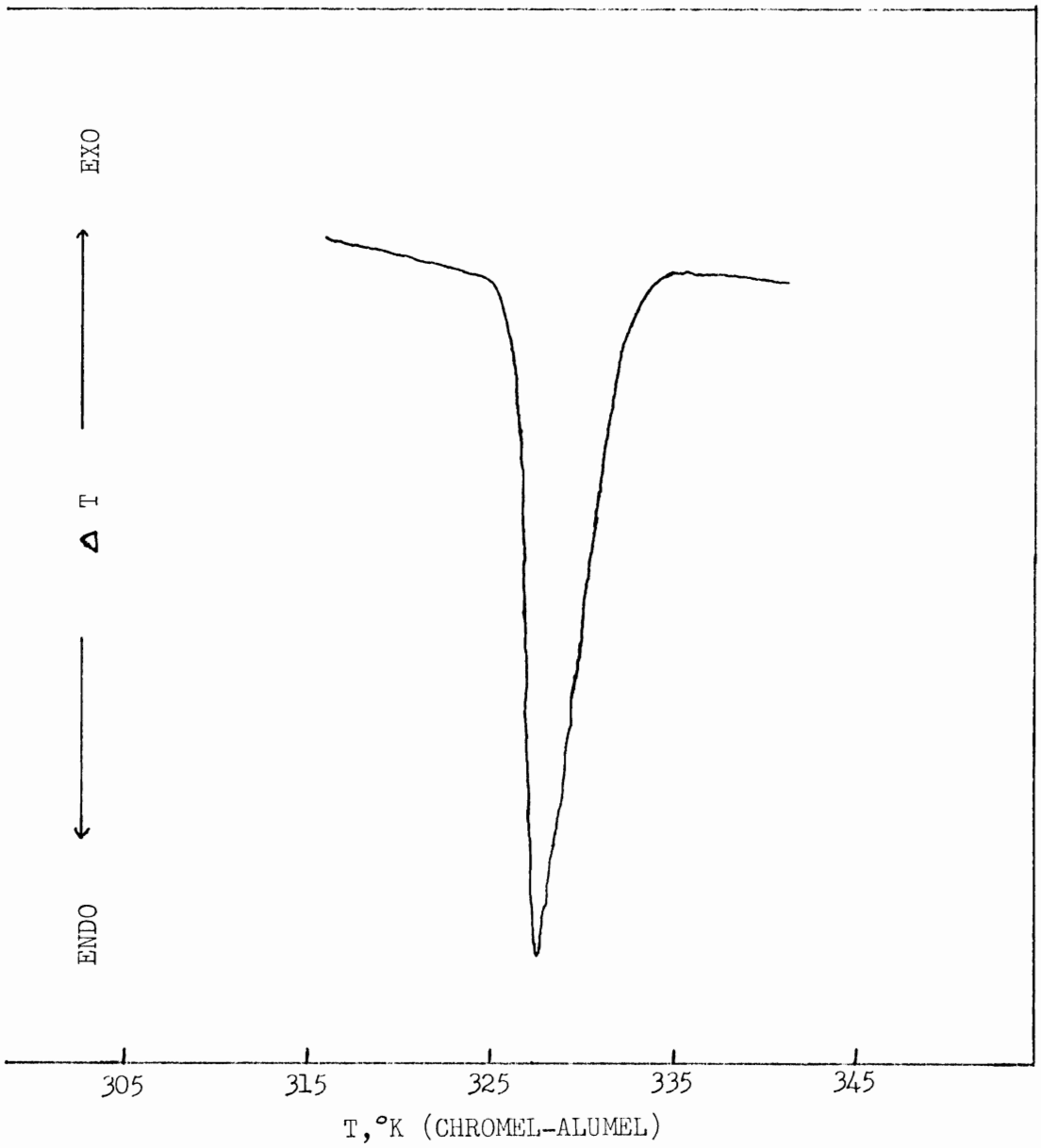

FIGURE A.15

DTA THERMOGRAM of NAPHTHALENE, RUN 17

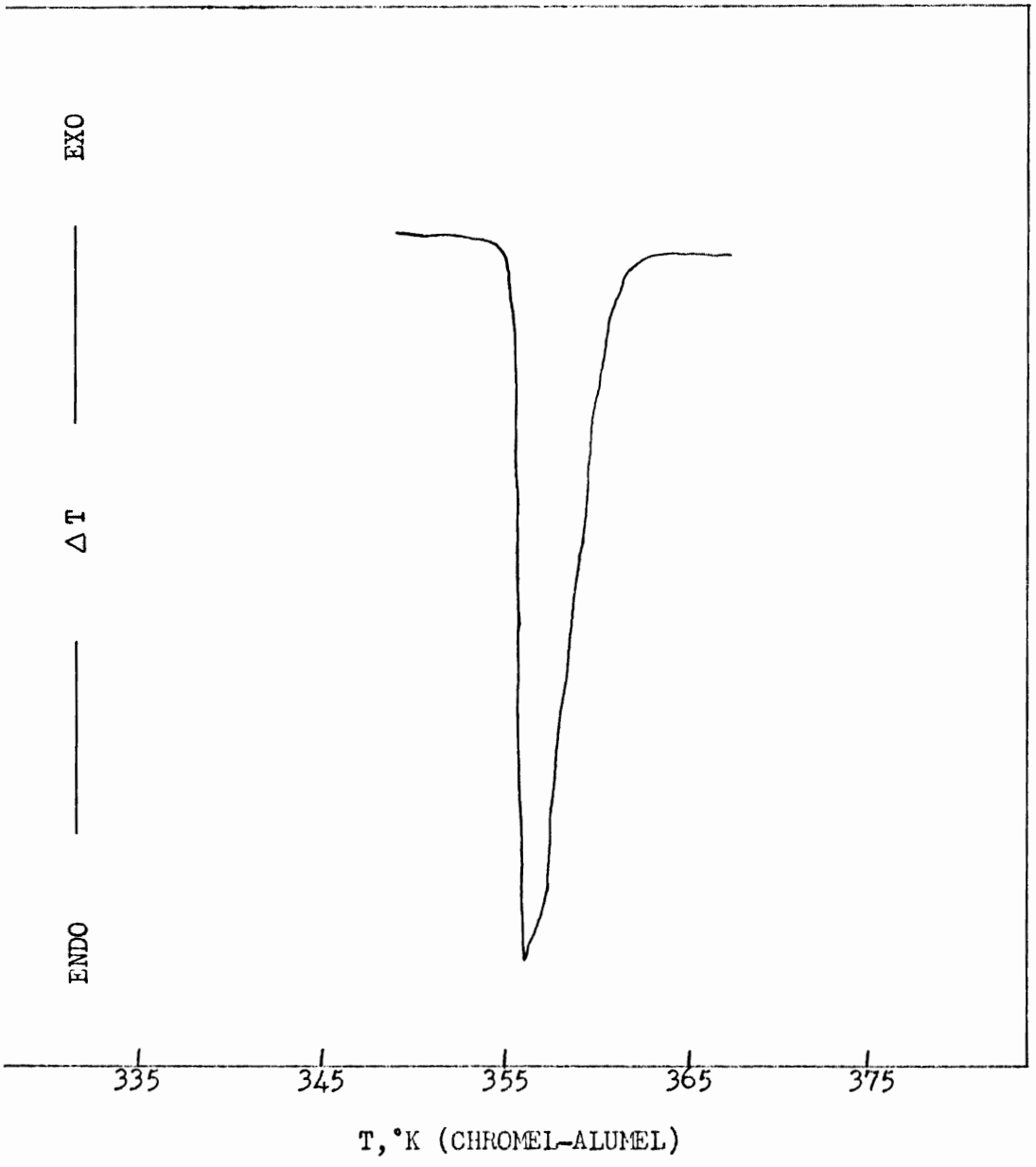

FIGURE A.16

DTA THERMOGRAM of BENZOIC ACID, RUN 5

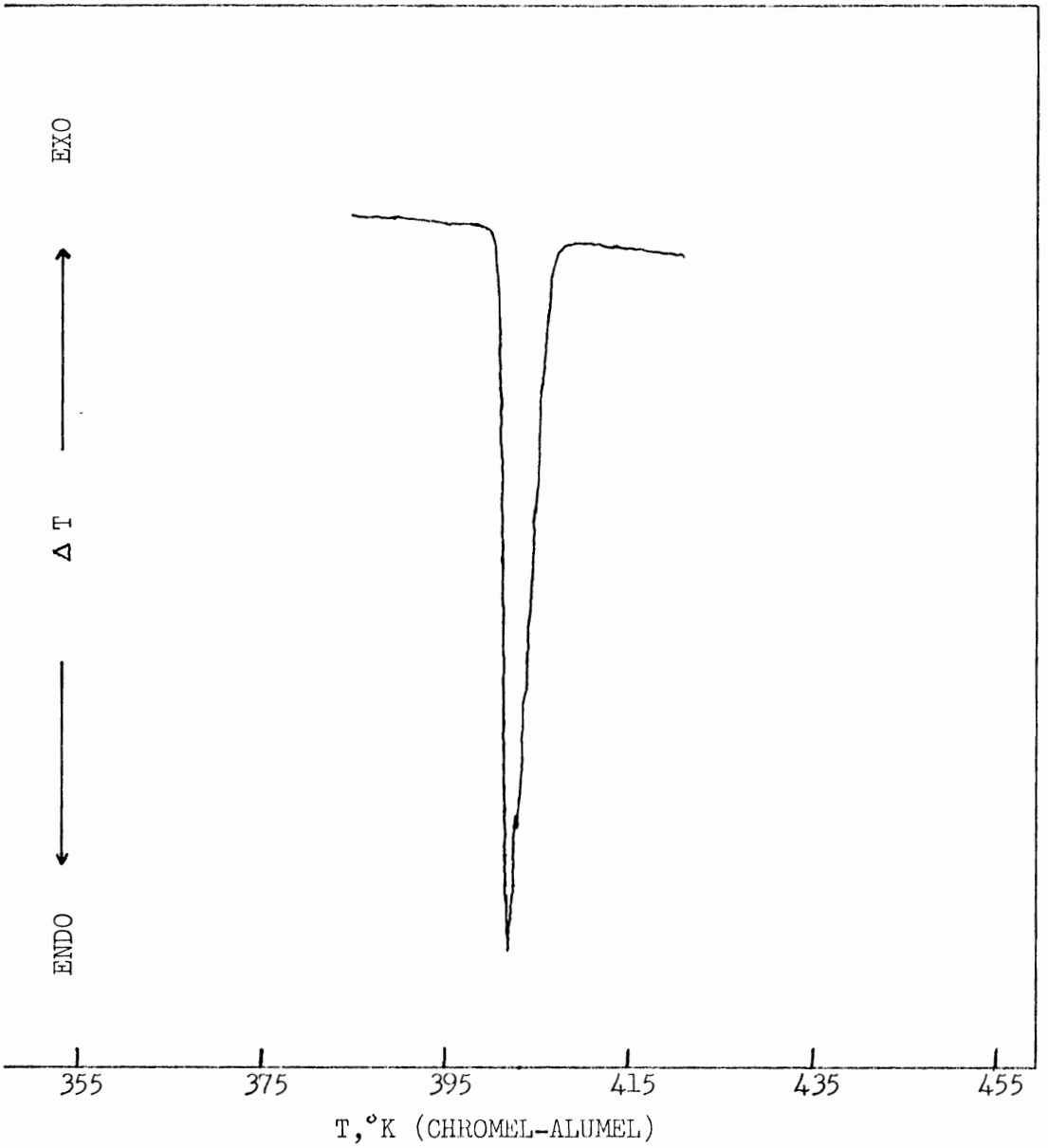

FIGURE A.17

DTA THERMOGRAM of ADIPIC ACID, RUN 13

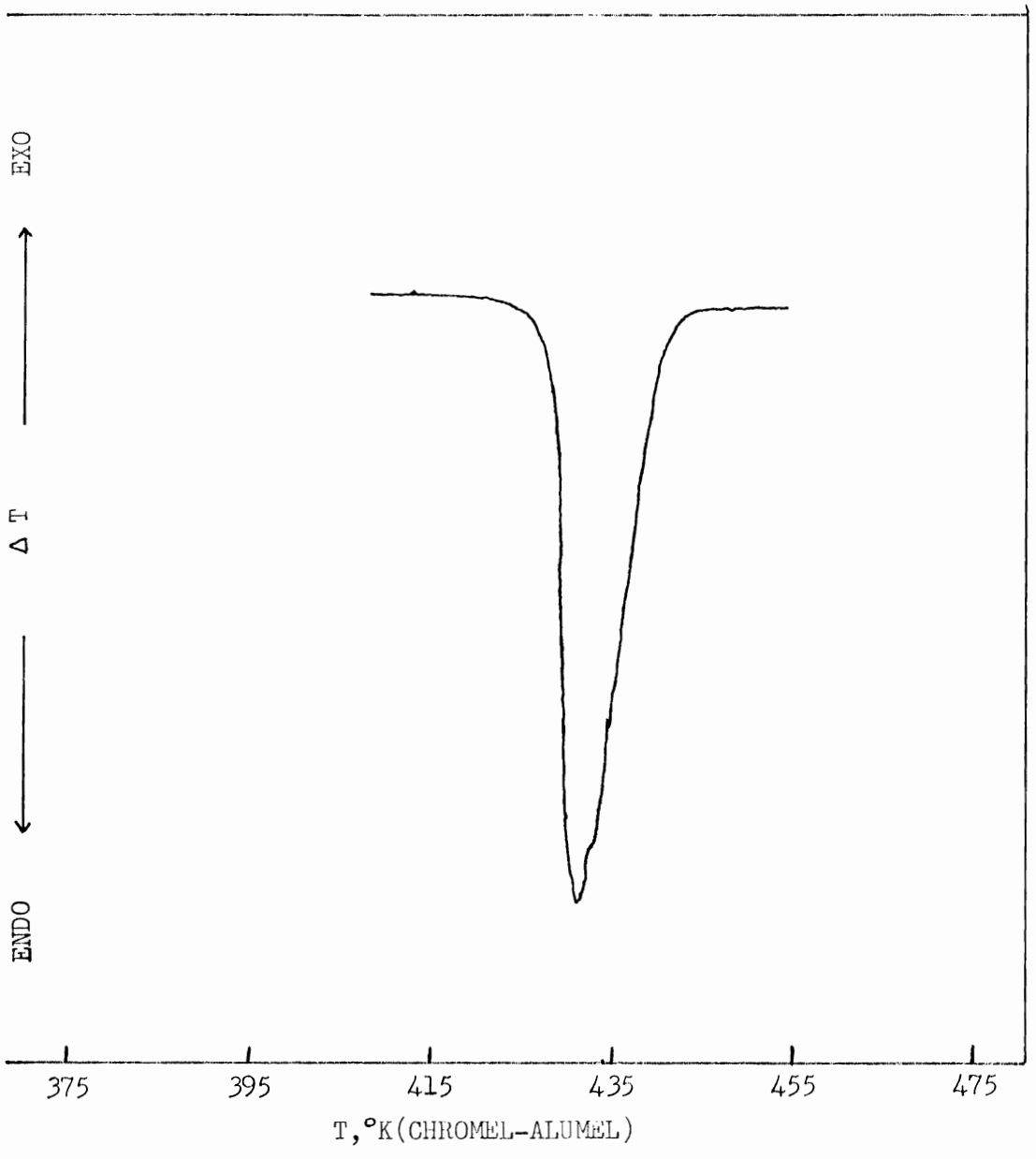

FIGURE A.18

DTA THERMOGRAM of POTASSIUM NITRATE, RUN 4

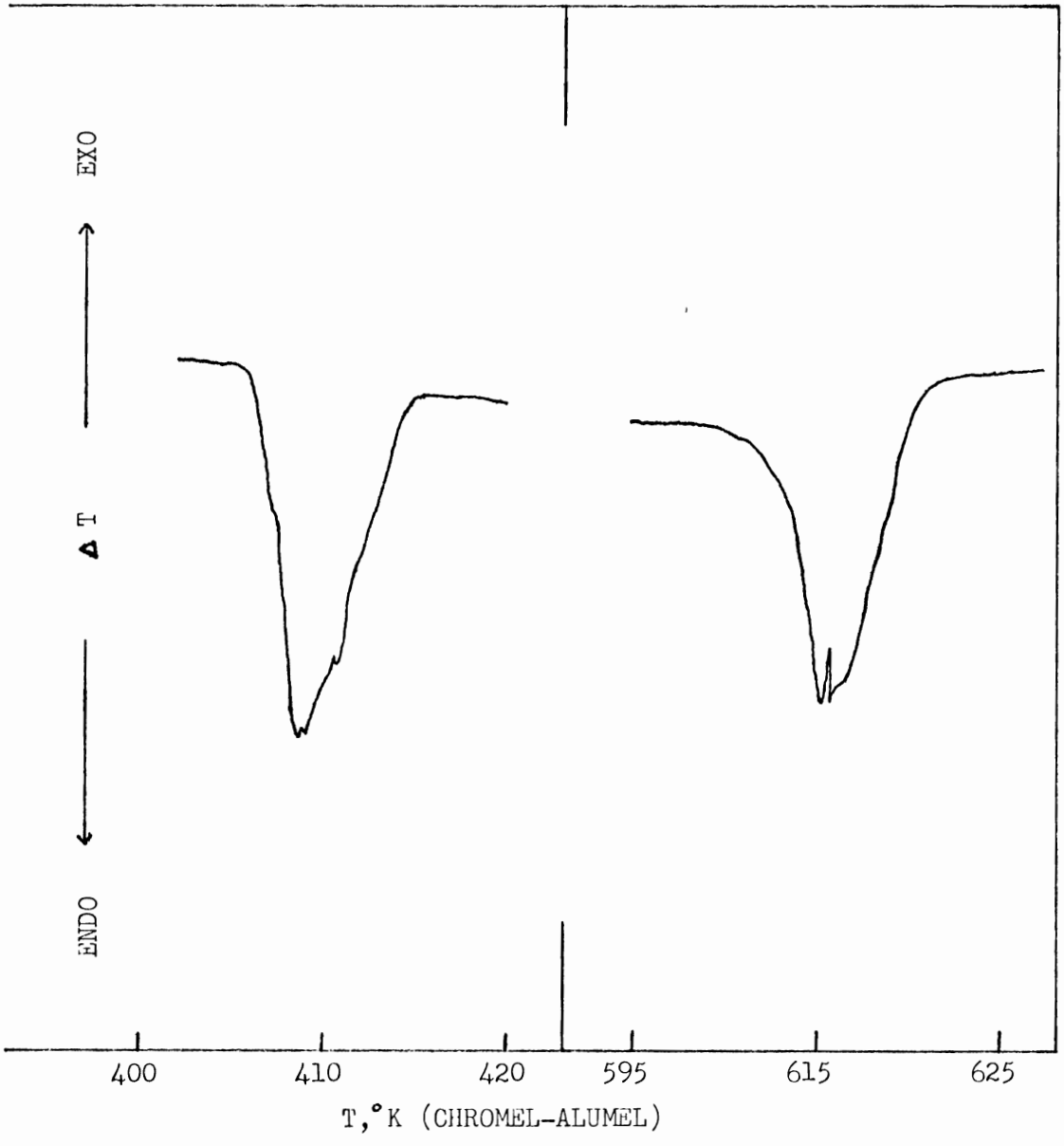

APPENDIX B

Experimental Data and Thermograms of Red Amorphous Selenium stored at 273°K

Table B.I

Area/mg and Observed Peak Temperature of the Endothermic and Exothermic Transitions in Red Amorphous Selenium #4

Run No.	Sample Wt. (mg)	Endotherm Area/mg	Endo. Temp. (°K)	Exotherm Area/mg	Exo. Temp. (°K)	Age (days)
1	12.474	20.3	327.1	41.1	368.3	350
2	11.412	18.3	328.3	40.3	369.0	476
3	17.714	21.7	326.8	44.0	368.6	476
4	16.507	20.1	324.5	41.8	368.3	748
5	14.928	20.3	324.9	43.3	368.0	748
6	18.006	22.2	324.1	42.4	368.7	748
7	16.960	18.7	324.3	45.0	368.3	748

Table B.II

Area/mg and Observed Peak Temperature of the Endothermic and Exothermic Transitions in Red Amorphous Selenium #5

Run No.	Sample Wt. (mg)	Endotherm Area/mg	Endo. Temp. (°K)	Exotherm Area/mg	Exo. Temp. (°K)	Age (days)
1	13.062	18.9	326.9	----	-----	337
2	14.231	20.3	325.8	42.0	365.6	337
3	6.220	21.3	325.7	----	-----	463
4	13.307	21.8	324.7	----	-----	463
5	12.241	20.8	325.5	40.8	365.0	463
7	9.249	----	-----	40.9	364.3	735
8	6.008	19.1	324.0	37.9*	364.2	735
9	7.690	16.7*	324.0	41.2	363.6	735
10	10.938	20.3	323.6	40.8	364.3	735

* Rejected at the 95% confidence level

Table B.III

Area/mg and Observed Peak Temperature of the Endothermic and Exothermic Transitions in Red Amorphous Selenium #6

Run No.	Sample Wt. (mg)	Endotherm Area/mg	Endo. Temp. (°K)	Exotherm Area/mg	Exo. Temp. (°K)	Age (days)
7	14.632	20.1	326.2	----	-----	160
8	13.954	20.4	325.8	40.3	365.9	160
9	10.002	23.4*	326.4	40.0	366.0	173
10	16.887	19.7	327.0	42.1	365.9	173
11	16.754	19.9	326.7	42.9	366.0	196
12	23.069	19.6	326.6	42.7	365.7	196
13	18.775	18.5	327.1	42.6	365.5	236
14	26.730	20.7	326.5	43.8	365.3	322
15	23.743	21.2	326.4	43.9	365.2	322
16	15.351	19.1	325.4	43.6	363.8	594
17	15.906	----	-----	43.4	363.7	594
18	7.540	18.2	326.4	41.2	364.8	594
19	11.617	19.7	325.5	42.1	364.5	594

* Rejected at the 95% confidence level

Table B.IV

Area/mg and Observed Peak Temperature of the Endothermic and Exothermic Transitions in Red Amorphous Selenium #7

Run No.	Sample Wt. (mg)	Endotherm Area/mg	Endo. Temp. (°K)	Exotherm Area/mg	Exo. Temp. (°K)	Age (days)
1	10.736	18.4	325.8	42.9	365.7	147
2	10.515	19.1	325.3	----	-----	147
4	12.711	-----	-----	41.5	365.4	160
5	12.335	17.7	327.0	40.9	364.9	166
6	9.674	18.2	325.8	42.3	365.2	166
7	10.324	20.5*	326.6	----	-----	183
8	12.193	18.7	326.2	----	-----	183
8.2	9.530	18.4	325.6	----	-----	188
9	10.472	19.2	326.5	40.6	364.8	223
10	10.264	20.2	325.6	42.8	364.1	309
11	13.934	18.9	325.1	42.4	364.2	309
12	9.868	19.6	326.9	40.9	364.4	581
13	11.021	18.7	326.3	42.5	364.1	581
14	7.493	18.2	325.2	40.6	364.4	581

* Rejected at the 95% confidence level

Table B.V

Area/mg and Observed Peak Temperature of the Endothermic and Exothermic Transitions in Red Amorphous Selenium #8

Run No.	Sample Wt. (mg)	Endotherm Area/mg	Endo. Temp. (°K)	Exotherm Area/mg	Exo. Temp. (°K)	Age (days)
1	16.620	----	-----	39.5	365.9	9
2	21.257	20.0	326.9	42.1	365.6	11
3	18.400	21.1	327.4	43.1	365.6	11
4	20.842	19.9	327.3	42.2	365.9	15
5	16.581	19.5	326.7	42.5	365.6	15
6	16.157	20.7	327.1	----	-----	15
7	22.885	20.1	327.1	----	-----	28
8	21.882	20.7	327.0	42.8	365.8	28
9	19.376	20.9	327.2	41.9	365.5	68
10	26.797	20.3	326.9	----	-----	154
11	27.343	21.2	326.4	41.5	365.3	154
12	14.107	20.6	325.9	42.0	364.4	425
13	12.688	20.8	326.4	40.0	364.7	425
14	15.785	20.3	326.0	40.3	364.8	425

Table B.VI

Area/mg and Observed Peak Temperature of the Endothermic and Exothermic Transitions in Red Amorphous Selenium #9

Run No.	Sample Wt. (mg)	Endotherm Area/mg	Endo. Temp. (°K)	Exotherm Area/mg	Exo. Temp. (°K)	Age (days)
2	14.340	19.9	326.6	----	-----	14
3	17.314	19.5	325.5	42.8	364.1	22
4	12.100	19.5	326.7	40.7	366.0	28
5	20.283	21.3	326.7	41.4	365.7	33
6	28.930	20.3	327.4	43.8	365.1	119
7	27.361	20.6	327.0	----	-----	119
8	16.125	19.5	327.0	42.7	365.3	119
9	11.778	18.8	325.2	41.8	363.1	389
10	12.247	19.9	325.3	42.1	363.4	389
11	18.700	18.7	325.8	41.8	363.2	389

Table B.VII

Area/mg and Observed Peak Temperature of the Endothermic and Exothermic Transitions in Red Amorphous Selenium #10, Group 5

Run No.	Sample Wt. (mg)	Endotherm Area/mg	Endo. Temp. (°K)	Exotherm Area/mg	Exo. Temp. (°K)	Age (days)
35	9.747	21.0	326.0	41.2	367.2	10
37	5.298	19.9	326.6	38.2	367.7	11
42	6.072	21.1	325.7	40.7	366.6	17
52	7.806	21.6	325.5	38.8	366.4	24
55	8.725	19.9	325.8	----	-----	29
59	8.541	21.1	327.1	38.0	366.3	102
60	7.964	21.8	326.8	40.6	366.1	102
67	8.906	----	-----	42.6	363.1	372
68	4.729	----	-----	36.5	363.6	372
69	6.171	18.0*	324.8	37.9	364.6	372
70	4.737	----	-----	38.0	364.5	372

* Rejected at the 95% confidence level

Table B.VIII

Area/mg and Observed Peak Temperature of the Endothermic and Exothermic Transitions in Red Amorphous Selenium #11, Group 7

Run No.	Sample Wt. (mg)	Endotherm Area/mg	Endo. Temp. (°K)	Exotherm Area/mg	Exo. Temp. (°K)	Age (days)
16	9.551	18.5	325.5	39.6	364.0	10
26	10.855	18.7	325.7	42.0*	363.3	23
30	8.816	19.6	326.4	39.0	363.9	88
31	9.680	18.8	326.0	39.2	364.1	88
41	4.285	----	-----	38.7	361.3	358
42	3.756	18.4	323.5	----	-----	358
43	8.982	17.9	323.3	39.1	361.1	358
44	8.441	16.0*	322.9	38.0	361.3	358

* Rejected at the 95% confidence level

Table B.IX

Experimental Data Accompanying Figures B.1 to B.8 *

Figure No.	Sample Wt. (mg)	Reference Wt. (mg)	Exo. Temp. (°K)	ΔT (°K/in)	Age (days)
B.1	15.4	73.9	327.7	0.2	53
B.2	17.3	51.9	328.7	0.1	199
B.3	15.3	----	328.1	0.1	14
B.4	16.4	73.9	327.7	0.2	40
B.5	15.8	51.9	327.6	0.1	186
B.6	18.0	51.9	327.4	0.1	45
B.7	13.7	51.9	329.5	0.1	32
B.8	13.4	37.3	327.5	0.1	191

* Rate of heating is 5°K/min

FIGURE B.1

DTA THERMOGRAM of RED AMORPHOUS SELENIUM #4, RUN 16

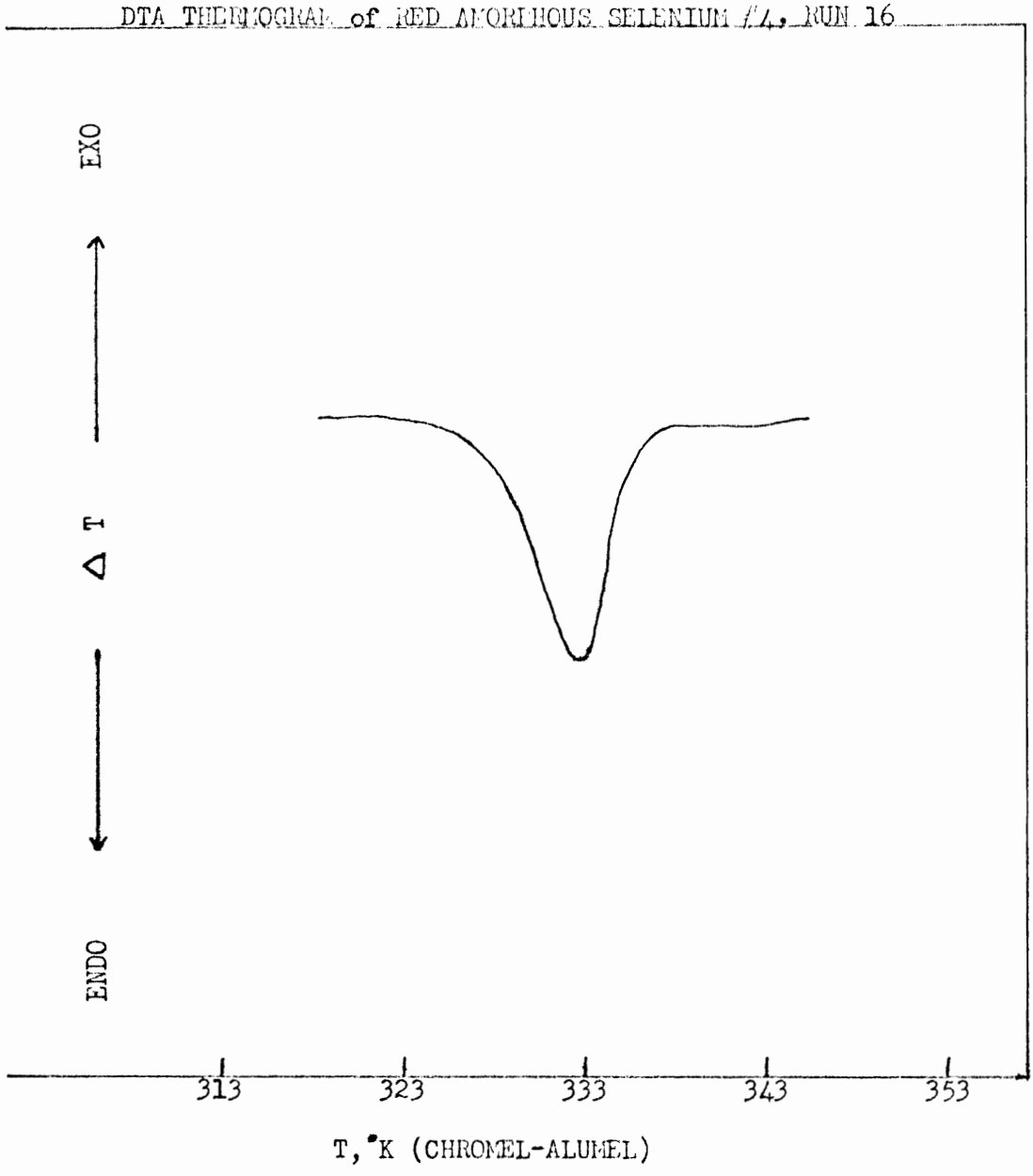

FIGURE B.2

DTA THERMOGRAM of RED AMORPHOUS SELENIUM #4, RUN 17

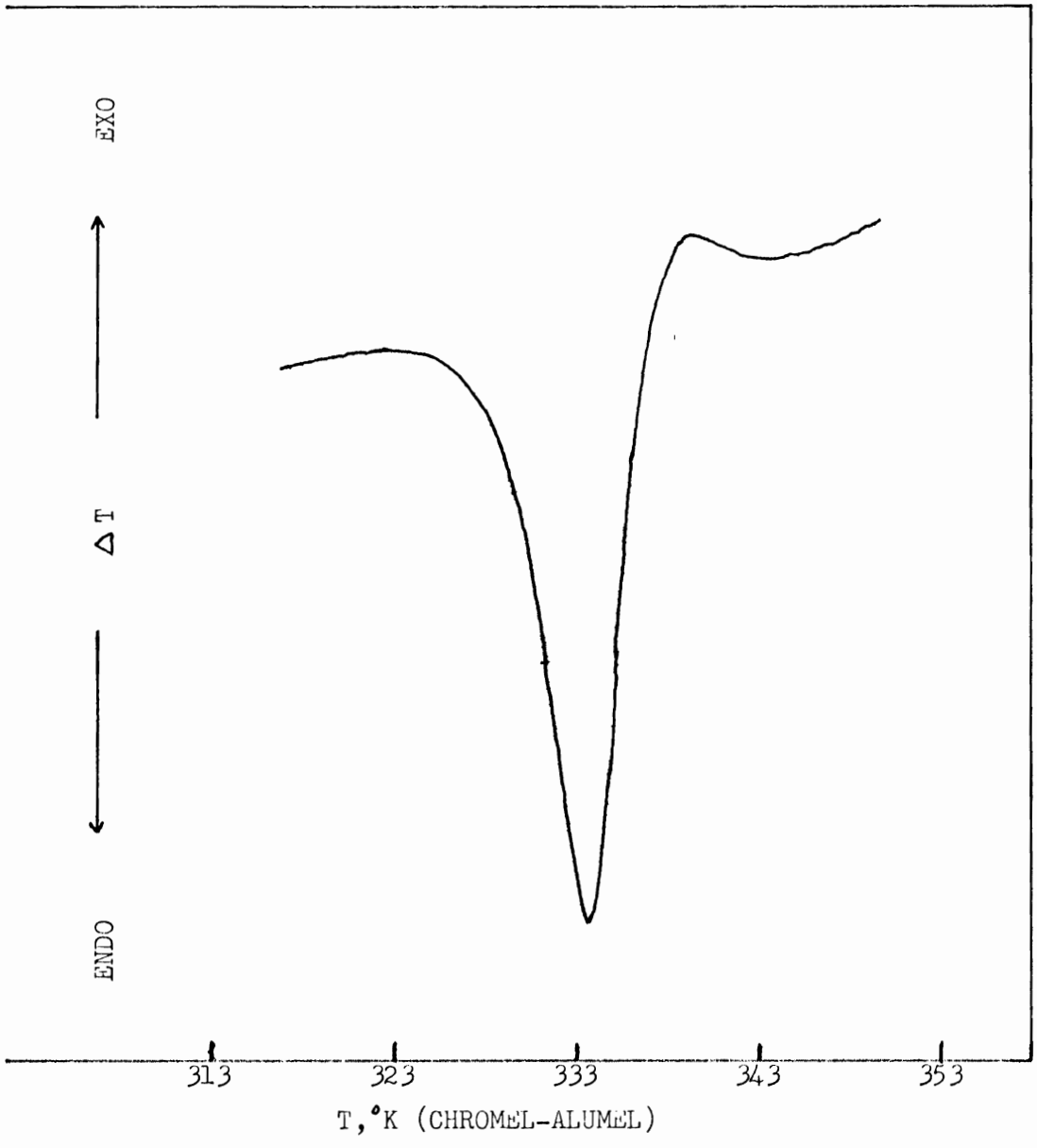

FIGURE B.3

DTA THERMOGRAM of RED AMORPHOUS SELENIUM #5, RUN 5

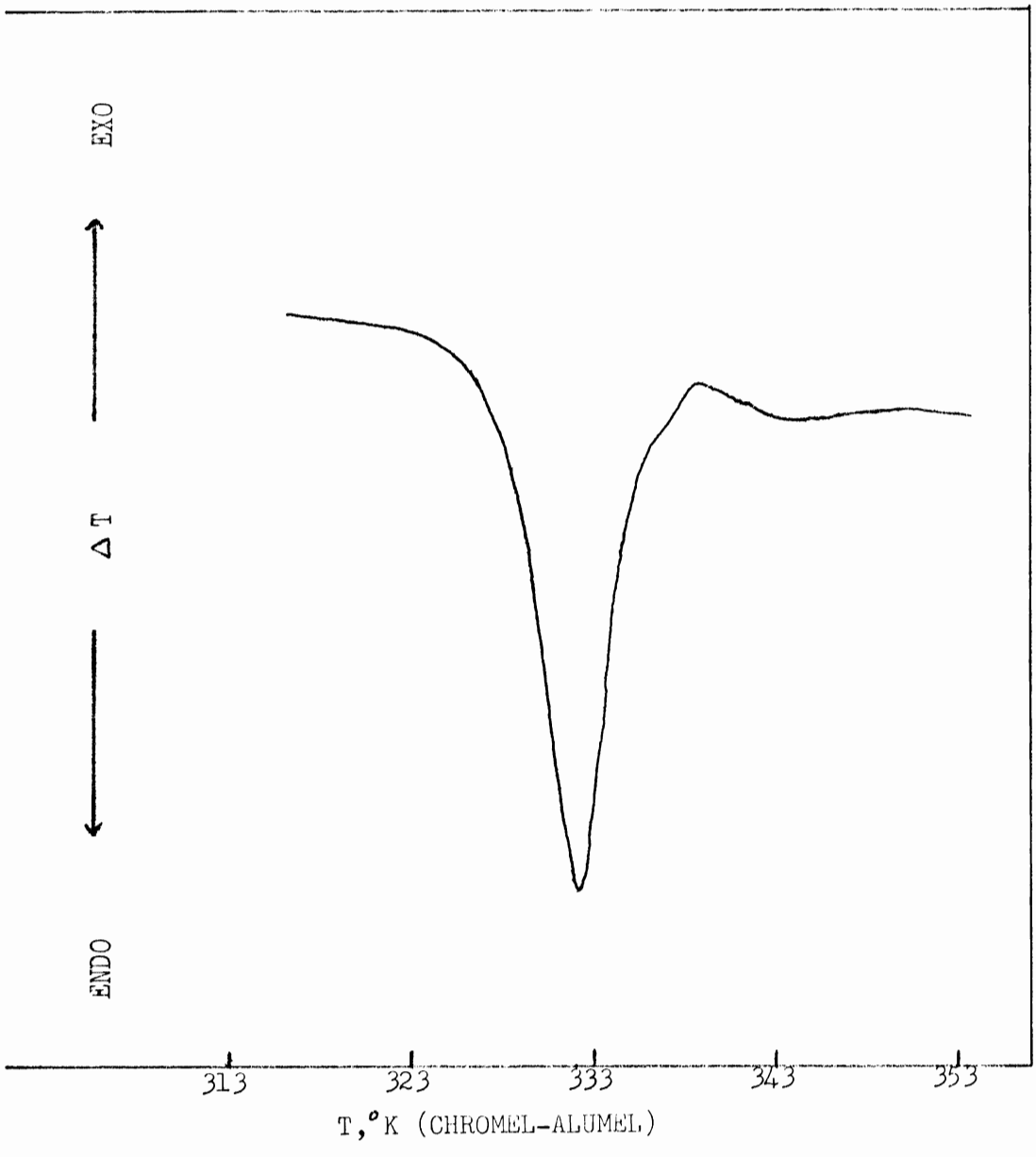

FIGURE B.4

DTA THERMOGRAM of RED AMORPHOUS SELENIUM #5, RUN 11

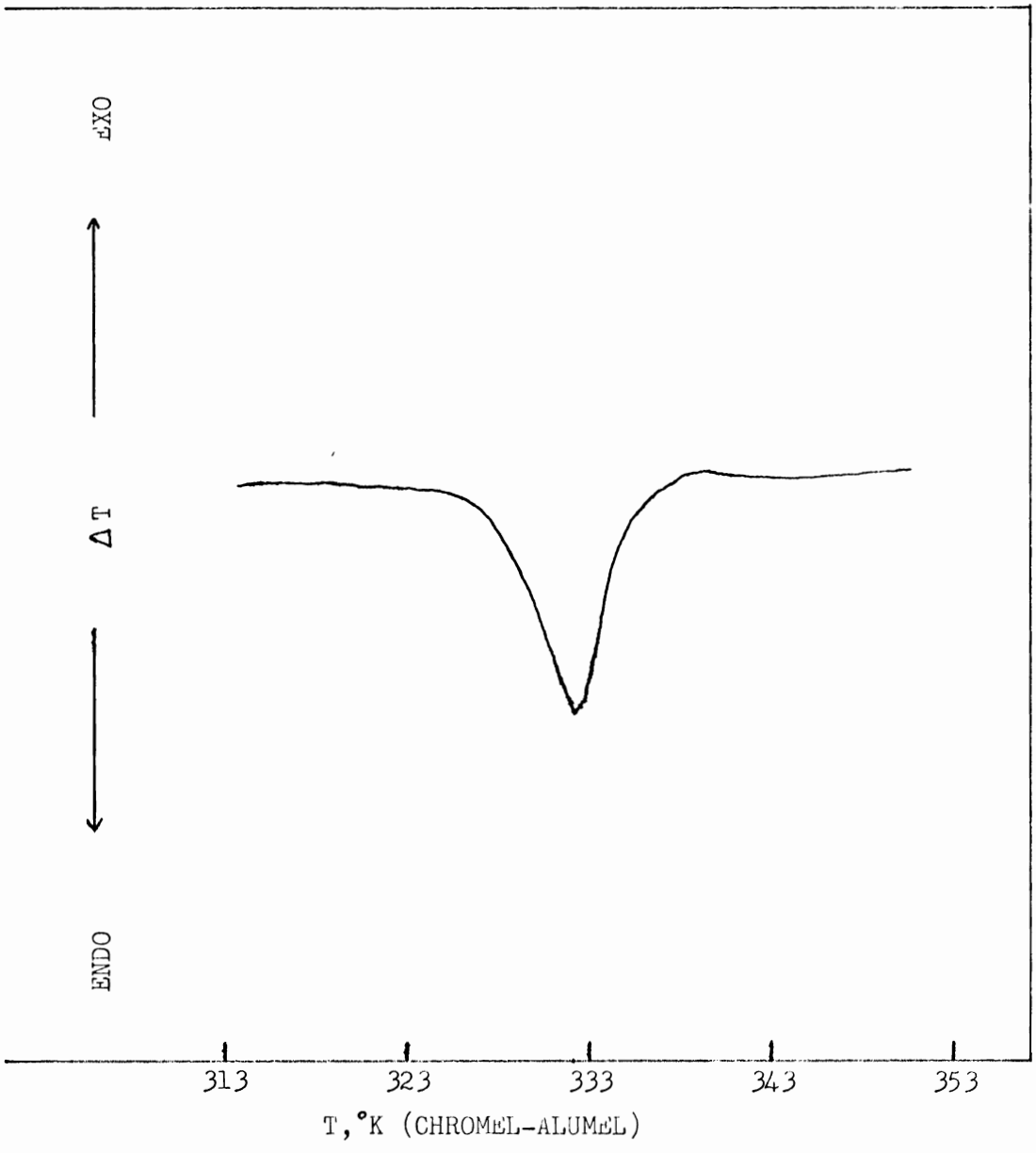

FIGURE B.5

DTA THERMOGRAM of RED AMORPHOUS SELENIUM #5, RUN 21

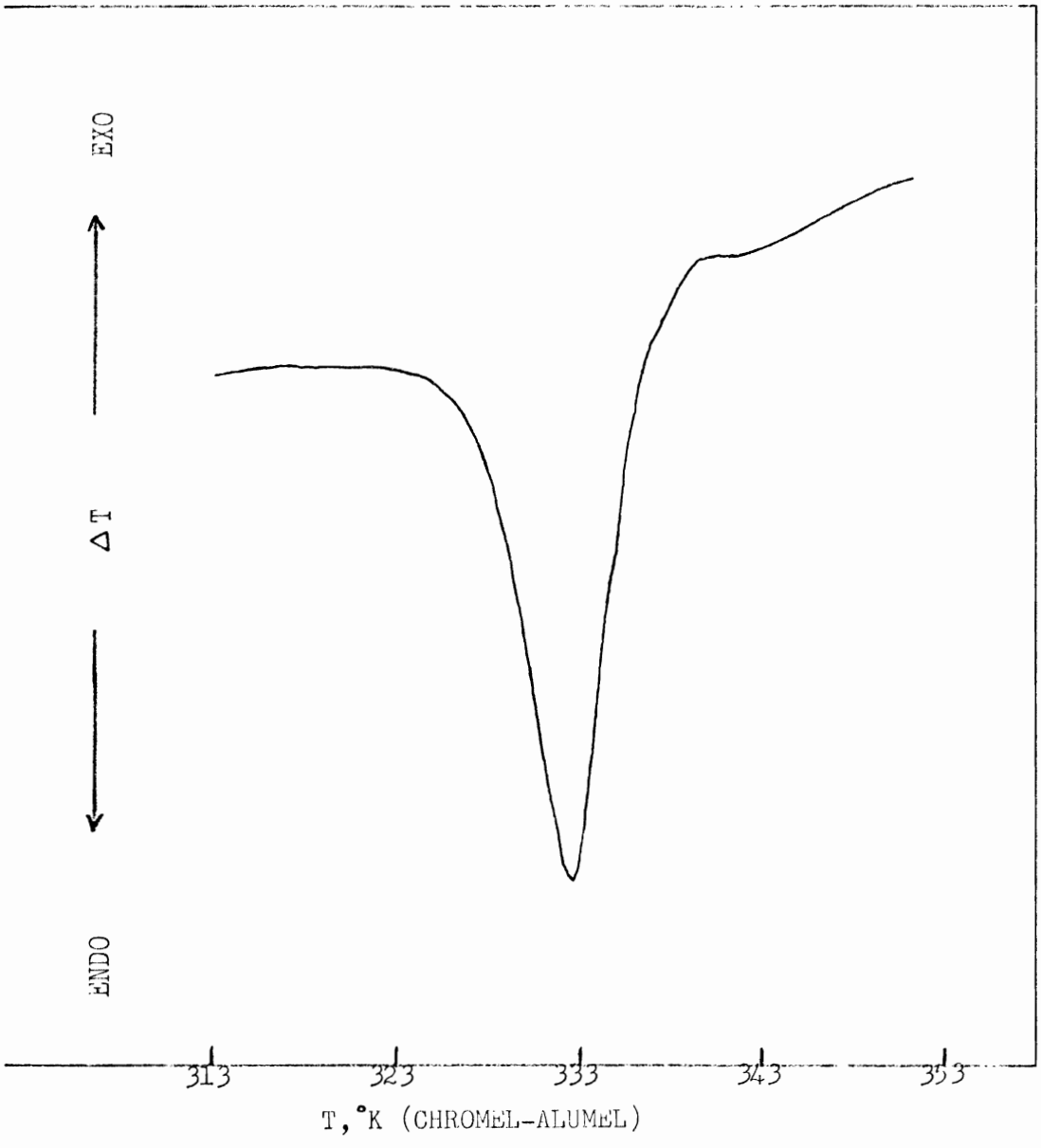

FIGURE B.6

DTA THERMOGRAM of RED AMORPHOUS SELENIUM #6, RUN 3

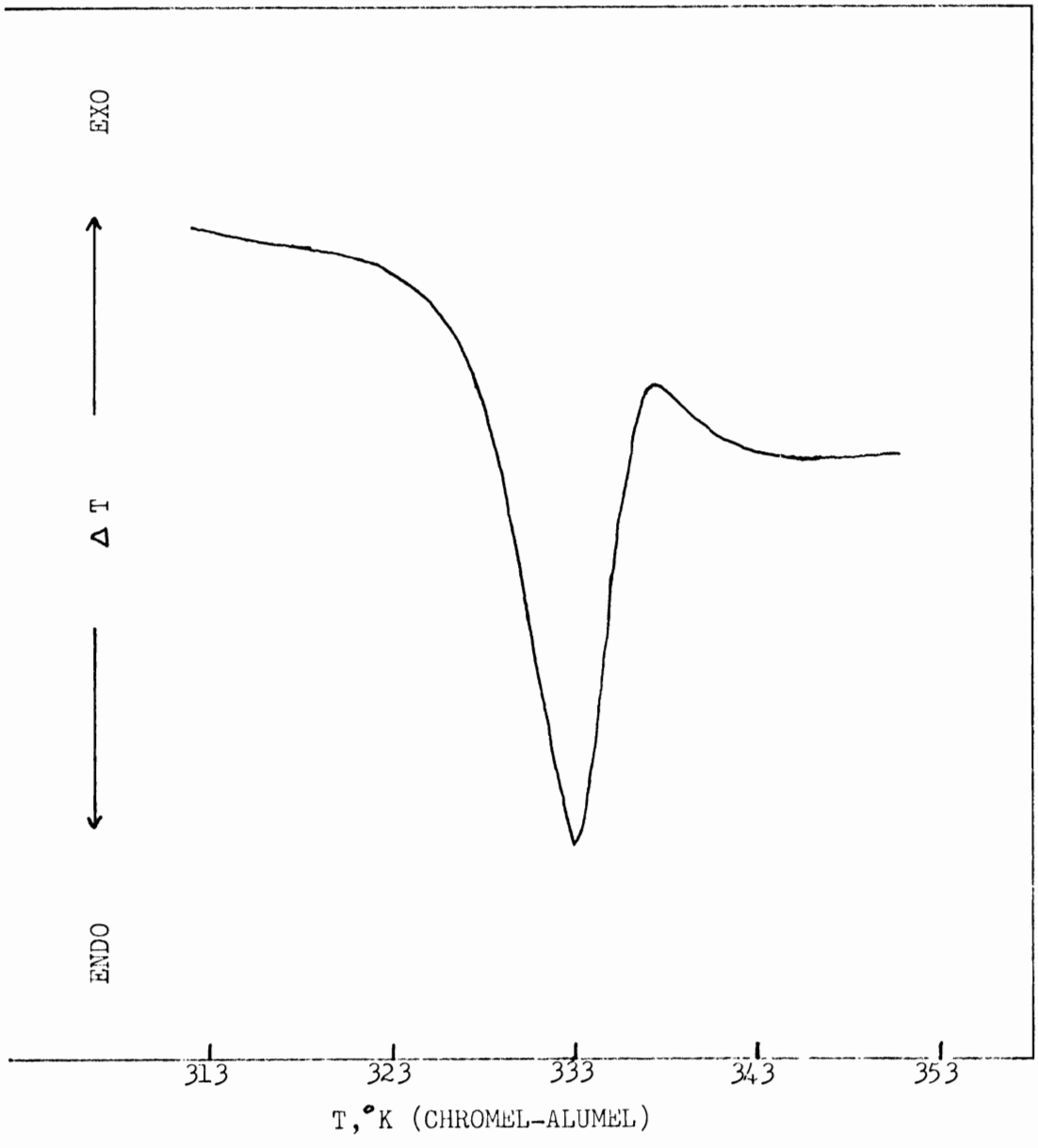

FIGURE B.7

DTA THERMOGRAM of RED AMORPHOUS SELENIUM #7, RUN 5

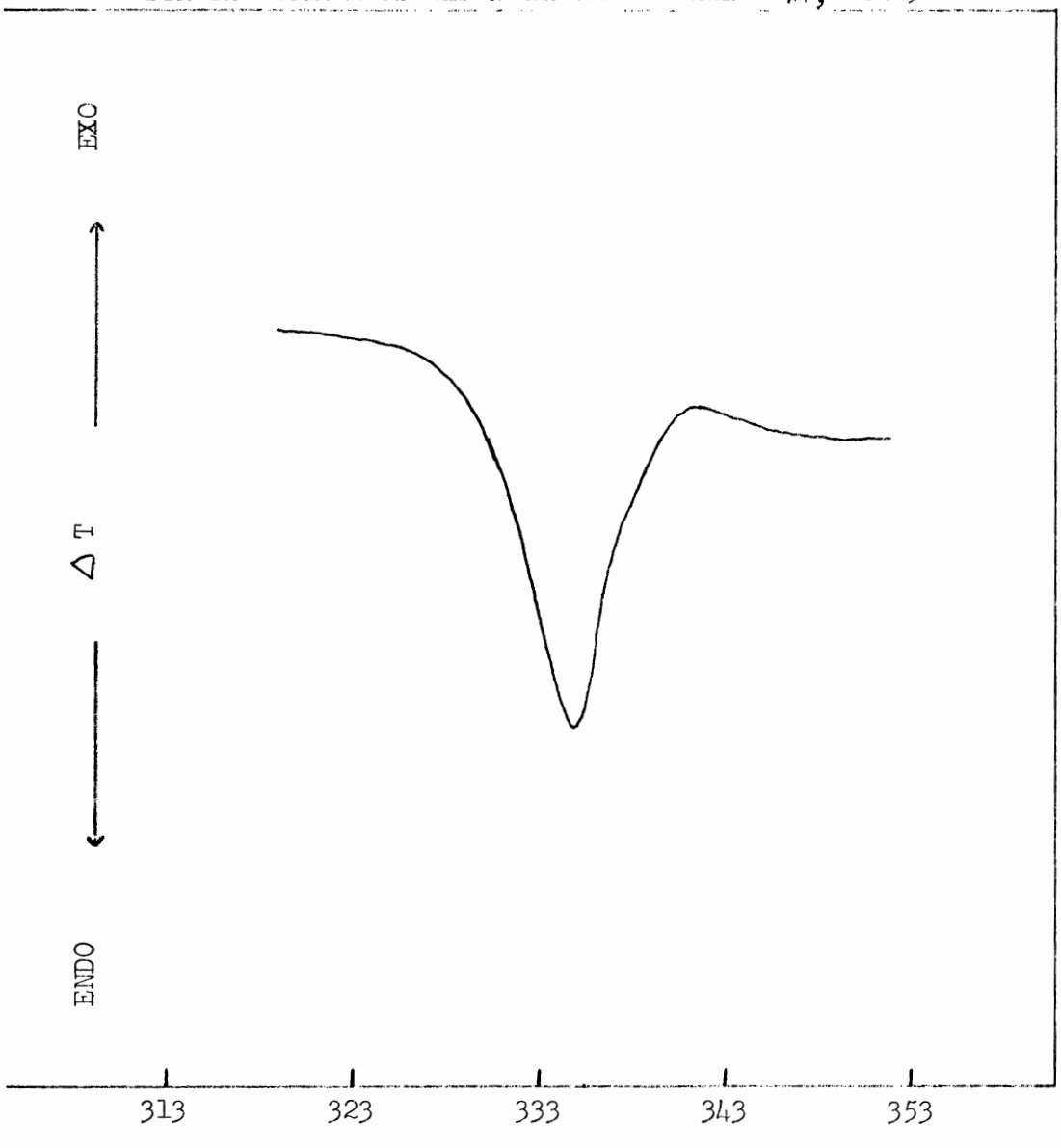

FIGURE B.8

DTA THERMOGRAM of RED AMORPHOUS SELENIUM #11, RUN 4

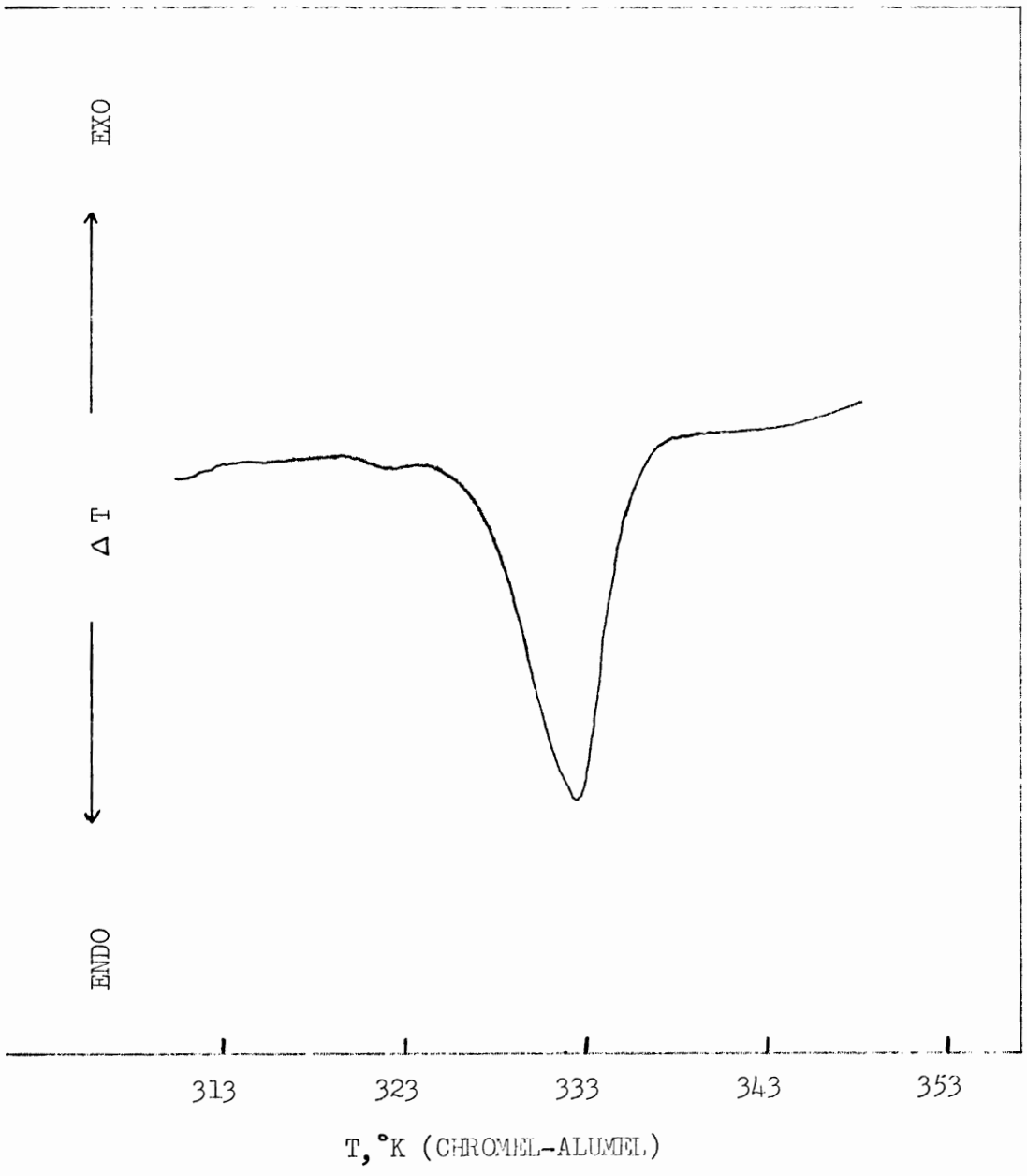

FIGURE B.9

DSC THERMOGRAM of RED AMORPHOUS SELENIUM #11, GROUP 7, RUN 44

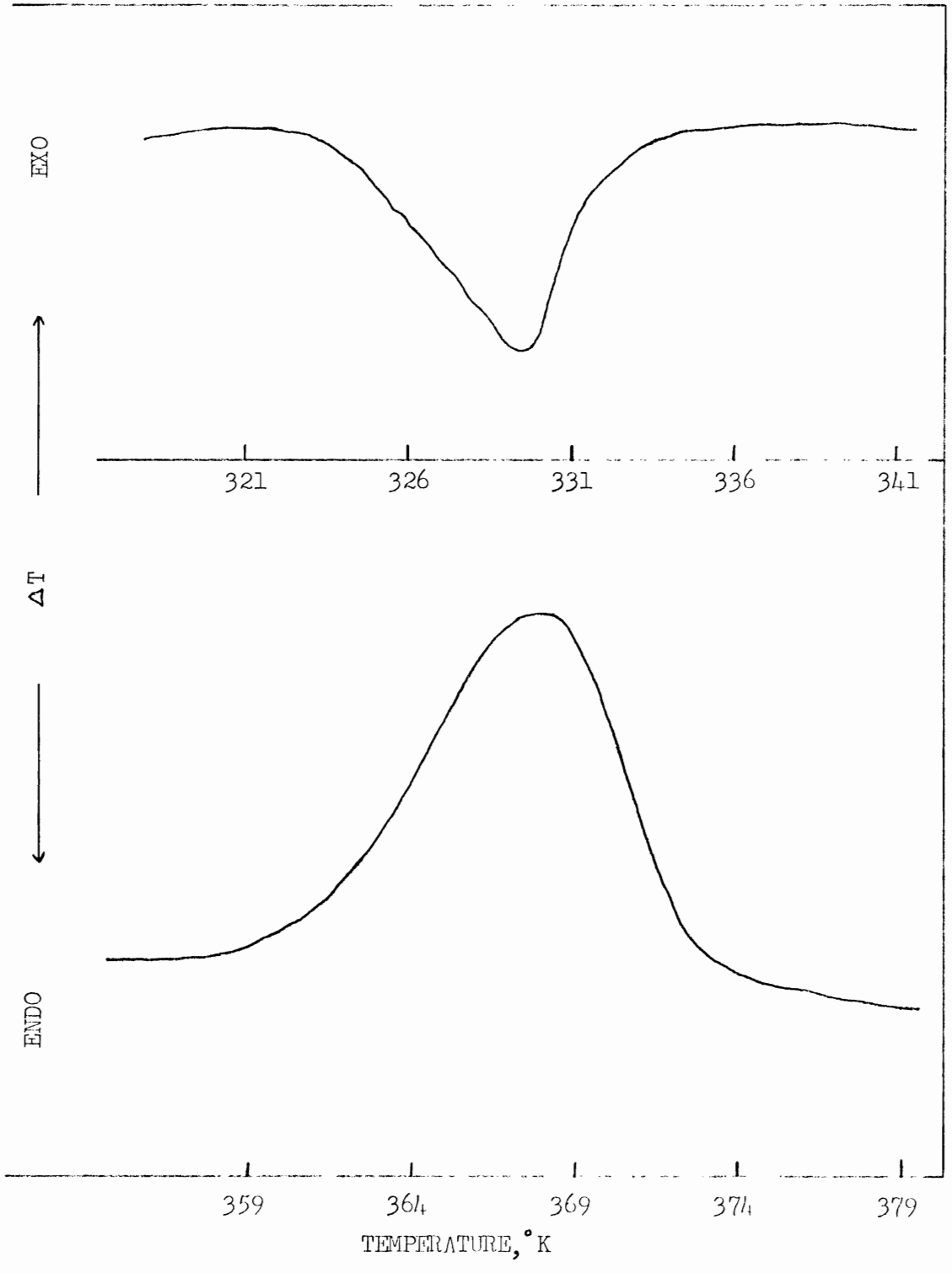

FIGURE B.10

DSC THERMOGRAM of RED AMORPHOUS SELENIUM #10, GROUP 5, RUN 59

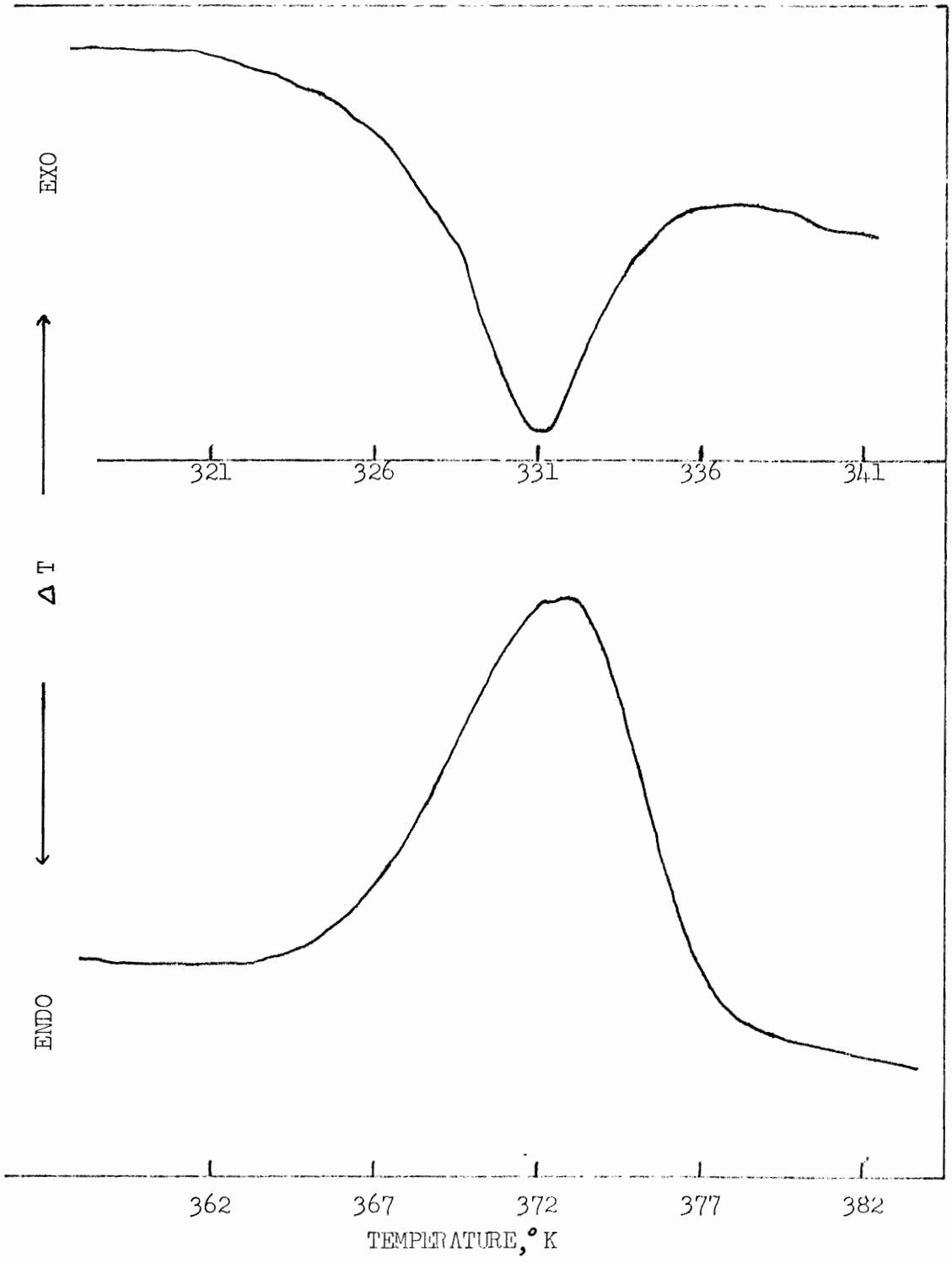

FIGURE B.11

DSC THERMOGRAM of RED AMORPHOUS SELENIUM #9, RUN 9

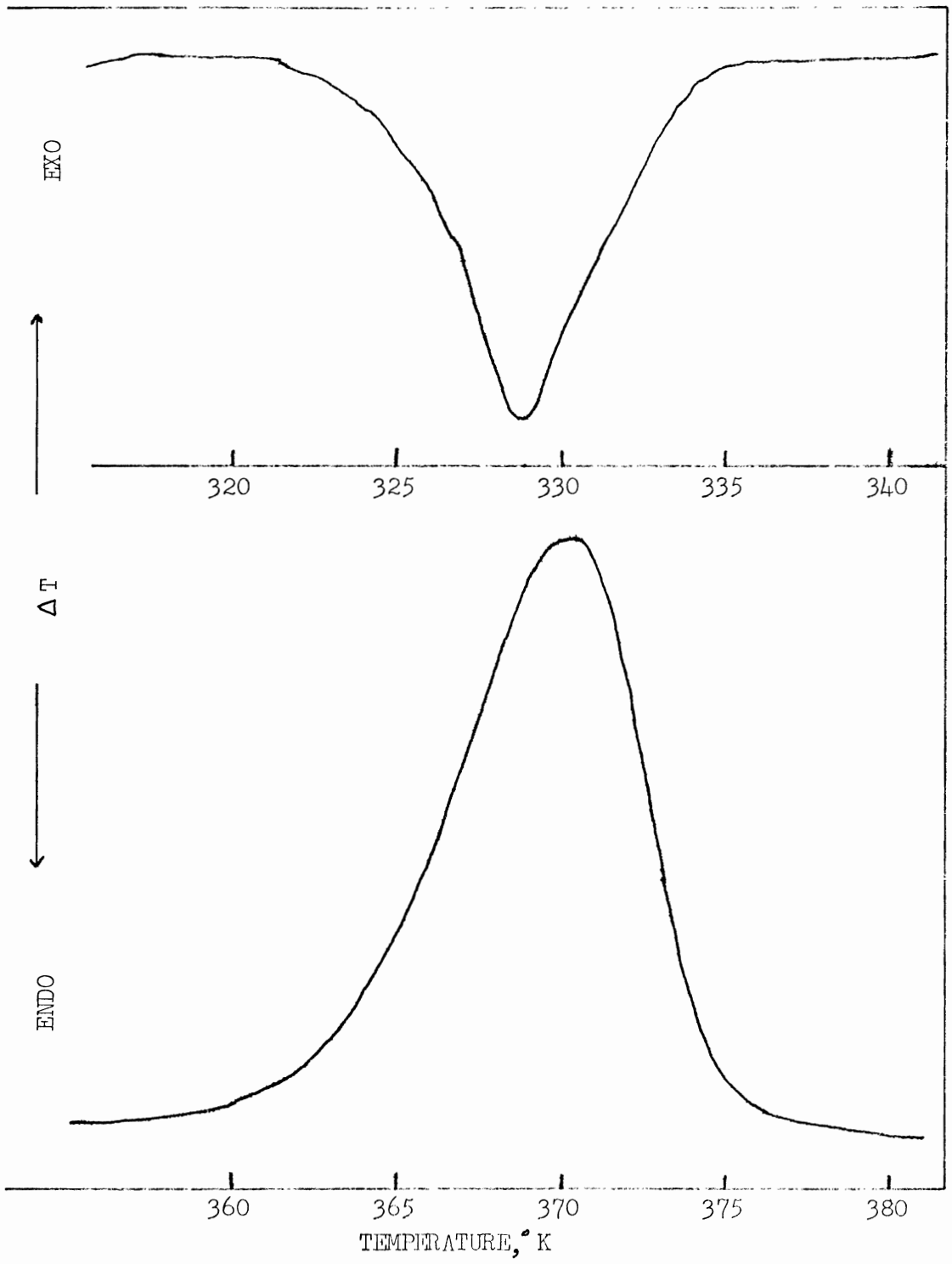

FIGURE B.12

DSC THERMOGRAM of RED AMORPHOUS SELENIUM #8, RUN 13

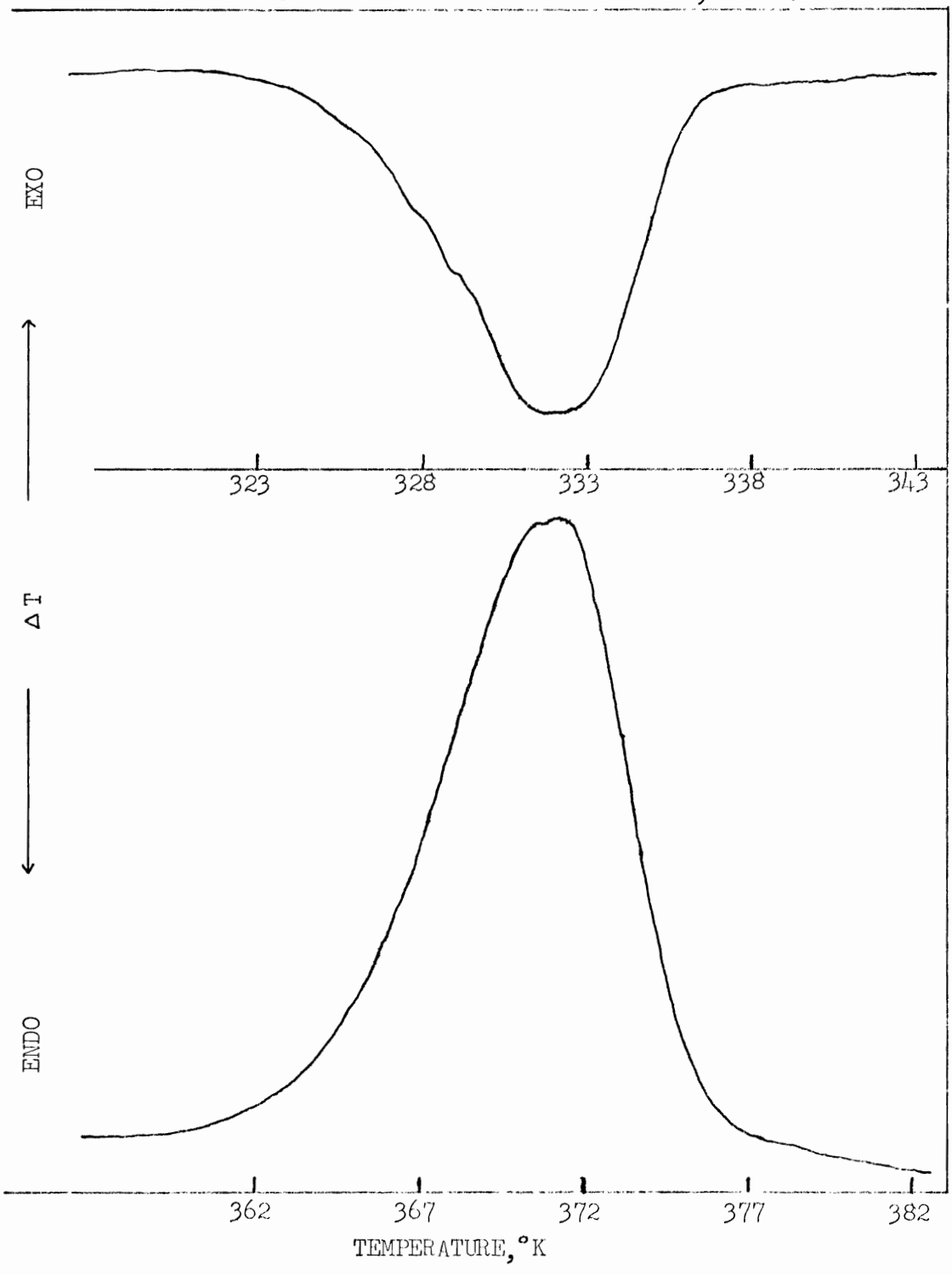

FIGURE B.13

DSC THERMOGRAM of RED AMORPHOUS SELENIUM #7, RUN 12

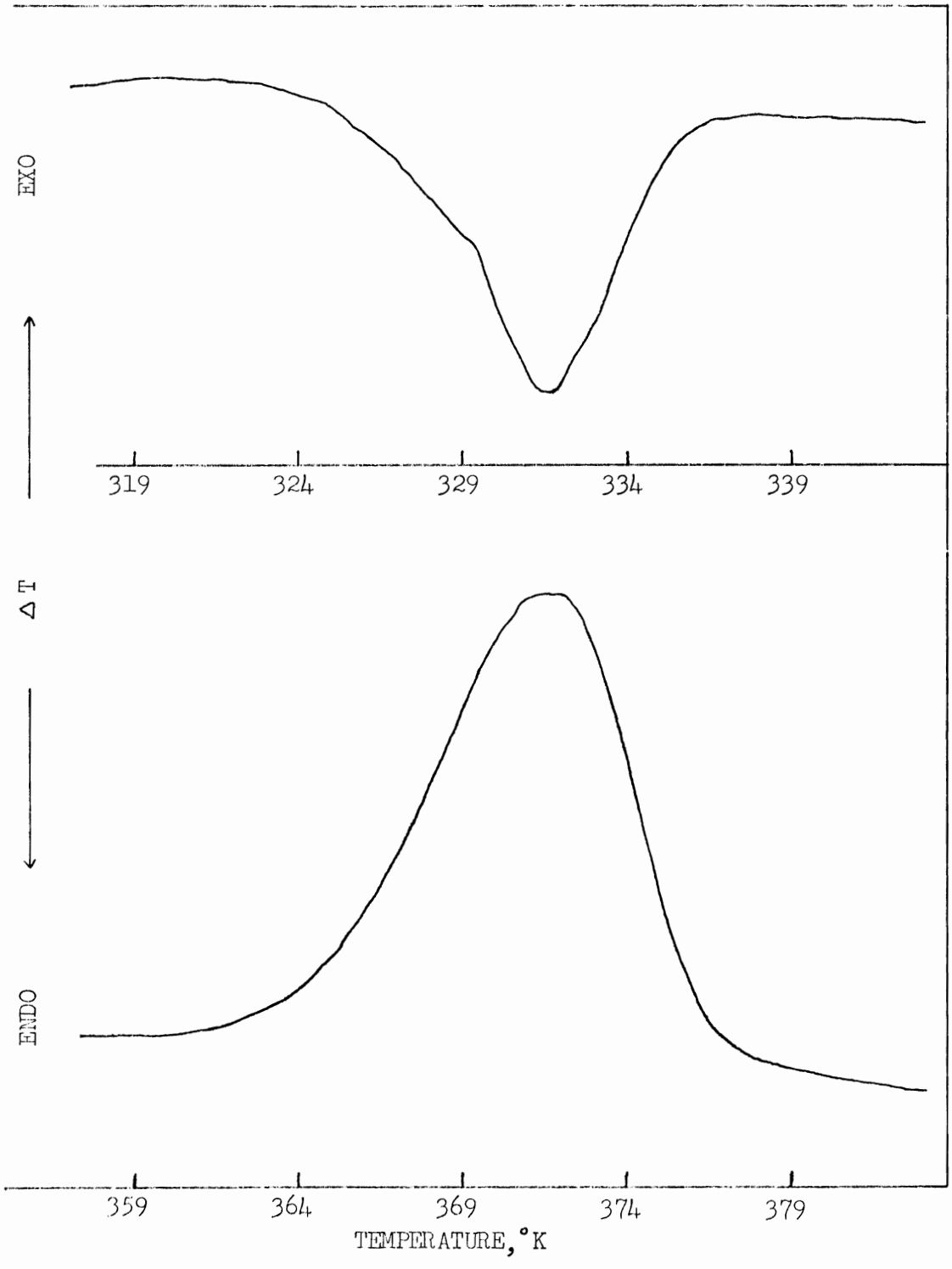

FIGURE B.14

DSC THERMOGRAM of RED AMORPHOUS SELENIUM #6, RUN 19

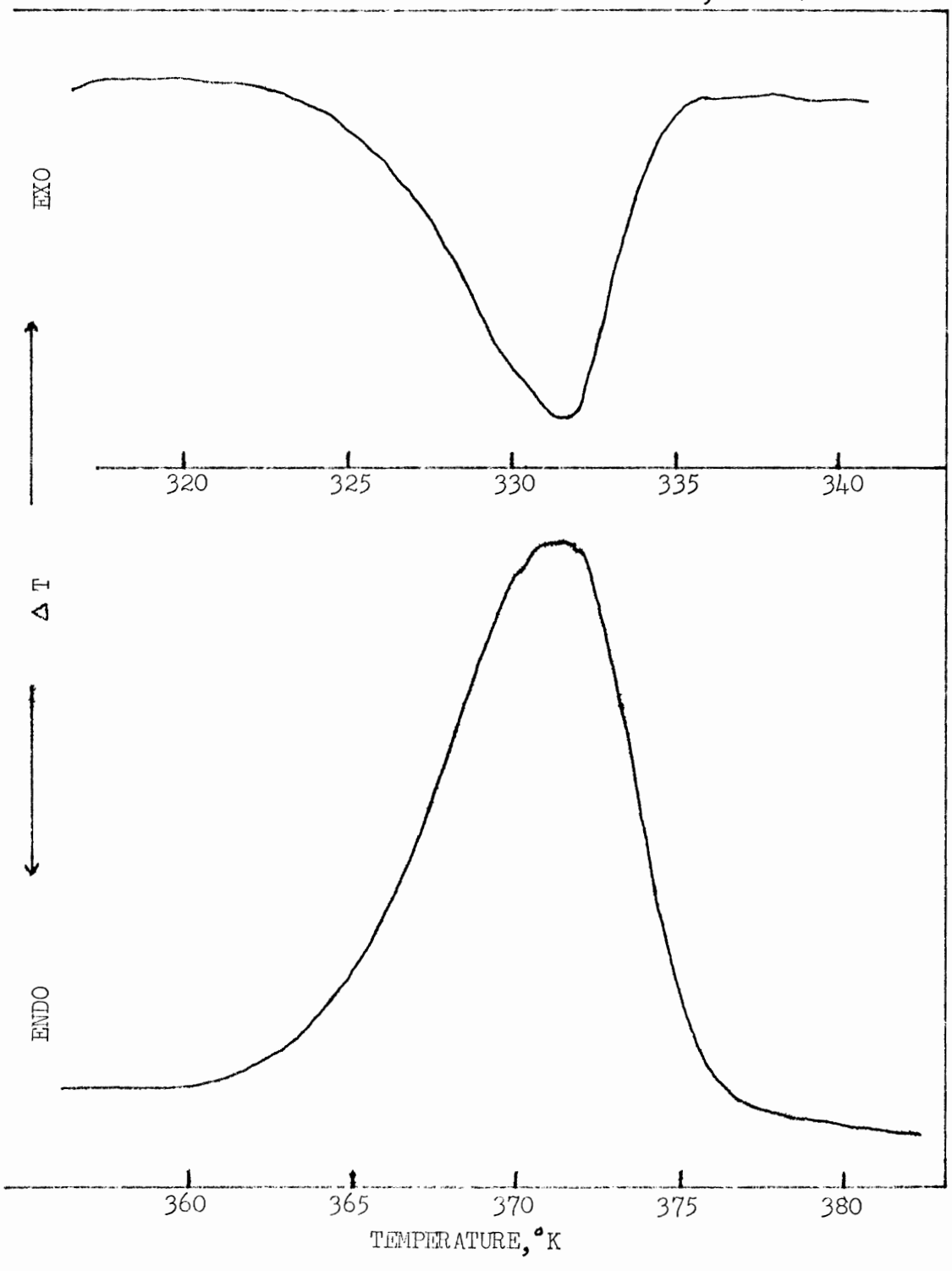

FIGURE B.15

DSC THERMOGRAM of RED AMORPHOUS SELENIUM #5, RUN 2

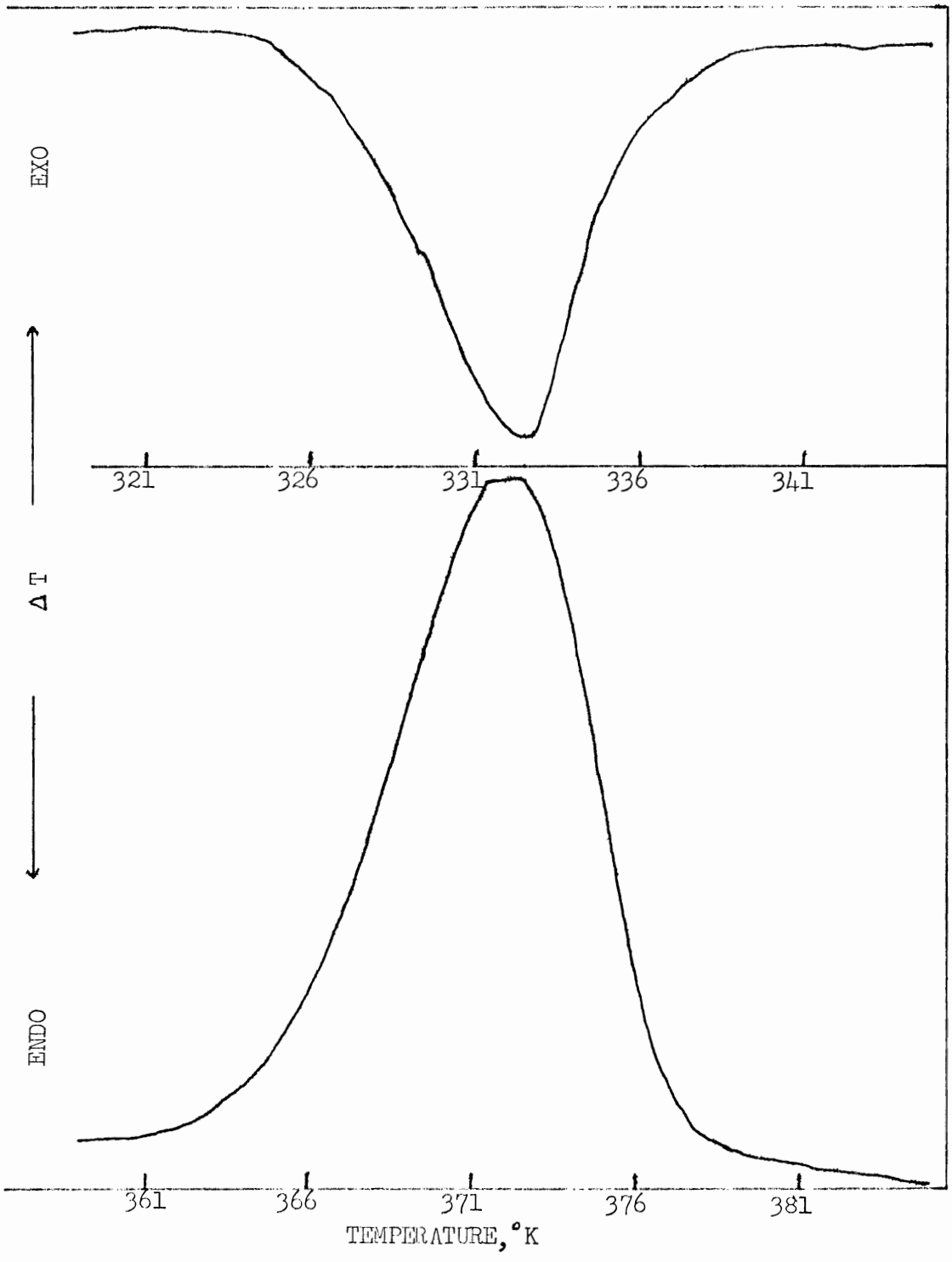

FIGURE B.16

DSC THERMOGRAM of RED AMORPHOUS SELENIUM #4, RUN 5

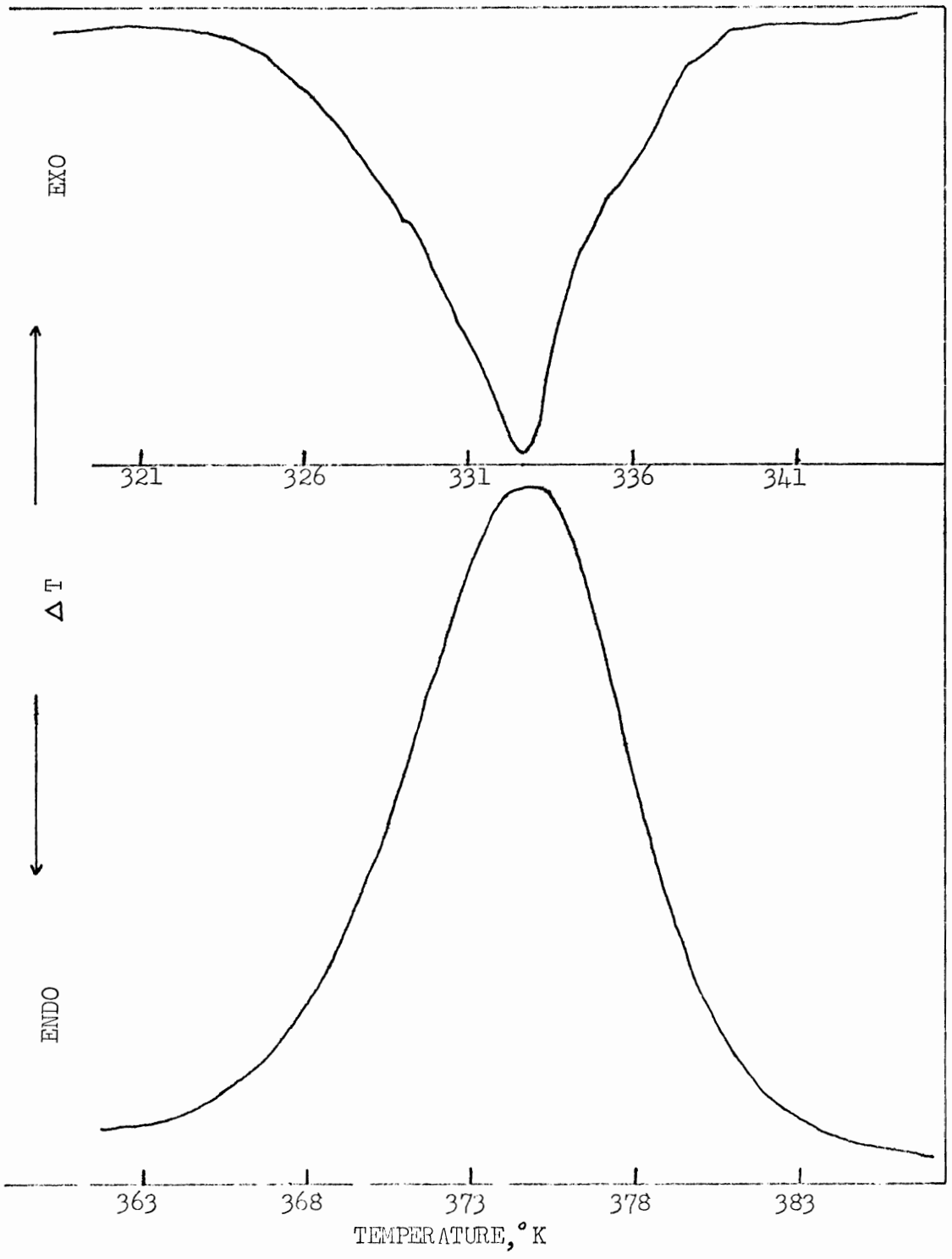

APPENDIX C

Low Temperature (77-323°K) Thermograms of Red Amorphous Selenium stored at 273°K

Table C.I

Experimental Data Accompanying Figures C.1 to C.12

Figure No.	Sample Wt. (mg)	Reference Wt. (mg)	Sample Atmosphere	ΔT (°K/in)	Age (days)
C.1	14.4	59.4	air	0.1	254
C.2	17.2	59.4	nitrogen/air	0.1	254
C.3	15.4	72.7	air	0.2	42
C.4	14.7	64.0	nitrogen	0.2	55
C.5	13.4	38.8	nitrogen	0.1	84
C.6	15.7	38.8	air	0.1	95
C.7	----	72.3	nitrogen	0.1	125
C.8	39.9	39.6	nitrogen	0.1	159
C.9	13.5	66.8	nitrogen	0.1	42
C.10	16.5	54.0	nitrogen	0.1	112
C.11	9.5	61.3	nitrogen	0.1	113
C.12	12.4	37.3	nitrogen	0.1	191

Table C.II

Temperature Corrections for Chromel-Alumel Thermocouples*

Correct Temperature (°K)	Observed Temperature (°K)
83	133
105	143
123	153
140	163
155	173
169	183
183	193
195	203
207	213
219	223
230	233
241	243
252	253
263-323	263-323
332	333
342	343
352	353
361	363
371	373

* Provided with the Du Pont 900 DTA instrument

FIGURE C.1A

DTA THERMOGRAM of RED AMORPHOUS SELENIUM #4,RUN 19

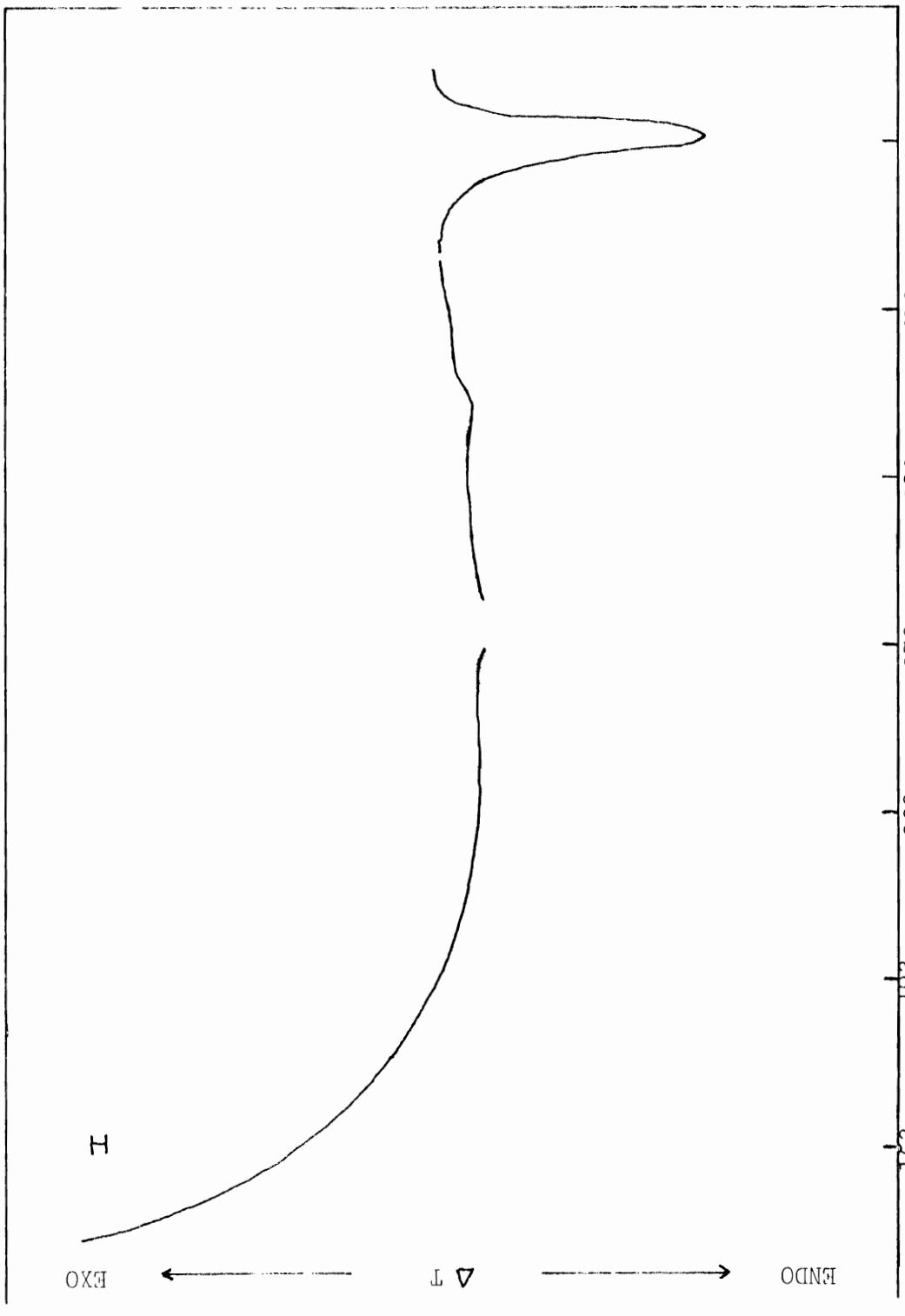

FIGURE C.1B

DTA THERMOGRAM of RED AMORPHOUS SELENIUM #4, RUN 19

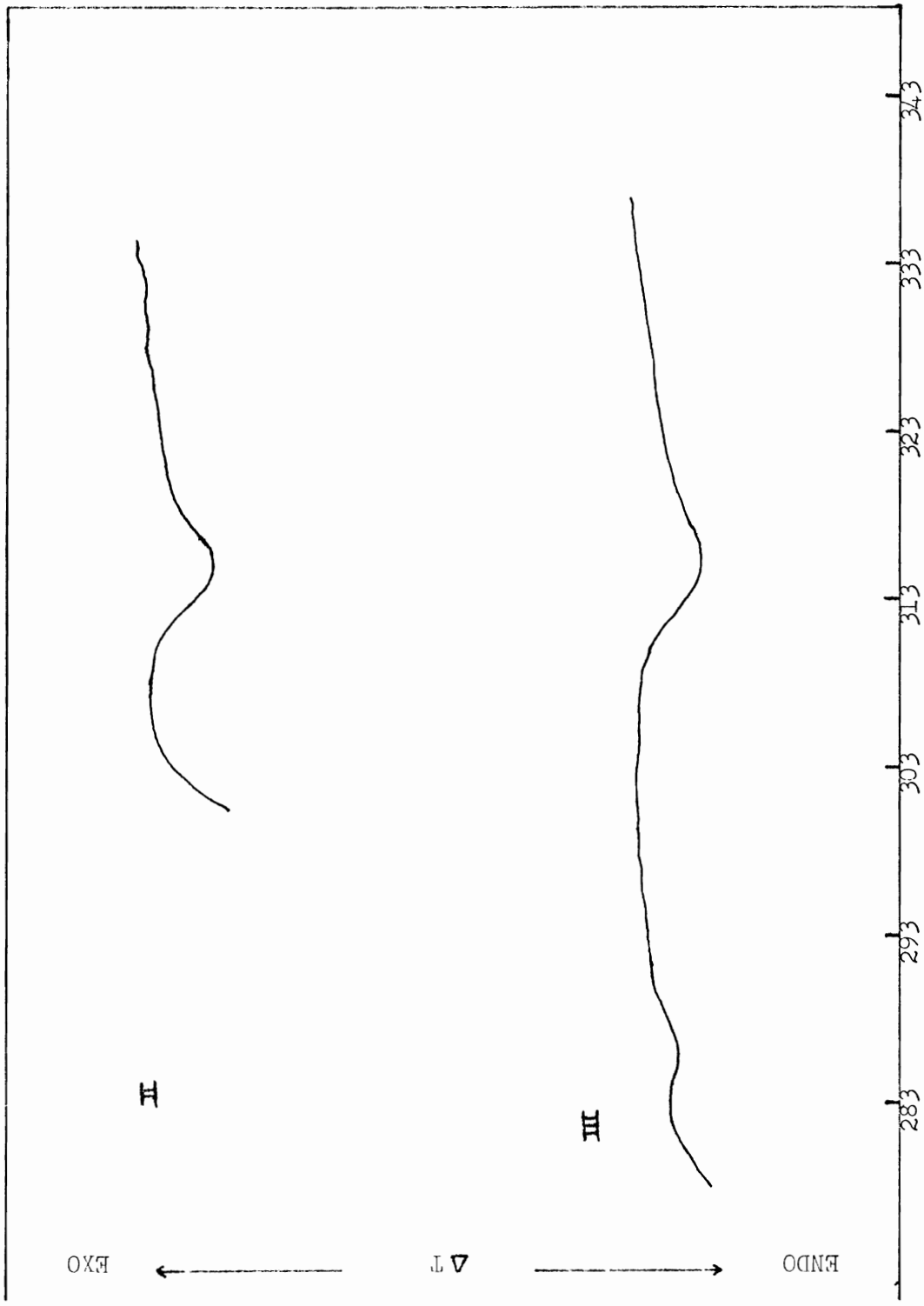

FIGURE C.2A

DTA THERMOGRAM of RED AMORPHOUS SELENIUM #4, RUN 18

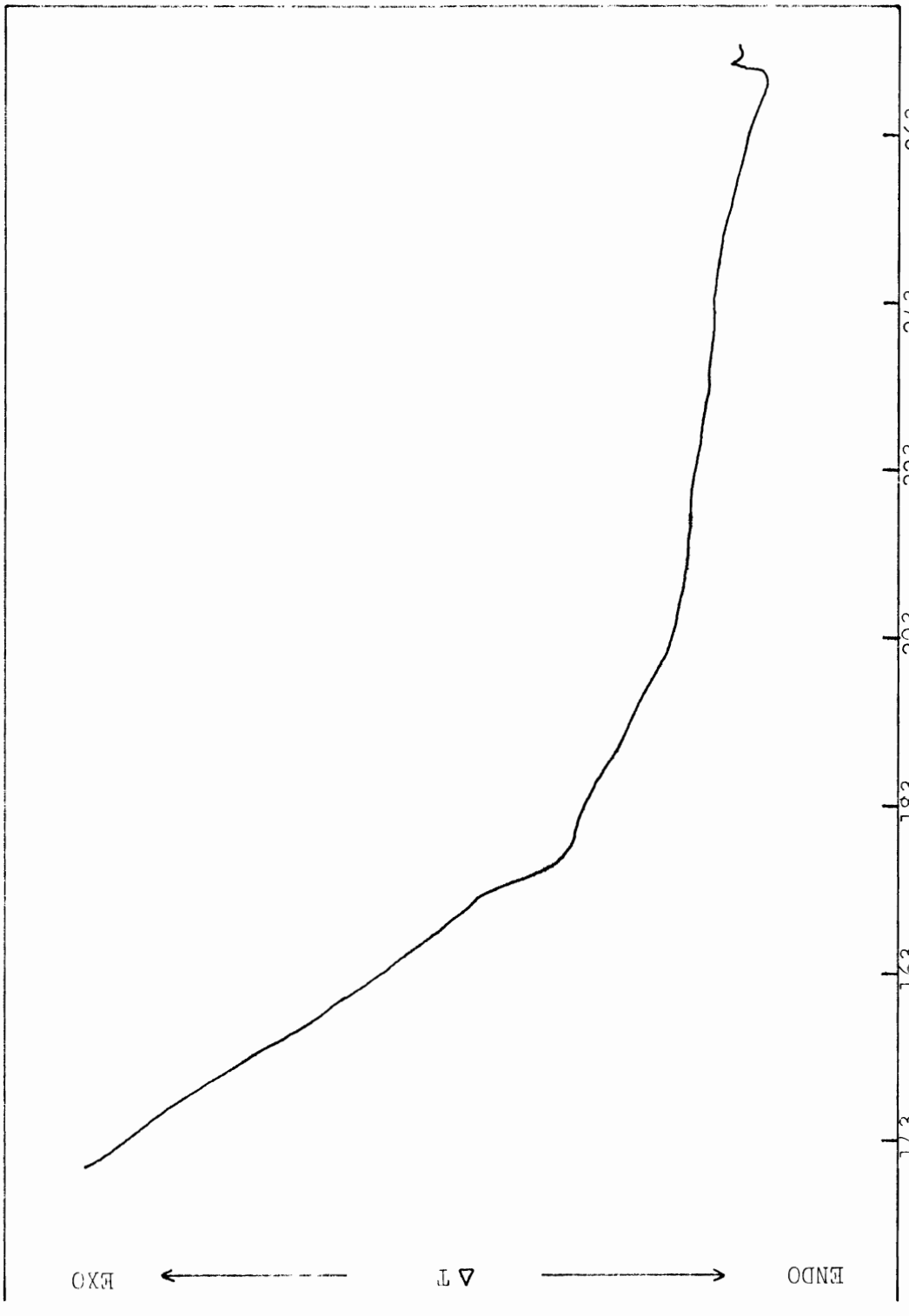

FIGURE C.2B

DTA THERMOGRAM of RED AMORPHOUS SELENIUM #4, RUN 18

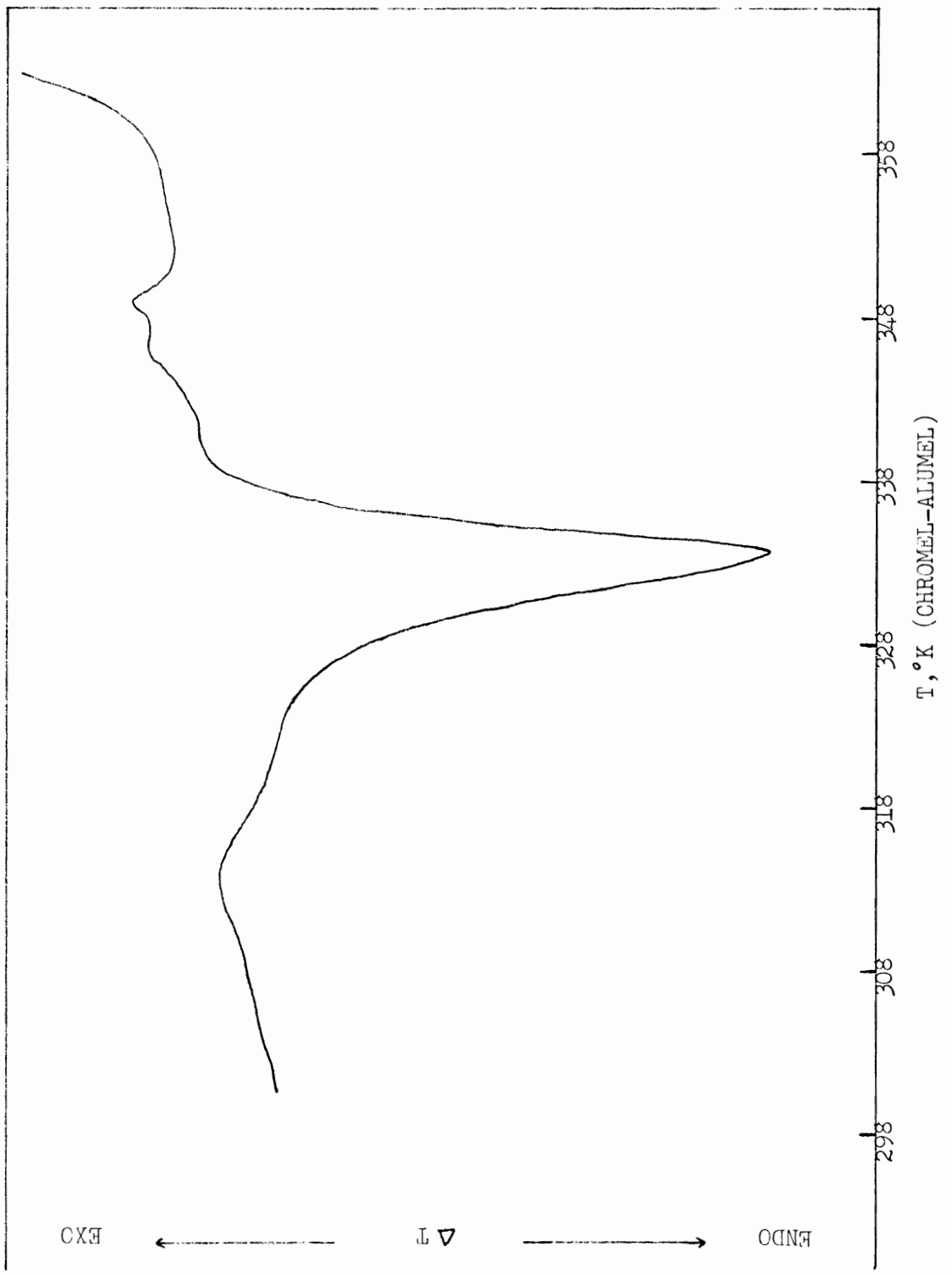

FIGURE C.3A

DTA THERMOGRAM of RED AMORPHOUS SELENIUM #5, RUN 12

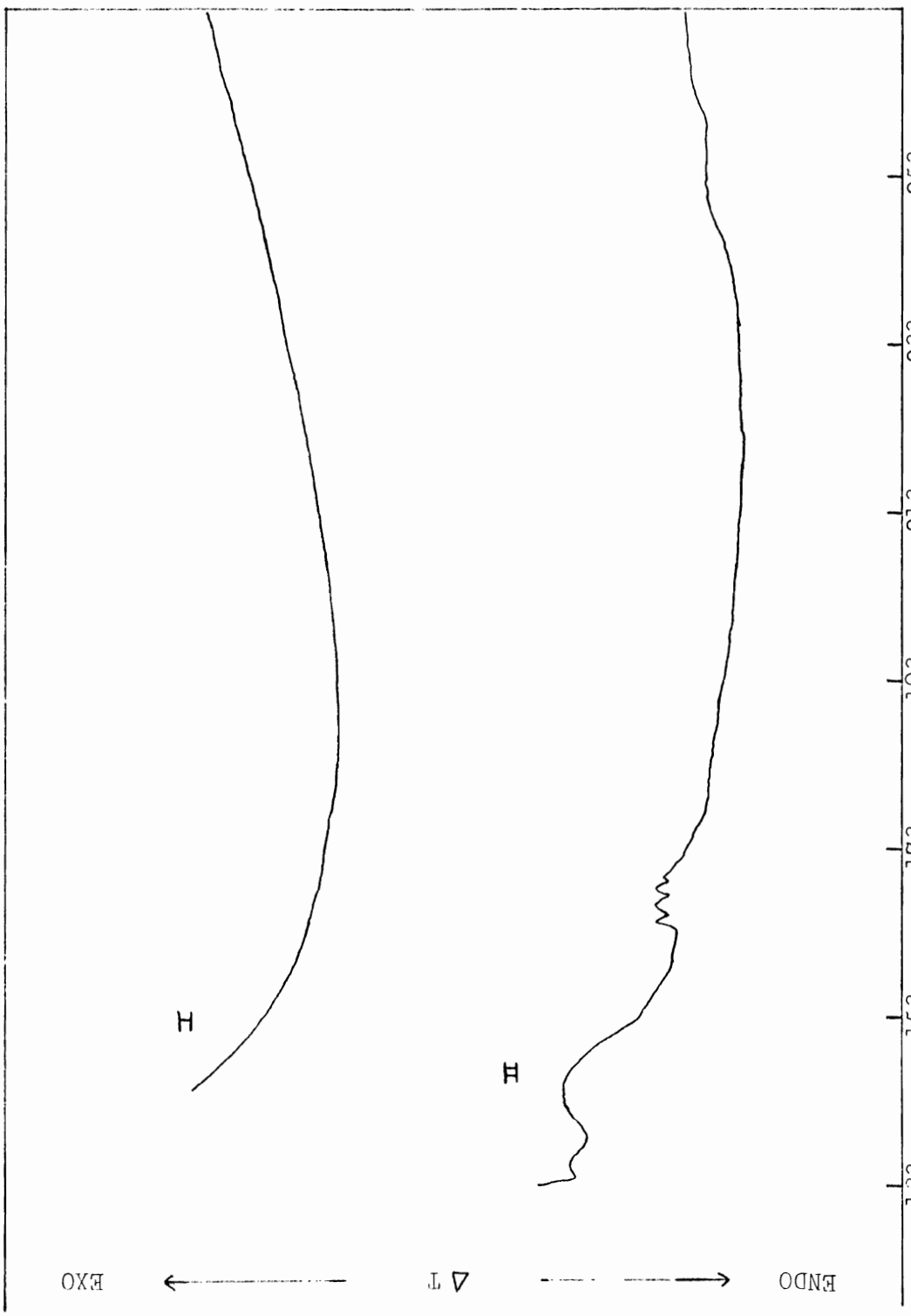

FIGURE C.4A

DTA THERMOGRAM of RED AMORPHOUS SELENIUM #5, RUN 13

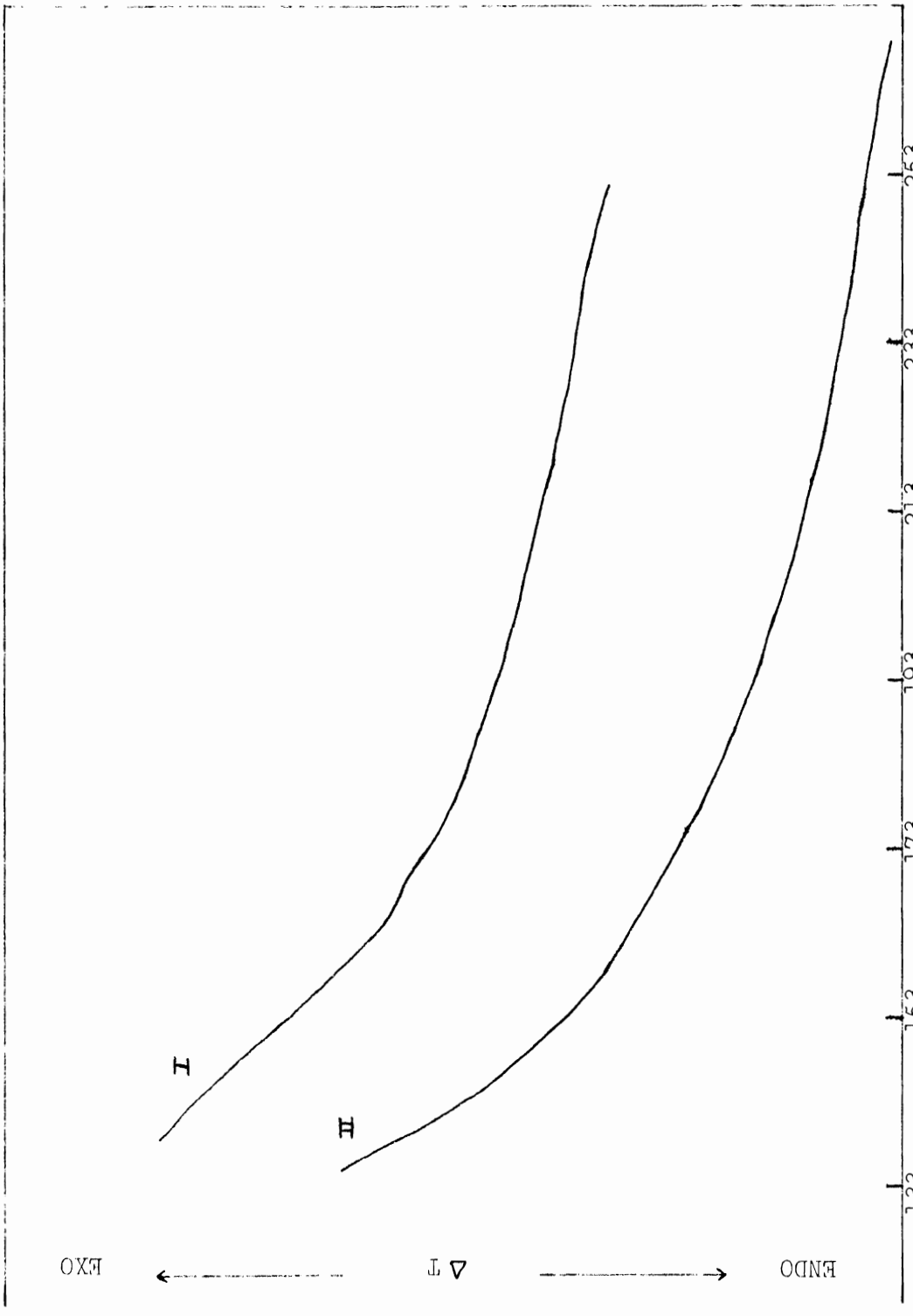

FIGURE C.5A

DTA THERMOGRAM of RED AMORPHOUS SELENIUM #5, RUN 16

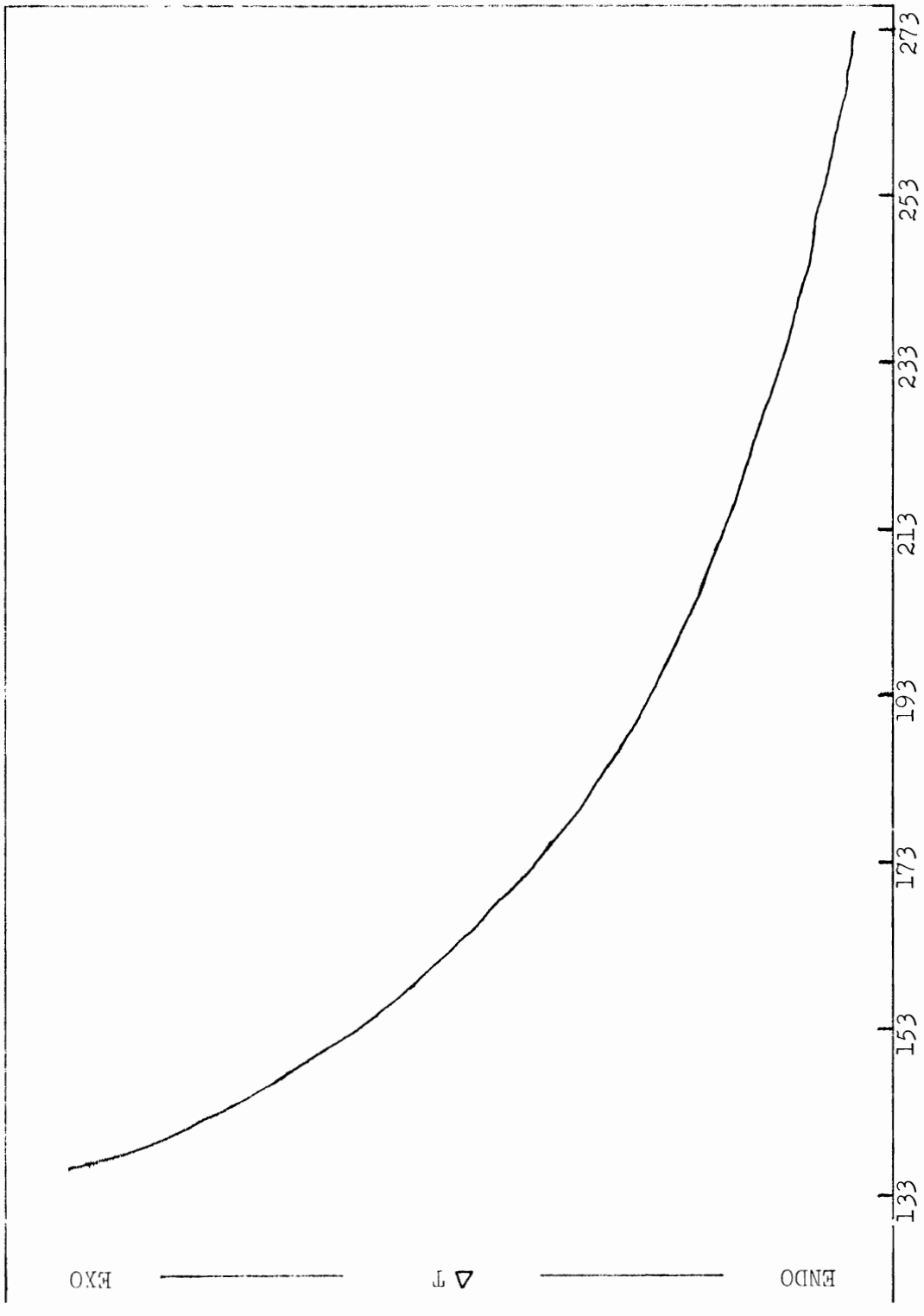

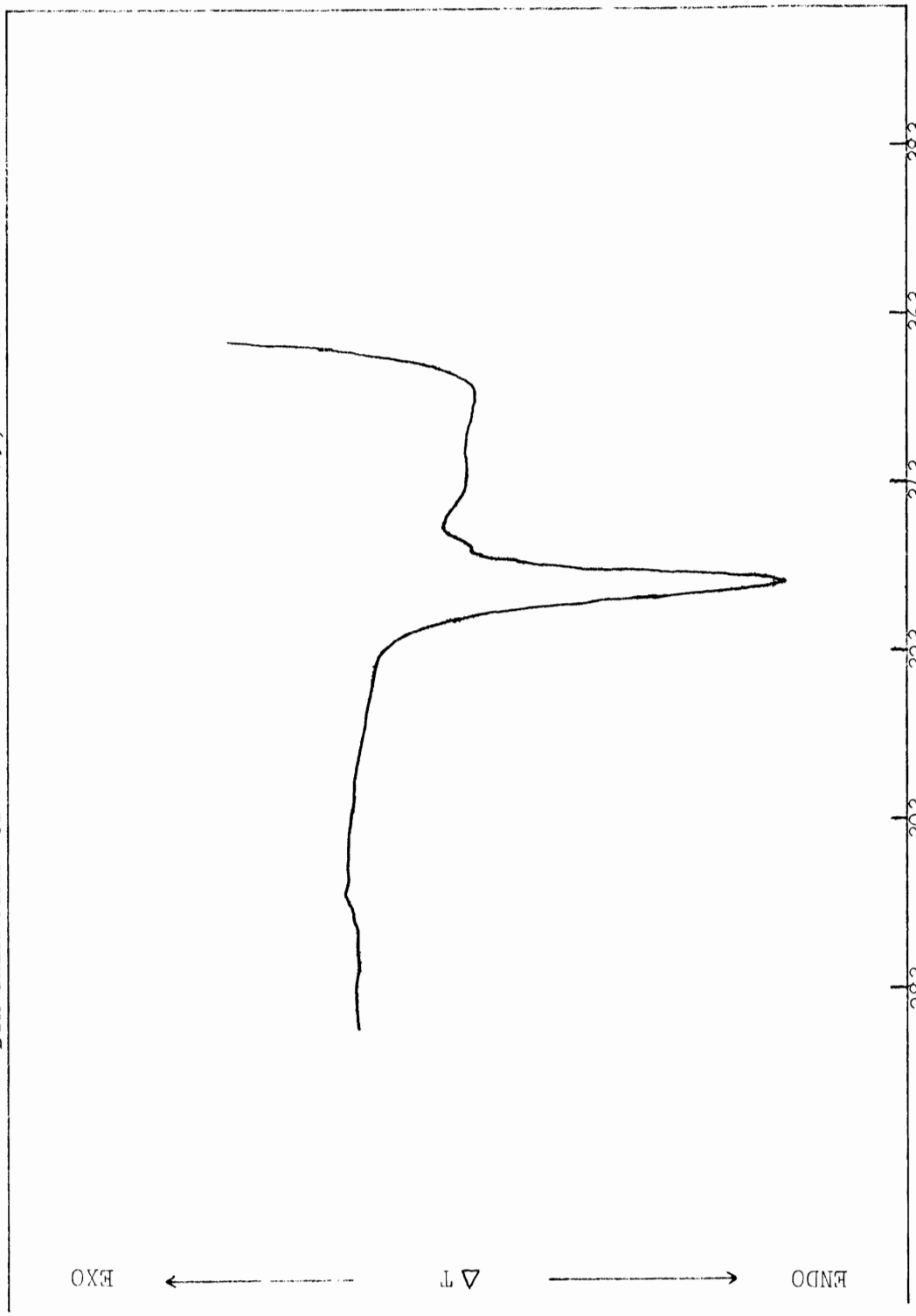

FIGURE C.5B

DTA THERMOGRAM of RED AMORPHOUS SELENIUM #5, RUN 16

FIGURE C.6A

DTA THERMOGRAM of RED AMORPHOUS SELENIUM #5, RUN 19

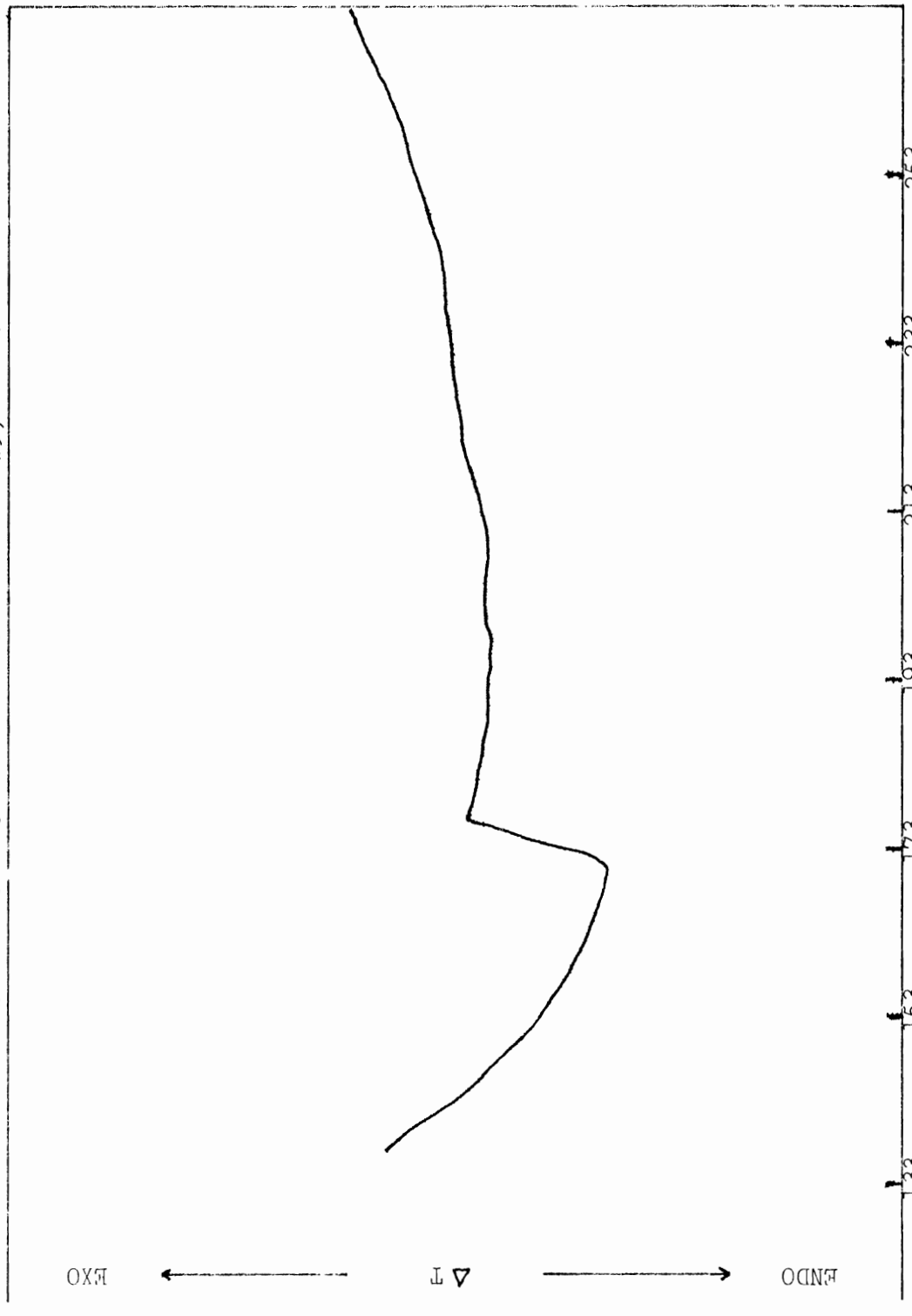

FIGURE C.6B

DTA THERMOGRAM of RED AMORPHOUS SELENIUM #5, RUN 19

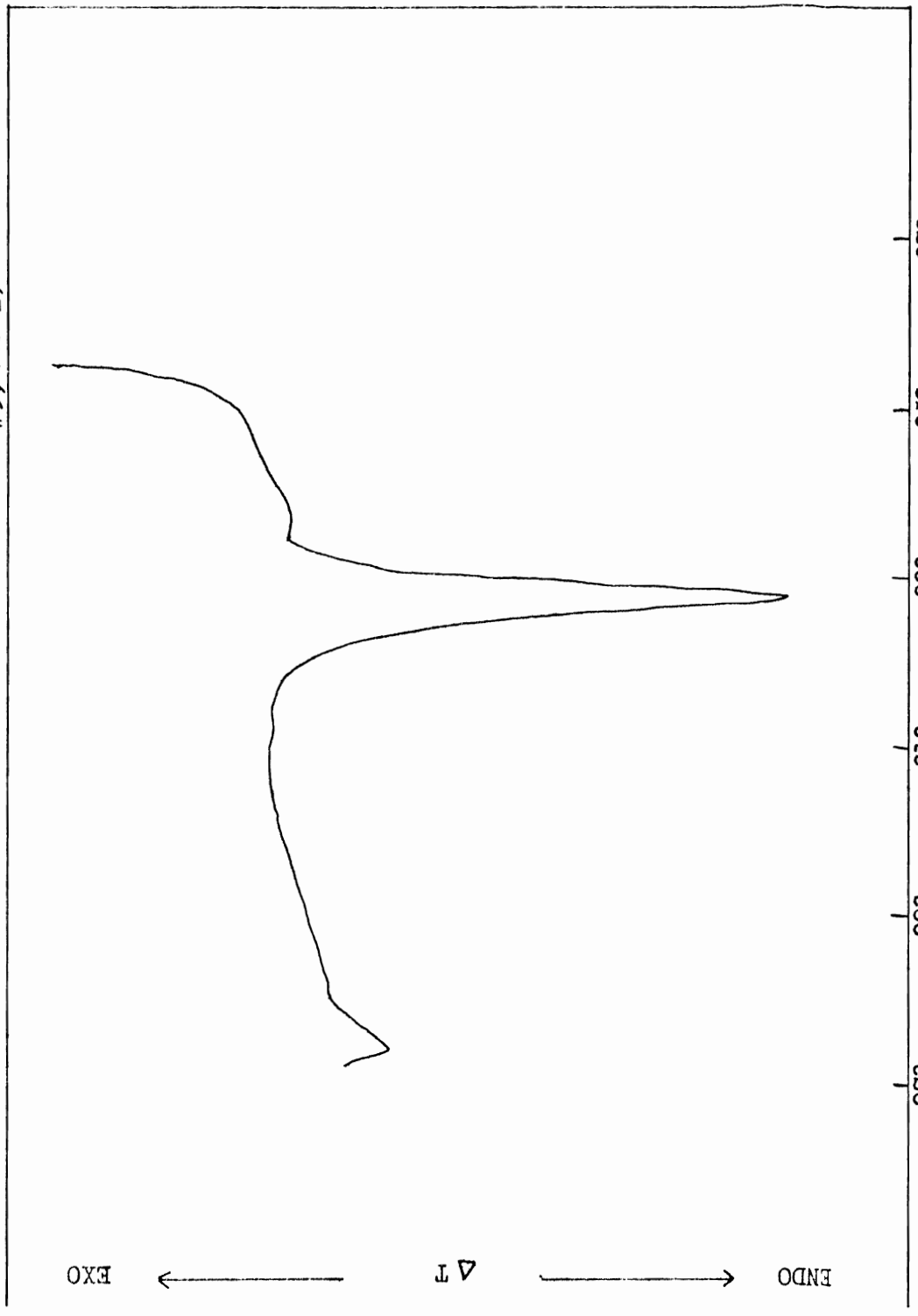

FIGURE C.7A

DTA THERMOGRAM of RED AMORPHOUS SELENIUM #6, RUN 6

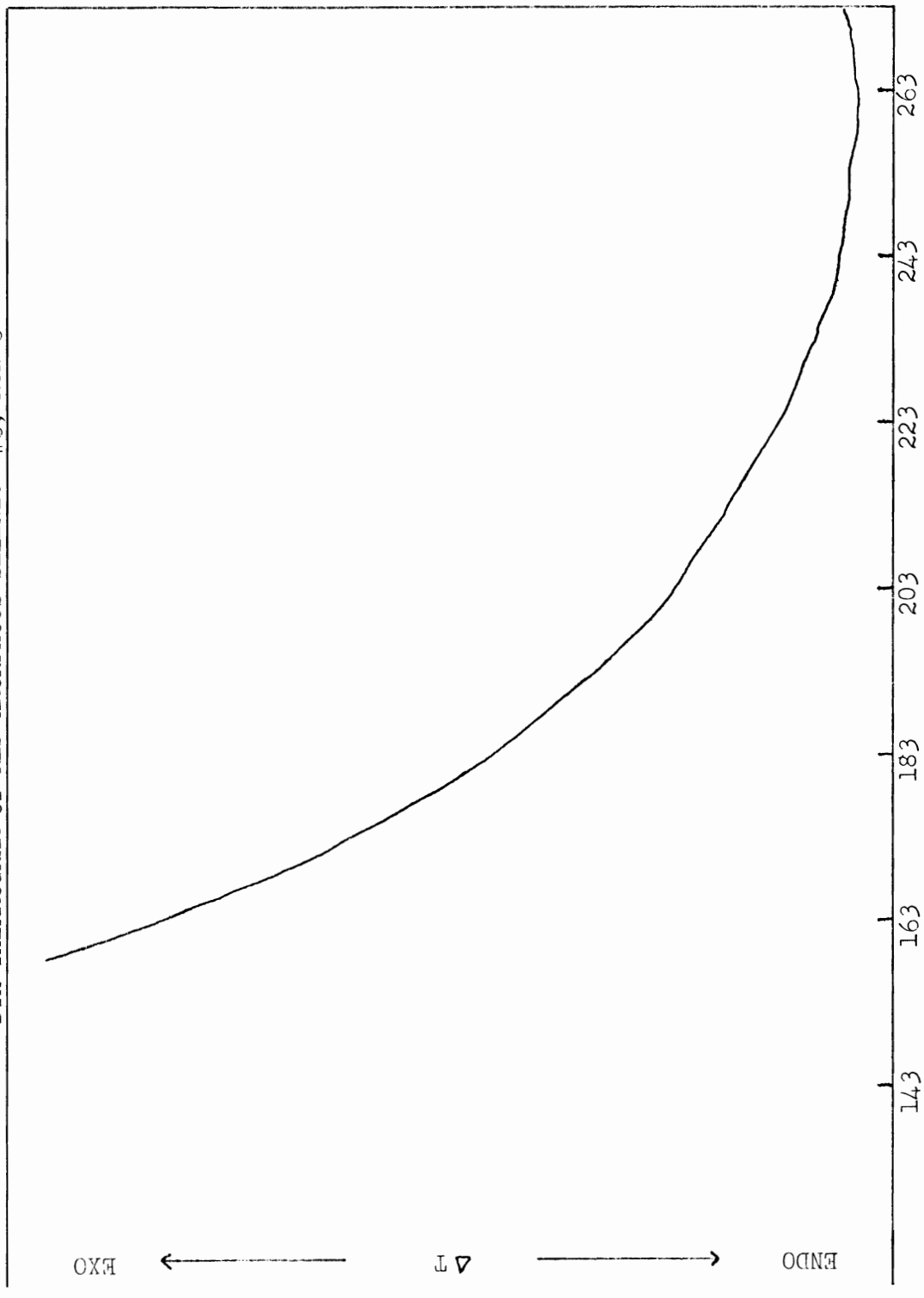

FIGURE C.7B

DTA THERMOGRAM of RED AMORPHOUS SELENIUM #6, RUN 6

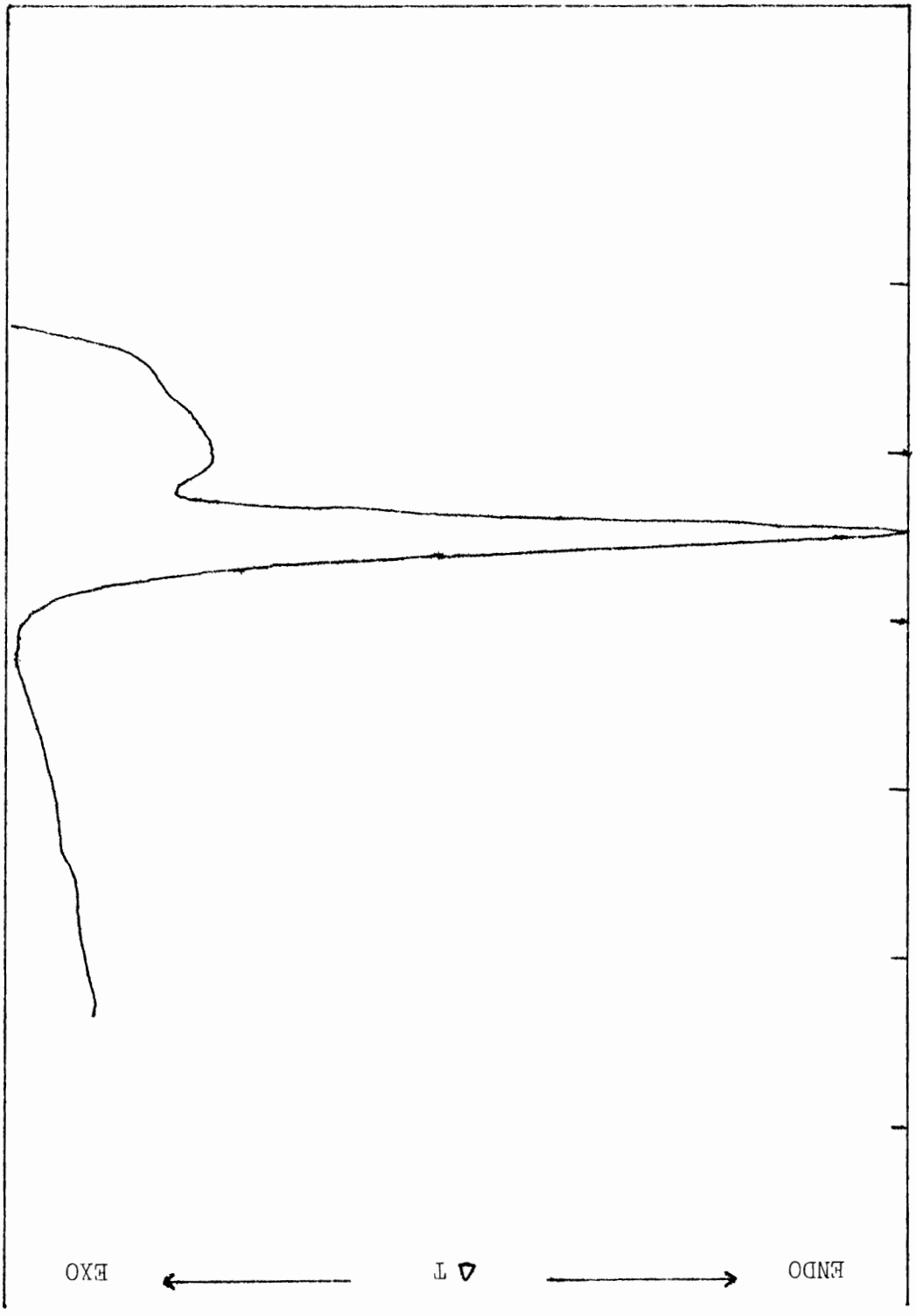

FIGURE C.8A

DTA THERMOGRAM of RED AMORPHOUS SELENIUM #6, RUN 8

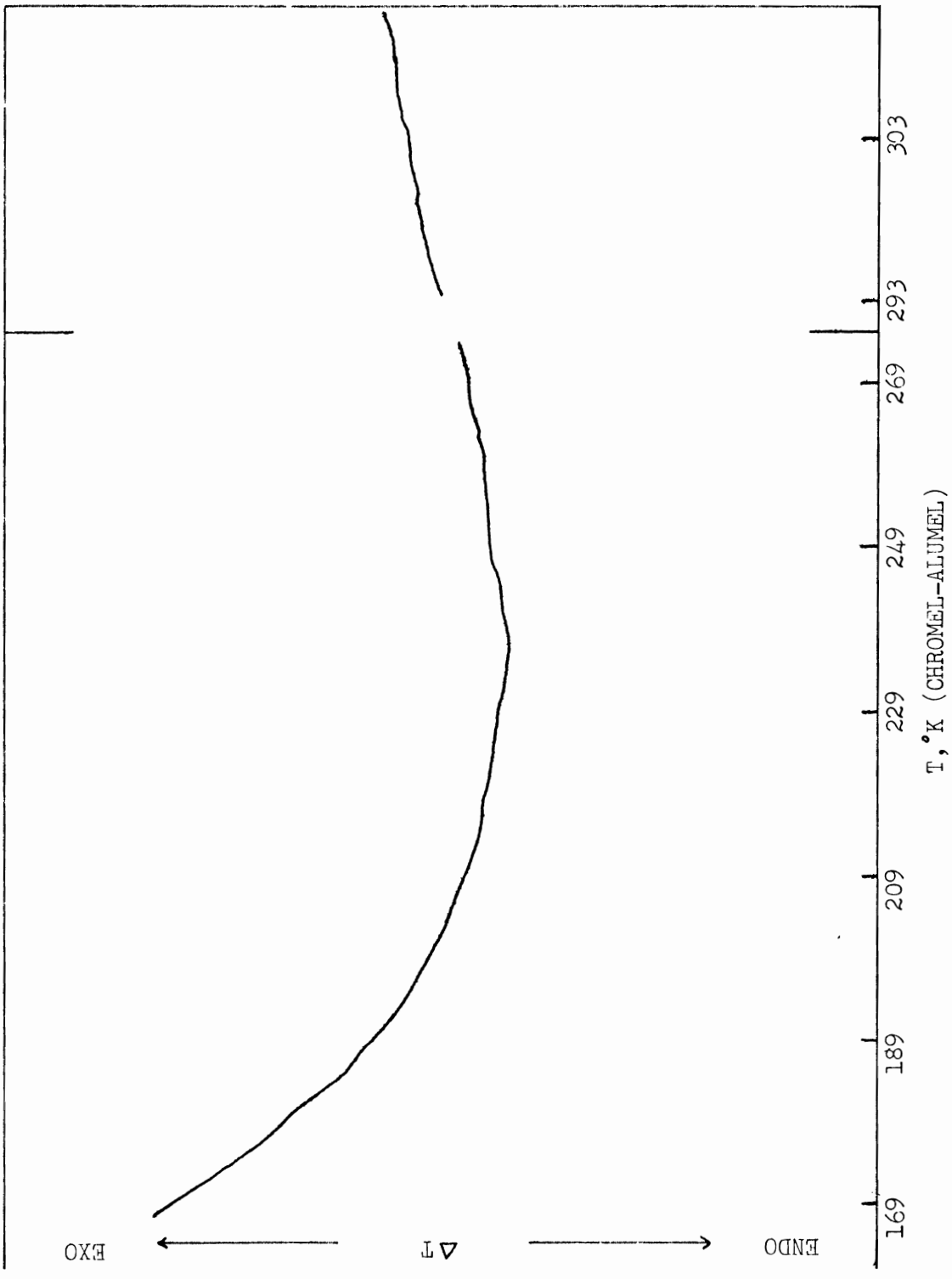

FIGURE C.9A

DTA THERMOGRAM of RED AMORPHOUS SELENIUM #7, RUN 6

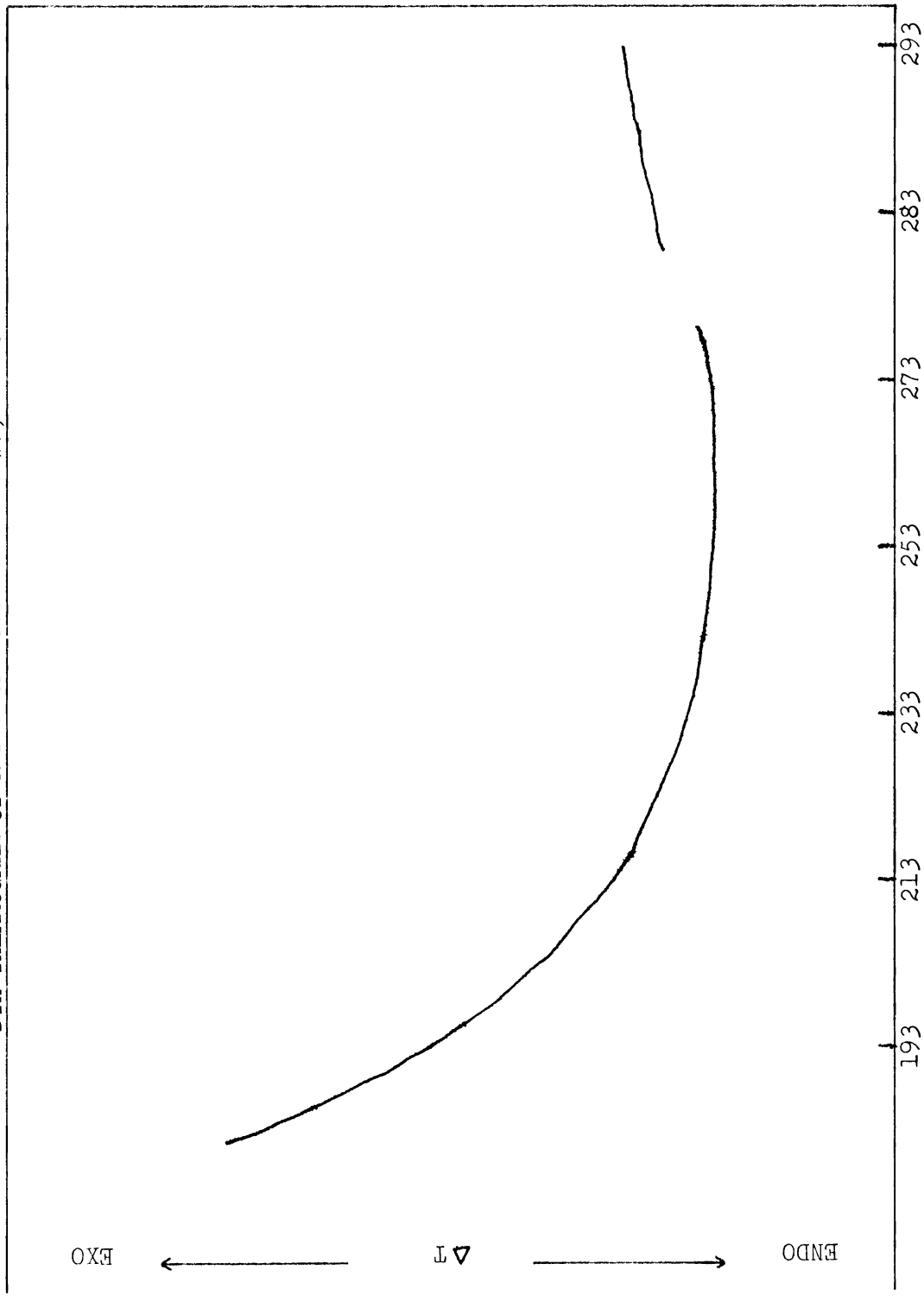

FIGURE C.9B

DTA THERMOGRAM of RED AMORPHOUS SELENIUM #7, RUN 6

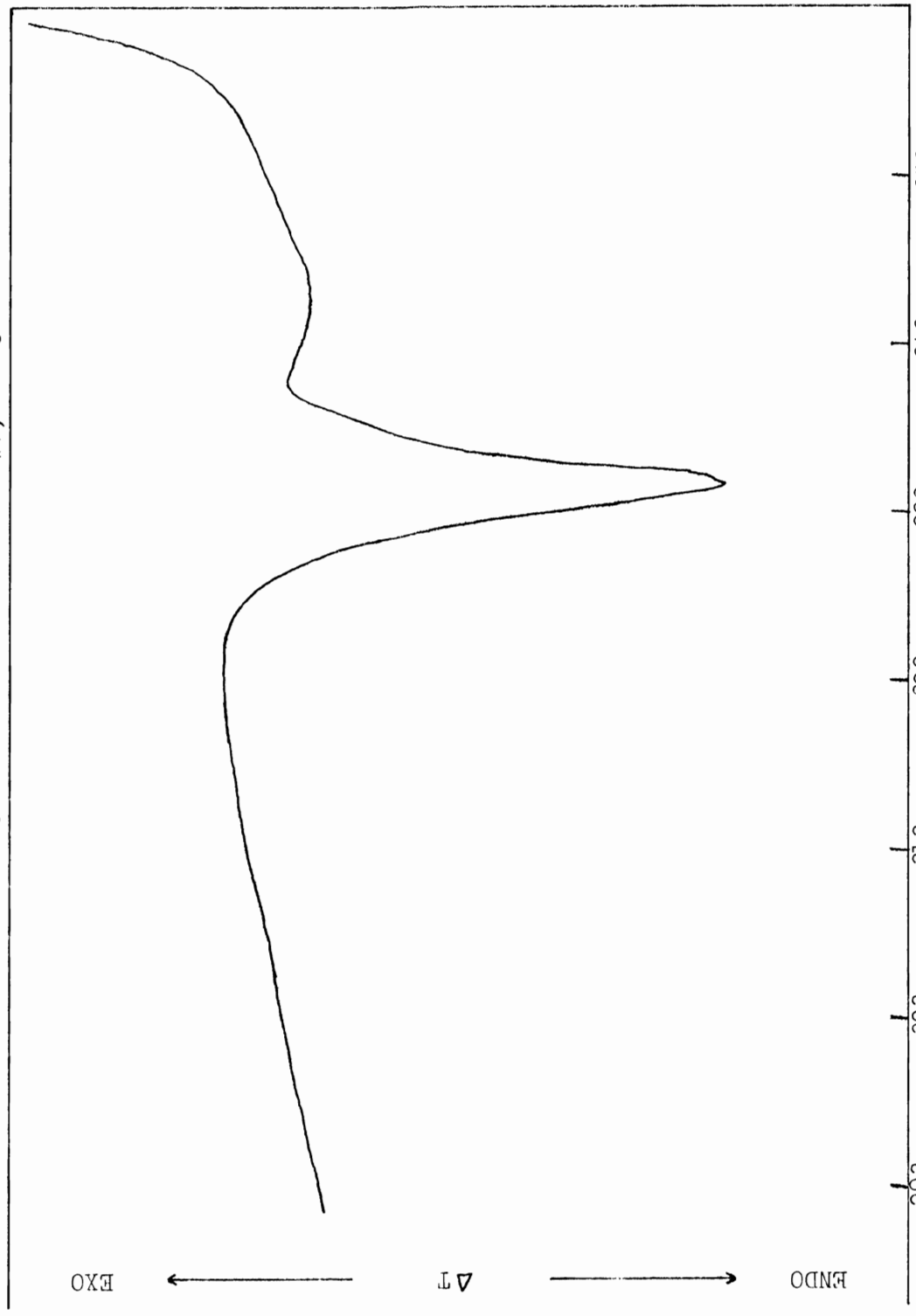

FIGURE C.10A

DTA THERMOGRAM of RED AMORPHOUS SELENIUM #7, RUN 9A

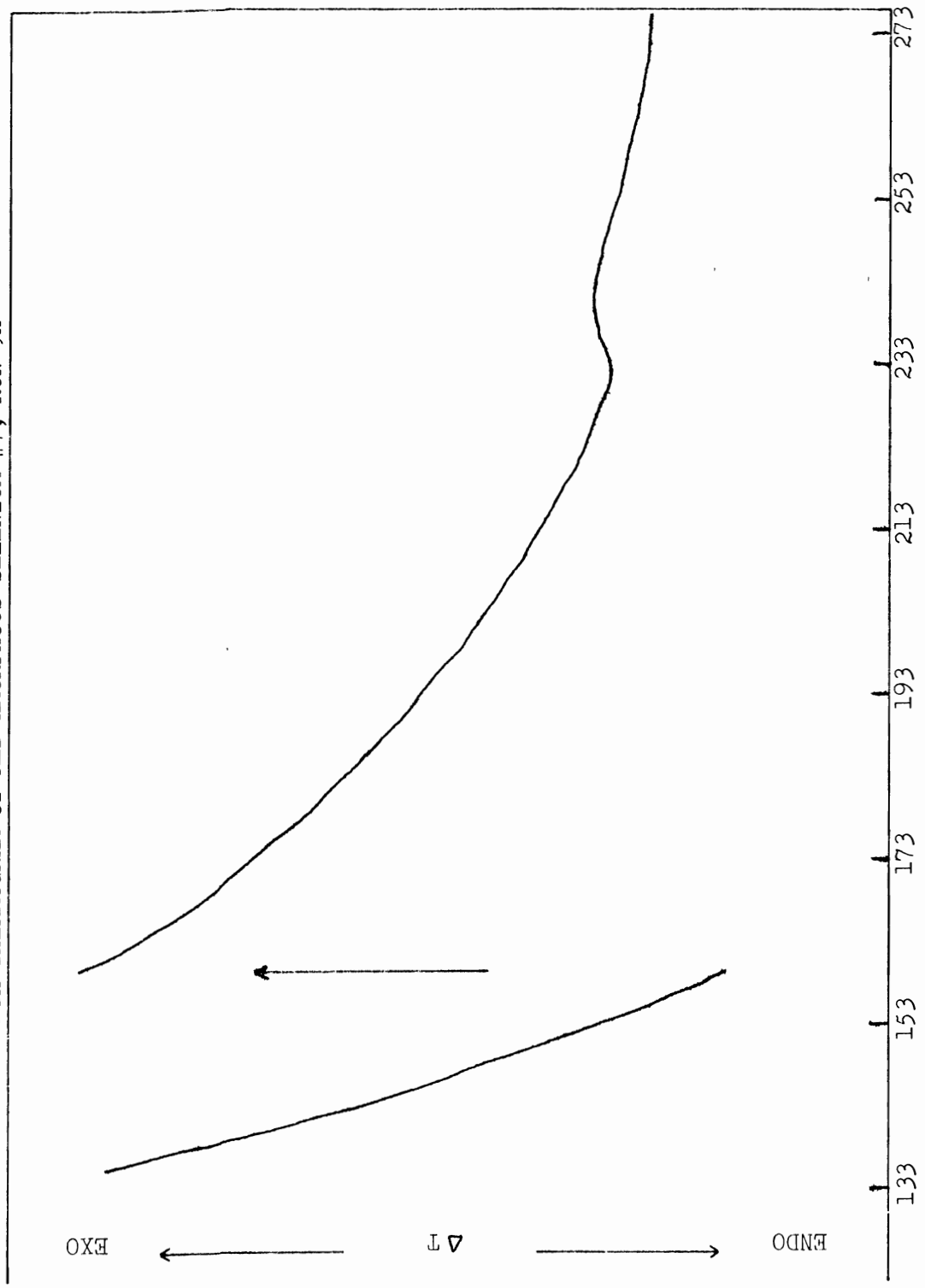

FIGURE C.10B

DTA THERMOGRAM of RED AMORPHOUS SELENIUM #7, RUN 9D

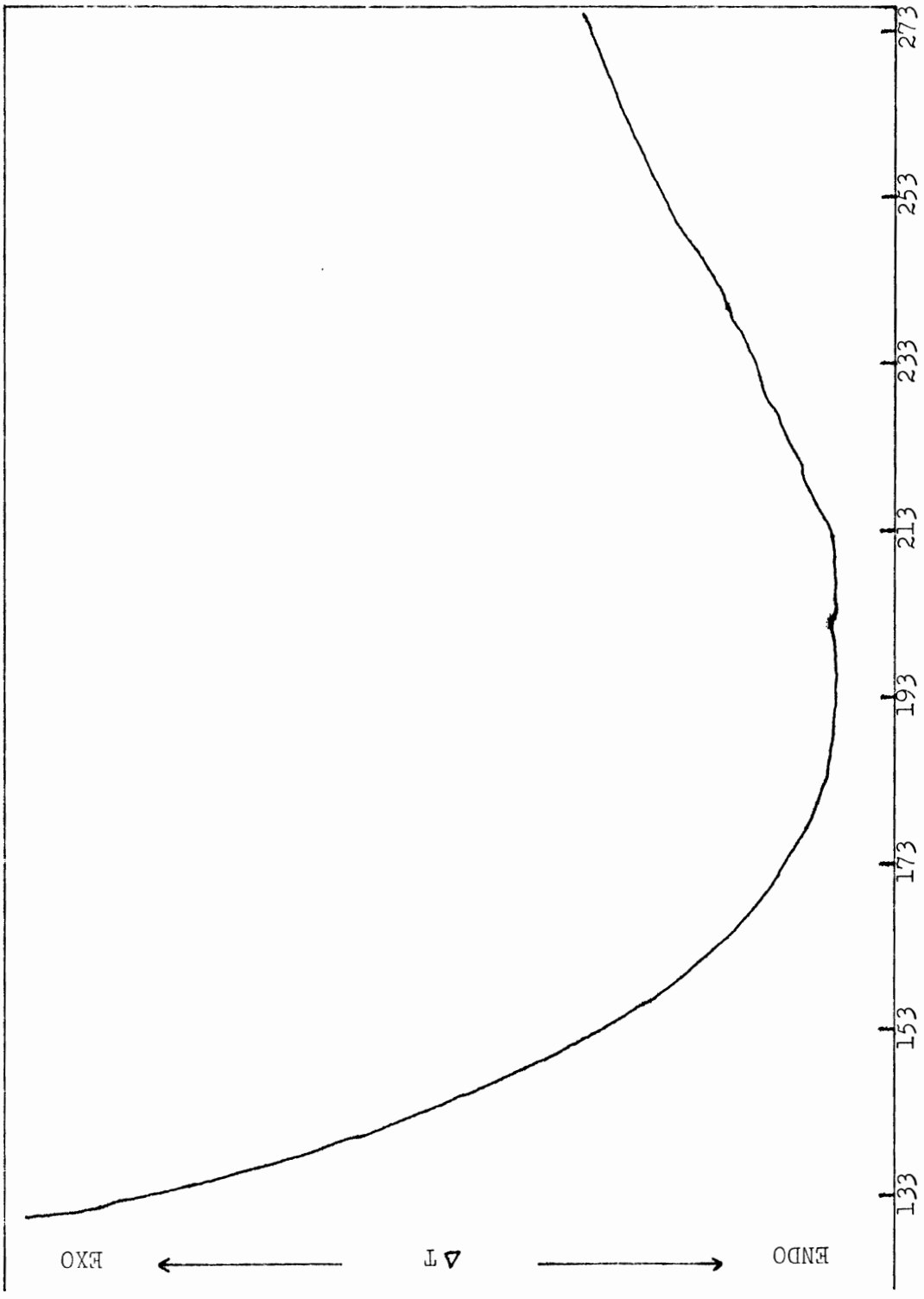

FIGURE C.10C

DTA THERMOGRAM of RED AMORPHOUS SELENIUM #7, RUN 9F

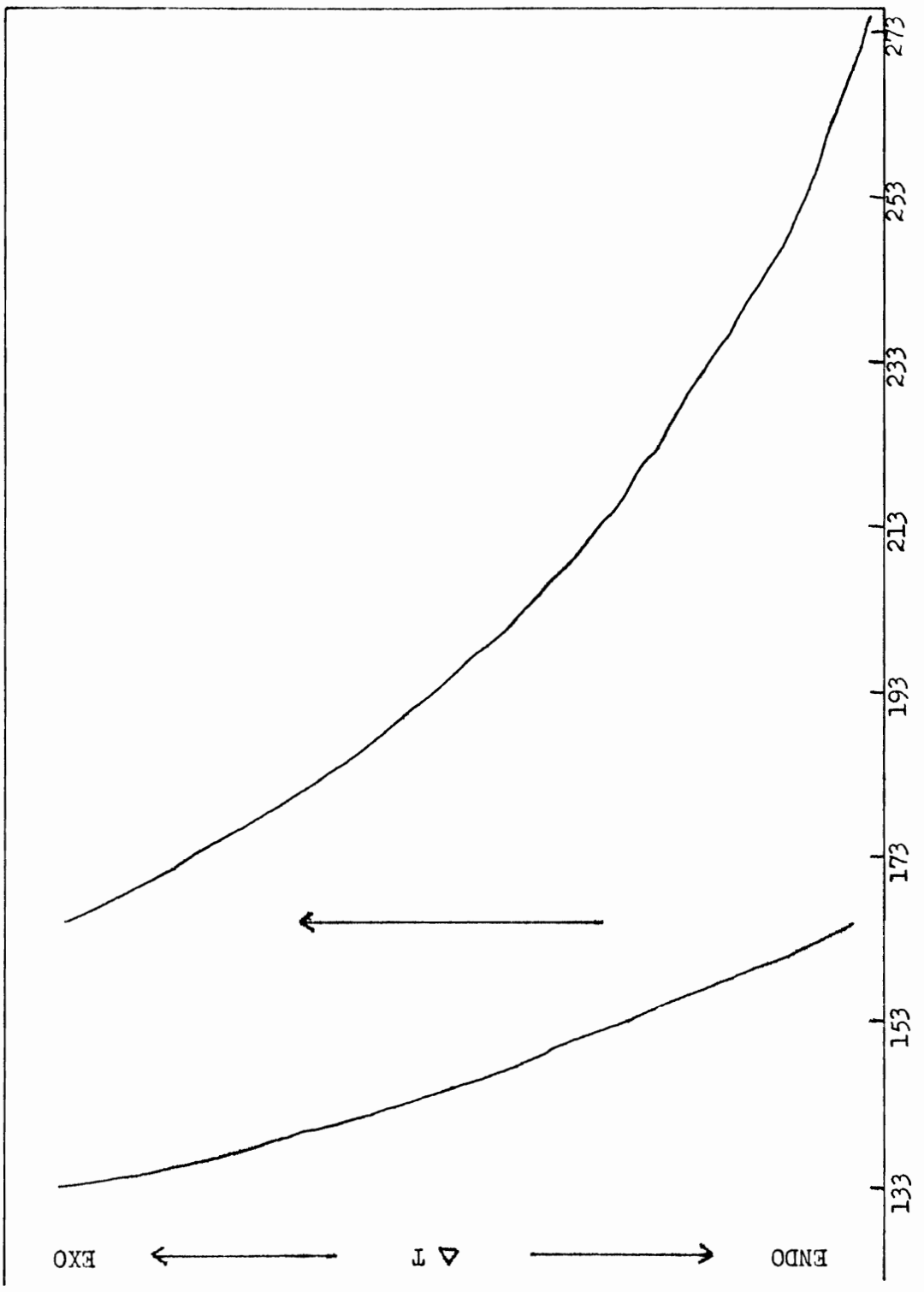

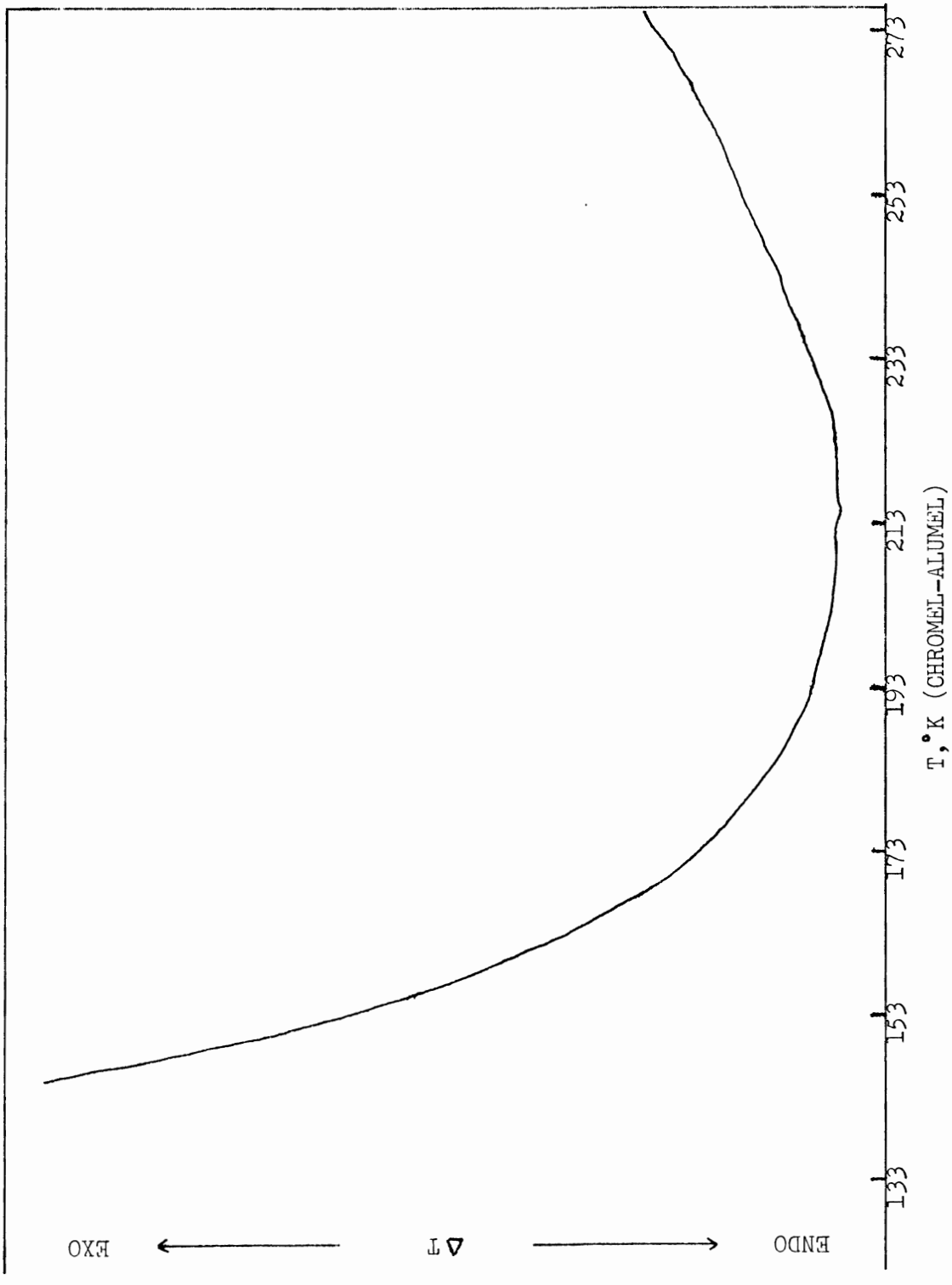

FIGURE C.10D

DTA THERMOGRAM of RED AMORPHOUS SELENIUM #7, RUN 9G

FIGURE C.10E

DTA THERMOGRAM of RED AMORPHOUS SELENIUM #7, RUN 9I

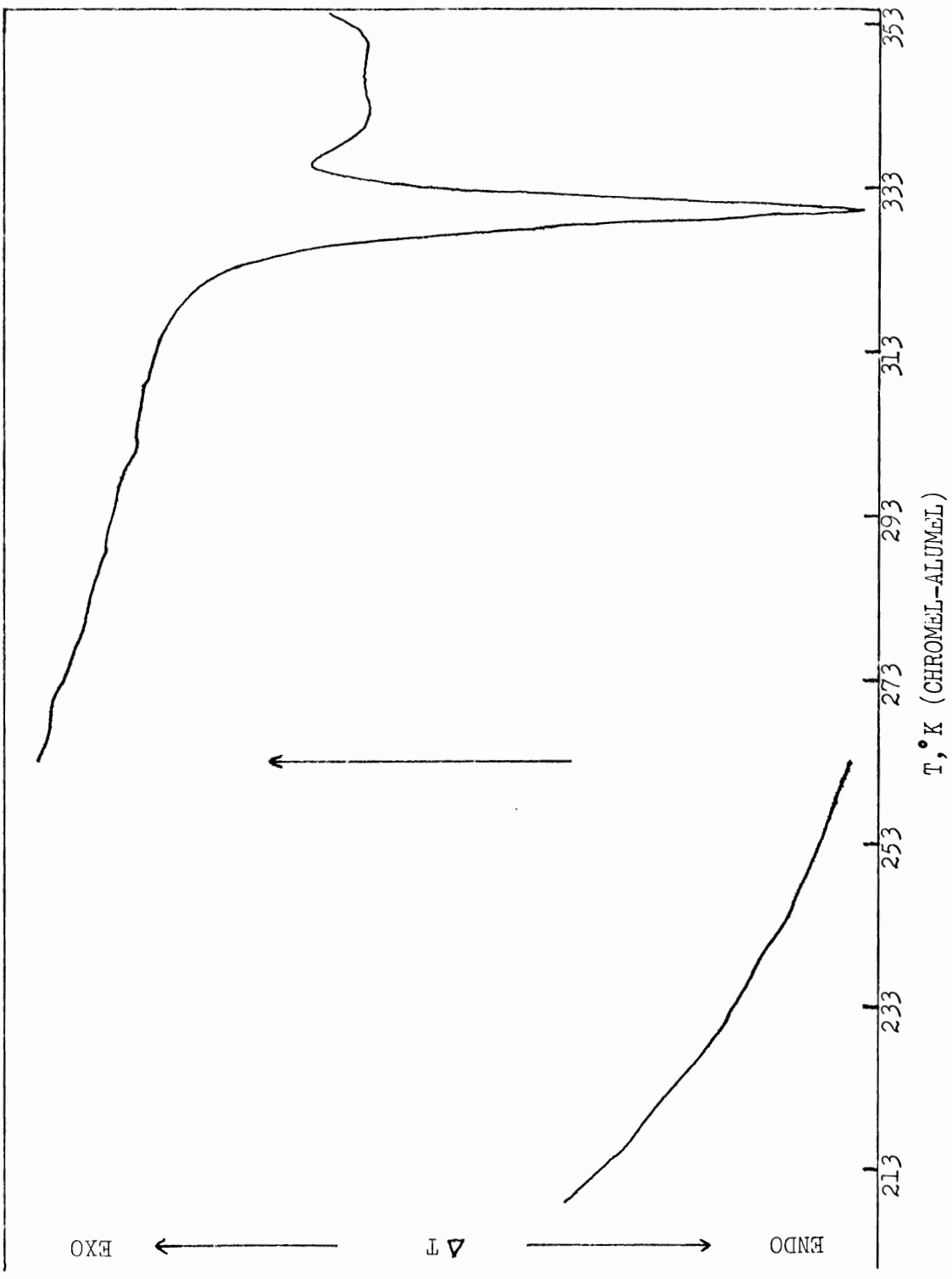

FIGURE C.11A

DTA THERMOGRAM of RED AMORPHOUS SELENIUM #7, RUN 10

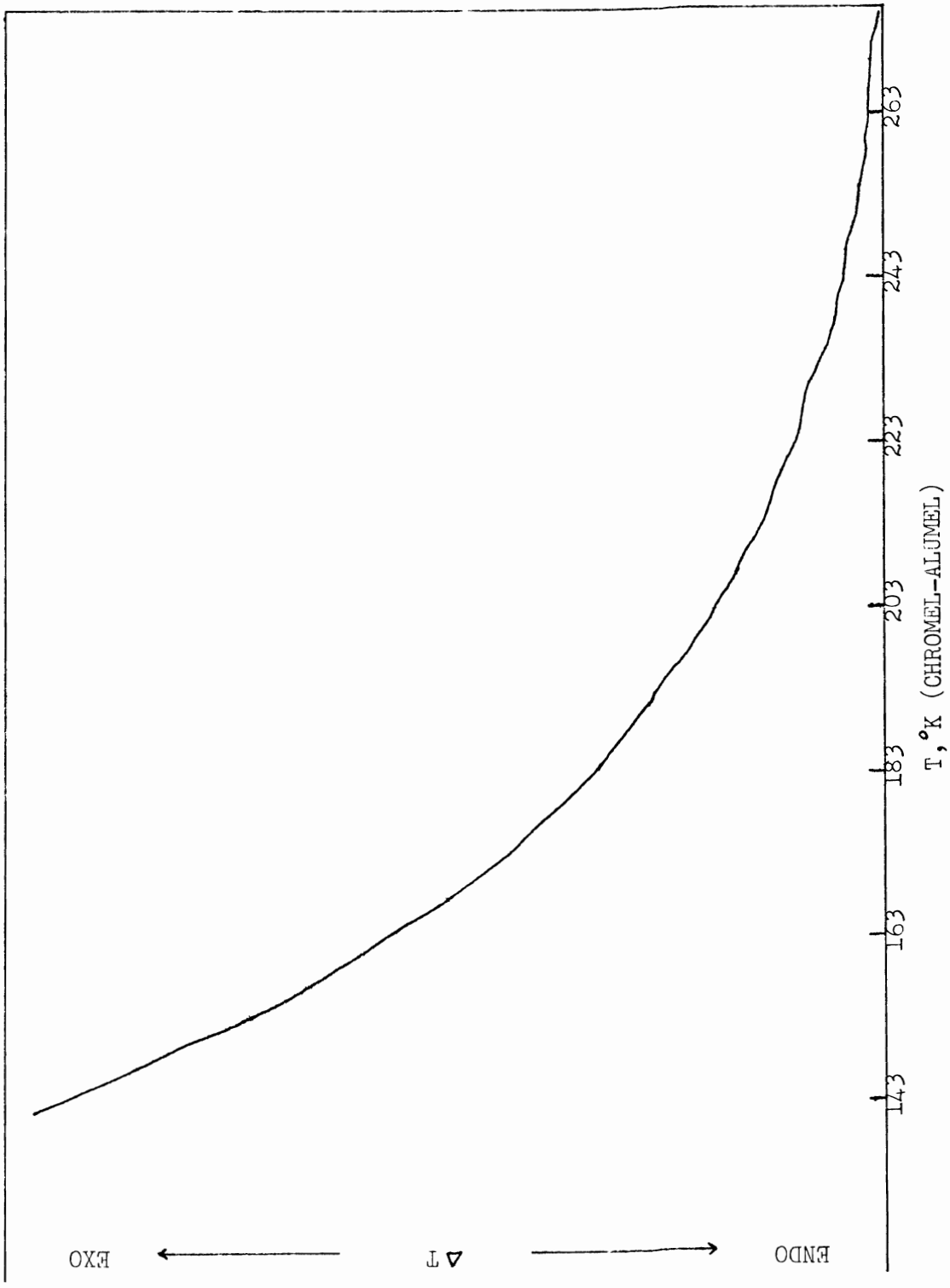

FIGURE C.12A

DTA THERMOGRAM of RED AMORPHOUS SELENIUM #11, GROUP 8, RUN 3

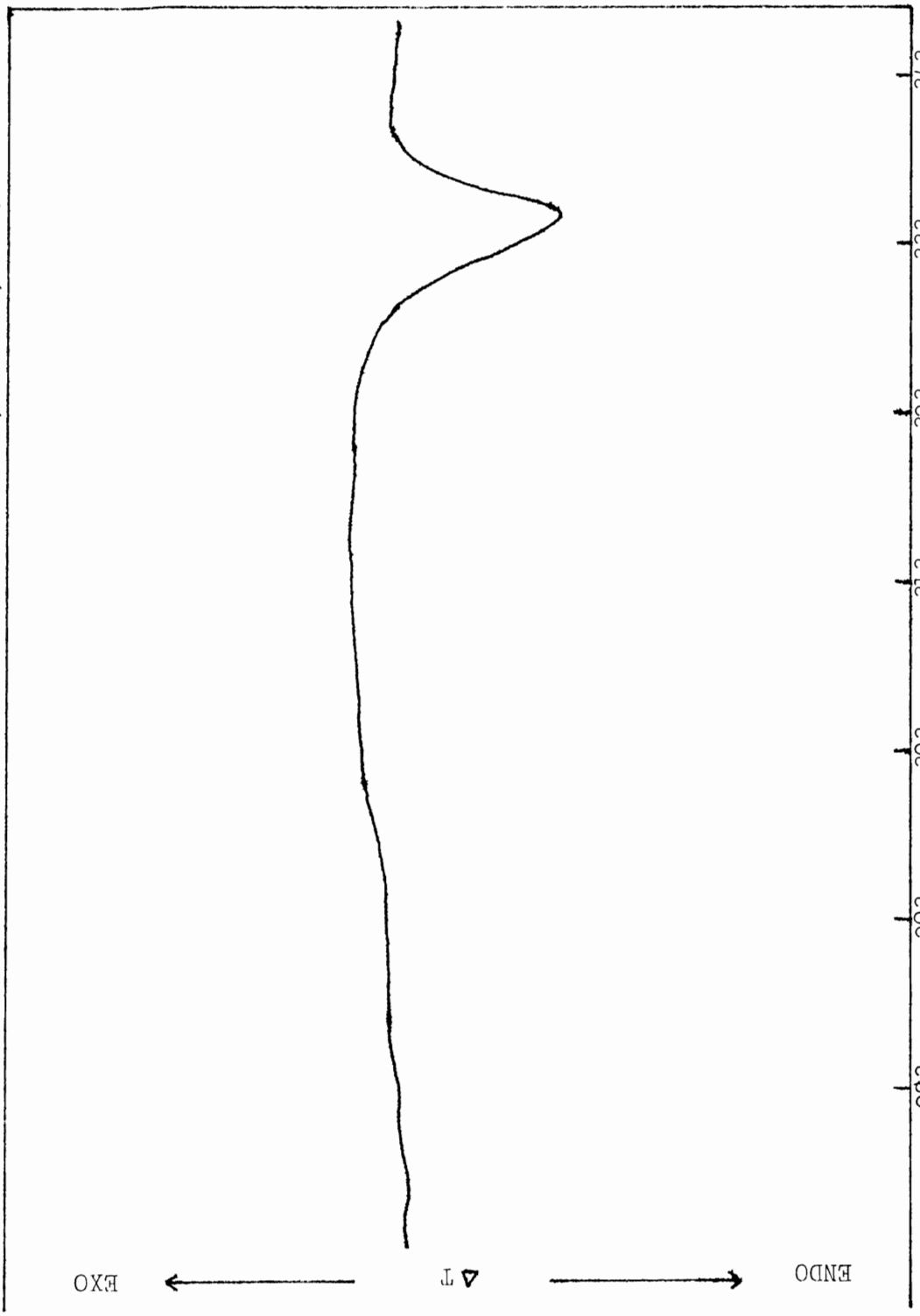

APPENDIX D

Effect of Variation of Drying Time and/or Storage Temperature on Red Amorphous Selenium

Table D.I

Experimental Data Accompanying Figures D.1 to D.56

Figure No.	Sample Wt. (mg)	Sample Age	Range Used
D.1	4.890	42 hr.	4
D.2	2.733	67 hr.	2
D.3	5.907	137 hr.	8
D.4	8.580	21 days	1
D.5	15.288	102 days	2
D.6	5.340	136 hr.	8
D.7	3.279	212 hr.	4
D.8	2.760	24 days	1
D.9	3.442	102 days	2
D.10	4.766	97 hr.	1
D.11	17.670	137 hr.	1
D.12	15.093	191 hr.	1
D.13	10.575	261 hr.	1
D.14	16.730	102 days	1
D.15	4.491	69 hr.	1
D.16	6.668	96 hr.	1
D.17	11.922	191 hr.	1
D.18	7.994	17 days	1
D.19	5.550	102 days	1
D.20	7.091	262 hr.	1
D.21	17.474	21 days	1
D.22	10.894	102 days	1
D.23	5.298	260 hr.	1

Table D.I (con't)

Figure No.	Sample Wt. (mg)	Sample Age	Range Used
D.24	7.806	24 days	1
D.25	7.964	102 days	1
D.26	6.171	372 days	1
D.27	14.879	31 hr.	1
D.28	9.161	48 hr.	1
D.29	11.731	162 hr.	1
D.30	8.490	23 days	1
D.31	18.923	88 days	1
D.32	5.207	32 hr.	4
D.33	5.789	23 days	1
D.34	14.923	88 days	1
D.35	15.700	48 hr.	1
D.36	12.960	162 hr.	1
D.37	17.714	21 days	1
D.38	9.627	88 days	1
D.39	5.760	46 hr.	1
D.40	14.535	11 days	1
D.41	11.885	23 days	1
D.42	13.163	88 days	1
D.43	13.661	53 hr.	1
D.44	18.456	21 days	1
D.45	17.517	88 days	1
D.46	13.300	53 hr.	1
D.47	13.816	11 days	1

Table D.I (con't)

Figure No.	Sample Wt. (mg)	Sample Age	Range Used
D.48	14.015	23 days	1
D.49	11.974	88 days	1
D.50	21.605	12 days	1
D.51	13.620	21 days	1
D.52	14.619	88 days	1
D.53	9.551	10 days	1
D.54	10.855	23 days	1
D.55	9.680	88 days	1
D.56	8.982	358 days	1

Table D.II

Area/mg and Observed Peak Temperature of the Endothermic and Exothermic Transitions in Red Amorphous Selenium #10, Group 3

Run No.	Sample Wt. (mg)	Endotherm Area/mg	Endo. Temp. (°K)	Exotherm Area/mg	Exo. Temp. (°K)	Age (days)
18	11.935	18.9	325.5	41.2	365.4	6
21	9.835	21.0	326.3	40.1	366.2	7
34	9.966	20.5	325.7	42.4	365.7	9
38	8.740	20.4	326.6	40.4	366.1	11
51	8.697	18.9	326.6	41.9	365.0	24
54	17.061	20.1	326.5	43.5	364.6	29

Table D.III

Area/mg and Observed Peak Temperature of the Exothermic Transition in Red Amorphous Selenium #10, Group 6

Run No.	Sample Wt. (mg)	Exotherm Area/mg	Exo. Temp. (°K)	Age (days)
36	15.767	41.7	367.1	10
40	7.091	36.3	367.9	11
44	7.018	39.1	367.8	17
47	17.474	41.9	367.3	21
56	10.636	36.0	367.6	29
63	9.835	42.3	367.5	102

Table D.IV

Area/mg and Observed Peak Temperature of the Exothermic Transition in Red Amorphous Selenium #11, Group 8

Run No.	Sample Wt. (mg)	Exotherm Area/mg	Exo. Temp. (K)	Age (days)
20	21.605	41.7	363.2	12
35	14.619	38.6	364.3	88
36	12.670	40.1	363.9	88

FIGURE D.1

DSC THERMOGRAM of RED AMORPHOUS SELENIUM #10, GROUP 2, RUN 5

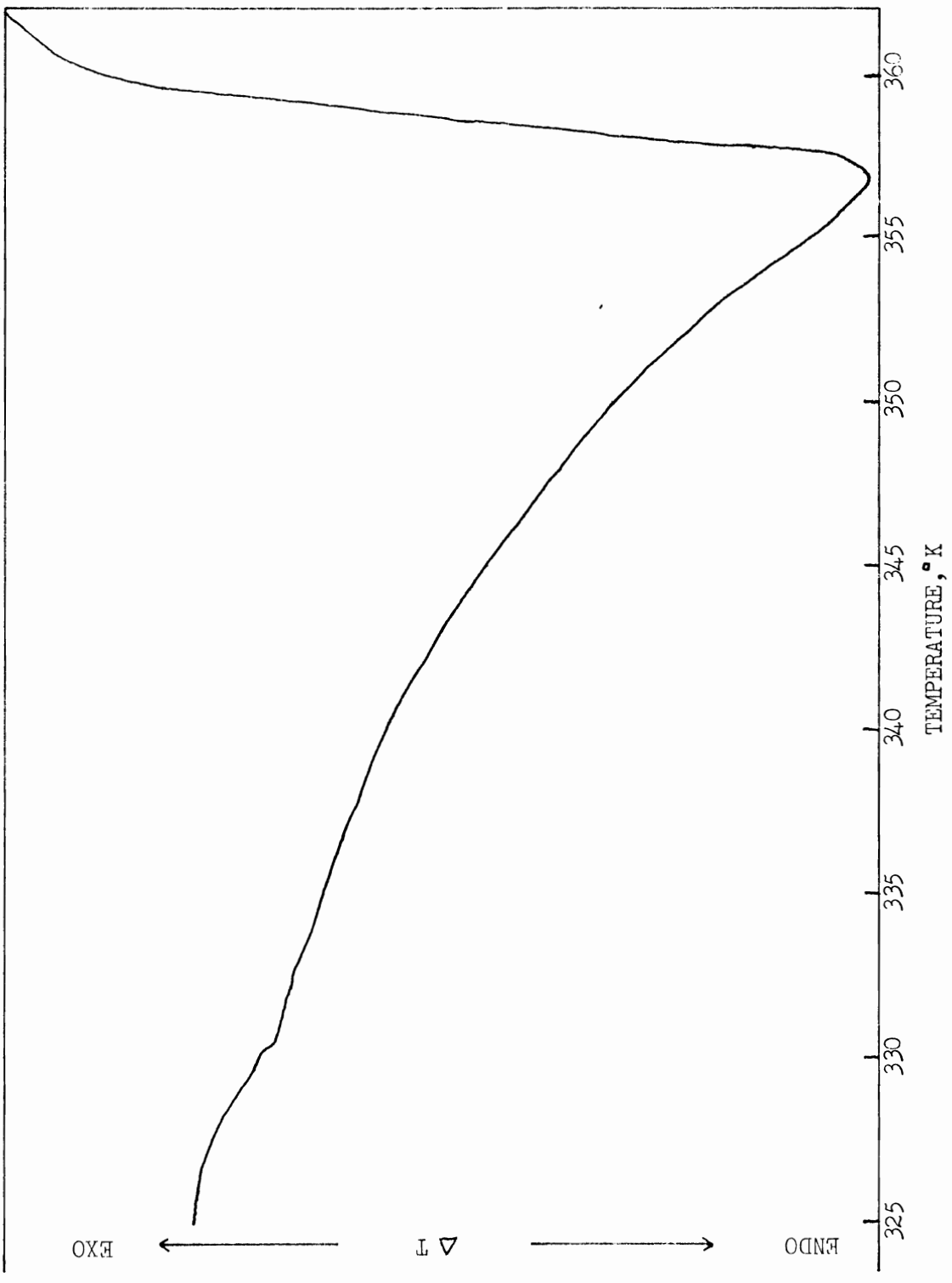

FIGURE D.2

DSC THERMOGRAM of RED AMORPHOUS SELENIUM #10, GROUP 2, RUN 10

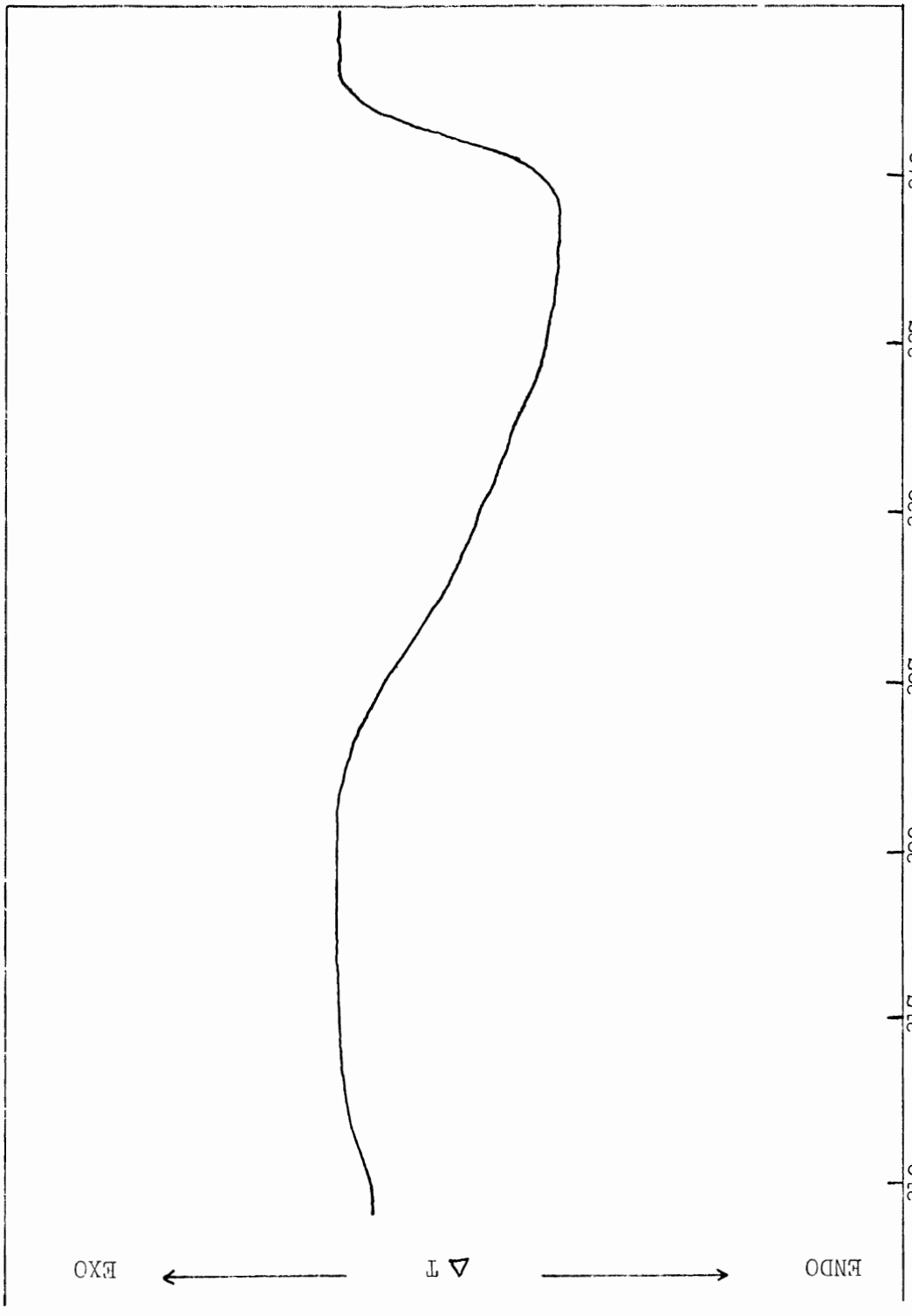

FIGURE D.3

DSC THERMOGRAM of RED AMORPHOUS SELENIUM #10, GROUP 2, RUN 19

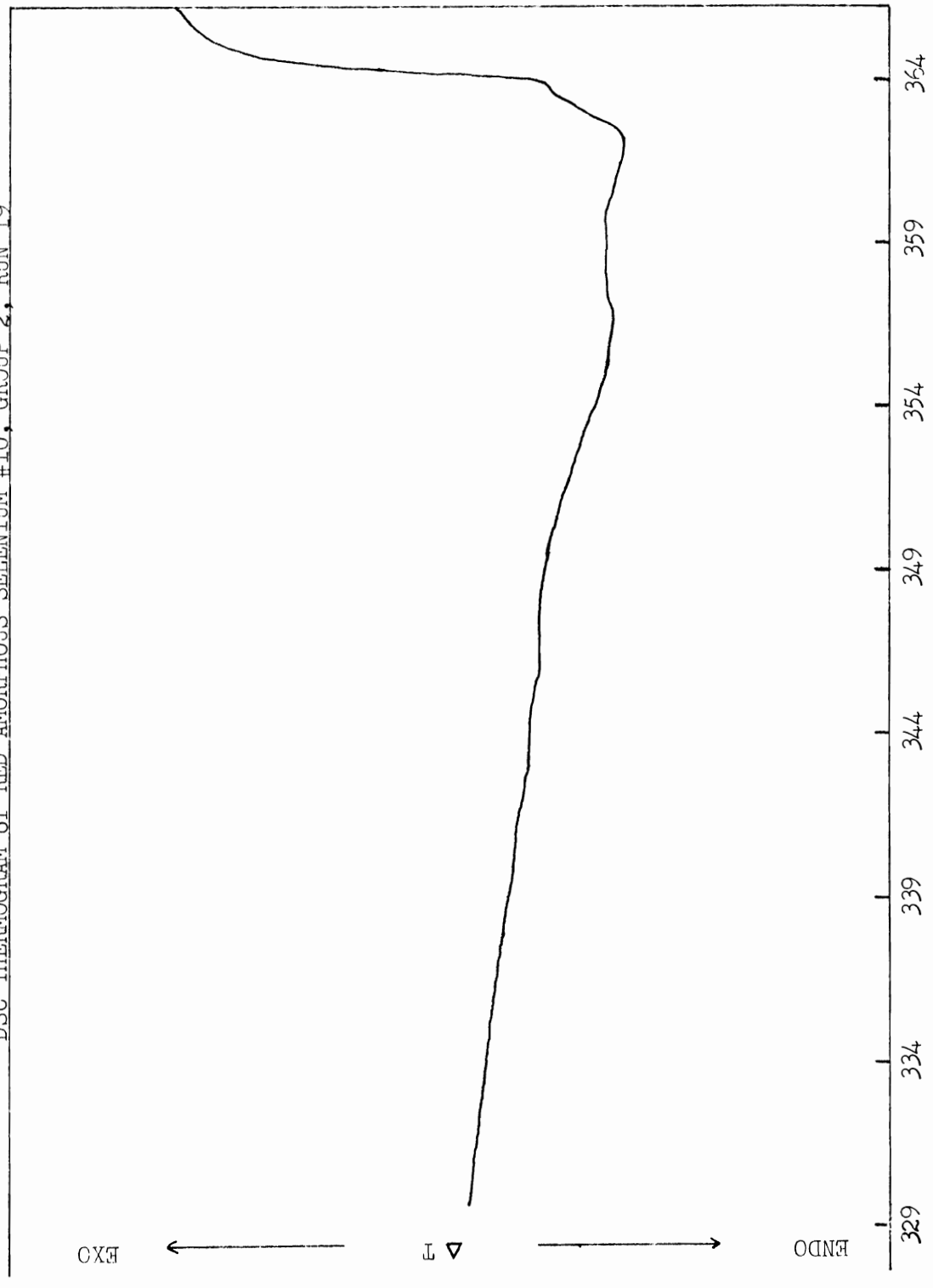

FIGURE D.4

DSC THERMOGRAM of RED AMORPHOUS SELENIUM #10, GROUP 2, RUN 49

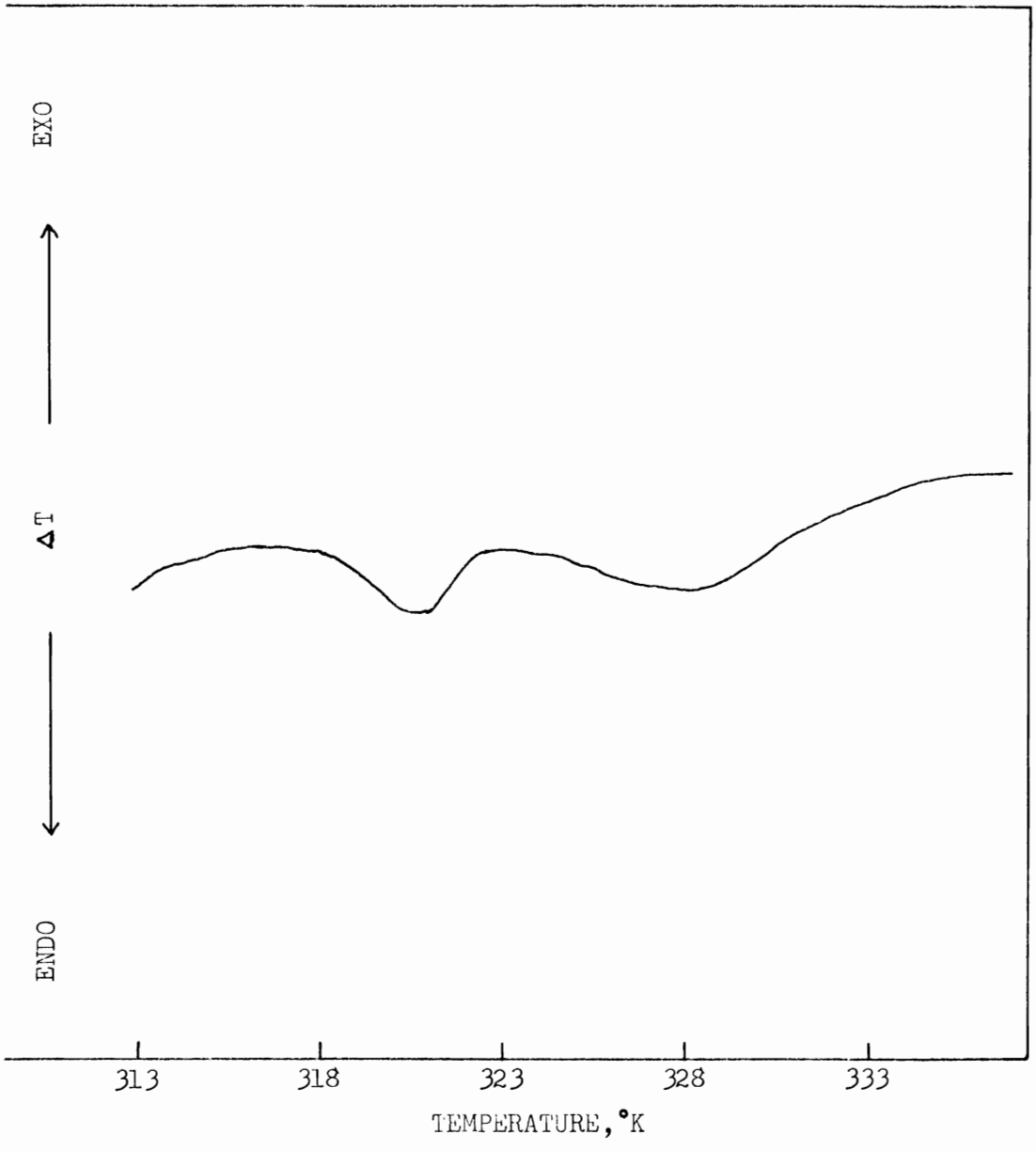

FIGURE D.5

DSC THERMOGRAM of RED AMORPHOUS SELENIUM #10, GROUP 2, RUN 66

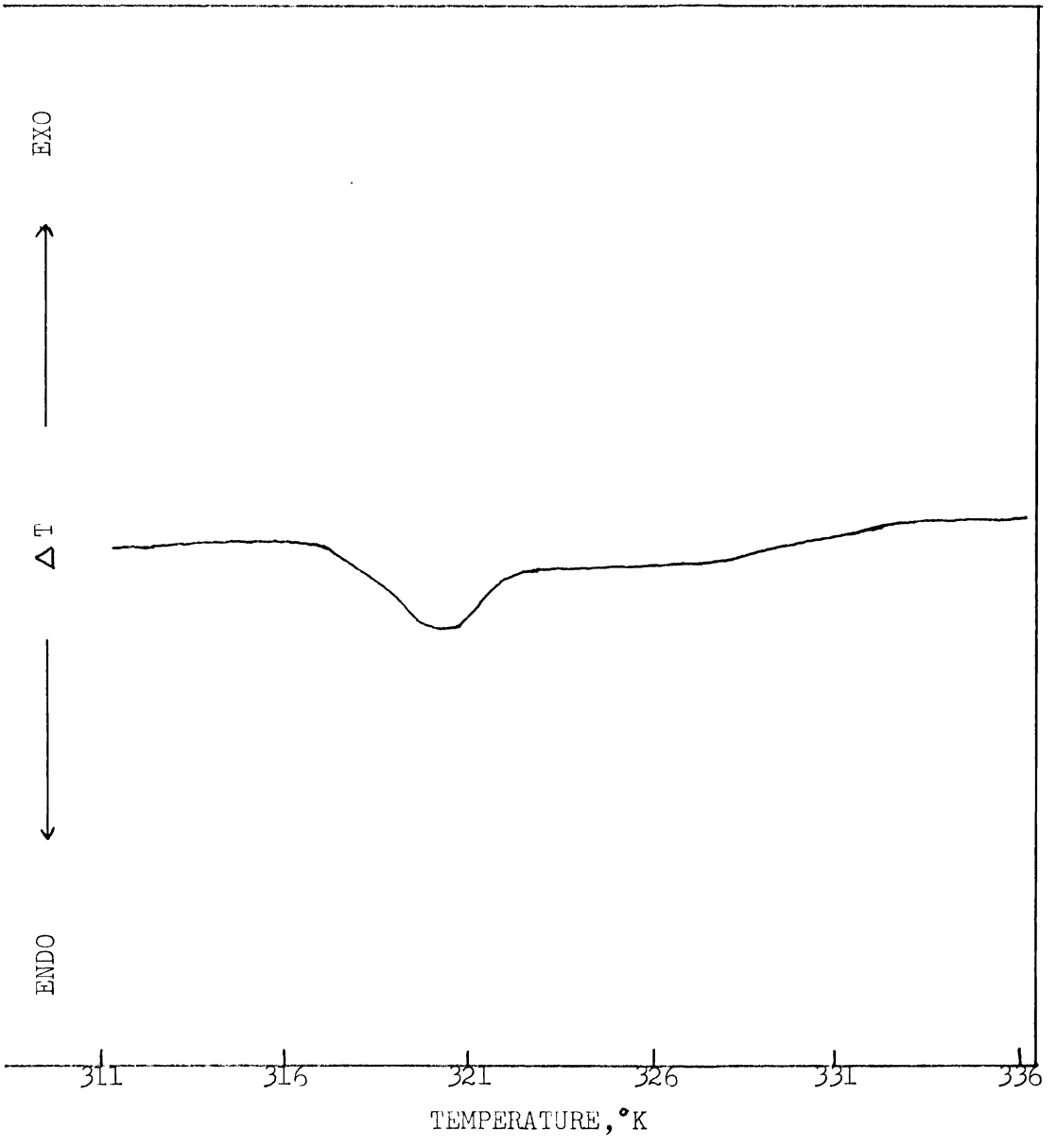

FIGURE D.6

DSC THERMOGRAM of RED AMORPHOUS SELENIUM #10, GROUP 1, RUN 17

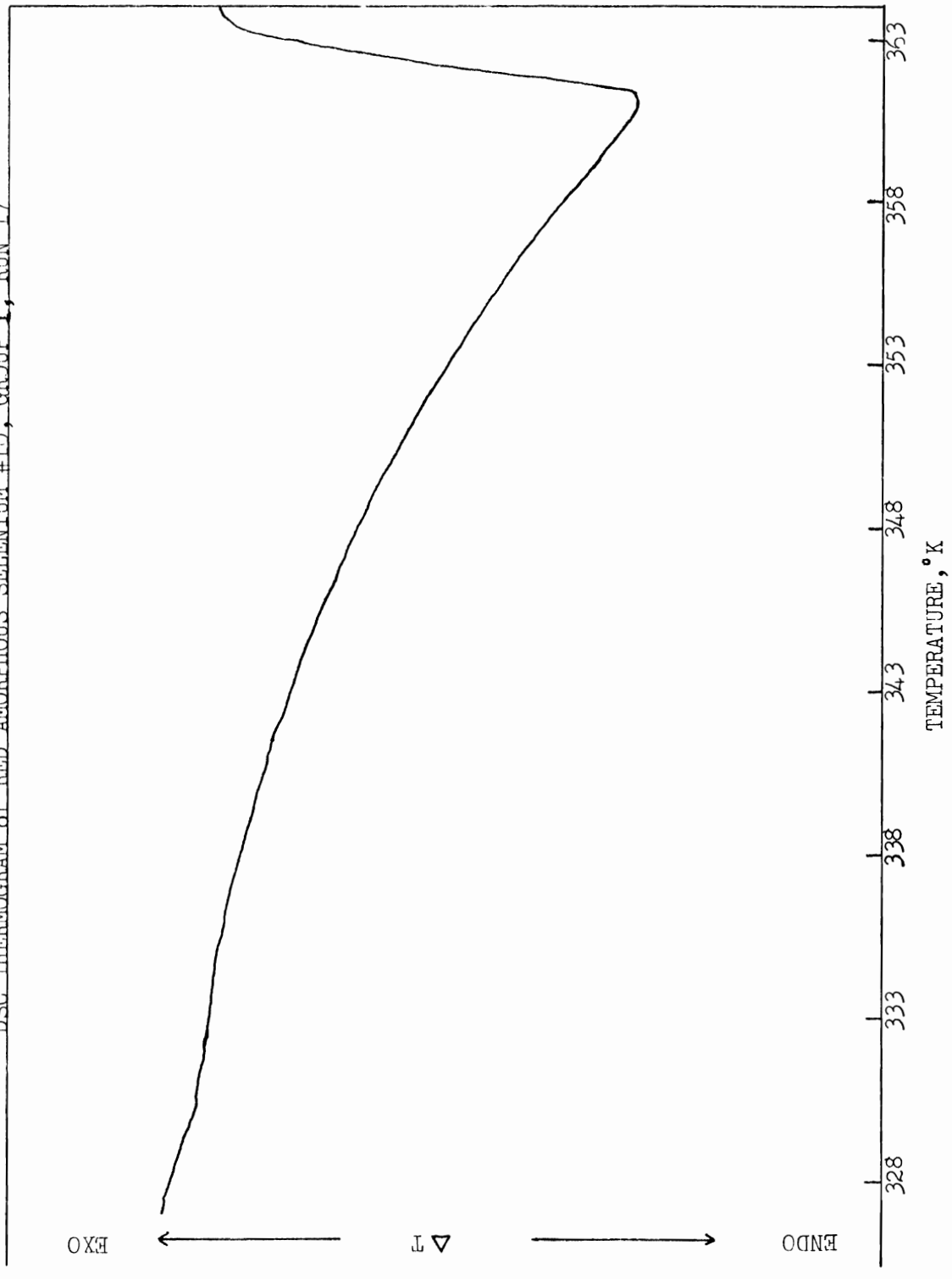

FIGURE D.7

DSC THERMOGRAM of RED AMORPHOUS SELENIUM #10, GROUP 1, RUN 31

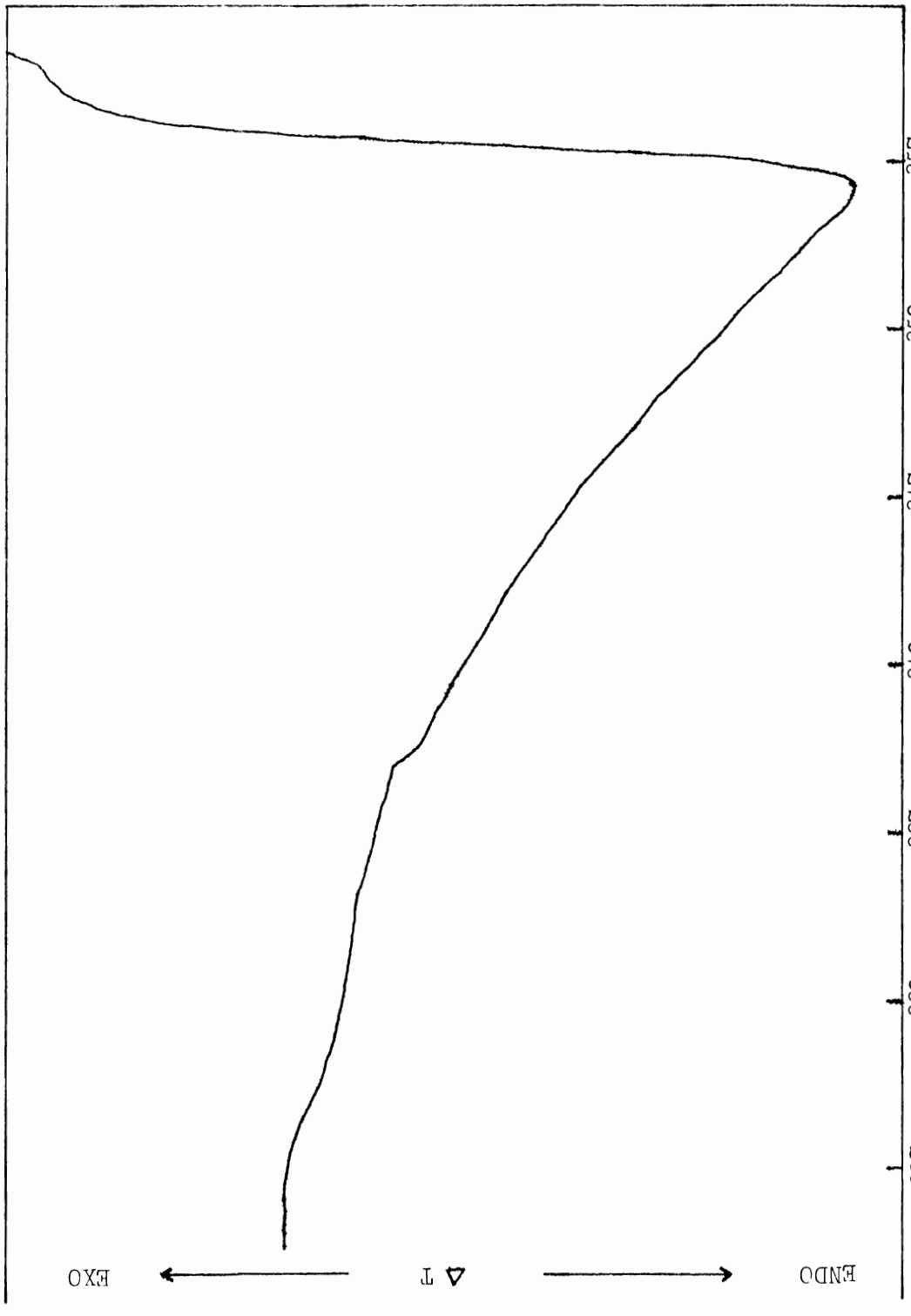

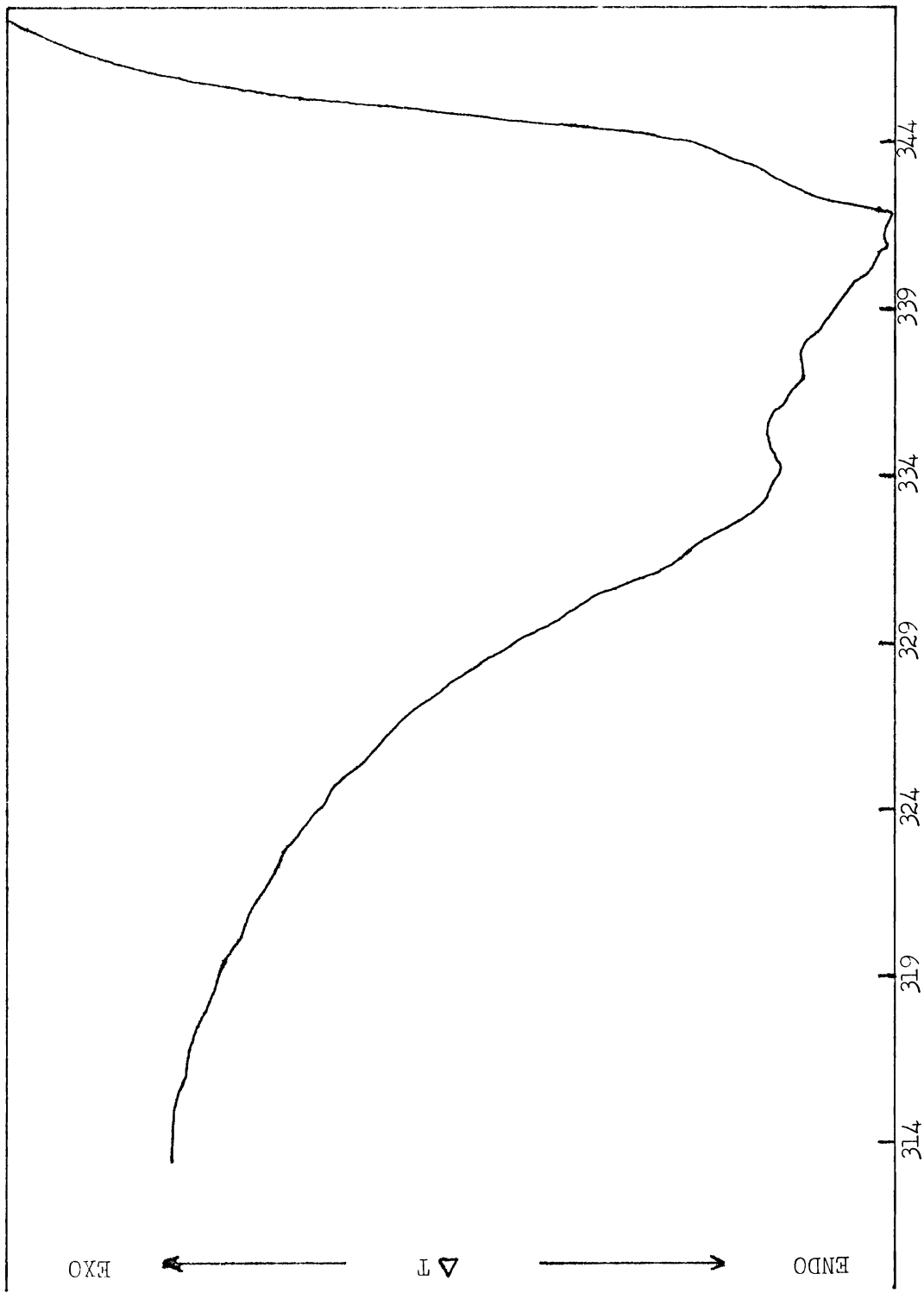

FIGURE D.8

DSC THERMOGRAM of RED AMORPHOUS SELENIUM #10, GROUP 1, RUN 50

FIGURE D.9

DSC THERMOGRAM of RED AMORPHOUS SELENIUM #10, GROUP 1, RUN 62

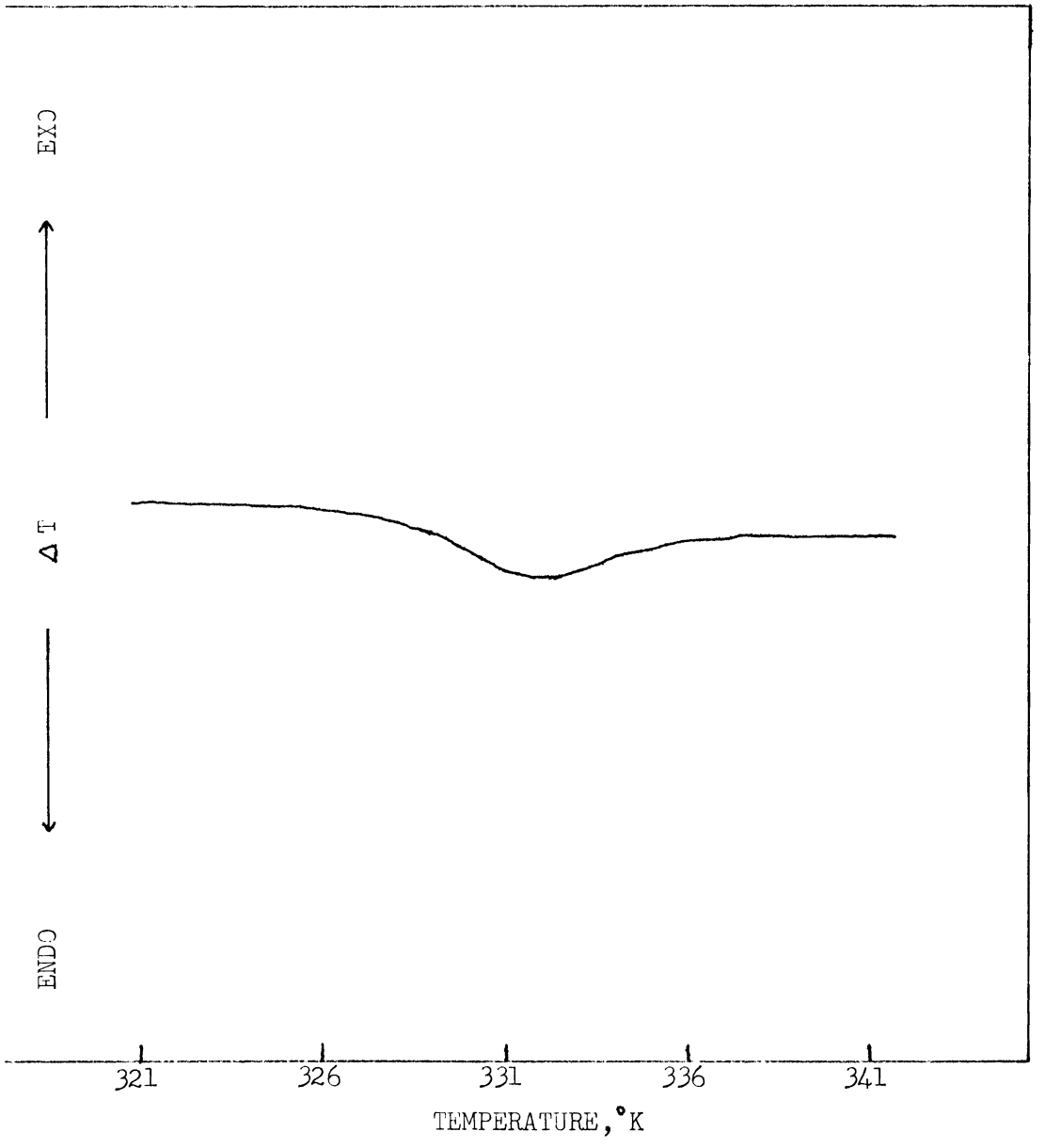

FIGURE D.10

DSC THERMOGRAM of RED AMORPHOUS SELENIUM #10, GROUP 4, RUN 14

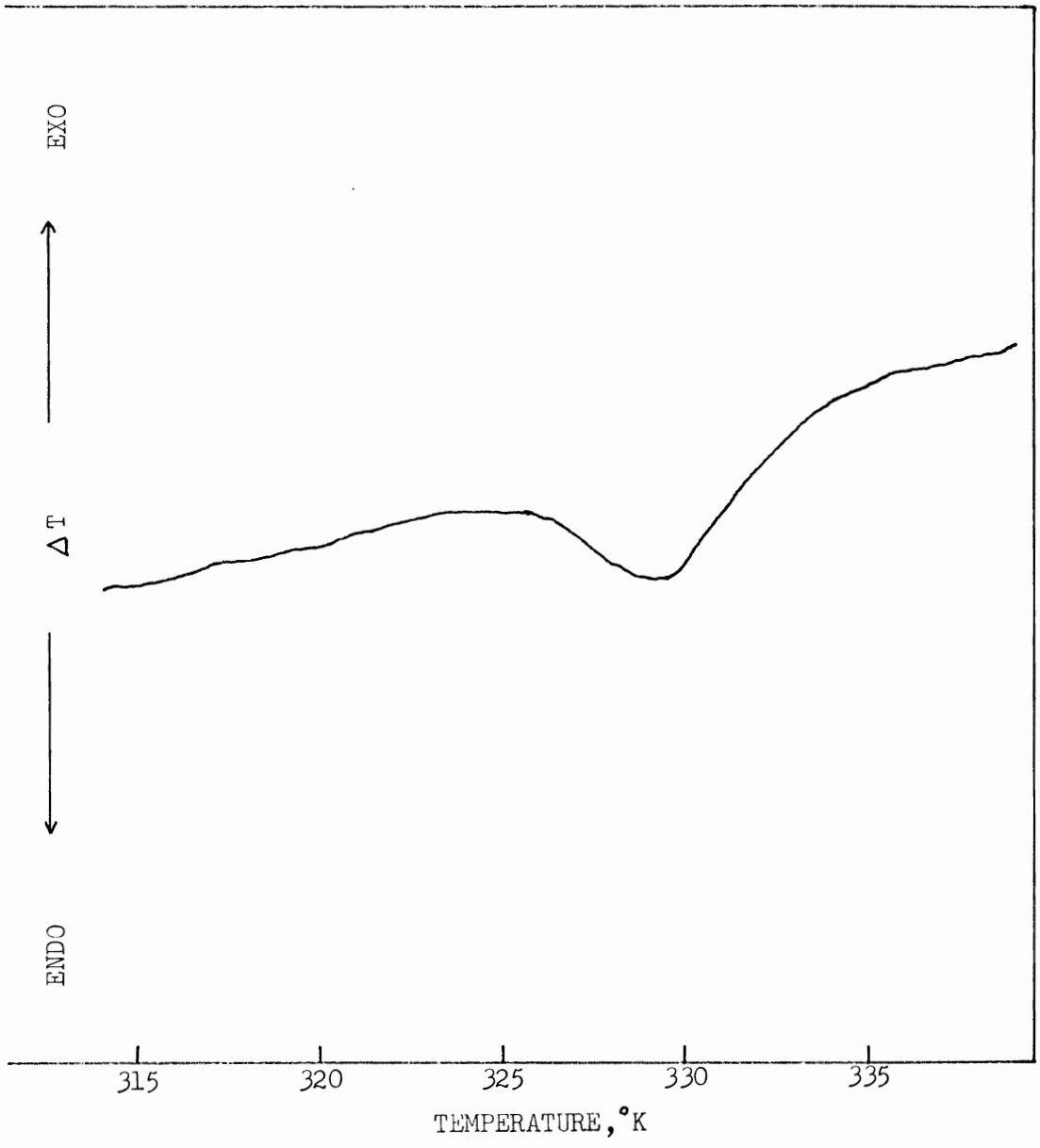

FIGURE D.11

DSC THERMOGRAM of RED AMORPHOUS SELENIUM #10, GROUP 4, RUN 20

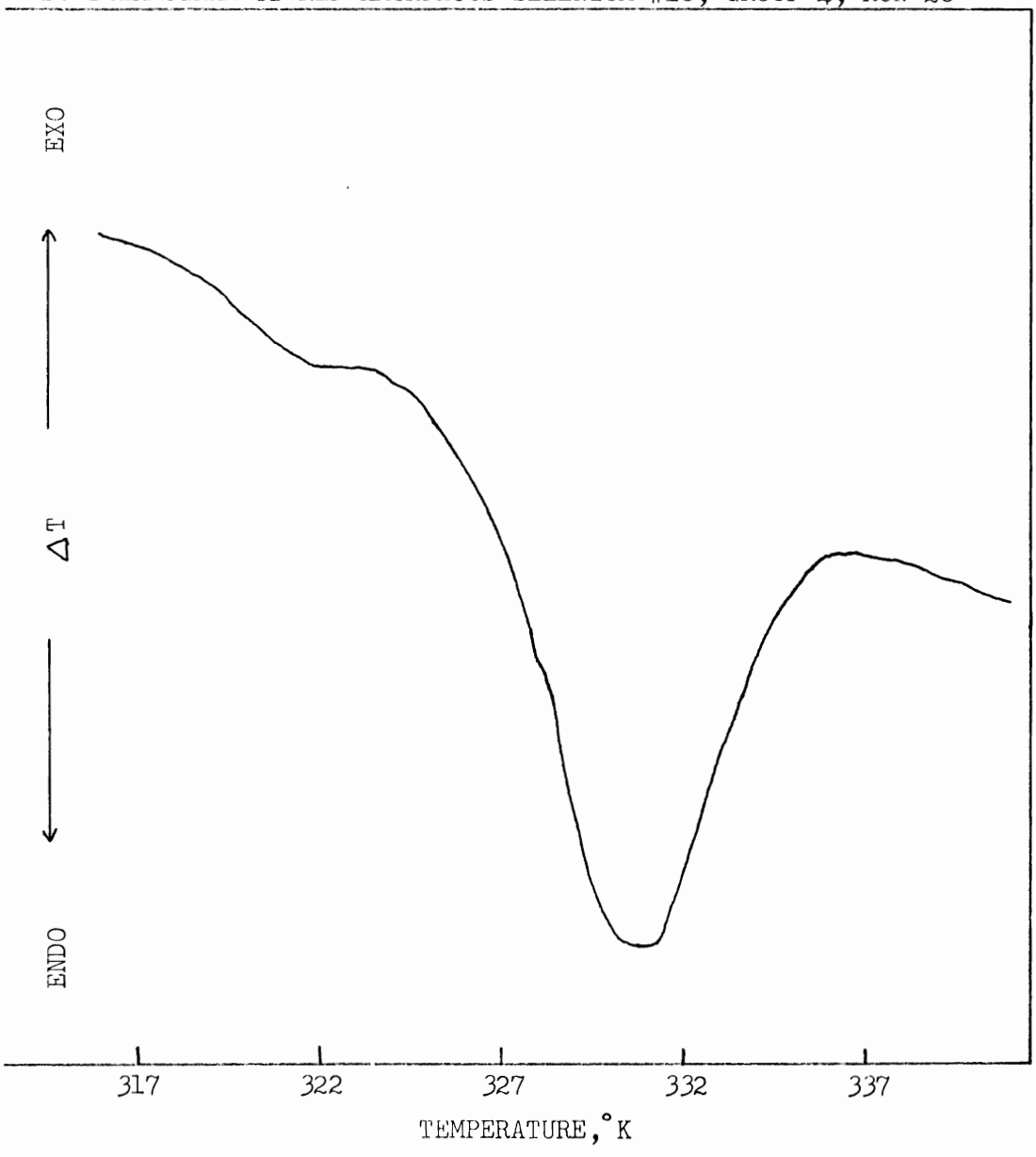

FIGURE D.12

DSC THERMOGRAM of RED AMORPHOUS SELENIUM #10, GROUP 4, RUN 28

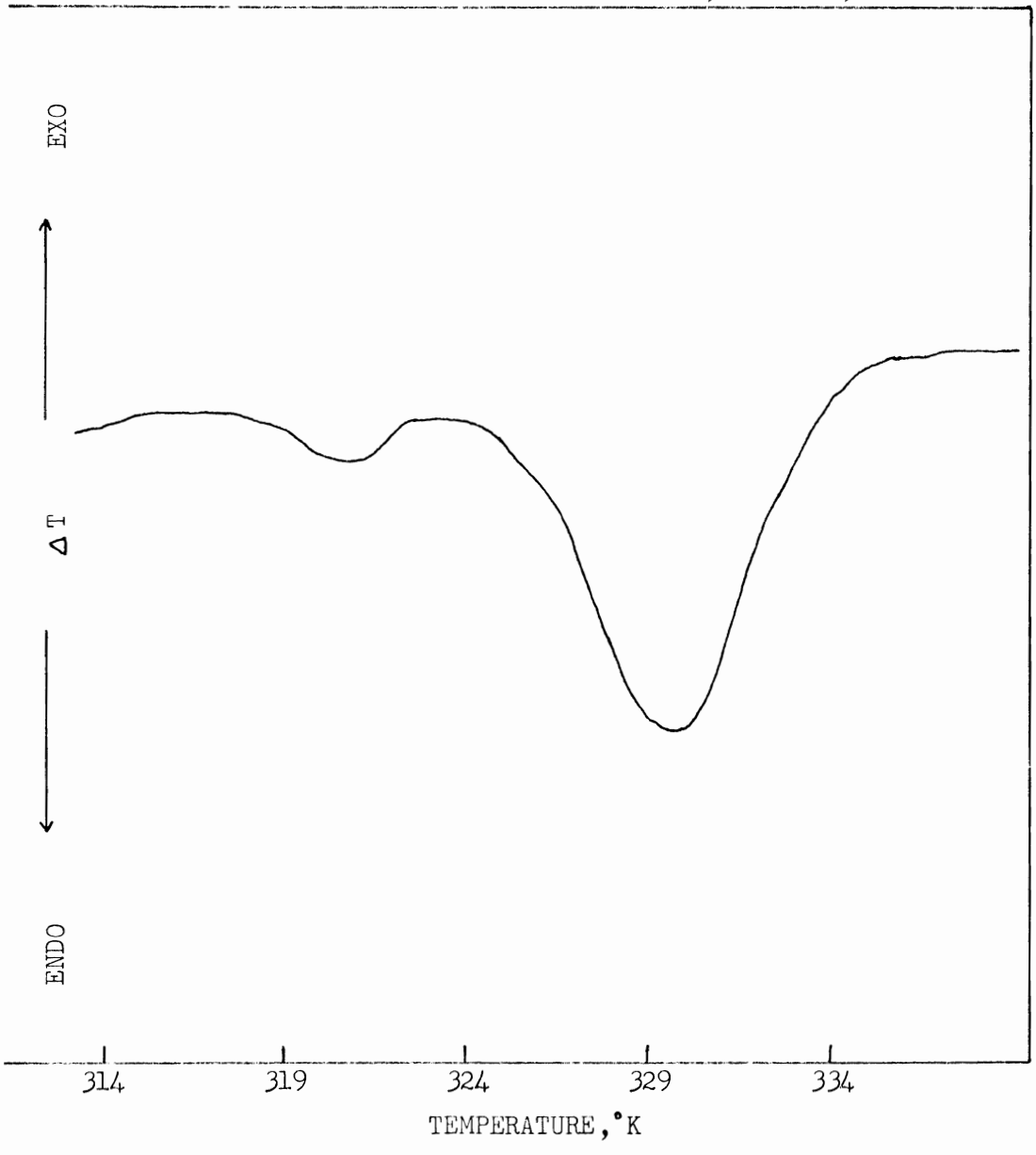

FIGURE D.13

DSC THERMOGRAM of RED AMORPHOUS SELENIUM #10, GROUP 4, RUN 39

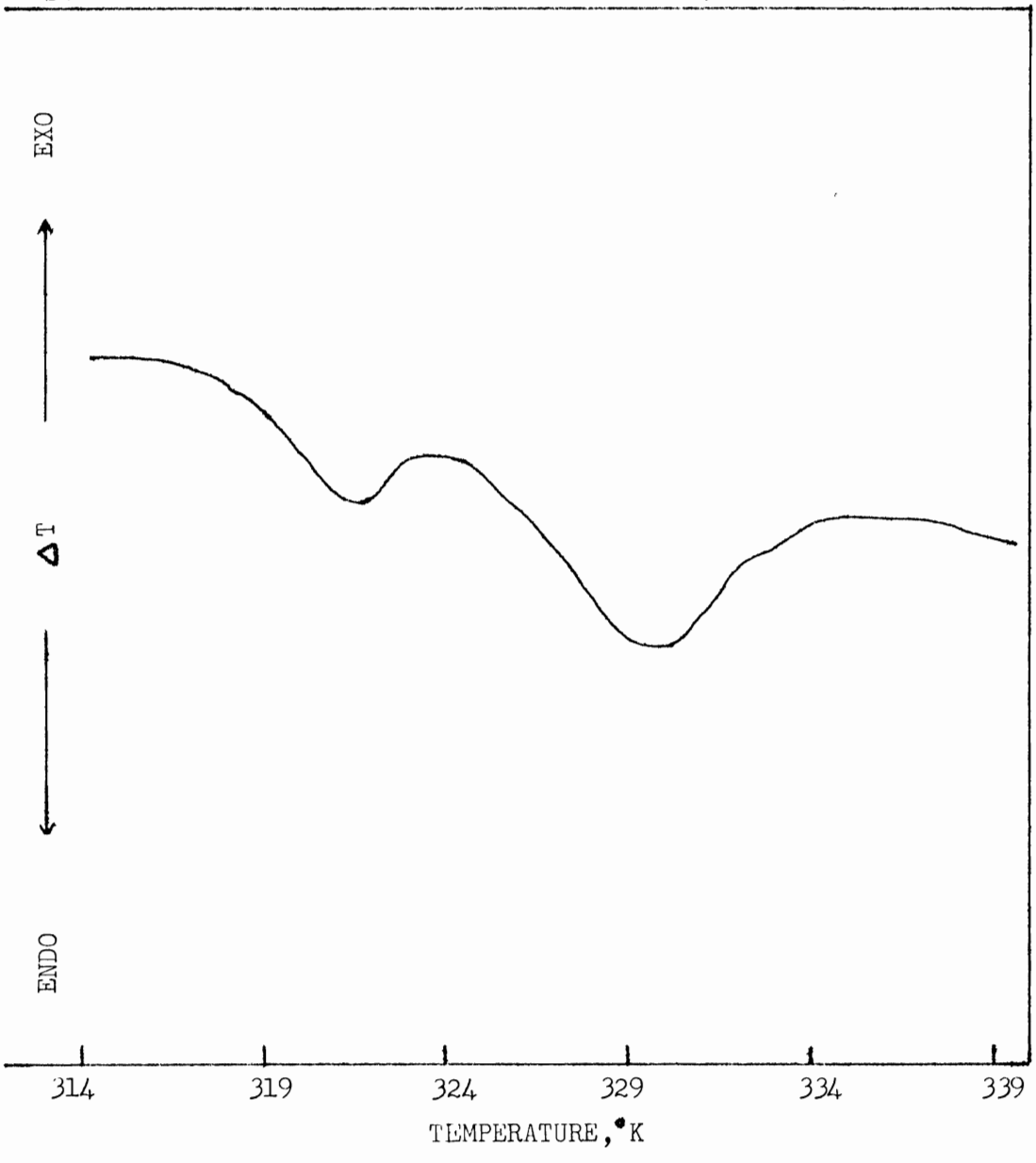

FIGURE D.14

DSC THERMOGRAM of RED AMORPHOUS SELENIUM #10, GROUP 4, RUN 65

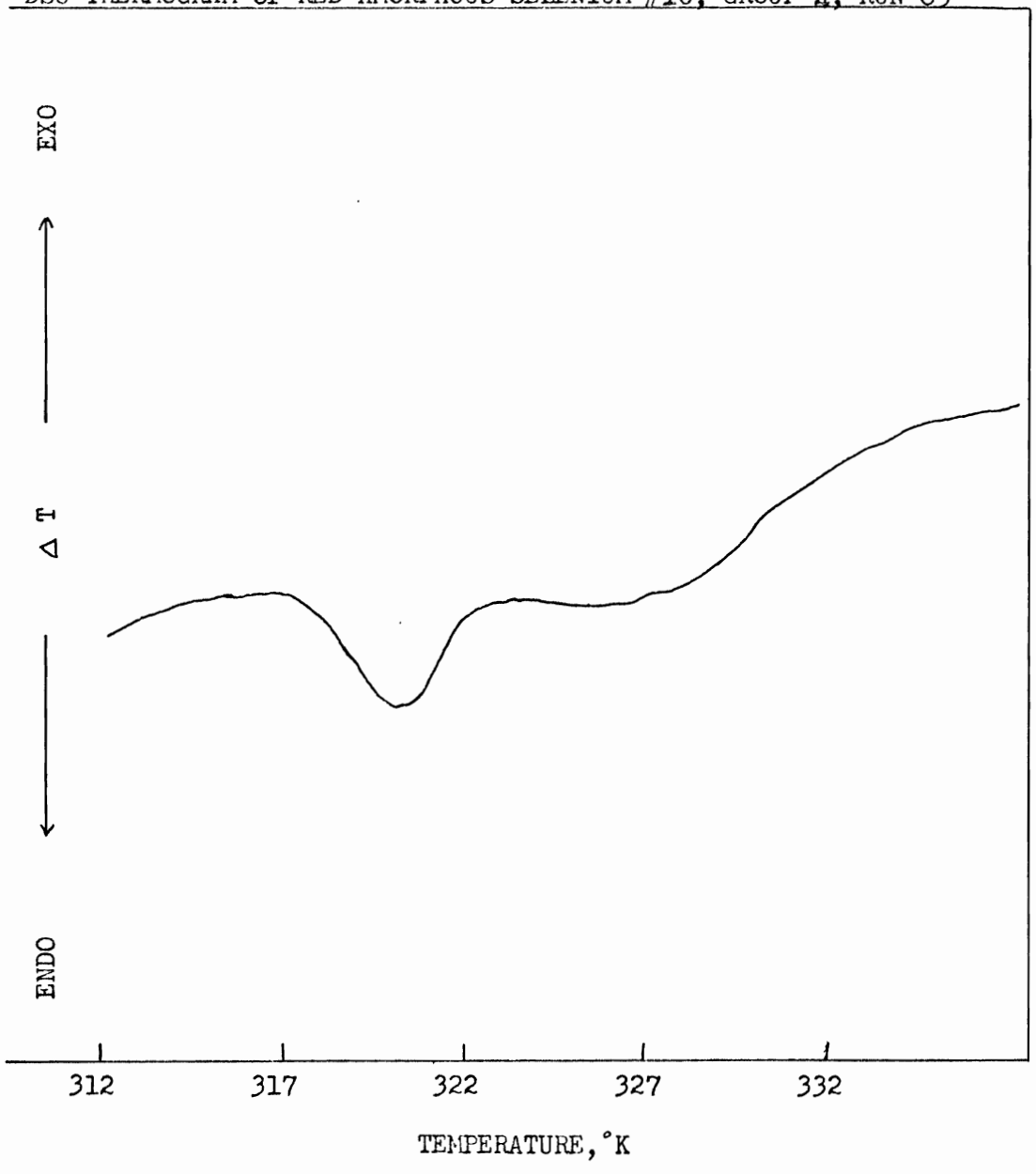

FIGURE D.15

DSC THERMOGRAM of RED AMORPHOUS SELENIUM #10, GROUP 3, RUN 12

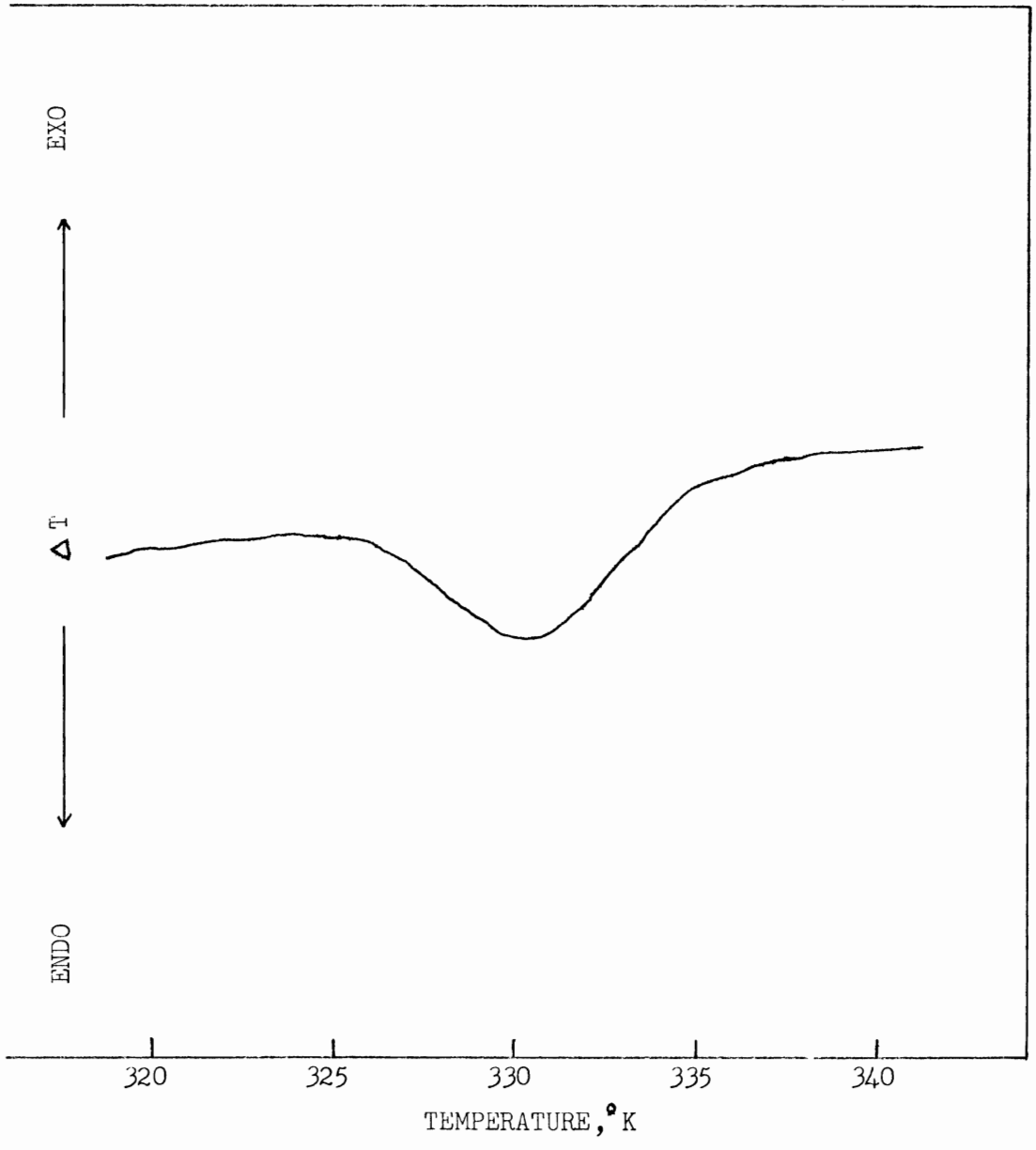

FIGURE D.16

DSC THERMOGRAM of RED AMORPHOUS SELENIUM #10, GROUP 3, RUN 13

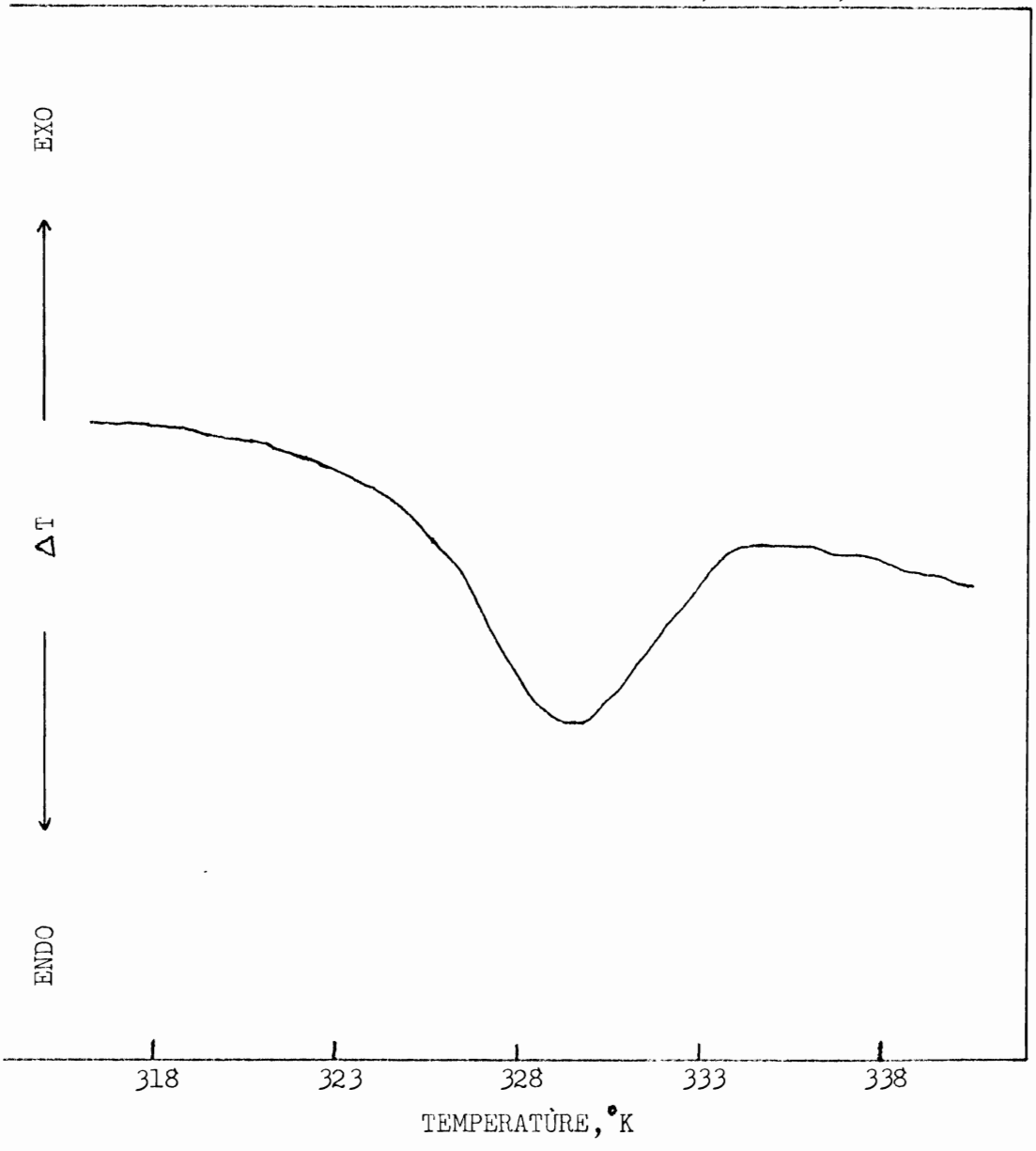

FIGURE D.17

DSC THERMOGRAM of RED AMORPHOUS SELENIUM #10, GROUP 3, RUN 29

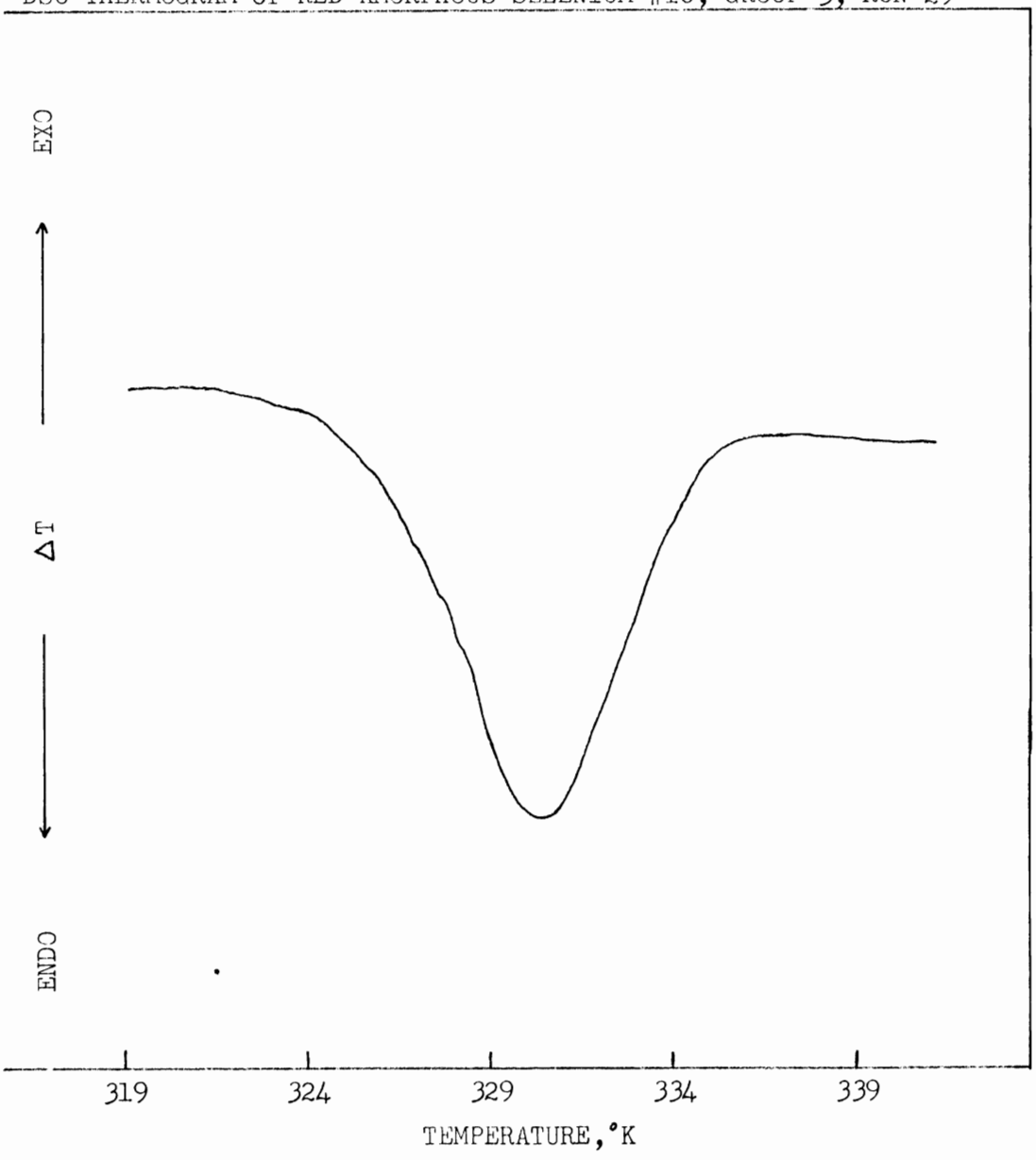

FIGURE D.18

DSC THERMOGRAM of RED AMORPHOUS SELENIUM #10, GROUP 3, RUN 41

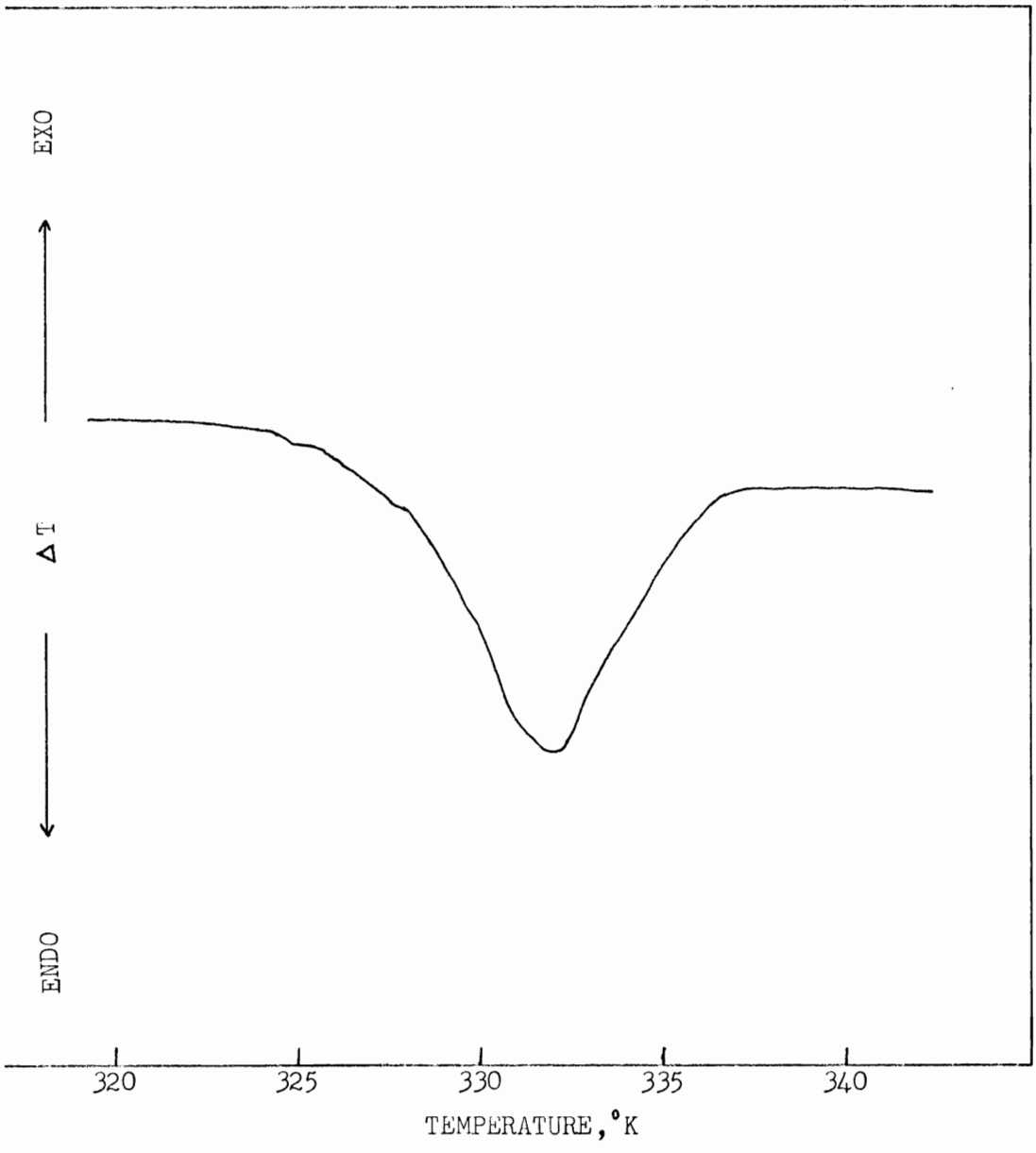

FIGURE D.19

DSC THERMOGRAM of RED AMORPHOUS SELENIUM #10, GROUP 3, RUN 61

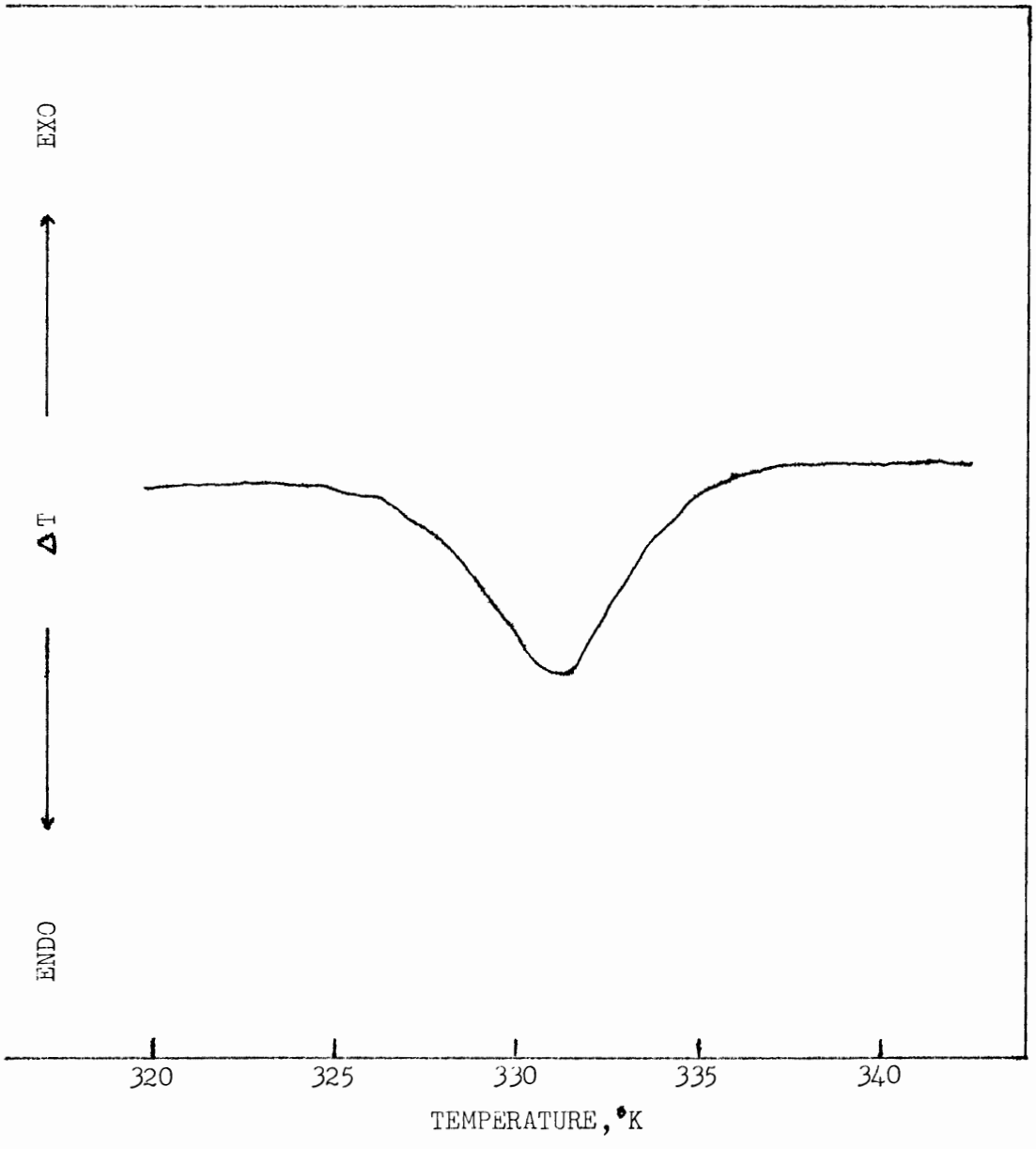

FIGURE D.20

DSC THERMOGRAM of RED AMORPHOUS SELENIUM #10, GROUP 6, RUN 40

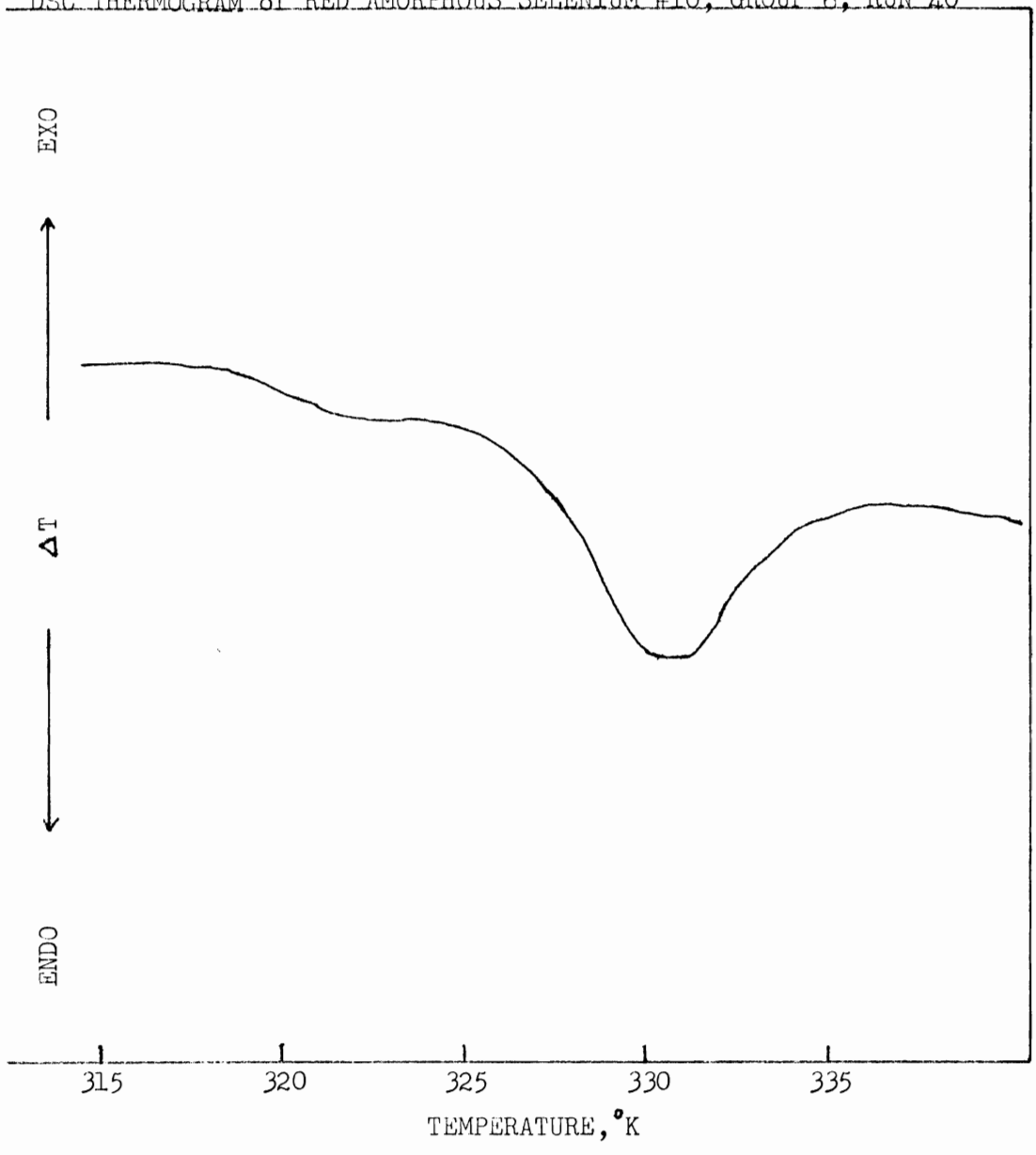

FIGURE D.21

DSC THERMOGRAM of RED AMORPHOUS SELENIUM #10, GROUP 6, RUN 47

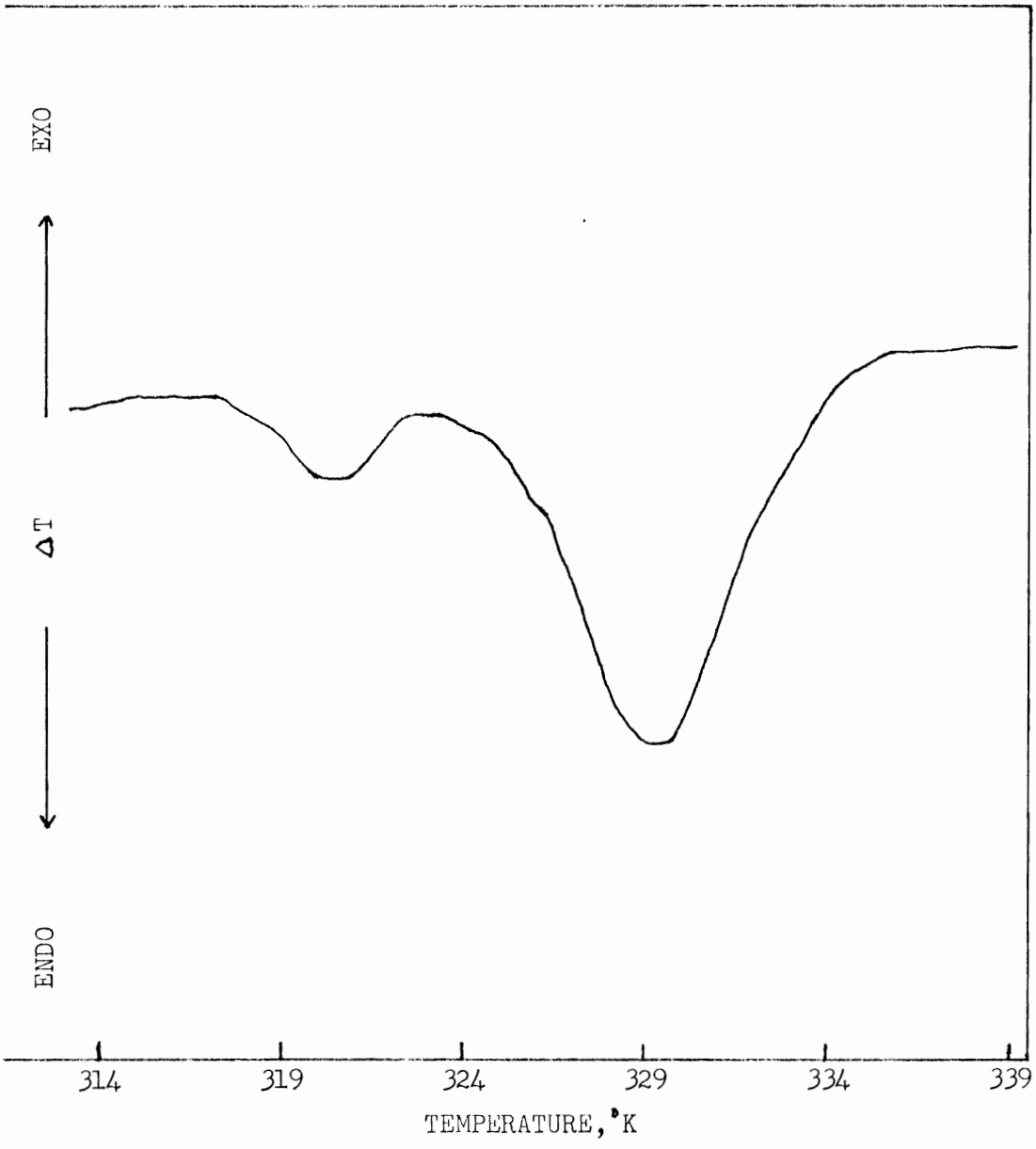

FIGURE D.22

DSC THERMOGRAM of RED AMORPHOUS SELENIUM #10, GROUP 6, RUN 64

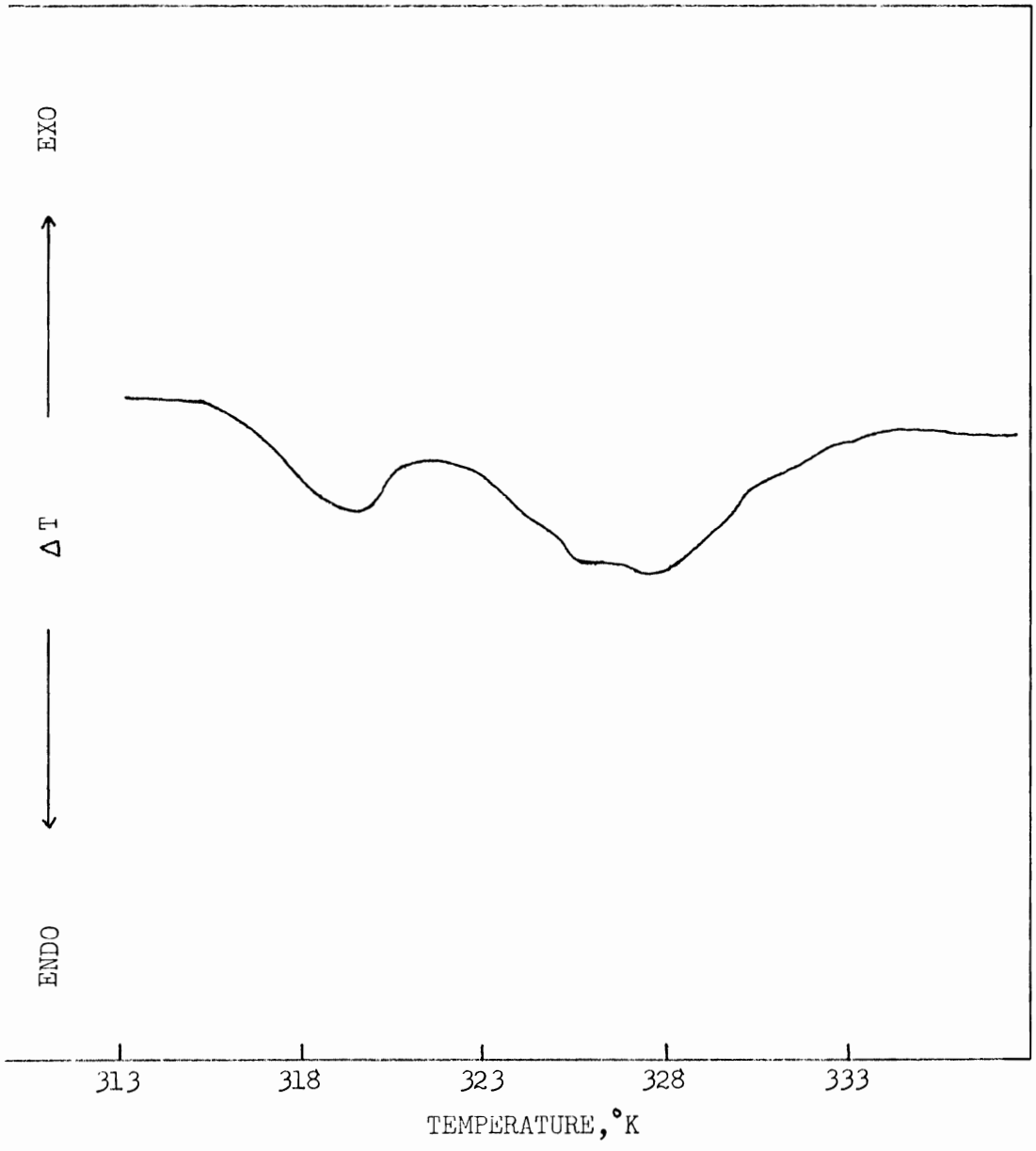

FIGURE D.23

DSC THERMOGRAM of RED AMORPHOUS SELENIUM #10, GROUP 5, RUN 37

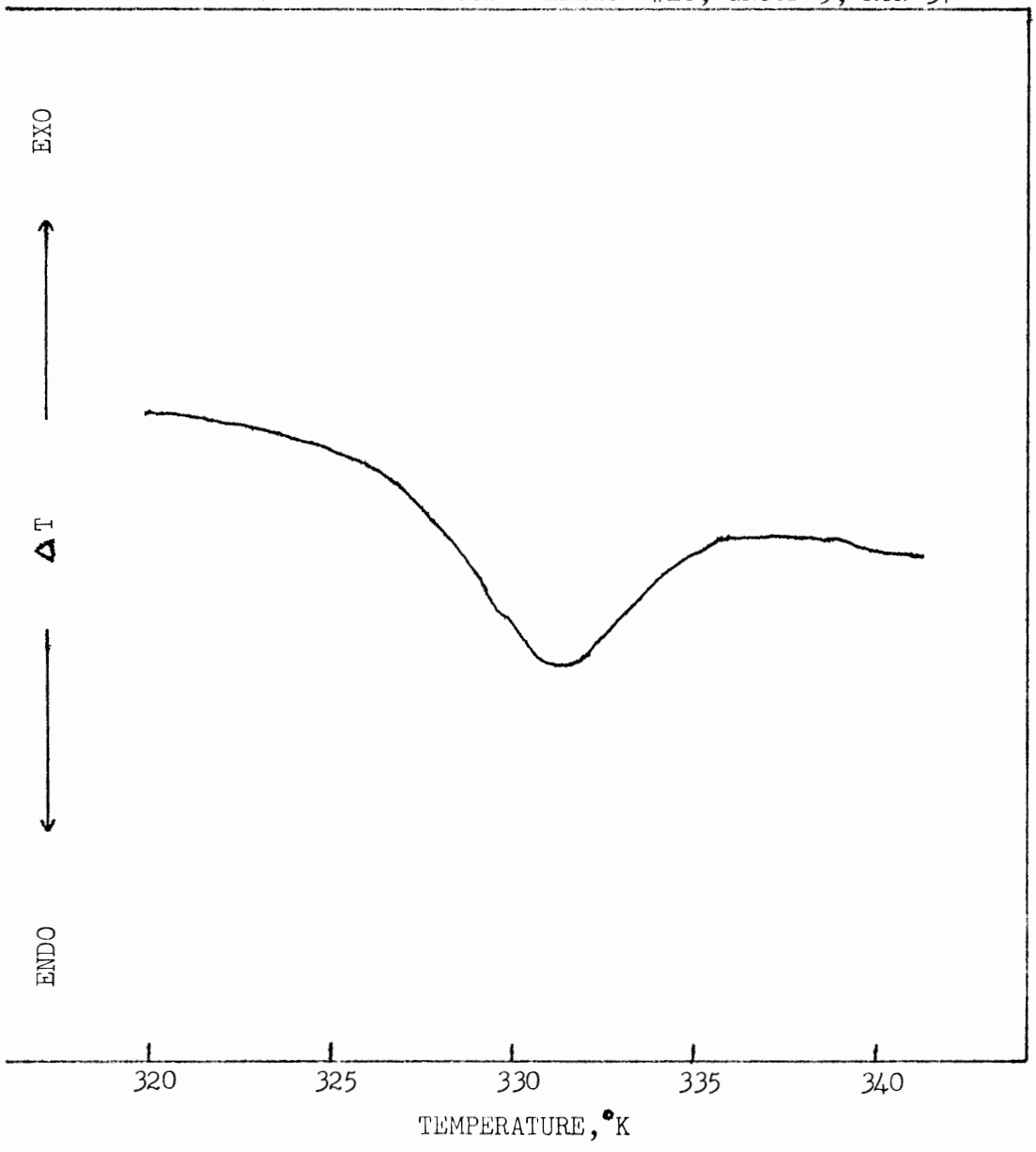

FIGURE D.24

DSC THERMOGRAM of RED AMORPHOUS SELENIUM #10, GROUP 5, RUN 52

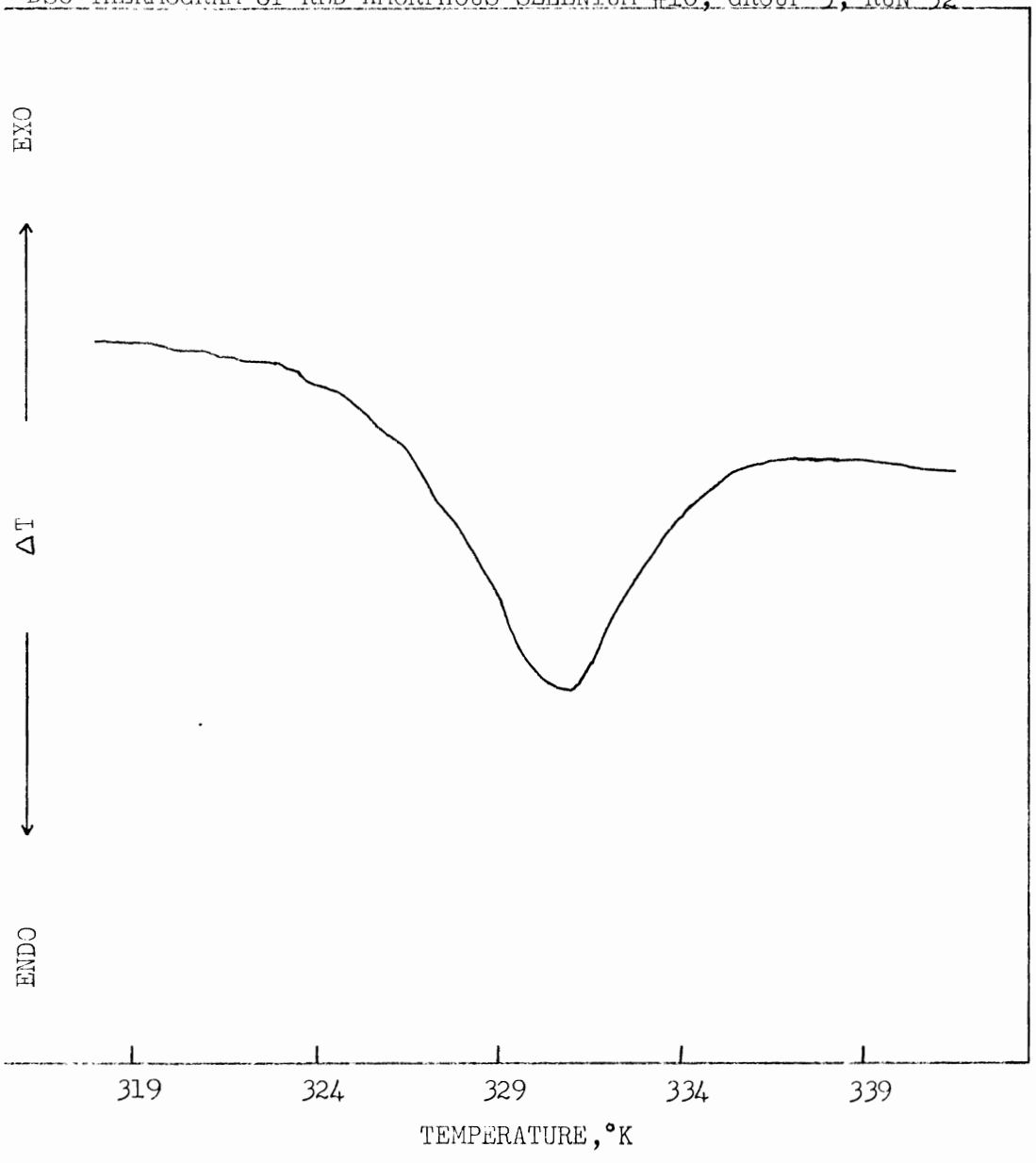

FIGURE D.25

DSC THERMOGRAM of RED AMORPHOUS SELENIUM #10, GROUP 5, RUN 60

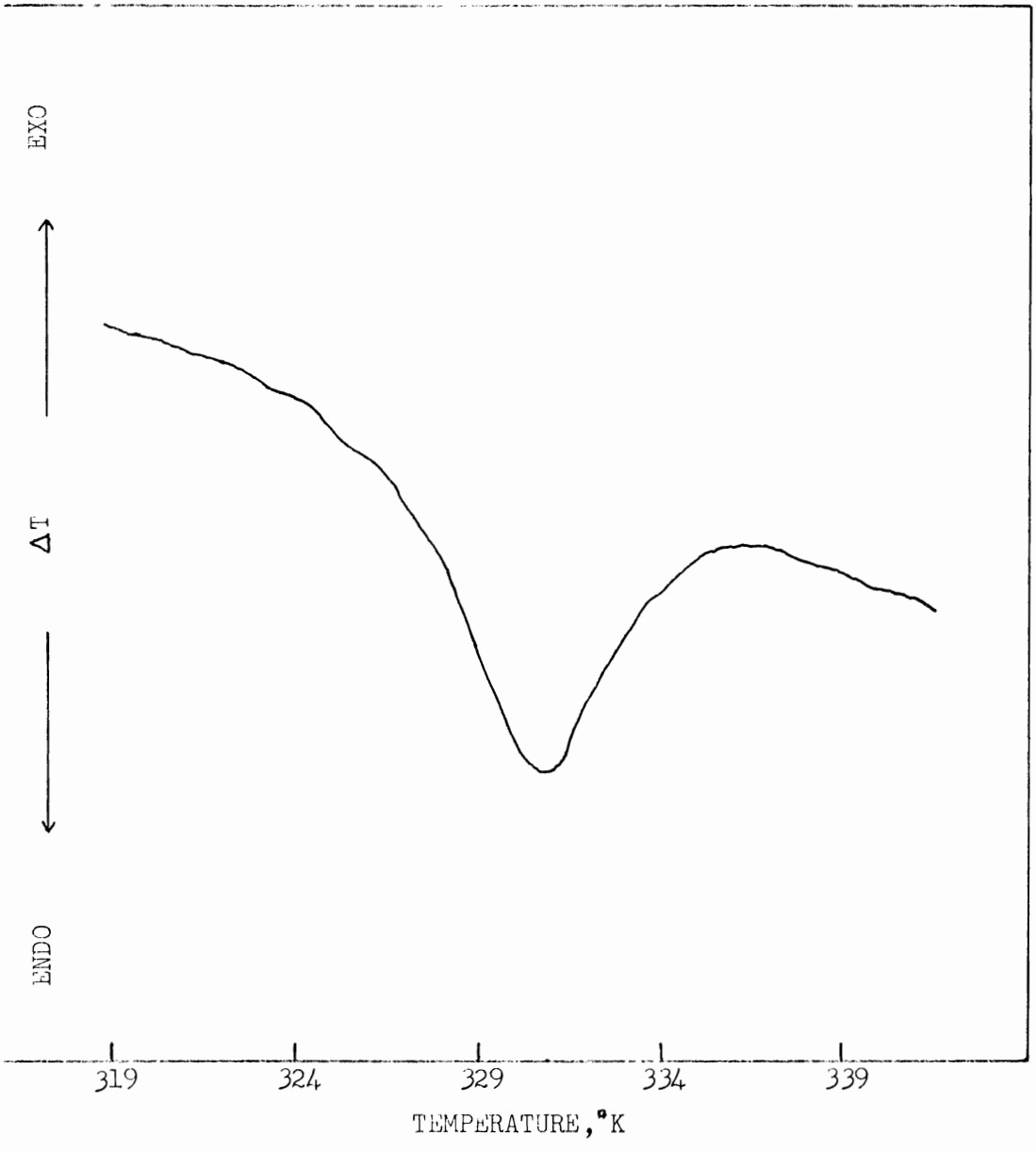

FIGURE D.26

DSC THERMOGRAM of RED AMORPHOUS SELENIUM #10, GROUP 5, RUN 69

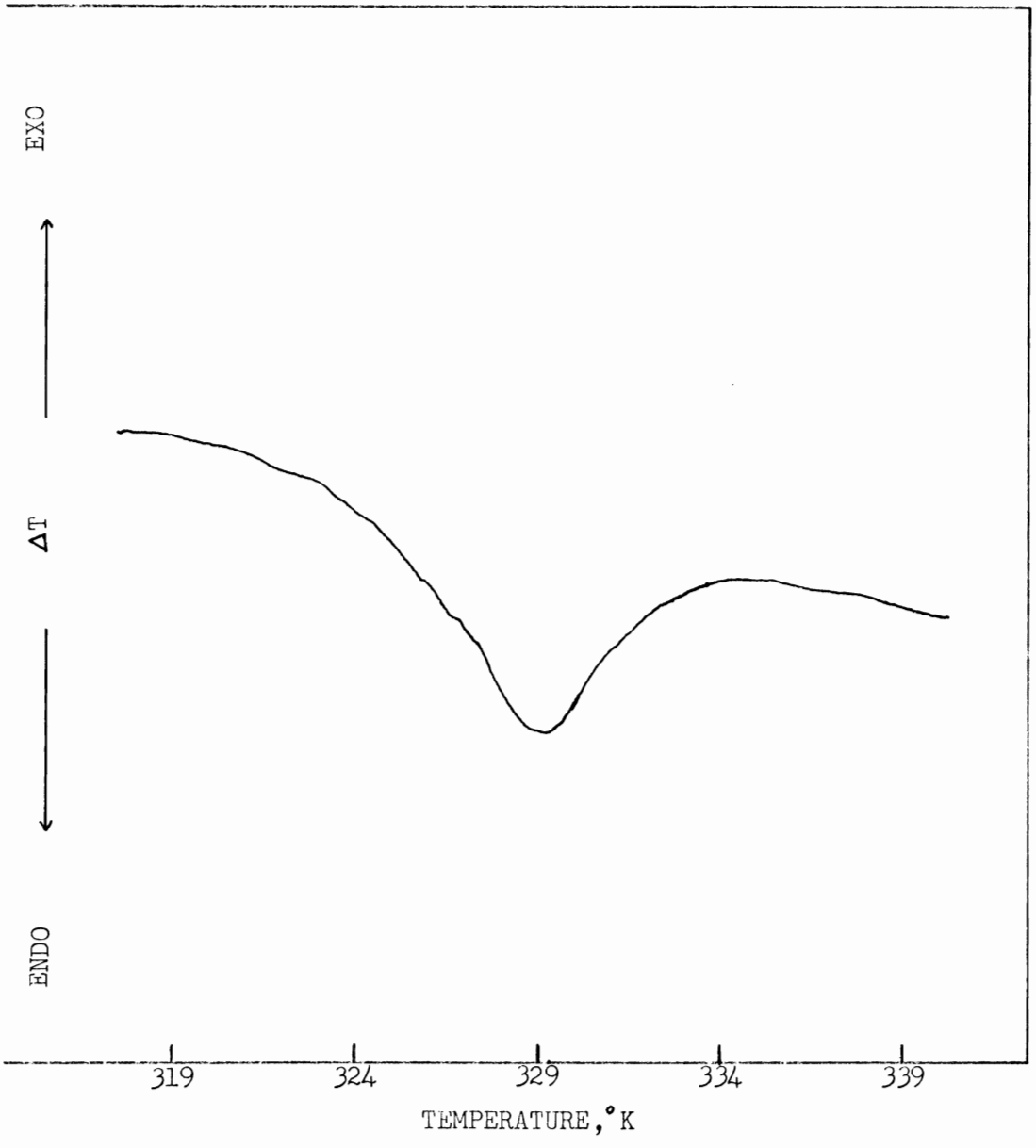

FIGURE D.27

DSC THERMOGRAM of RED AMORPHOUS SELENIUM #11, GROUP 2, RUN 1

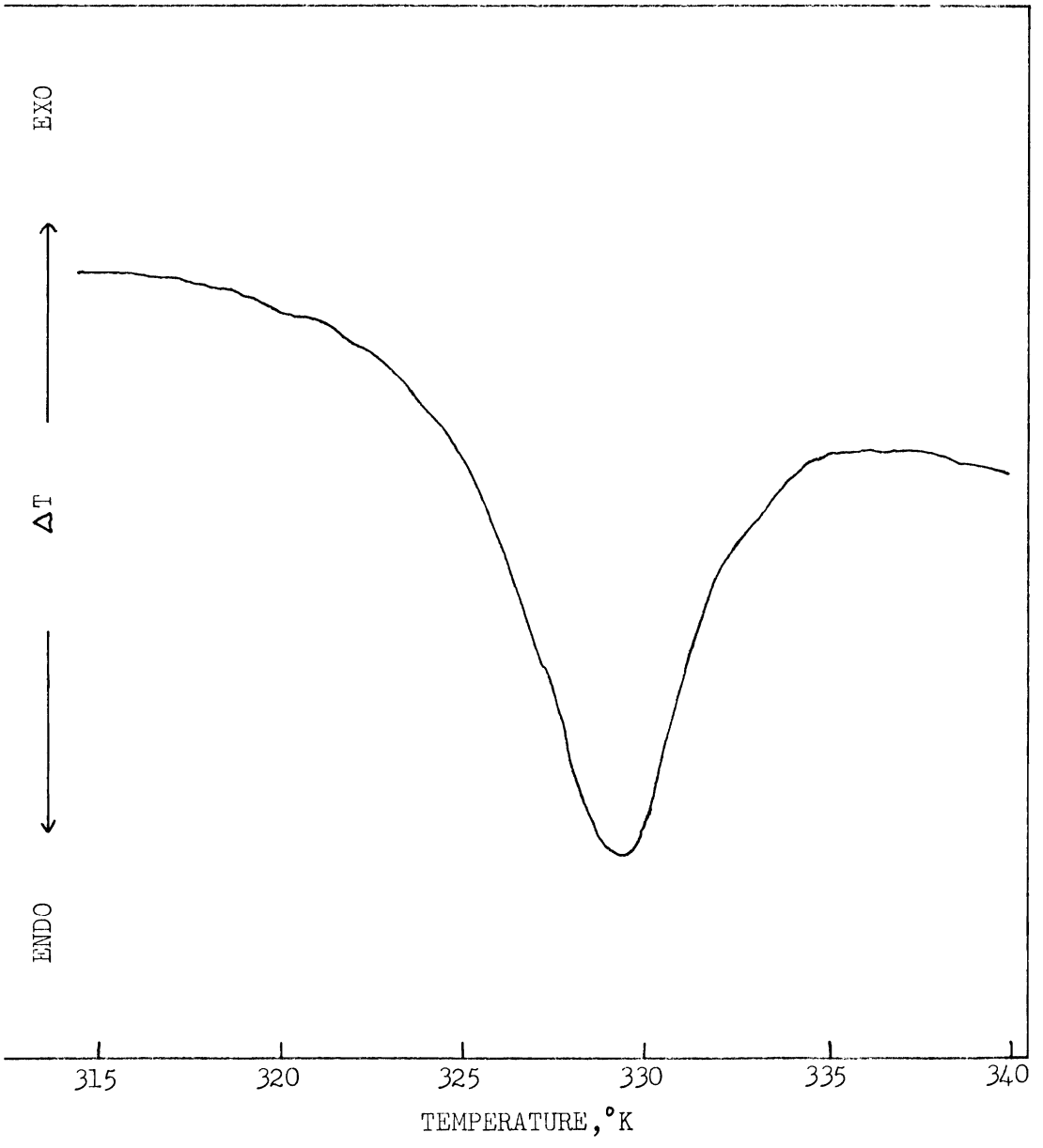

FIGURE D.28

DSC THERMOGRAM of RED AMORPHOUS SELENIUM #11, GROUP 2, RUN 7

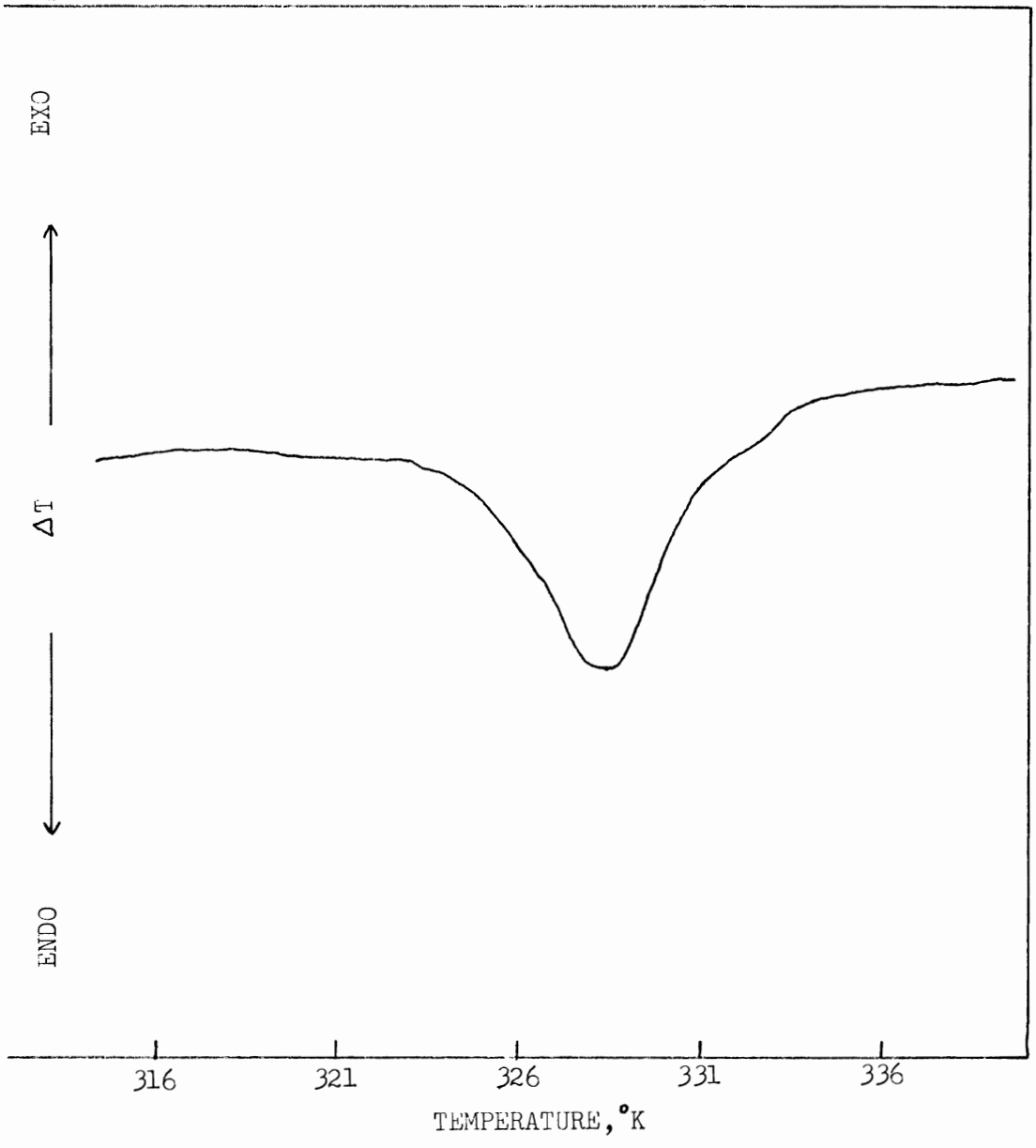

FIGURE D.29

DSC THERMOGRAM of RED AMORPHOUS SELENIUM #11, GROUP 2, RUN 13

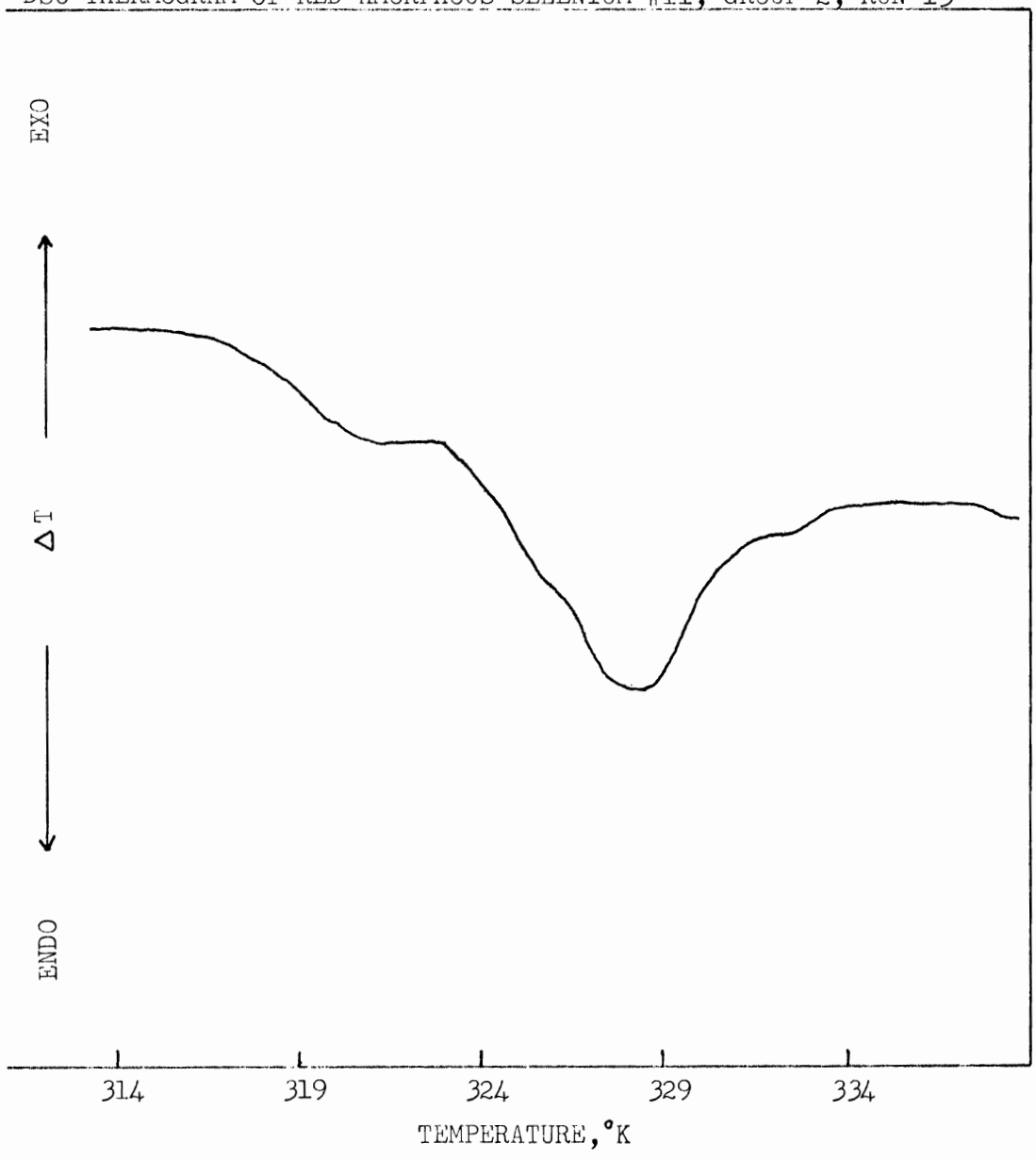

FIGURE D.30

DSC THERMOGRAM of RED AMORPHOUS SELENIUM #11, GROUP 2, RUN 25

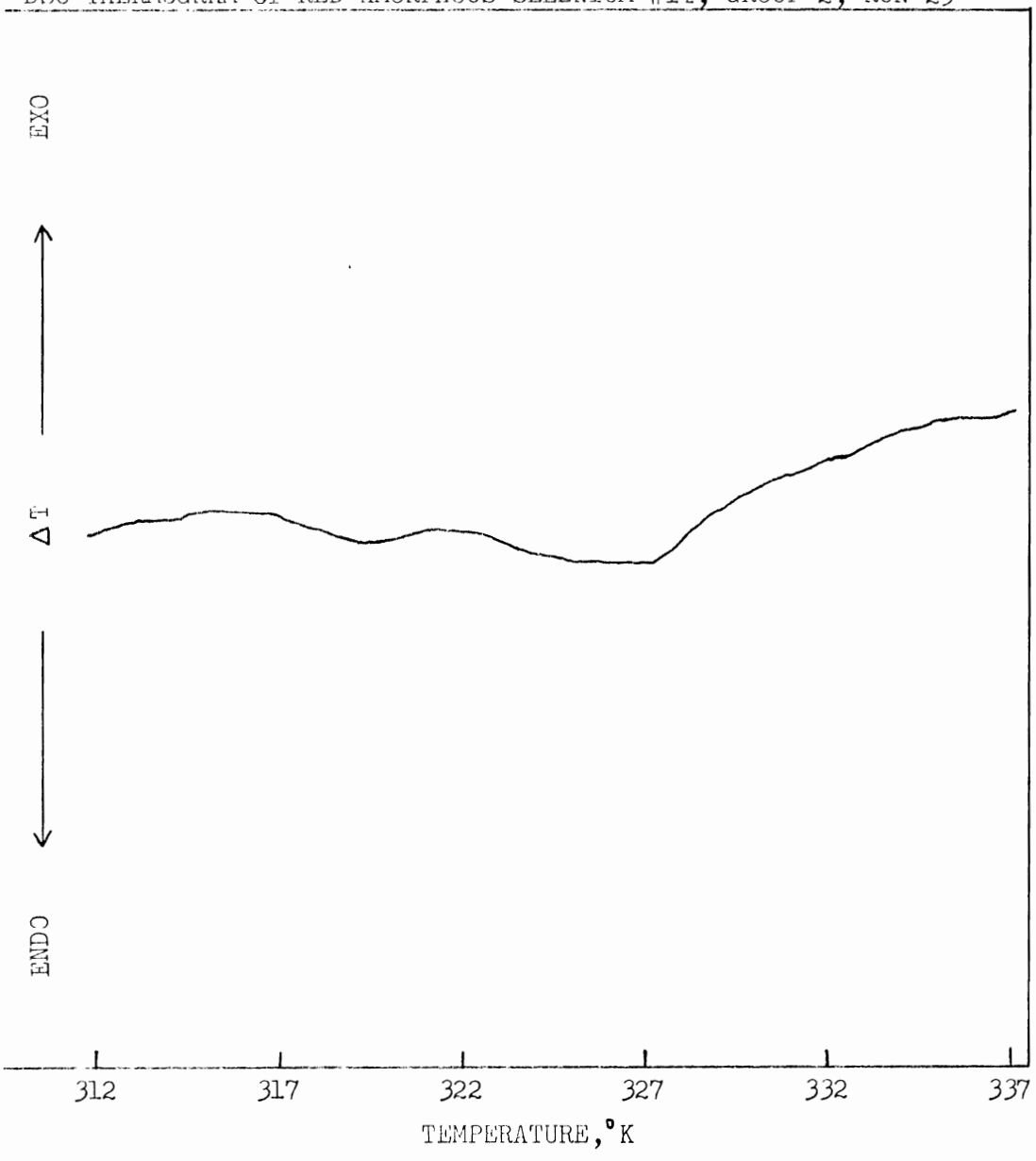

FIGURE D.31

DSC THERMOGRAM of RED AMORPHOUS SELENIUM #11, GROUP 2, RUN 39

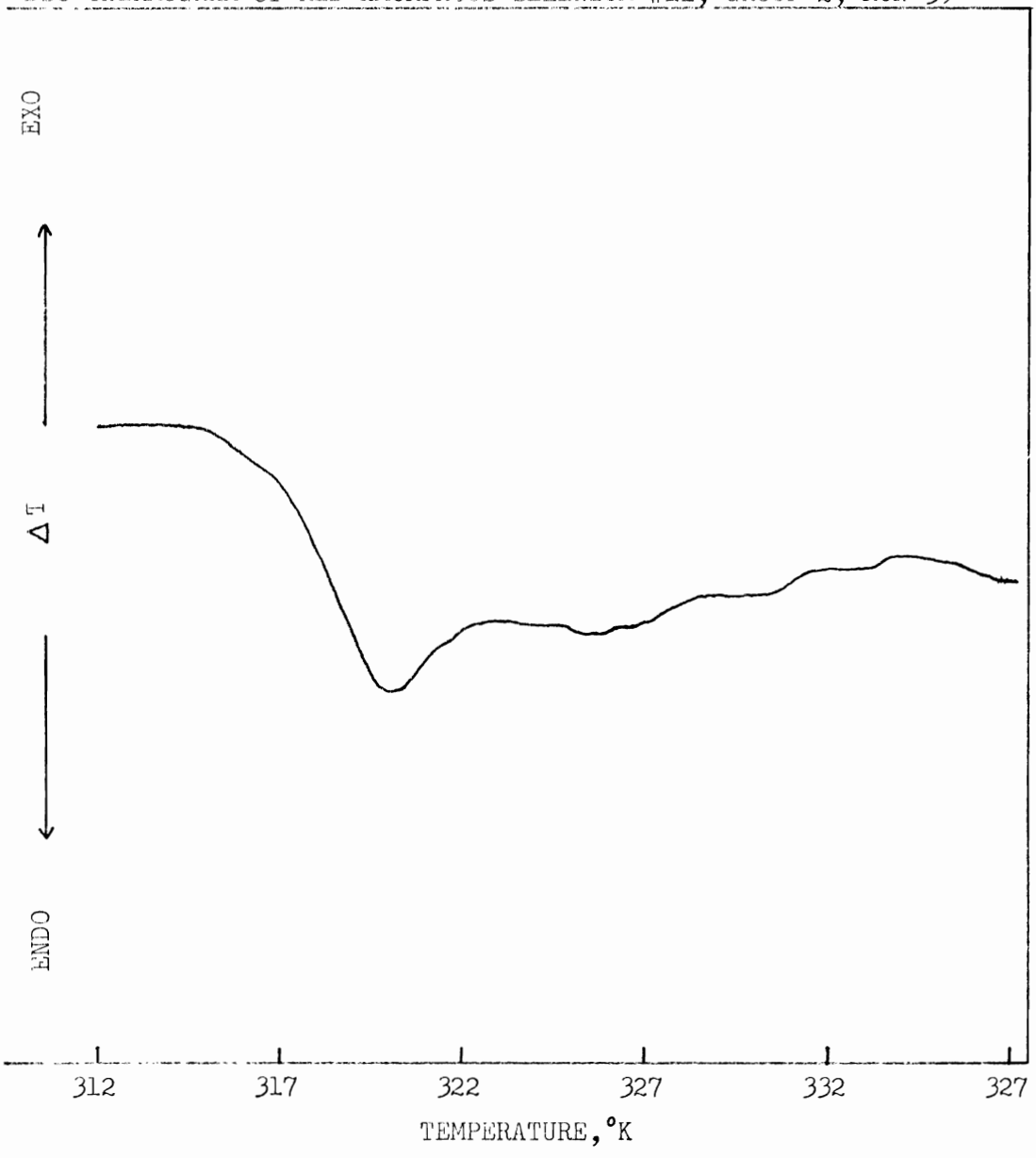

FIGURE D.32

DSC THERMOGRAM of RED AMORPHOUS SELENIUM #11, GROUP 1, RUN 3

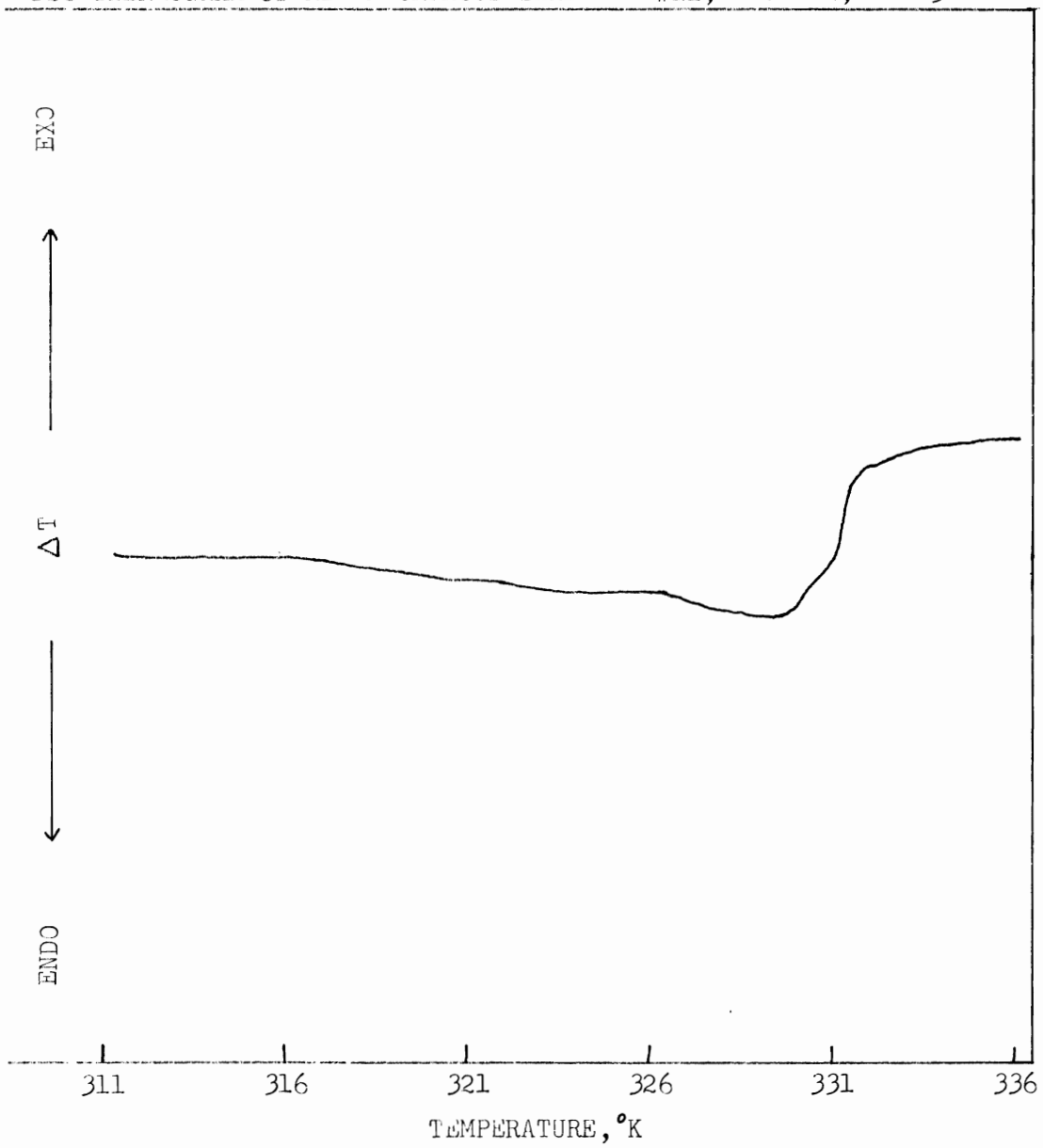

FIGURE D.33

DSC THERMOGRAM of RED AMORPHOUS SELENIUM #11, GROUP 1, RUN 29

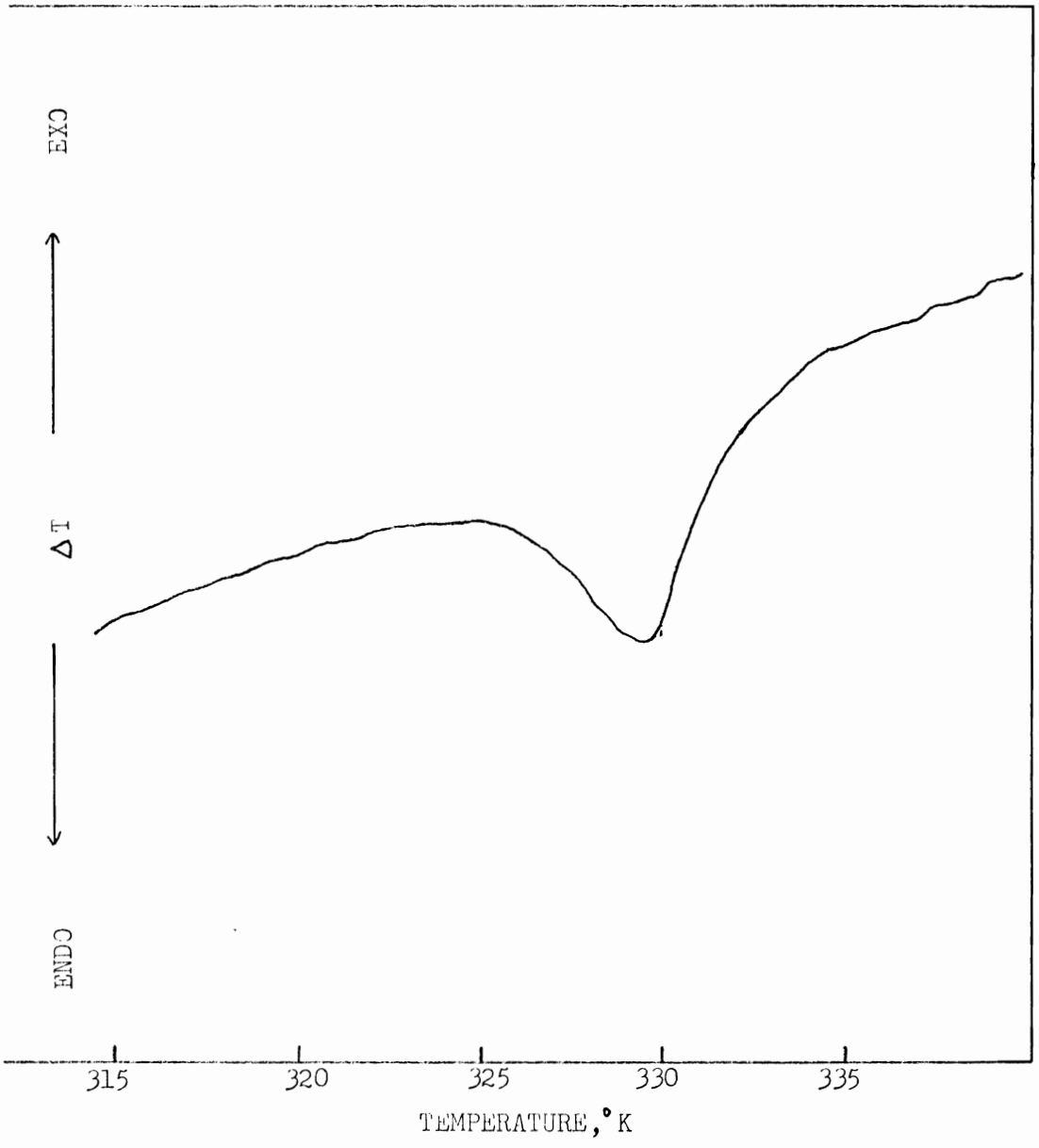

FIGURE D.34

DSC THERMOGRAM of RED AMORPHOUS SELENIUM #11, GROUP 1, RUN 34

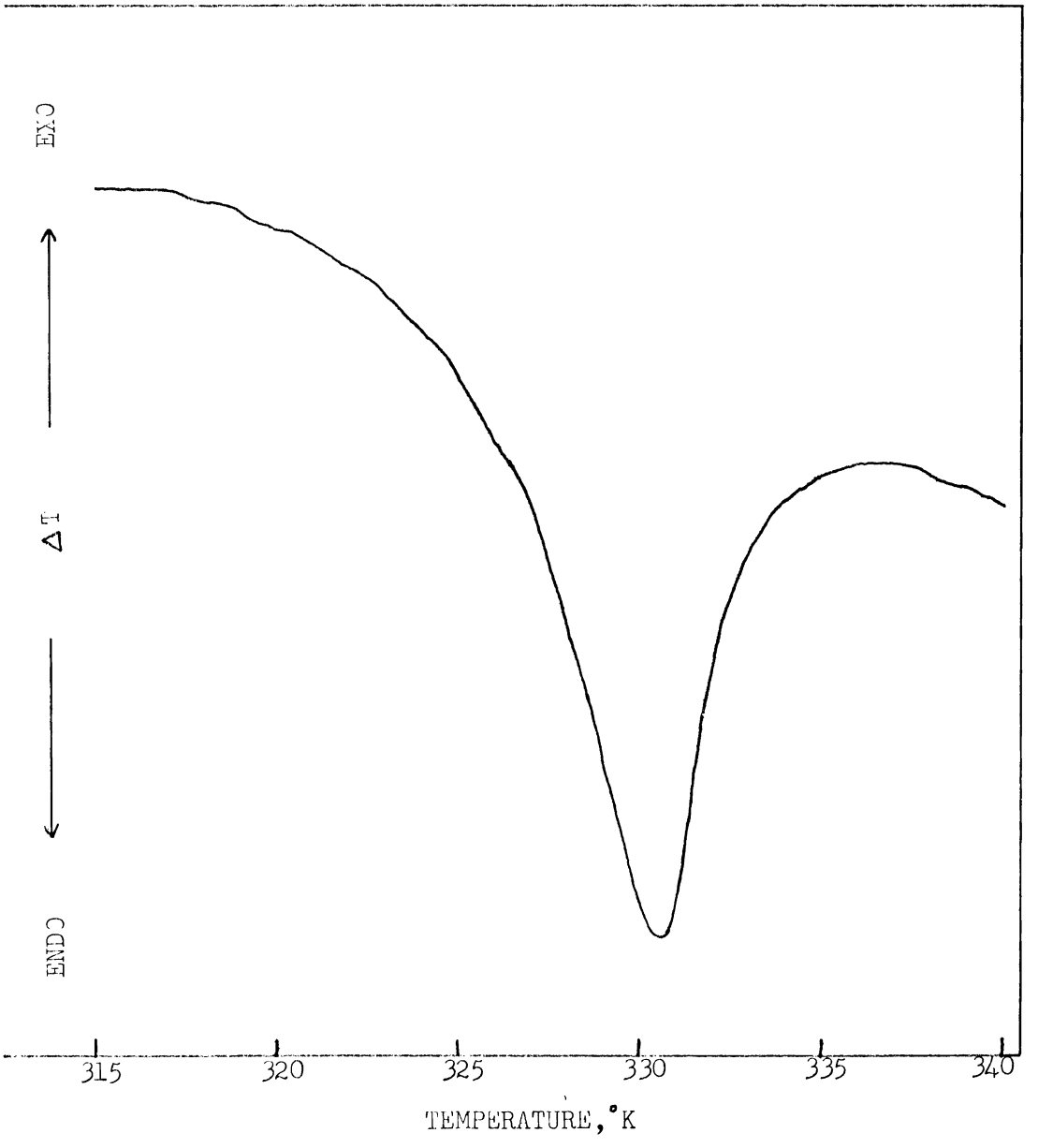

FIGURE D.35

DSC THERMOGRAM of RED AMORPHOUS SELENIUM #11, GROUP 4, RUN 6

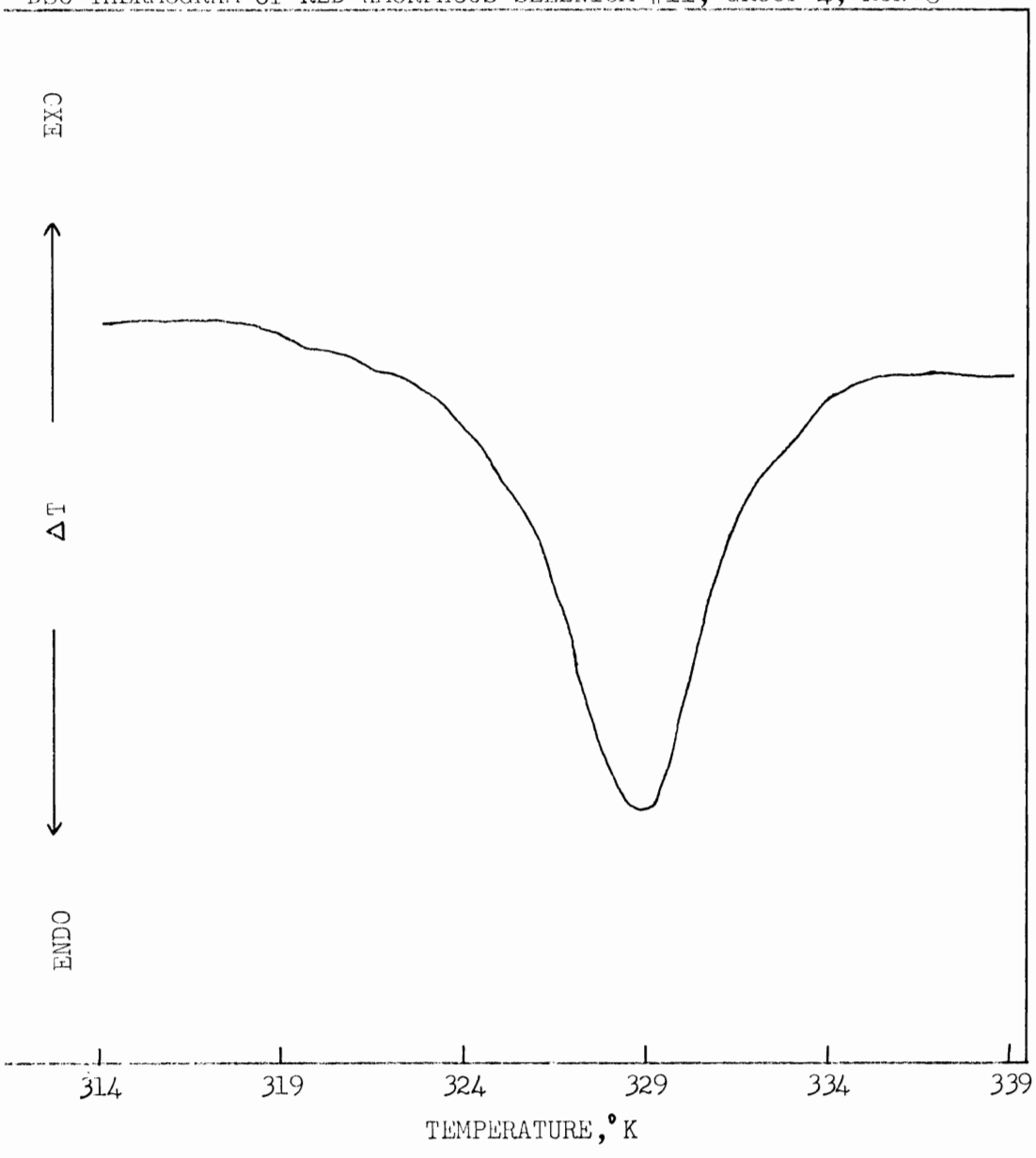

FIGURE D.36

DSC THERMOGRAM of RED AMORPHOUS SELENIUM #11, GROUP 4, RUN 14

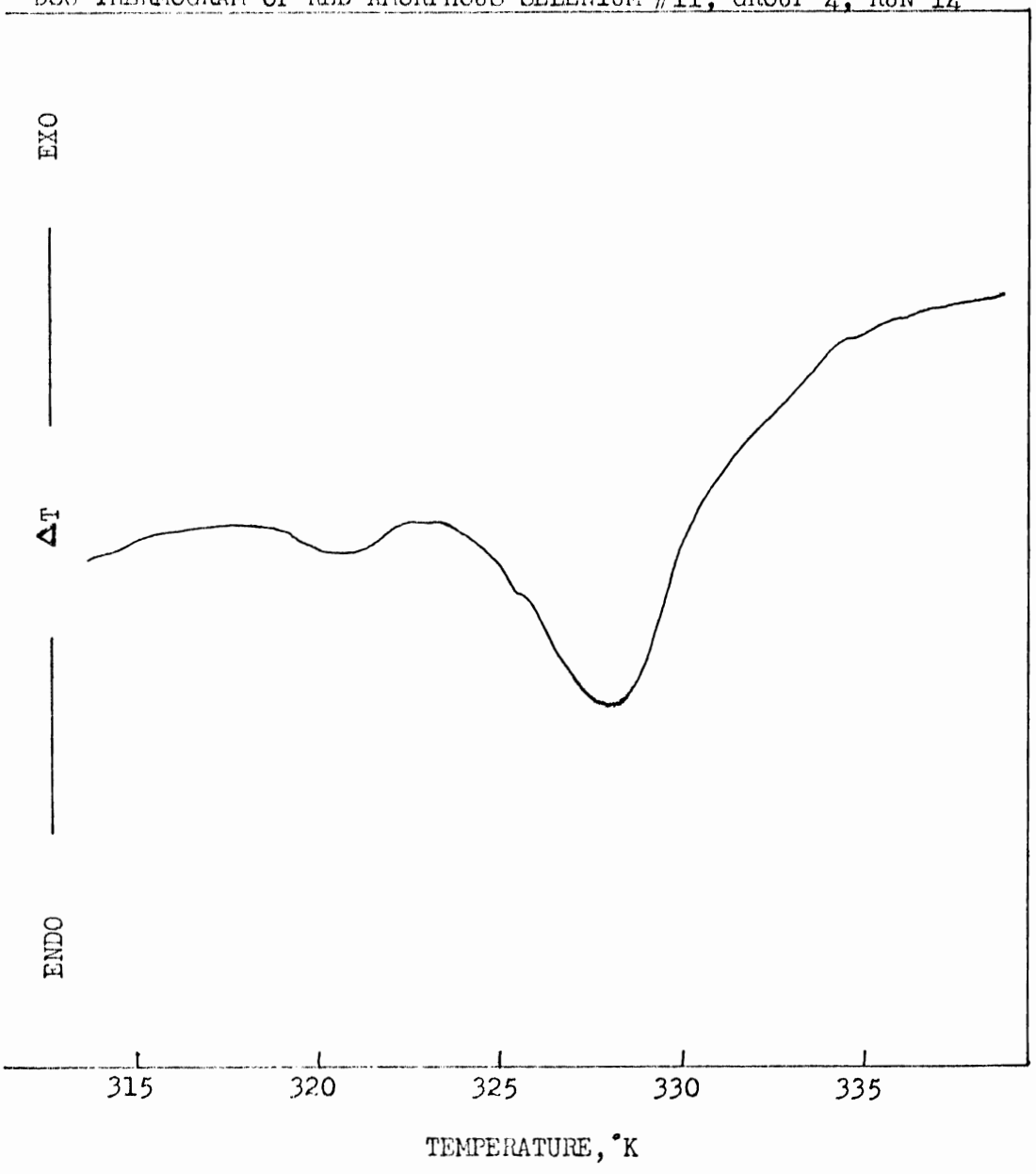

FIGURE D.37

DSC THERMOGRAM of RED AMORPHOUS SELENIUM #11, GROUP 4, RUN 23

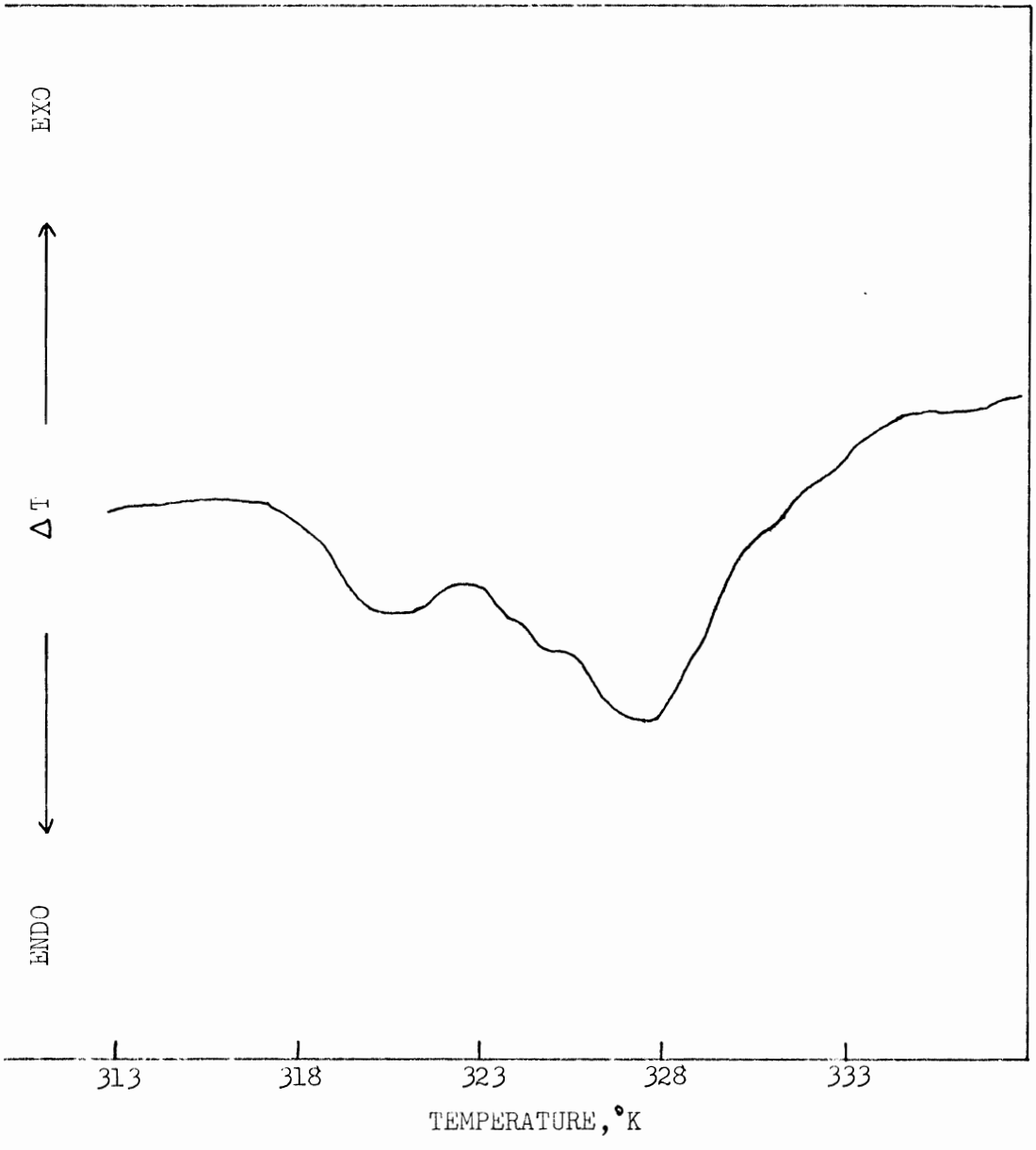

FIGURE D.38

DSC THERMOGRAM of RED AMORPHOUS SELENIUM #11, GROUP 4, RUN 40

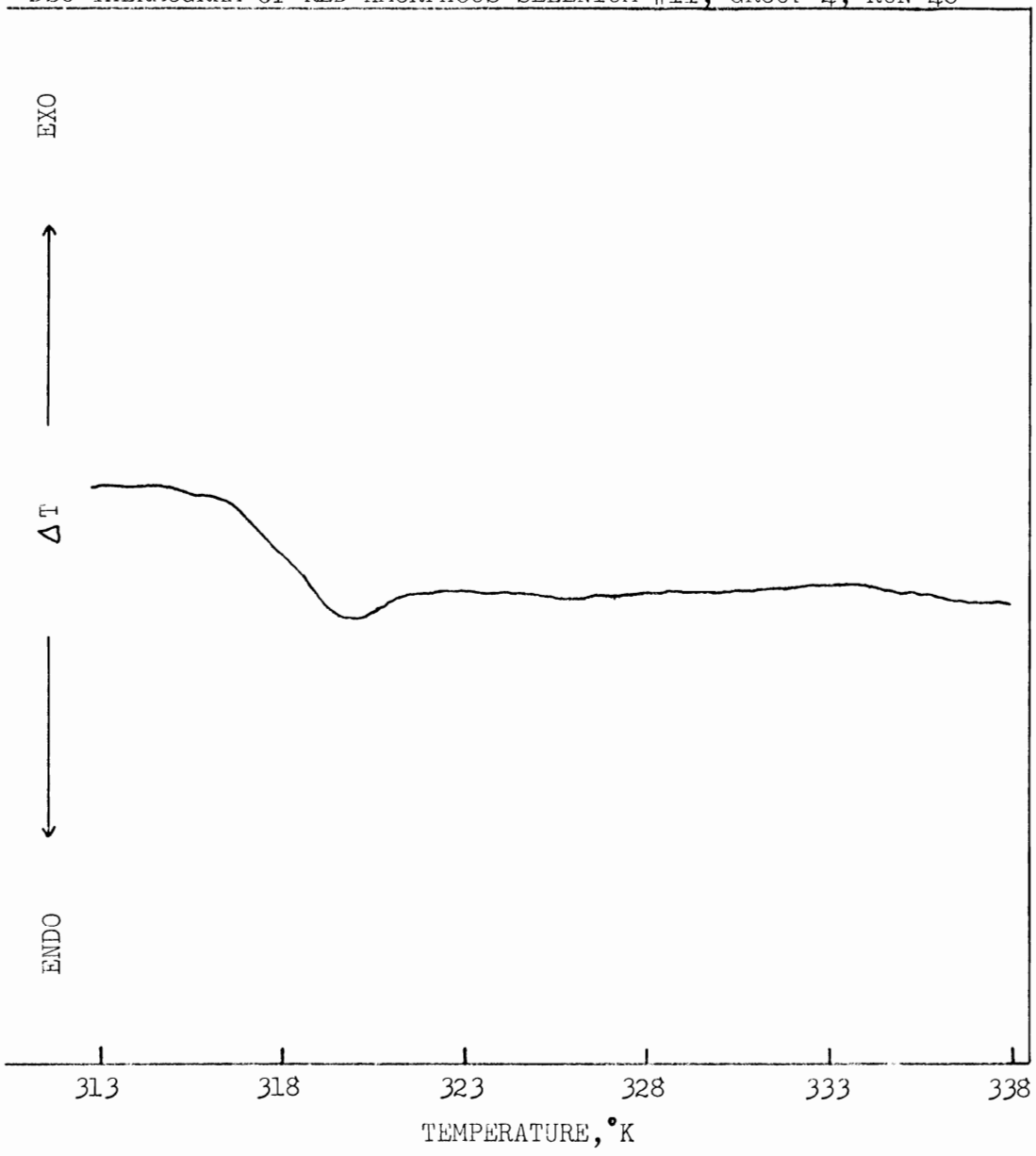

FIGURE D.39

DSC THERMOGRAM of RED AMORPHOUS SELENIUM #11, GROUP 3, RUN 4

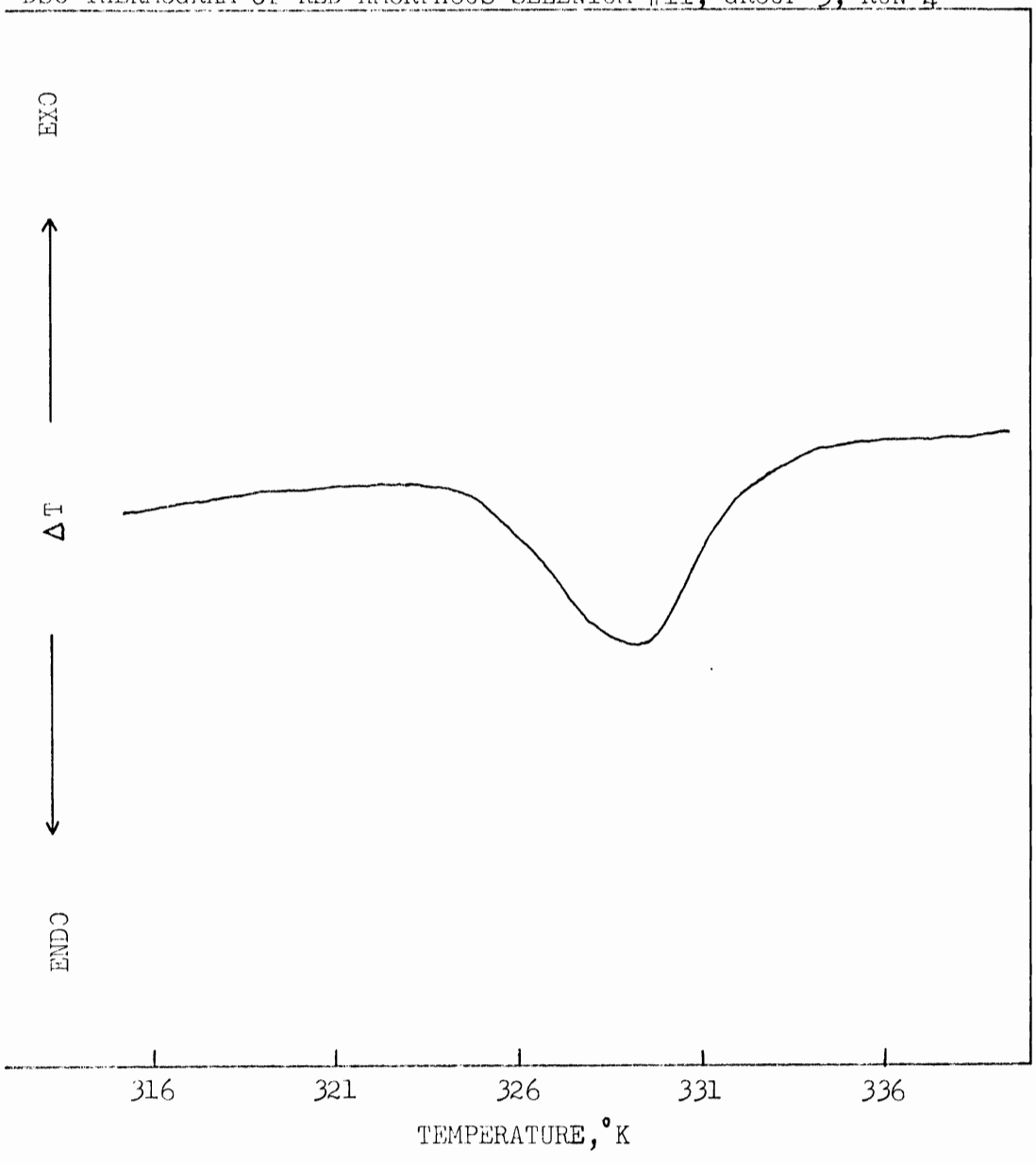

FIGURE D.40

DSC THERMOGRAM of RED AMORPHOUS SELENIUM #11, GROUP 3, RUN 18

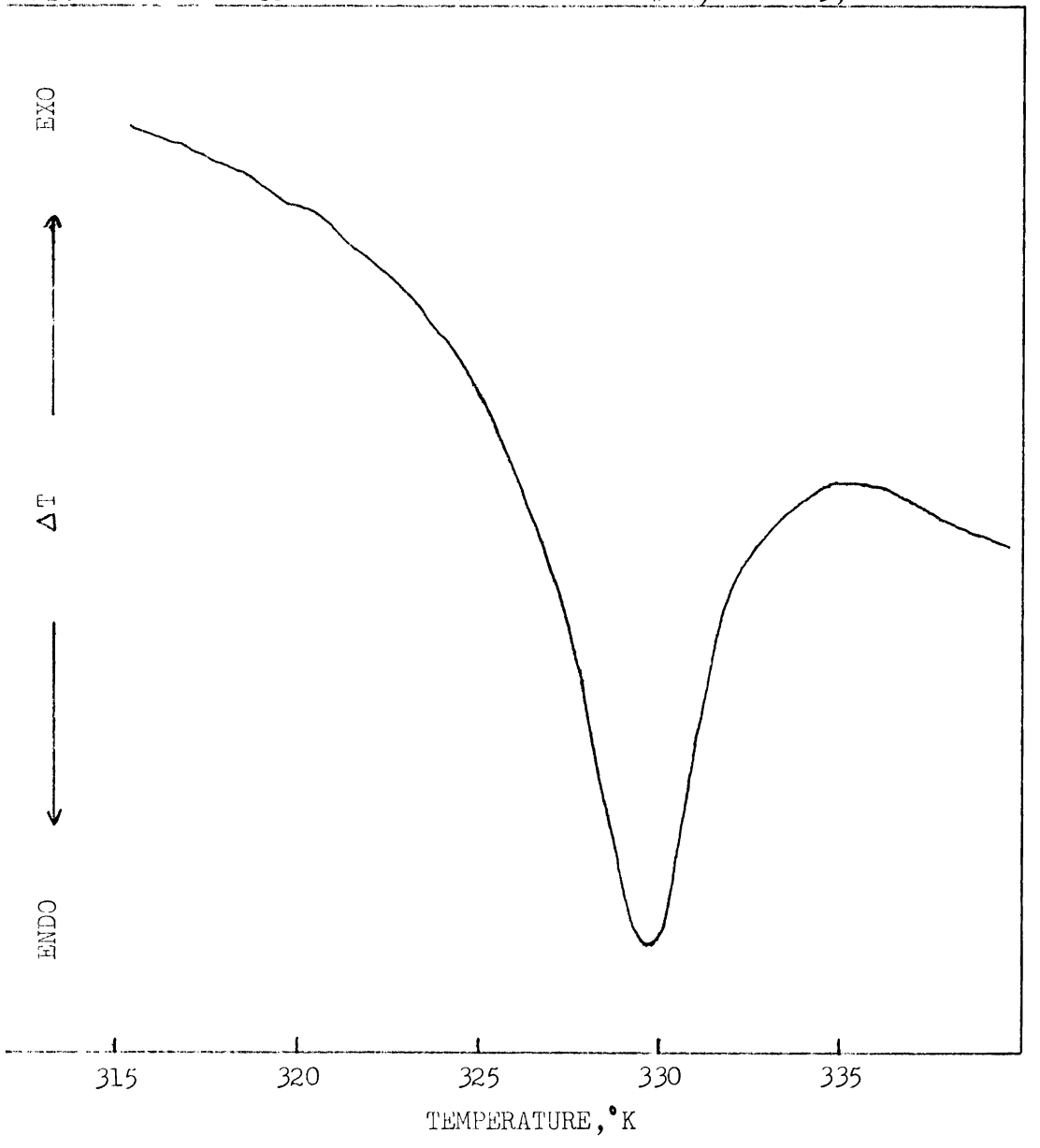

FIGURE D.41

DSC THERMOGRAM of RED AMORPHOUS SELENIUM #11, GROUP 3, RUN 28

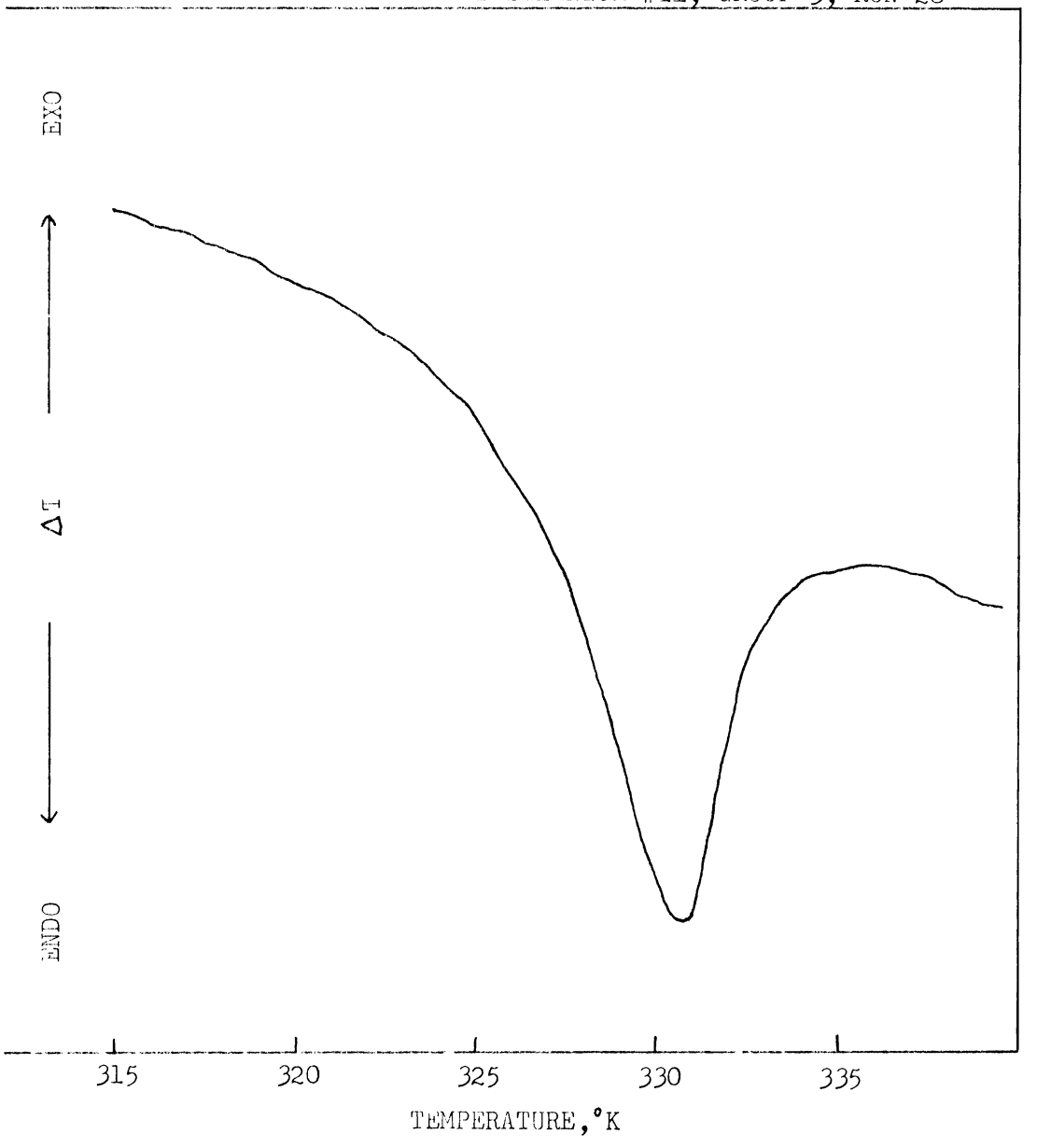

FIGURE D.42

DSC THERMOGRAM of RED AMORPHOUS SELENIUM #11, GROUP 3, RUN 33

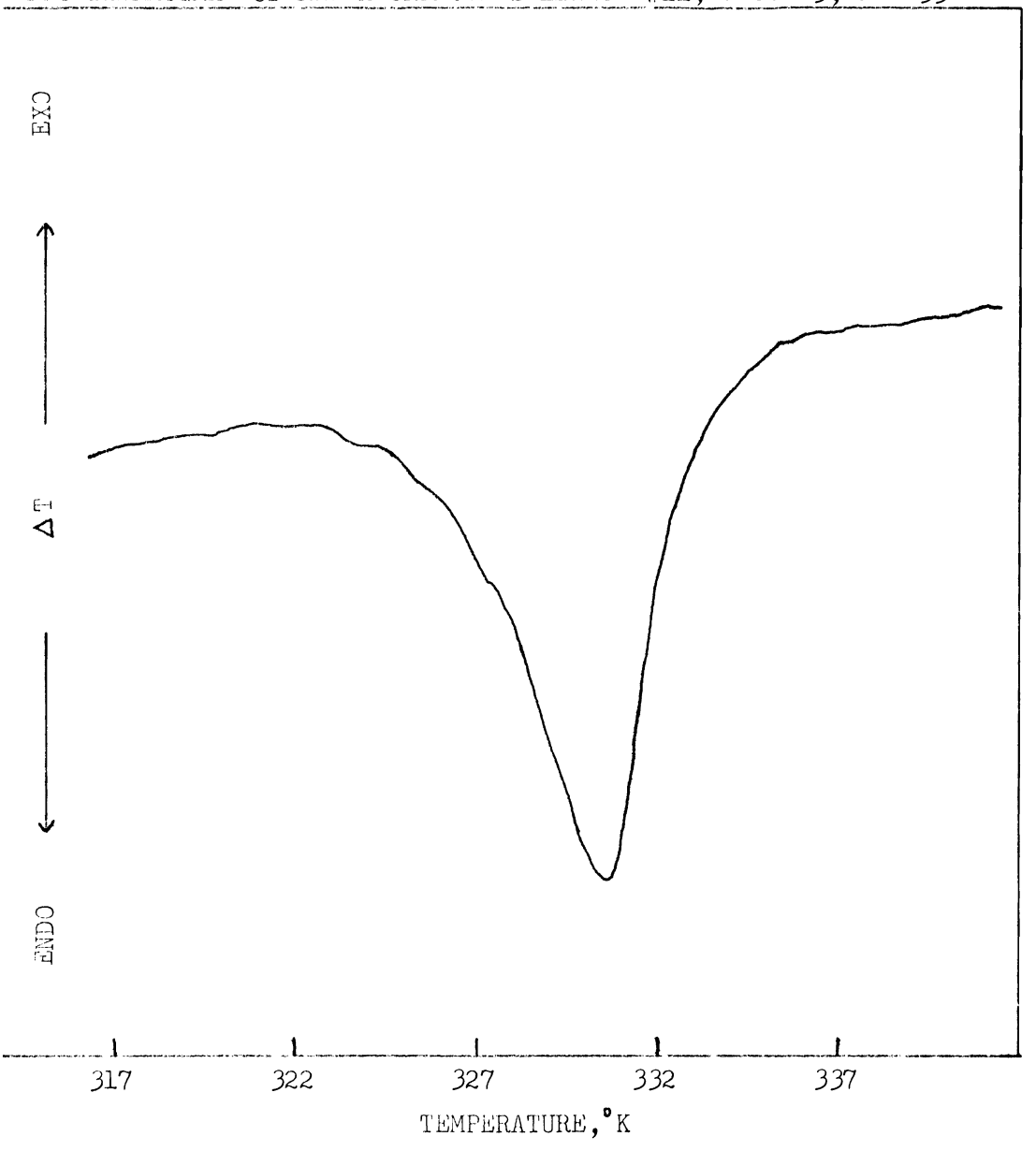

FIGURE D.43

DSC THERMOGRAM of RED AMORPHOUS SELENIUM #11, GROUP 6, RUN 9

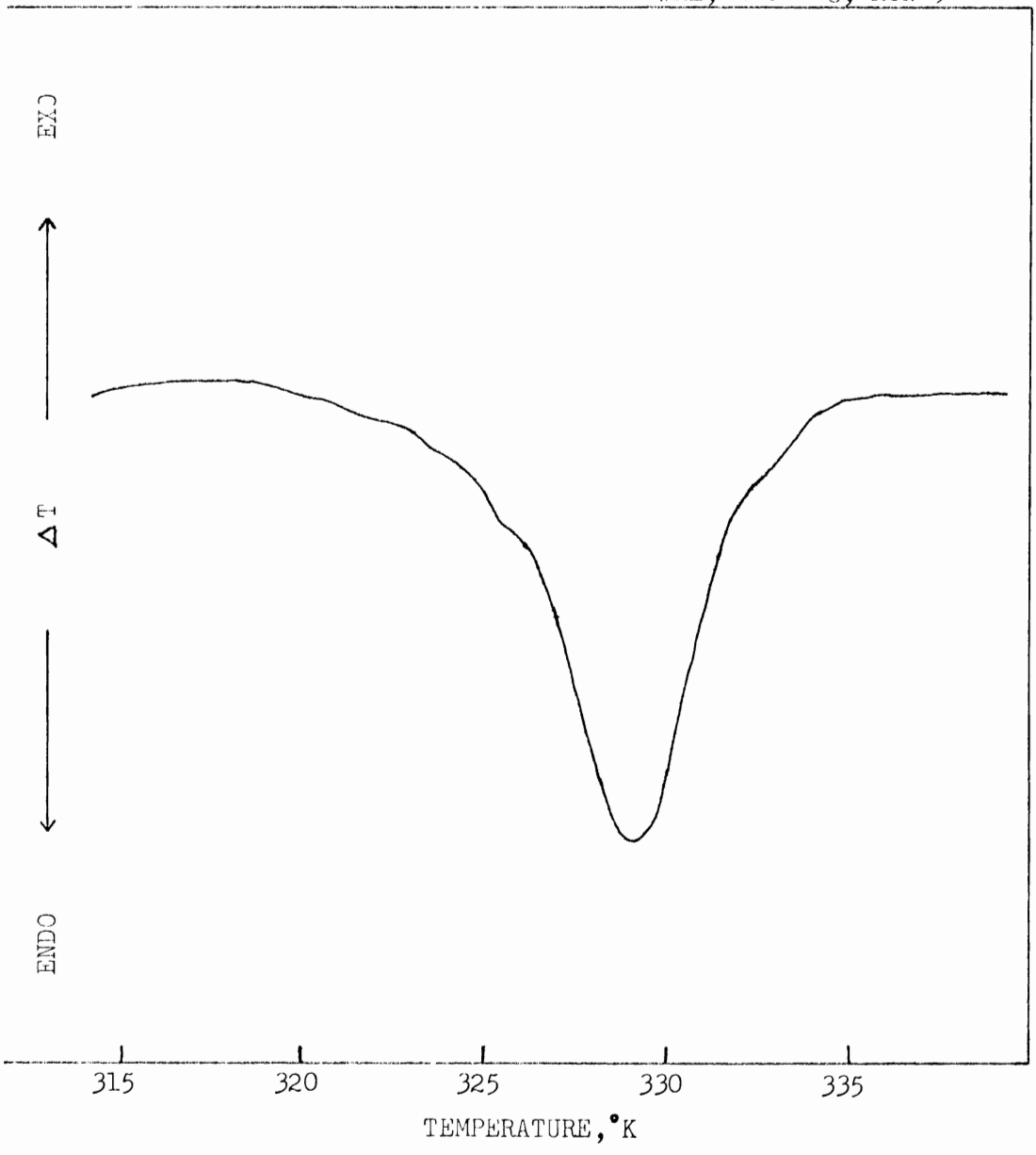

FIGURE D.44

DSC THERMOGRAM of RED AMORPHOUS SELENIUM #11, GROUP 6, RUN 22

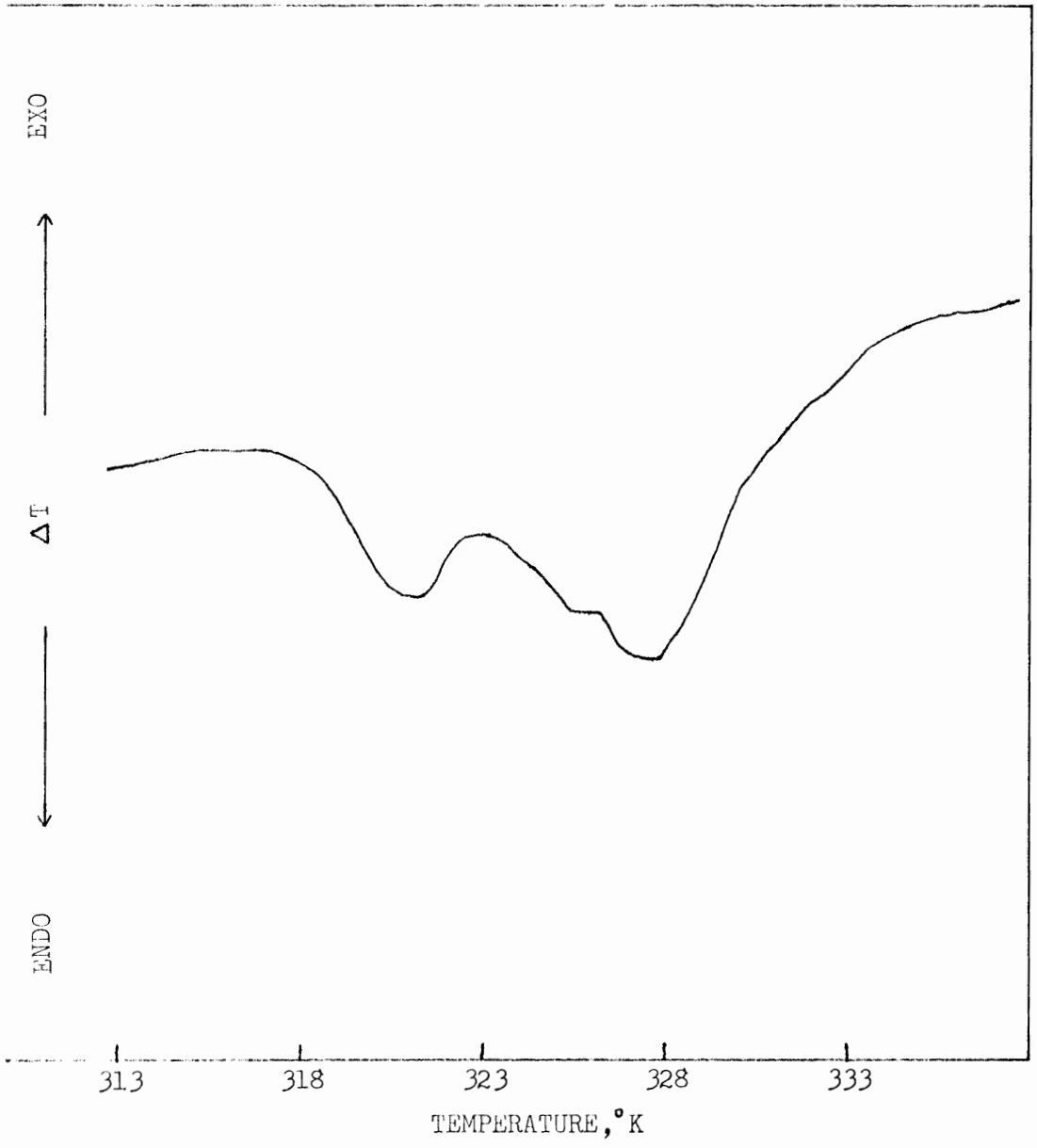

FIGURE D.45

DSC THERMOGRAM of RED AMORPHOUS SELENIUM #11, GROUP 6, RUN 37

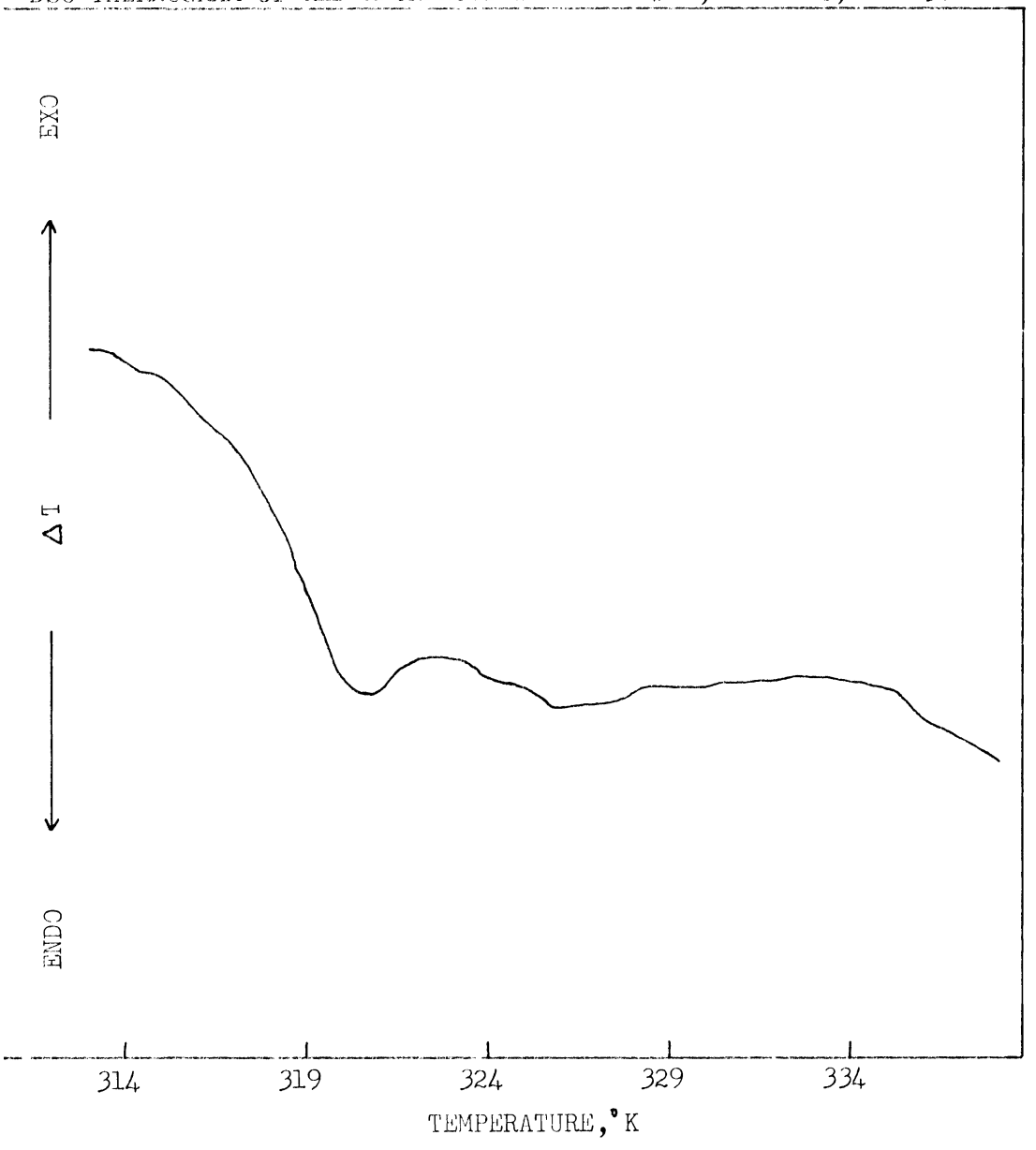

FIGURE D.46

DSC THERMOGRAM of RED AMORPHOUS SELENIUM #11, GROUP 5, RUN 8

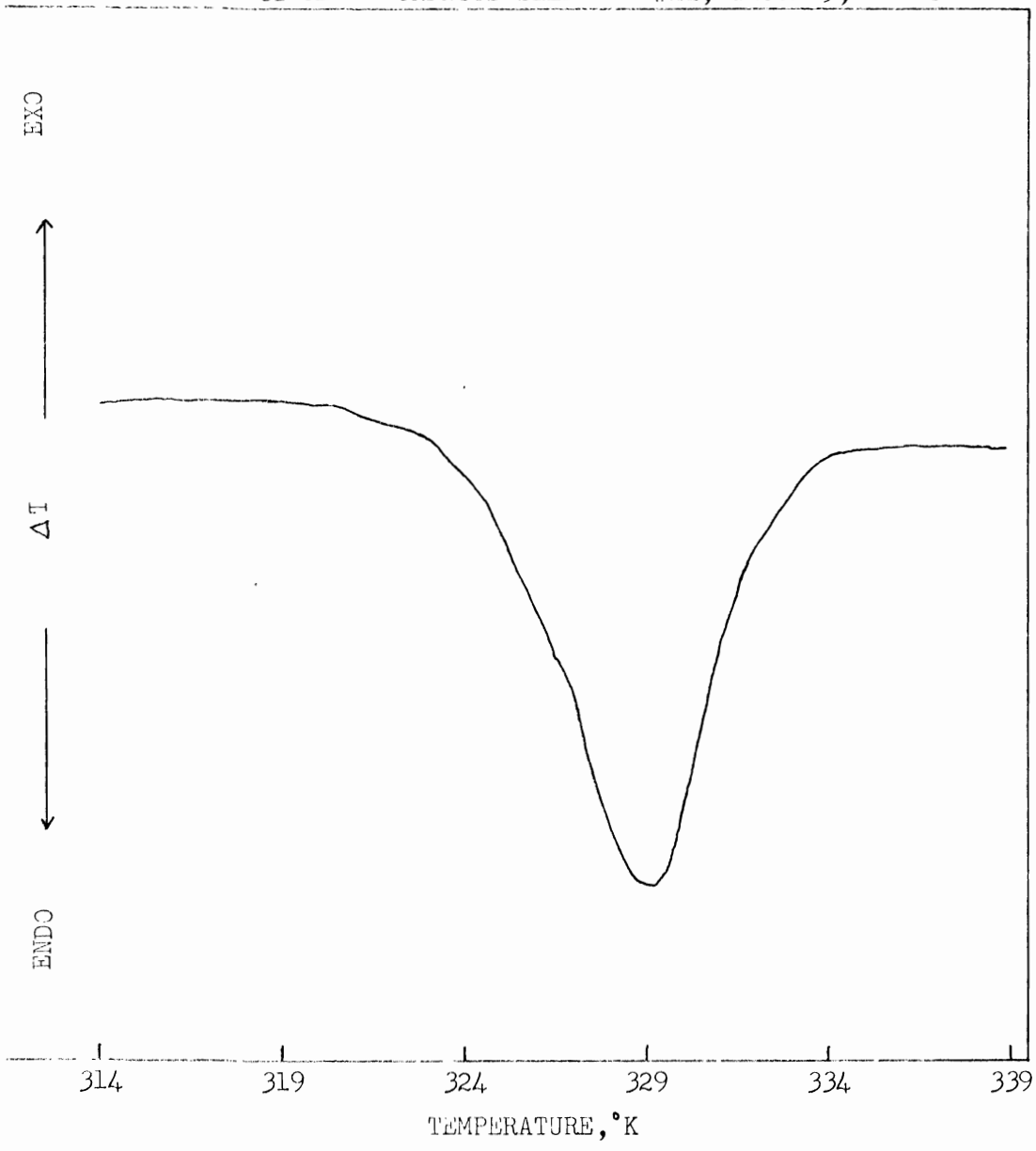

FIGURE D.47

DSC THERMOGRAM of RED AMORPHOUS SELENIUM #11, GROUP 5, RUN 17

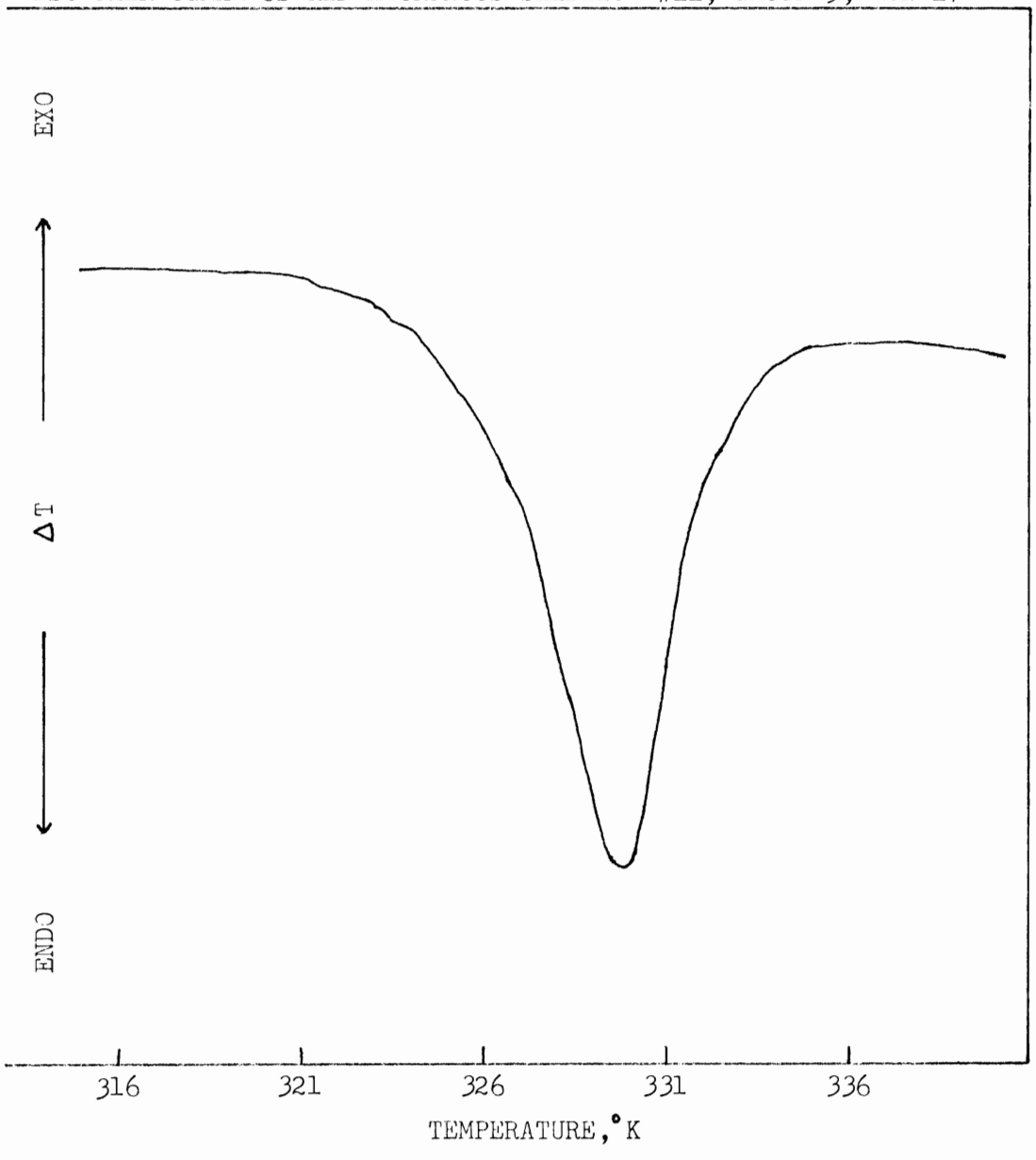

FIGURE D.48

DSC THERMOGRAM of RED AMORPHOUS SELENIUM #11, GROUP 5, RUN 27

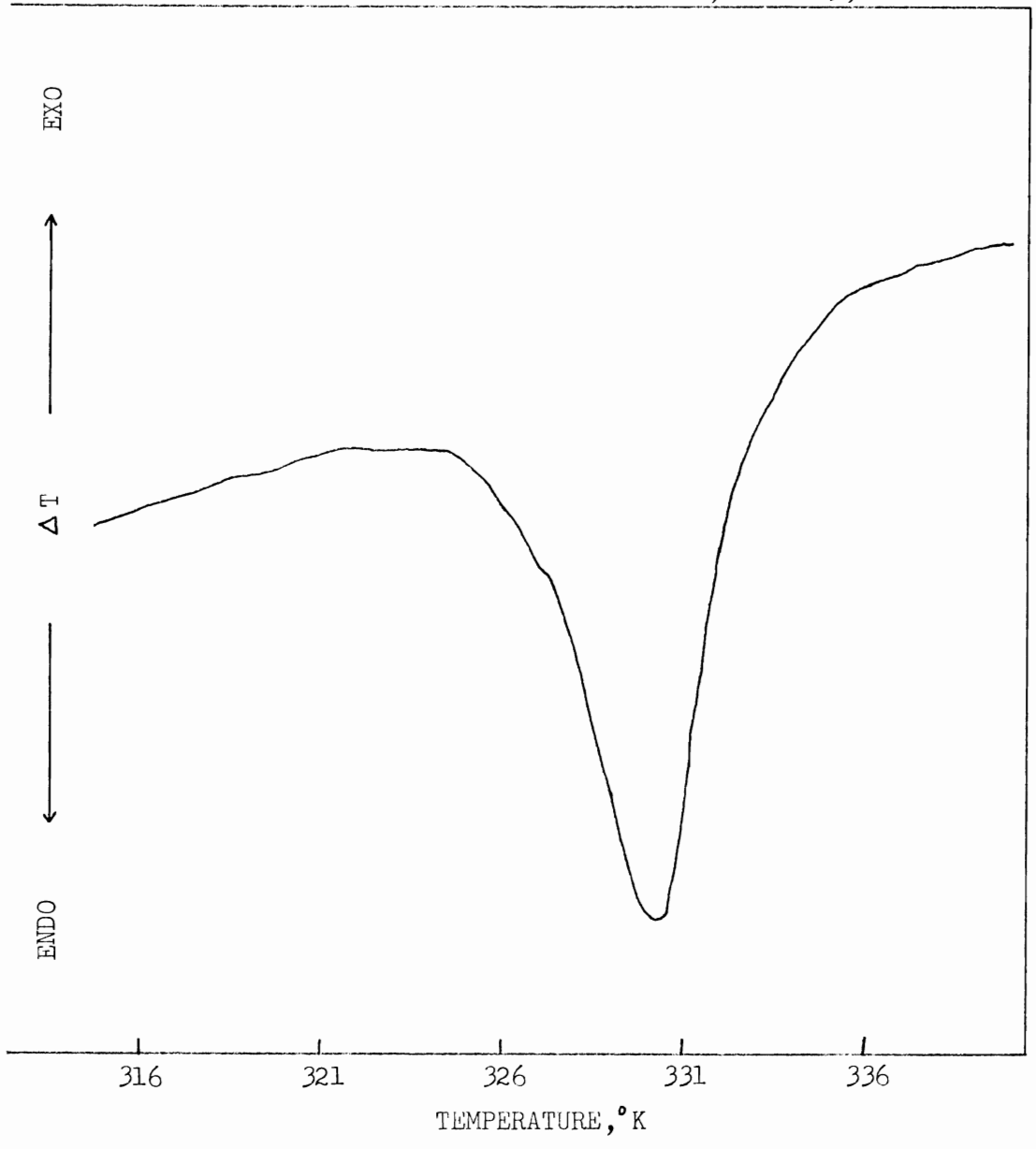

FIGURE D.49

DSC THERMOGRAM of RED AMORPHOUS SELENIUM #11, GROUP 5, RUN 32

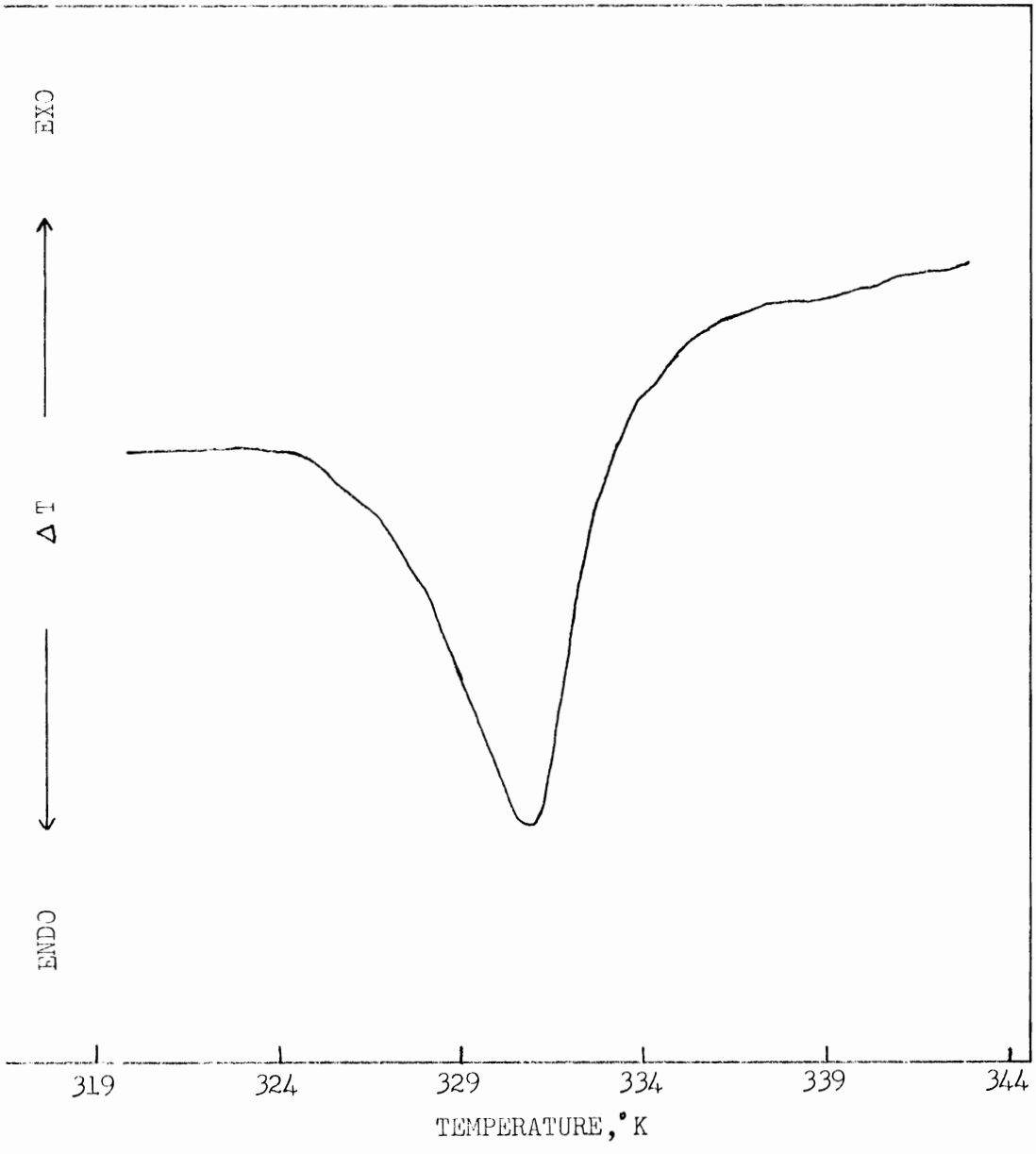

FIGURE D.50

DSC THERMOGRAM of RED AMORPHOUS SELENIUM #11, GROUP 8, RUN 20

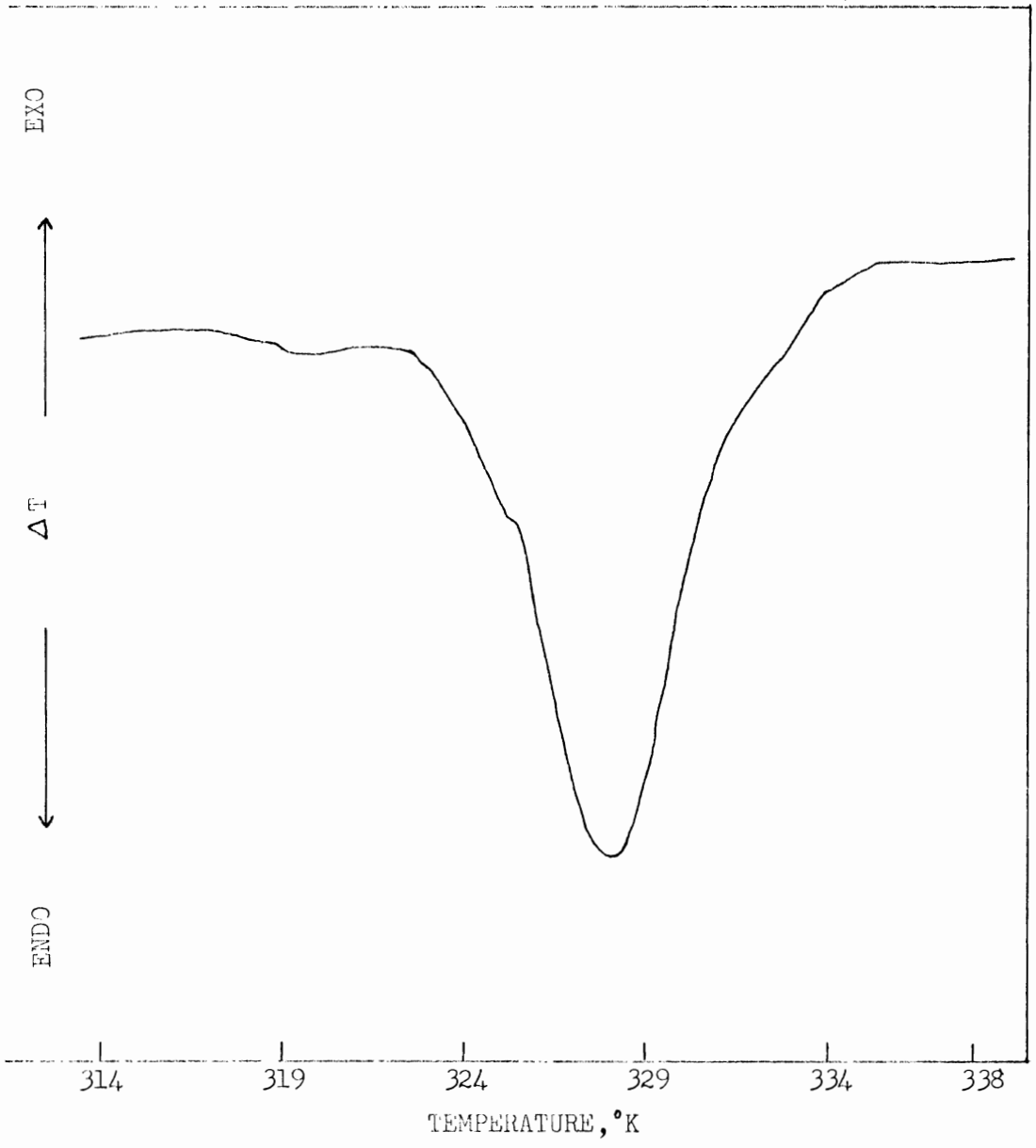

FIGURE D.51

DSC THERMOGRAM of RED AMORPHOUS SELENIUM #11, GROUP 8, RUN 21

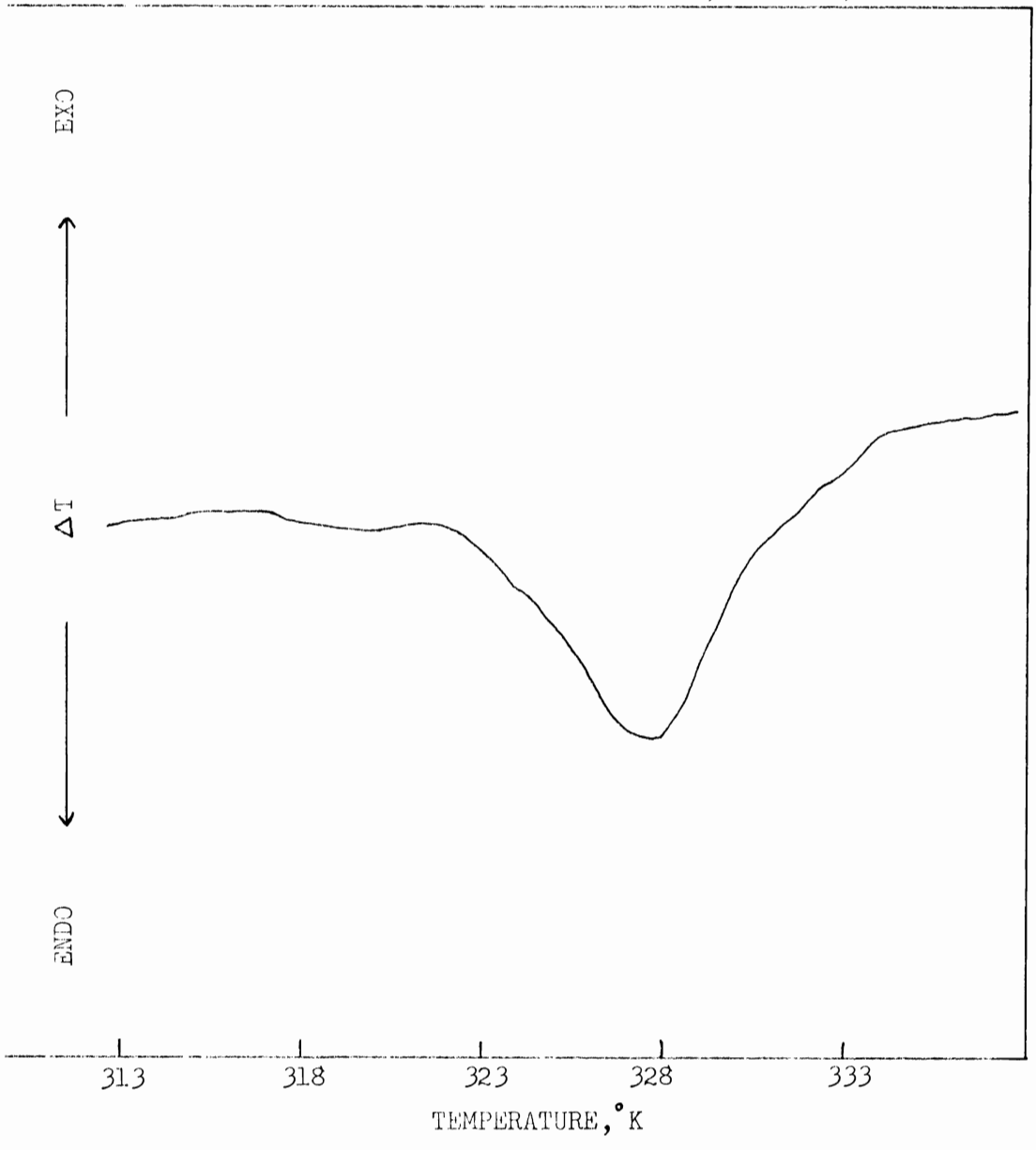

FIGURE D.52

DSC THERMOGRAM of RED AMORPHOUS SELENIUM #11, GROUP 8, RUN 35

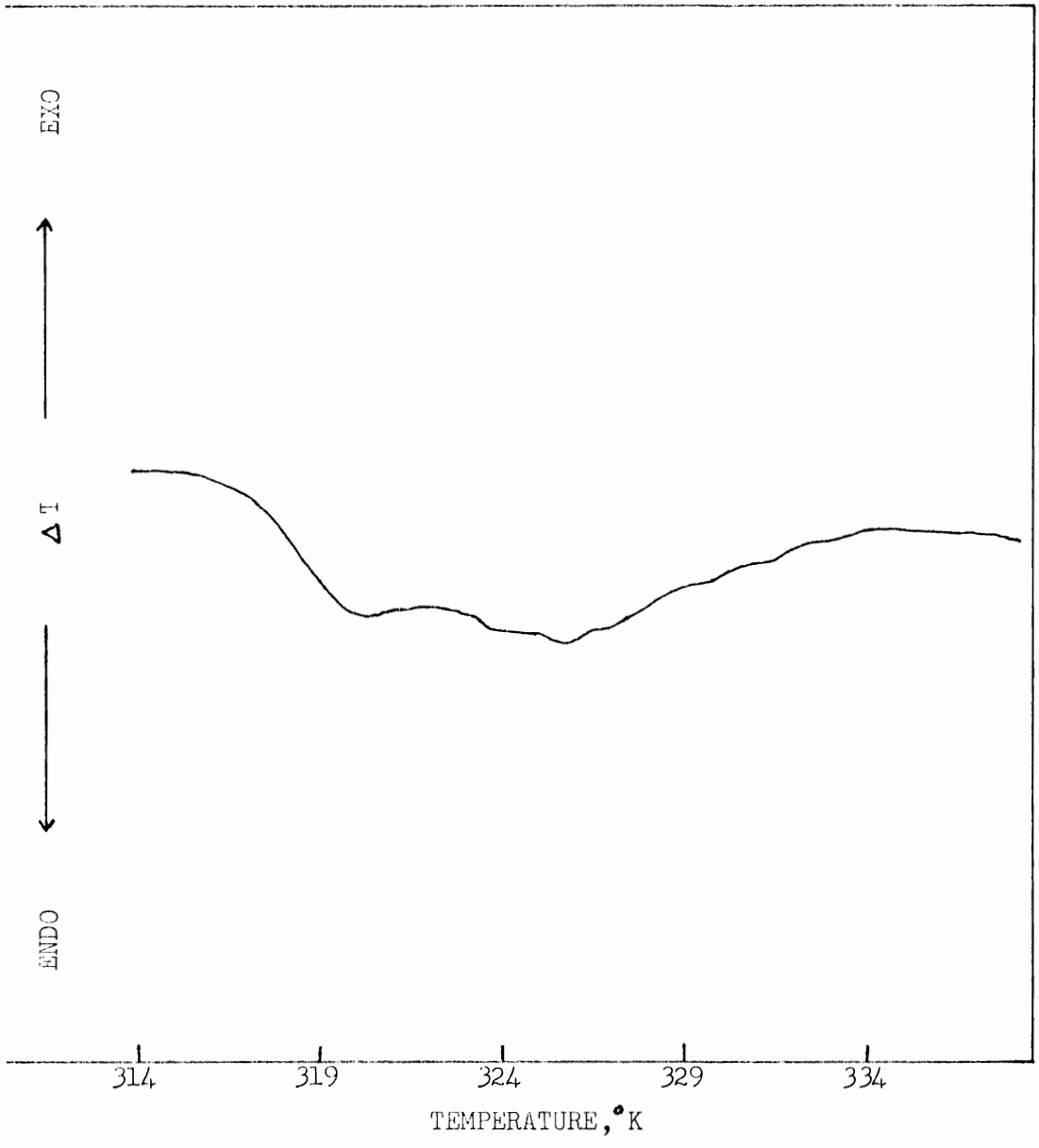

FIGURE D.53

DSC THERMOGRAM of RED AMORPHOUS SELENIUM #11, GROUP 7, RUN 16

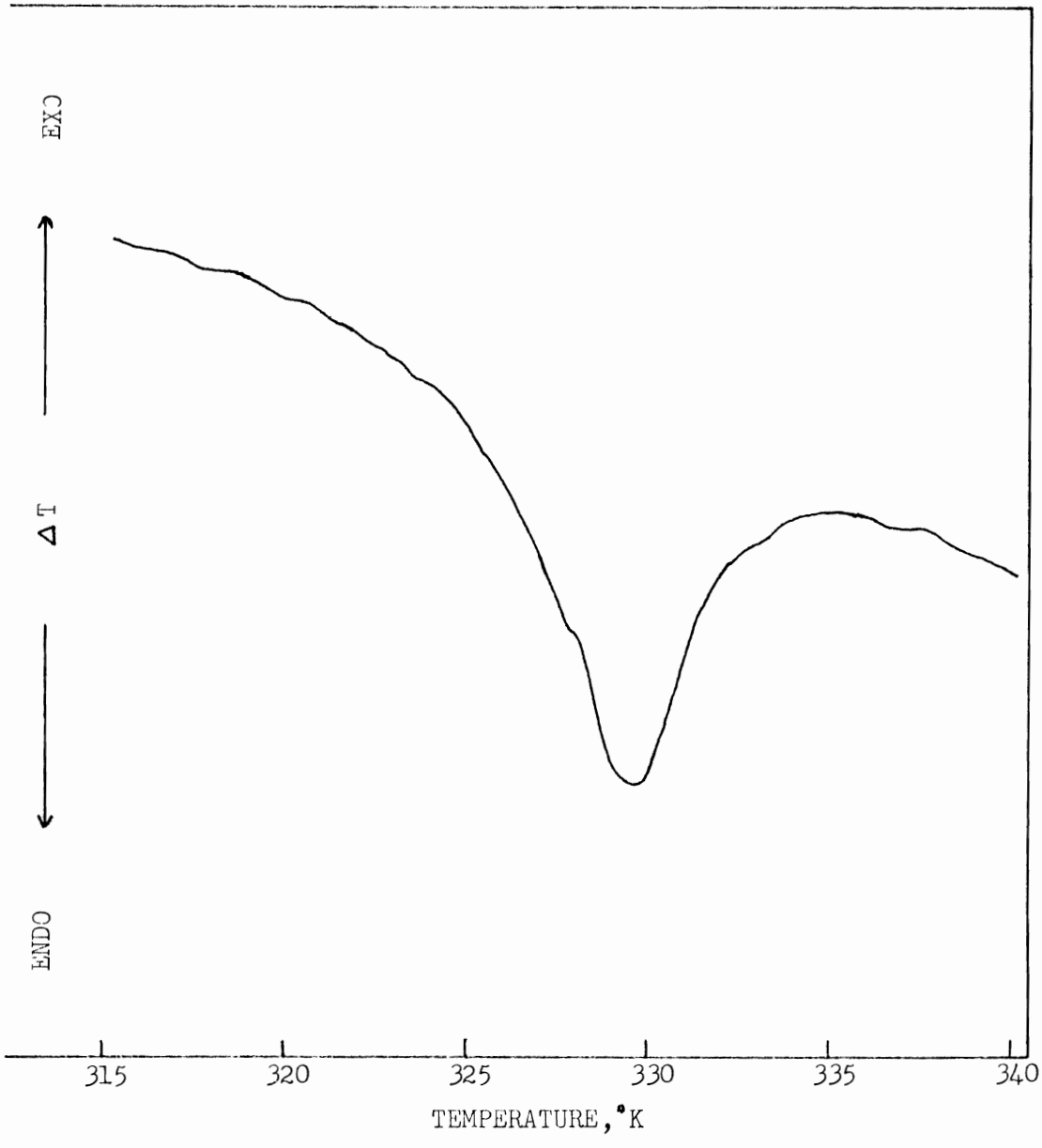

FIGURE D.54

DSC THERMOGRAM of RED AMORPHOUS SELENIUM #11, GROUP 7, RUN 26

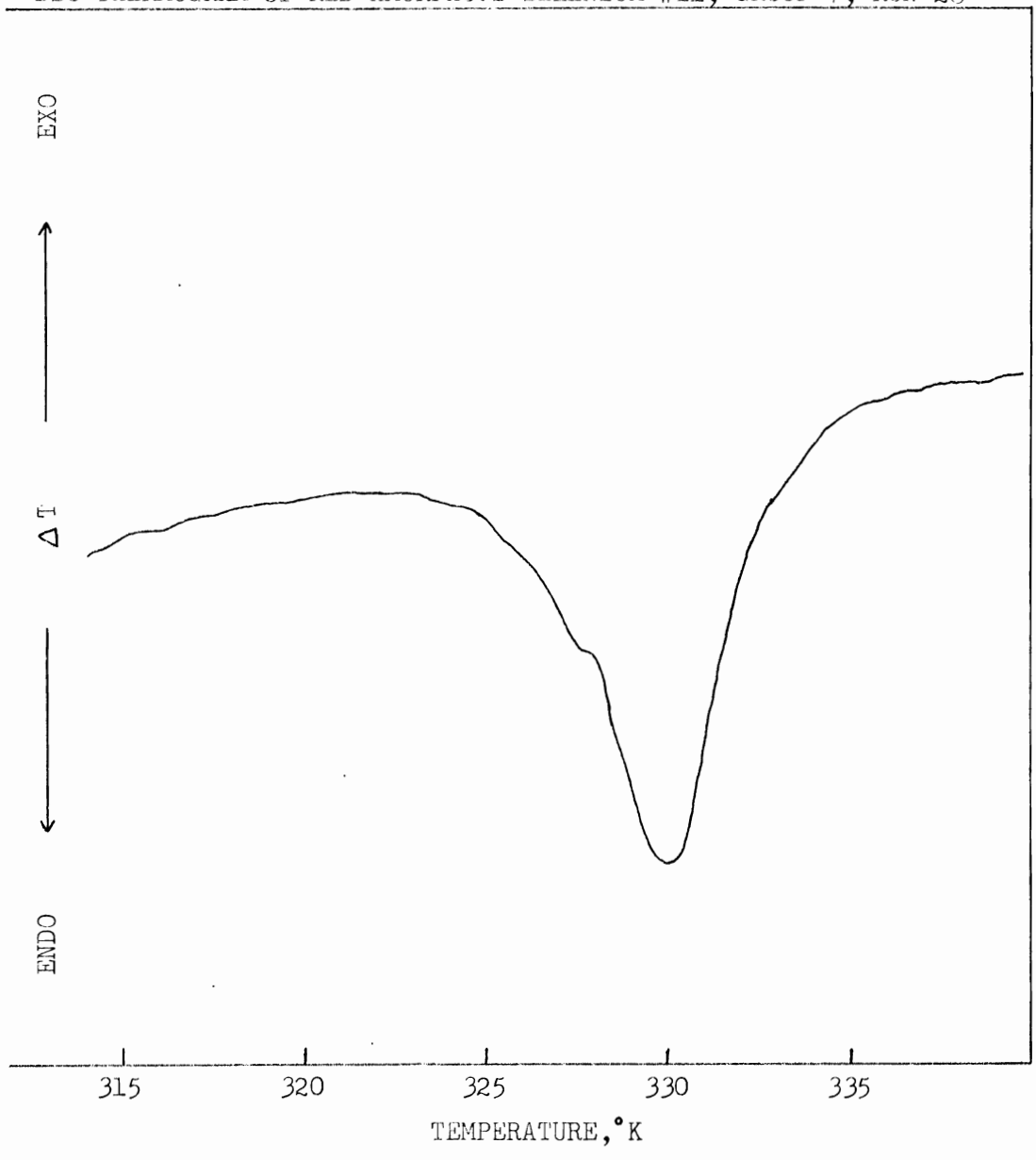

FIGURE D.55

DSC THERMOGRAM of RED AMORPHOUS SELENIUM #11, GROUP 7, RUN 31

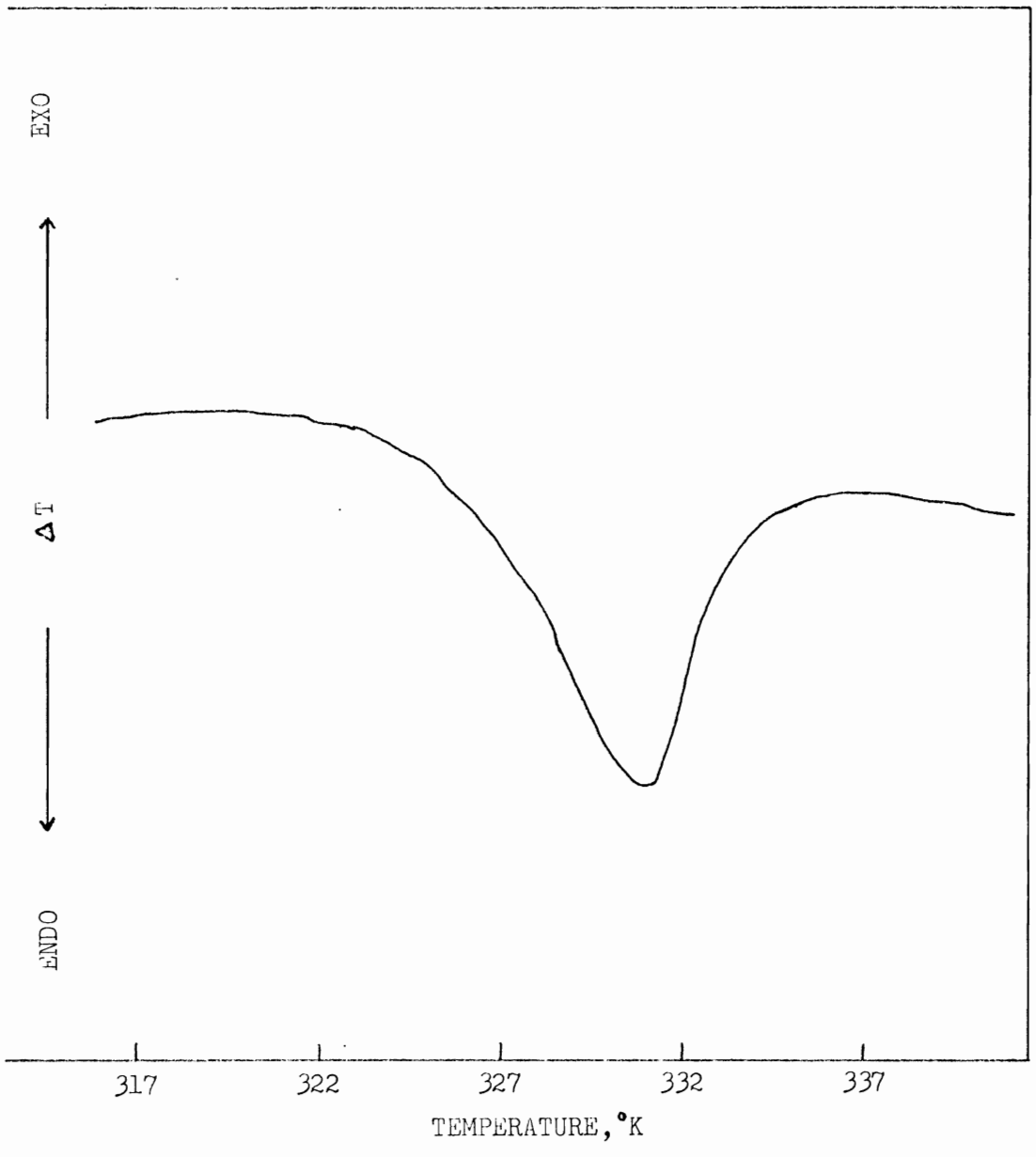

FIGURE D.56

DSC THERMOGRAM of RED AMORPHOUS SELENIUM #11, GROUP 7, RUN 43

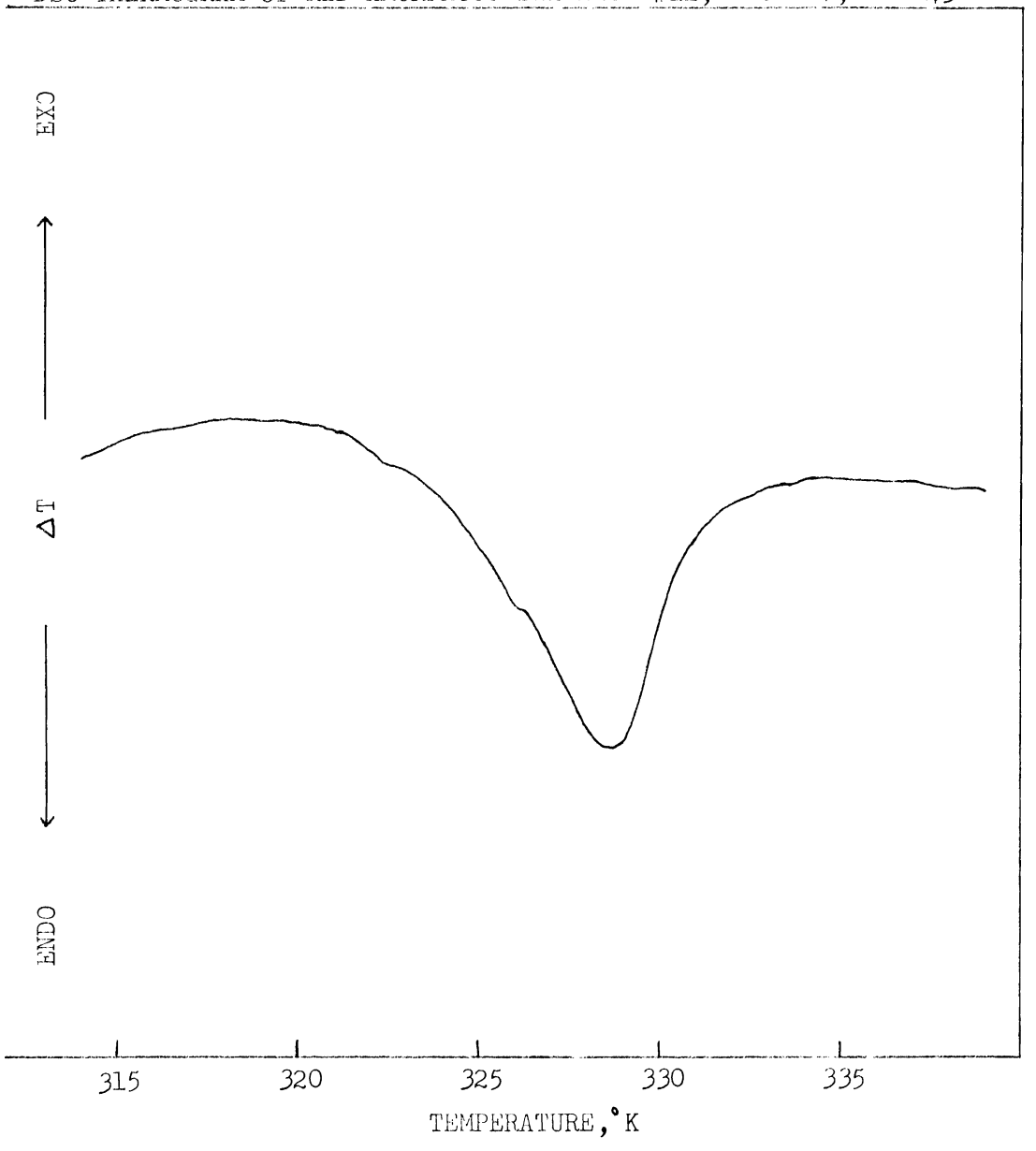

APPENDIX E

Miscellaneous Thermograms

FIGURE E.1

DSC THERMOGRAMS of RED AMORPHOUS SELENIUM #8; T=313°K before runs

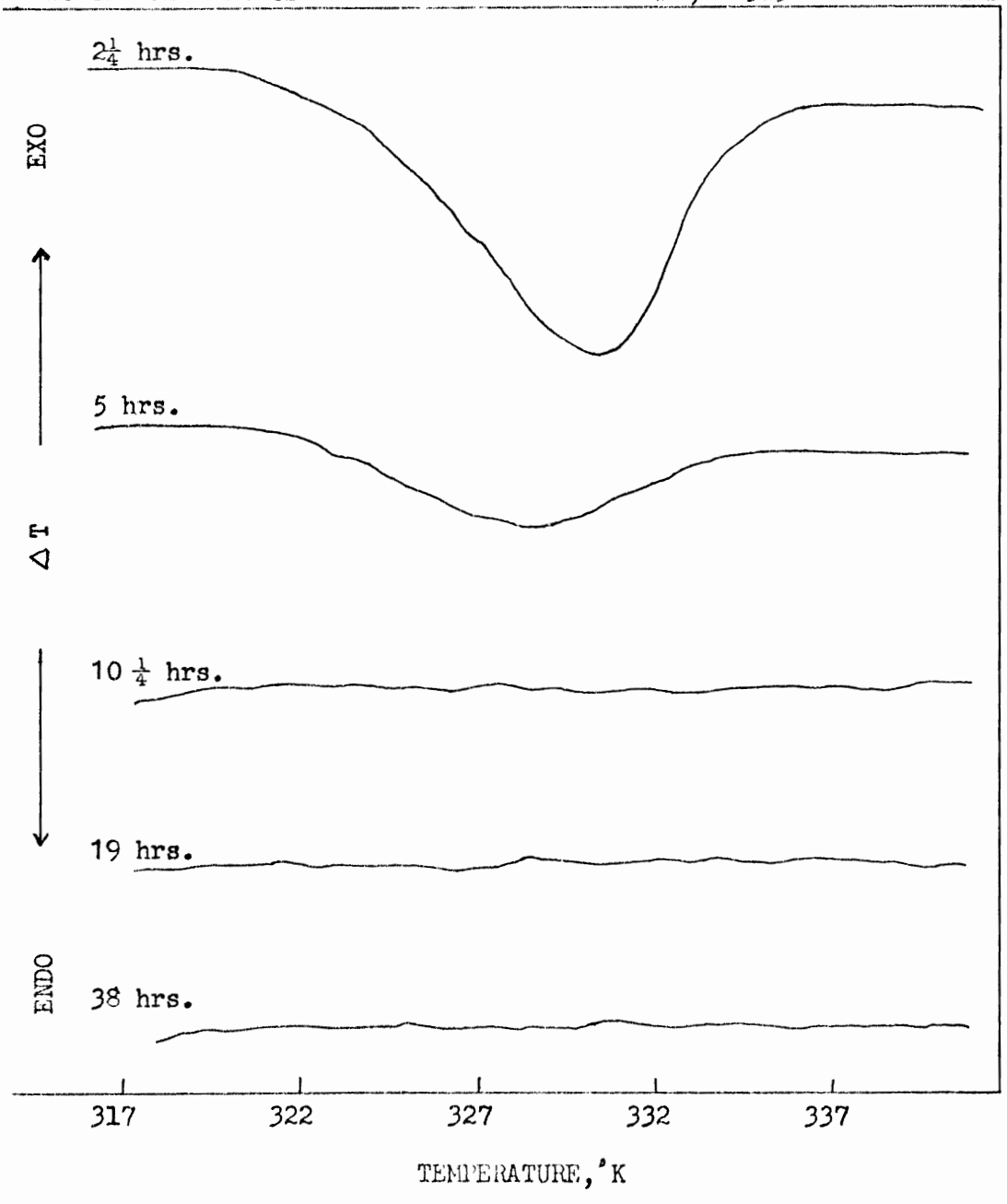

FIGURE E.2

DSC THERMOGRAMS of RED AMORPHOUS SELENIUM #5 SAMPLE

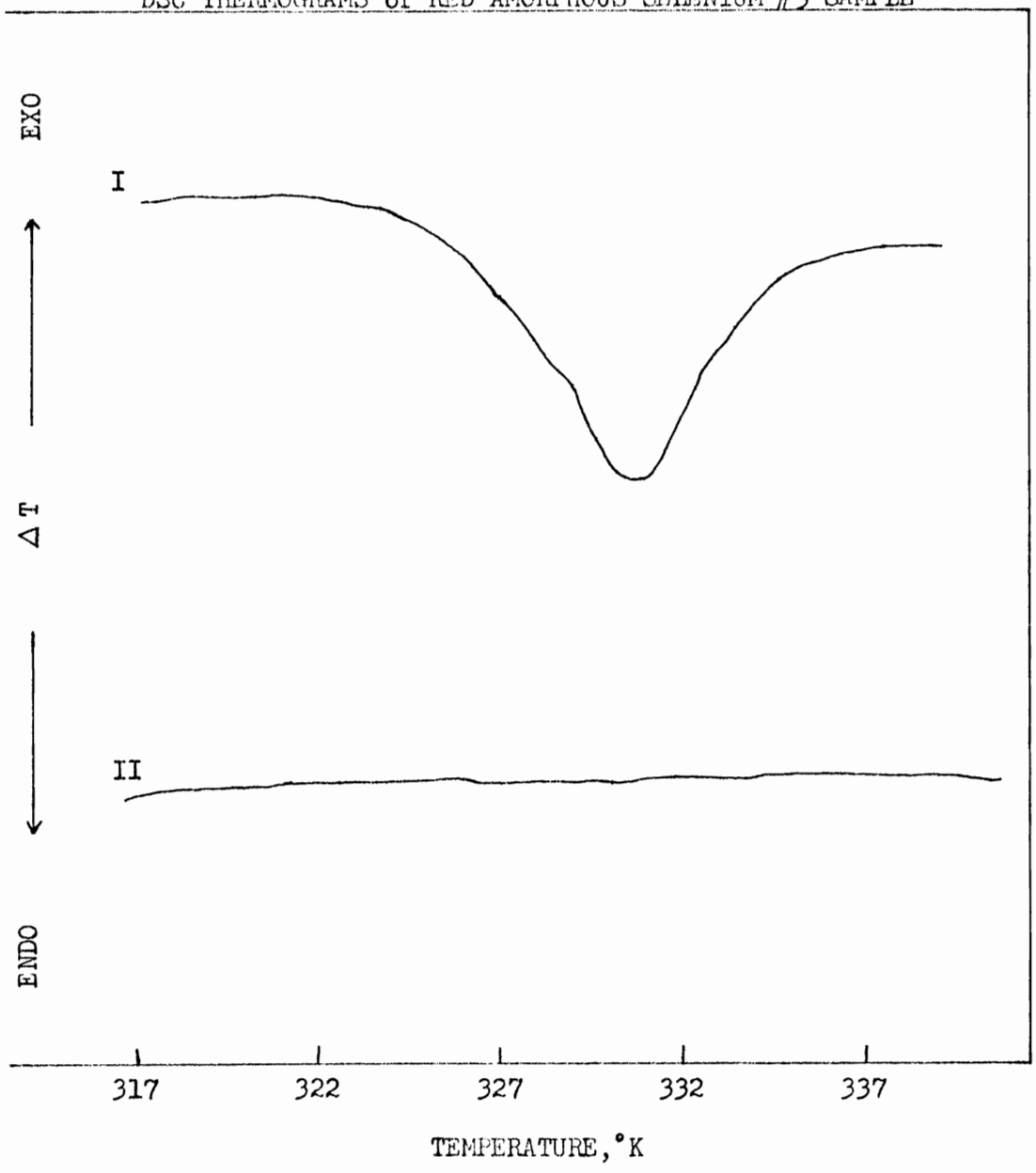

FIGURE E.3

DSC THERMOGRAMS of RED AMORPHOUS SELENIUM #5 SAMPLE

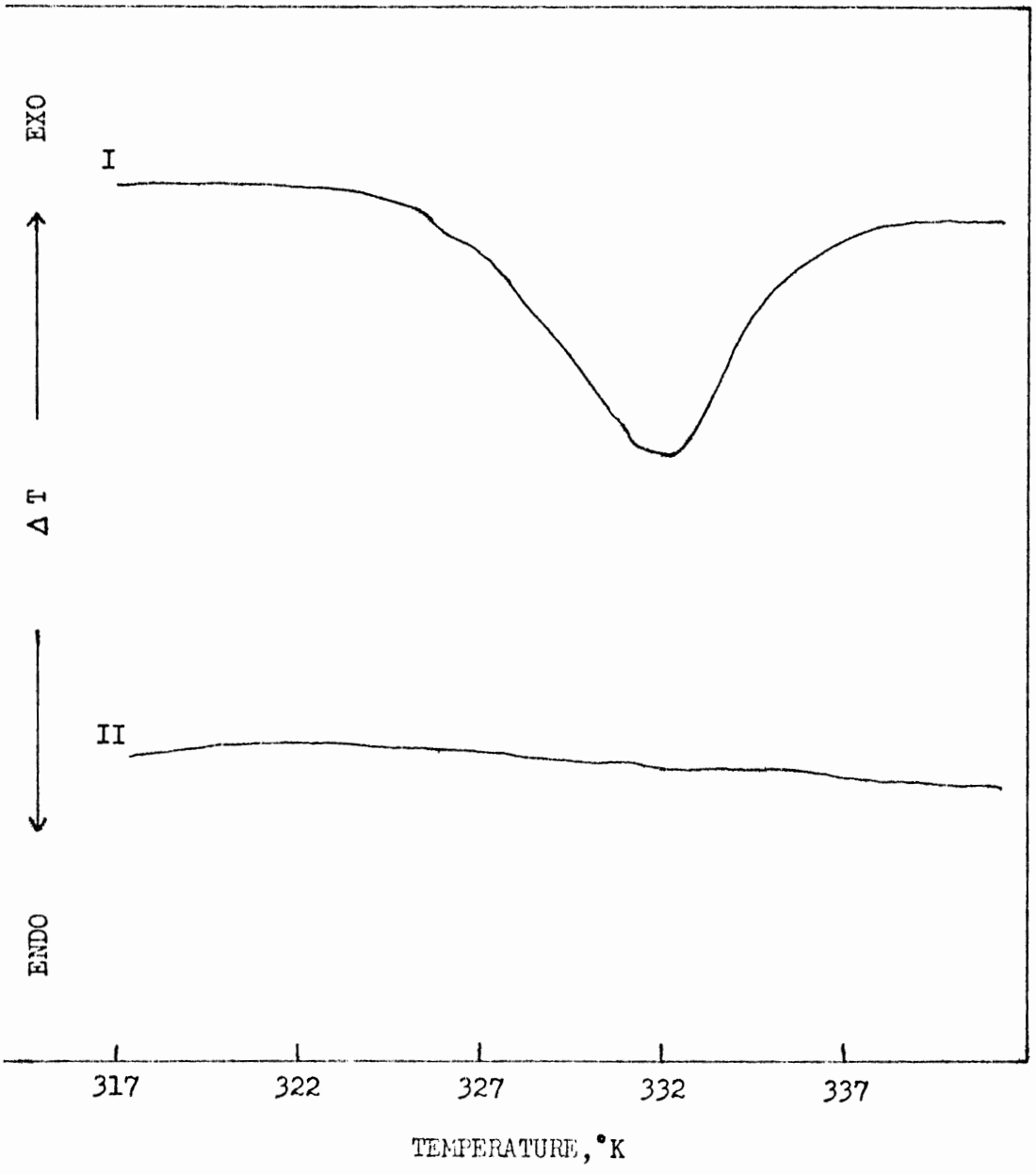

FIGURE E.4

DSC THERMOGRAM of POLY(ETHYLENE TEREPHTHALATE)

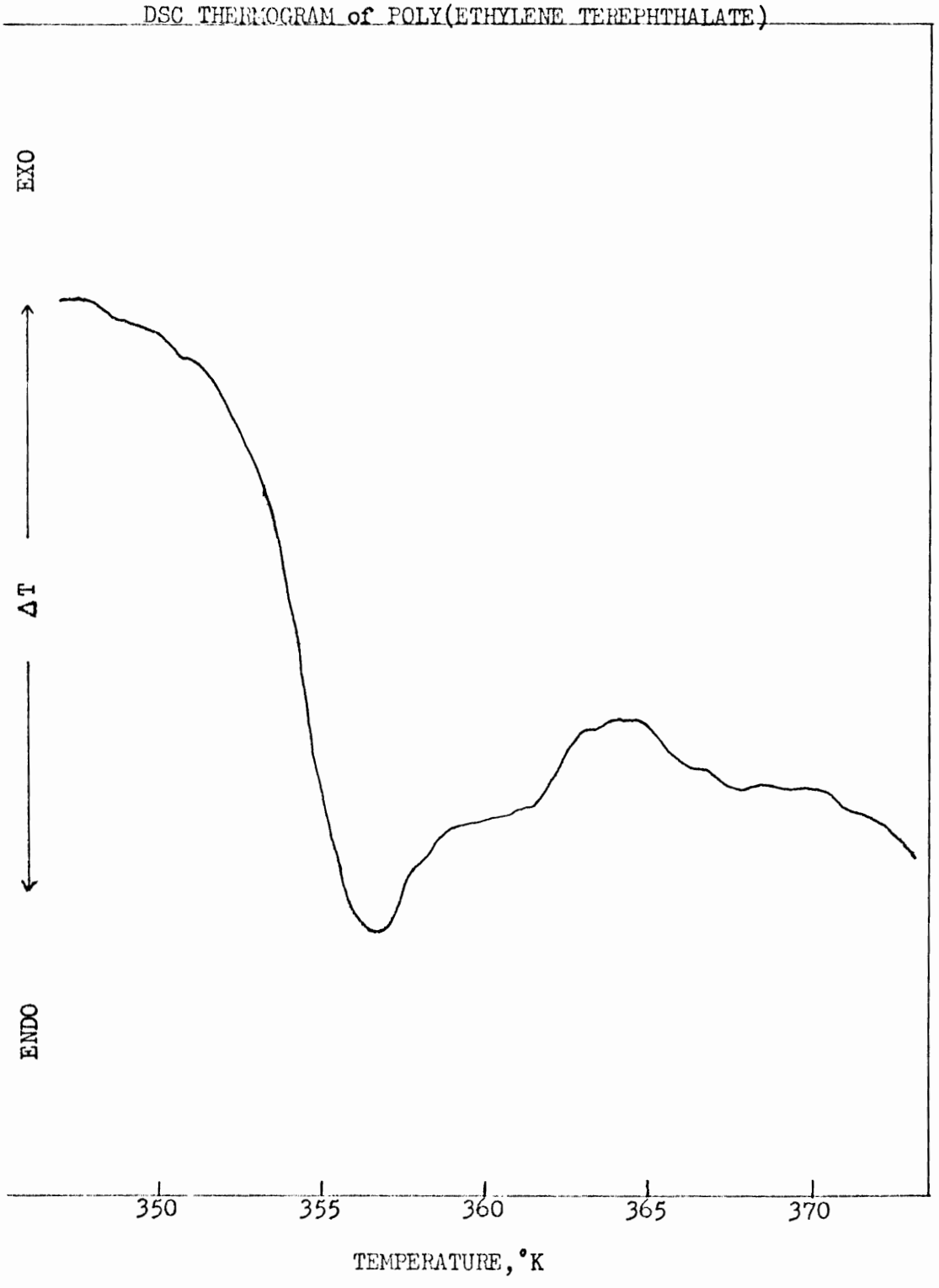

FIGURE E.5

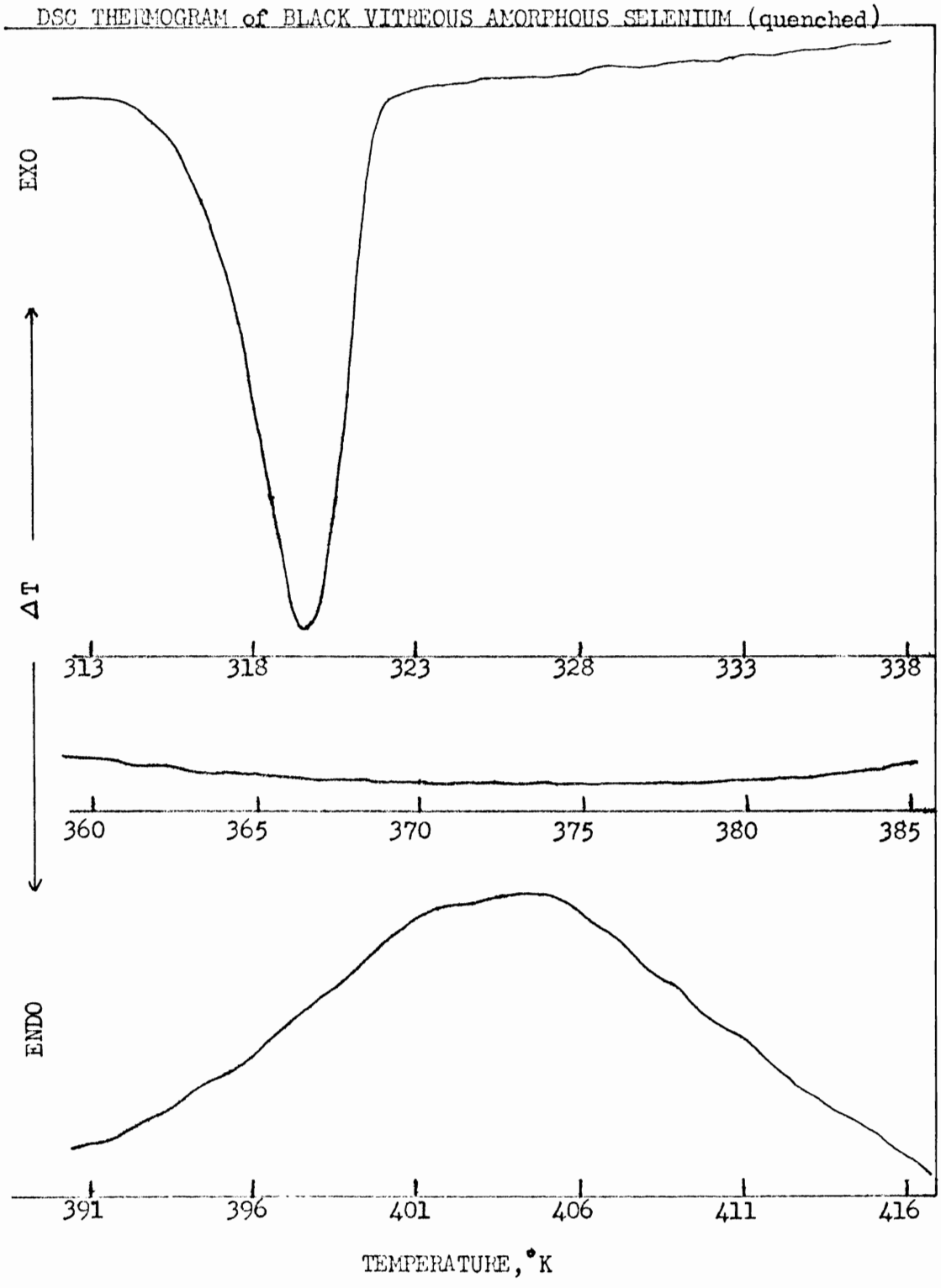
DSC THERMOGRAM of BLACK VITREOUS AMORPHOUS SELENIUM (quenched)
EXO
ΔT
ENDO
313
318
323
328
333
338
360
365
370
375
380
385
391
396
401
406
411
416
TEMPERATURE, °K

FIGURE E.6

DSC THERMOGRAM of BLACK VITREOUS AMORPHOUS SELENIUM (slow cooled)

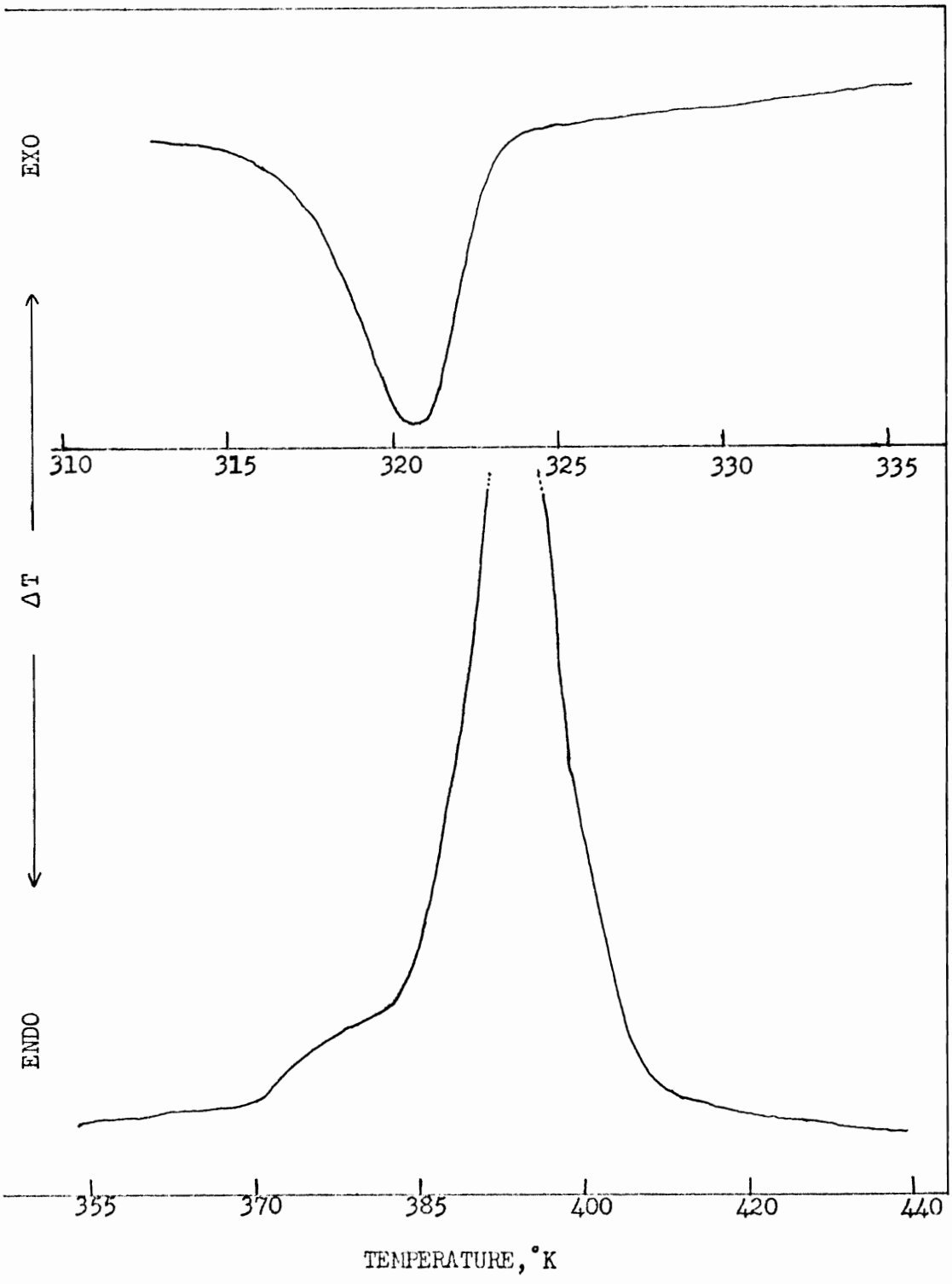

FIGURE E.7

DSC THERMOGRAM of RED AMORPHOUS SELENIUM #11, GROUP 8 (aged)

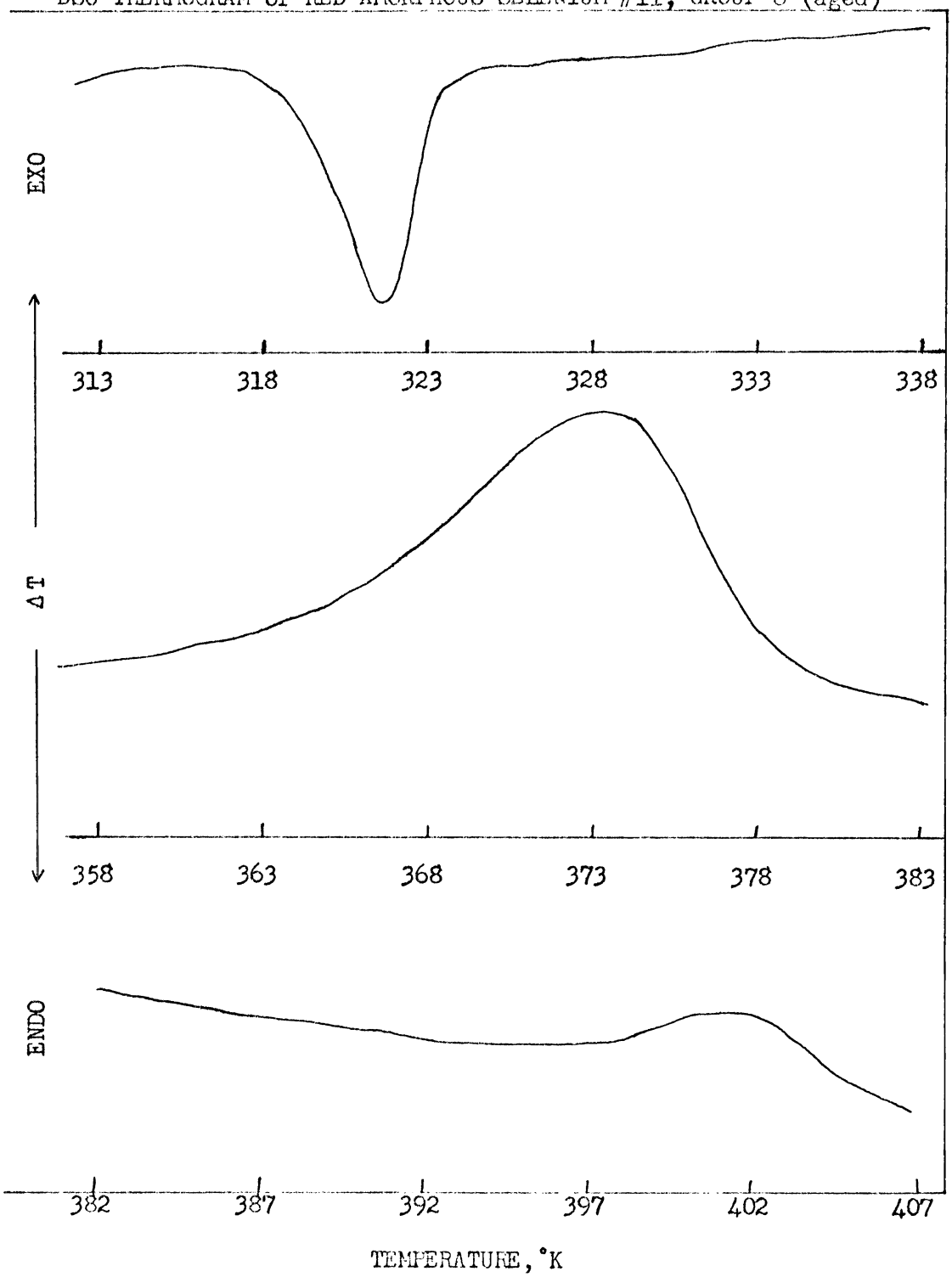

FIGURE E.8

DSC THERMOGRAM of RED AMORPHOUS AND BLACK VITREOUS AMORPHOUS SELENIUM

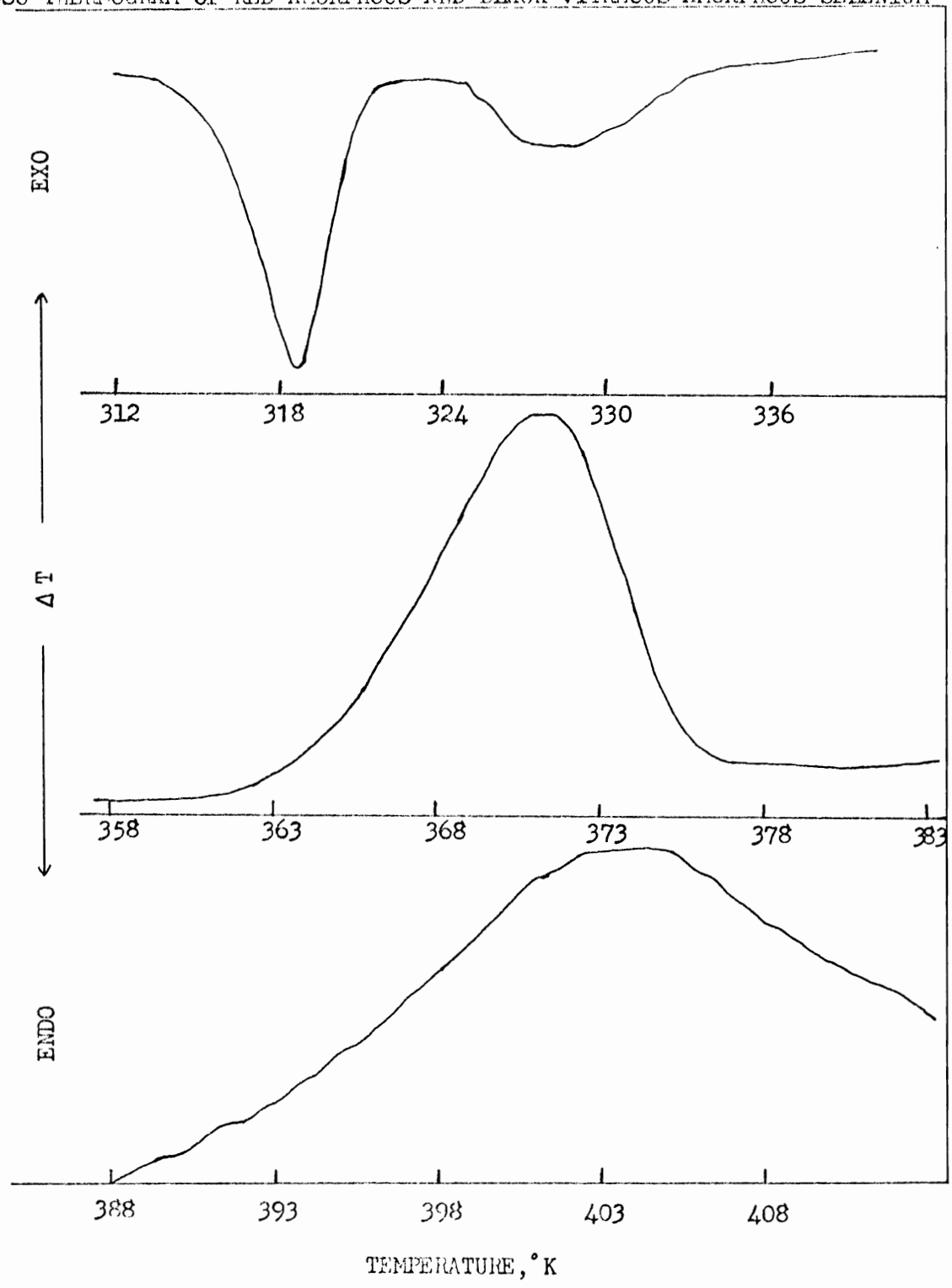

BIBLIOGRAPHY

1. Bagnall K. W., "The Chemistry of Selenium, Tellurium and Polonium," Elsevier Publishing Co., Amsterdam, 1966.

2. Bauer G. (ed.), "Handbook of Preparative Inorganic Chemistry," Eng. trans'n, 1, Academic Press, New York, 1963.

3. Remy H., "Treatise on Inorganic Chemistry," trans. Anderson J. S., 1, Elsevier Publishing Co., New York, 1956.

4. Henisch H. K., "Rectifying Semi-Conductor Contacts," Oxford Univ. Press, 1957.

5. Braested R. C., "Comprehensive Inorganic Chemistry," 8: S, Se, Te, Po and O, Van Nostrand Co. Ltd., New York, 1961.

6. Durrant P. J. and Durrant B., "Introduction to Advanced Inorganic Chemistry," Wiley, New York, 1962.

7. Addison W. E., "The Allotropy of the Elements," Oldbourne Book Co. Ltd., London, 1964.

8. Chizhikov D. M. and Schastlivyi V. P., "Selenium and Selenides," trans. Elkin E. M., Collet's Ltd., Wellingborough, England, 1968.

9. Cherin P. and Unger P., "The Physics of Selenium and Tellurium," ed. Cooper W. C., Pergamon, New York, 1969, p. 228-9.

10. Gobrecht H., "The Physics of Selenium and Tellurium," ed. Cooper W. C., Pergamon, New York, 1969, p. 87-101.

11. Lucovsky G., "The Physics of Selenium and Tellurium," ed. Cooper W. C., Pergamon, New York, 1969, p. 256.

12. Mooradian A. and Wright G. B., "The Physics of Selenium and Tellurium," ed. Cooper W. C., Pergamon, New York, 1969, p. 269.

13. Keezer R. C., "The Physics of Selenium and Tellurium," ed. Cooper W. C., Pergamon, New York, 1969, p. 103.

14. Miyazawa T., J. Polymer Sci. 55, 215-31 (1961).

15. Cherin P. and Unger P., Inorganic Chem. 6(8), 1589-91 (1967).

16. Breuche E. and Schuetz W., Z. Phys. 199(1), 135-40 (1967).

17. Cherin P. and Unger P., Acta Cryst. S21(7), A46 (1968).

18. Mort J., J. Appl. Phys. 38, 3414 (1967).

19. Vedam K., Miller D. L. and Ray R., J. Appl. Phys. 37, 3432 (1966).

20. Stuke J., "The Physics of Selenium and Tellurium," ed. Cooper W. C., Pergamon, New York, 1969, p. 4.

21. Burbank R. D., Acta Cryst. 4, 140 (1951).

22. Marsh R. E., Pauling L. and McCullough J. D., Acta Cryst. 6, 71 (1953).

23. Abdullayev G. B., Asadov Yu. G. and Mamedov K. P., "The Physics of Selenium and Tellurium," ed. Cooper W. C., Pergamon, New York, 1969, p. 186-88.

24. Cherin P. and Unger P., "The Physics of Selenium and Tellurium," ed. Cooper W. C., Pergamon, New York, 1969, p. 226-27.

25. Andrievsky A. I. and Nabitovich I. D., Nauk. Zapiski L'vov. Politekhn. Inst. 1958(57), 82-92.

26. Andrievsky A. I., Nabitovich I. D. and Kripyakevich P. I., Doklady Akad. Nauk SSSR 124(2), 321-23 (1959).

27. Similetov S. A., Kristallografiya 4(4), 629 (1959).

28. Andrievsky A. I. and Nabitovich I. D., Kristallografiya 5, 465-66 (1960).

29. Griffiths C. H. and Sang H., "The Physics of Selenium and Tellurium," ed. Cooper W. C., Pergamon, New York, 1969, p. 152.

30. Griffiths C. H. and Sang H., "The Physics of Selenium and Tellurium," ed. Cooper W. C., Pergamon, New York, 1969, p. 142.

31. Abdullayev G. B., Asadov Yu. G. and Mamedov K. P., "The Physics of Selenium and Tellurium," ed. Cooper W. C., Pergamon, New York, 1969, p. 179.

32. Prosser V., "Proc. Int. Conf. Semicond. Phys. Prague, 1960," Academic Press, New York, 1961.

33. Gattow G. and Heinrich G., Z. anorg. u. allg. Chem. 331, 275-86 (1964).

34. Ato S. and Ichioka K., Repts. Sci. Research Inst. (Japan) 32, 27-39 (1956).

35. Tarayan V. M. and Arstamyan Zh. M., Akad. Nauk. Armianskoi SSR, Izv. Seriya Khim. Nauk 15(5), 415 (1962).

36. Gobrecht H., "The Physics of Selenium and Tellurium," ed. Cooper W. C., Pergamon, New York, 1969, p. 96-7.

37. Gattow G. and Heinrich G., Z. anorg. u. allg. Chem. 331, 287-88 (1964).

38. Kharlamov I. P. and Golubeva G. F., Trudy Tsentral. Nauk.-Issledov. Lab. 1956(4), 147-51; Chem. Abst's 56, 1256d (1962).

39. Hamada K., Sasaki H. and Negita H., J. Sci. Hiroshima Univ., Ser. A-II 29(1), 33-39 (1965).

40. Dunoyer J. M., Compt.Rend. 226, 1524 (1948).

41. Griffiths C. H. and Sang H., "The Physics of Selenium and Tellurium," ed. Cooper W. C., Pergamon, New York, 1969, p. 138, 143.

42. Tsuzuki R., Nippon Kinzoku Gakkaishi 25, 721-23 (1961).

43. Sato T. and Kaneko H., Tech. Repts. Tohoku Univ., Sendai, Japan 14(2), 45-54 (1950).

44. Eisenberg A. and Tobolsky A. V., J. Am. Chem. Soc. 87(10), 2108 (1965).

45. Eisenberg A. and Tobolsky A. V., Frick Chem. Lab., Tech. Rept. No. RLT 29, Apr. 15, (1960).

46. Briegleb G., Naturwiss. 17, 51 (1929).

47. Briegleb G., Z. physik. Chem. A144, 321,340 (1929).

48. Beckmann E. and Pfeiffer, after reference (3), p. 743.

49. Andrade E. N., Phil. Mag. 17, 497,698 (1934).

50. Keezer R. C. and Bailey M. W., Mat. Res. Bull. 2, 185 (1967).

51. Keezer R. C., "The Physics of Selenium and Tellurium," ed. Cooper W. C., Pergamon, New York, 1969, p. 104.

52. Gee G., Trans. Faraday Soc. 48, 515 (1952).

53. Krebs H. and Marsh W., Z. anorg. Chemie 263, 305 (1950).

54. Lucovsky G., Keezer R. C., Mooradian A., Taylor W. and Wright G. B., Solid State Comm. 5, 113 (1967).

55. Lucovsky G., Keezer R. C. and Burstein E., Solid State Comm. 5, 439 (1967).

56. Lucovsky G., "The Physics of Selenium and Tellurium," ed. Cooper W. C., Pergamon, New York, 1969, p. 260-4.

57. Srb I. and Vaško A., Czech. J. Phys. B13, 827 (1963).

58. Vaško A., "The Physics of Selenium and Tellurium," ed. Cooper W. C., Pergamon, New York, 1969, p. 250.

59. Grimminger H., Grüninger H. and Richter H., Naturwiss. 42, 256 (1955).

60. Herre H. and Richter H., Naturwiss. 44, 31 (1957).

61. Herre H. and Richter H., Z. Naturforsch. 13a, 874 (1958).

62. Lucovsky G., "The Physics of Selenium and Tellurium," ed. Cooper W. C., Pergamon, New York, 1969, p. 276.

63. Axmann A., Gissler W. and Springer T., "The Physics of Selenium and Tellurium," ed. Cooper W. C., Pergamon, New York, 1969, p. 304.

64. Mande C. and Patil R. W., Ind. J. Appl. Phys. 3(10), 401-2 (1965).

65. Vedam K., Miller D. L. and Ray R., J. Appl. Phys. 37(9), 3432-4 (1966).

66. Lucovsky G., "The Physics of Selenium and Tellurium," ed. Cooper W. C., Pergamon, New York, 1969, p. 255.

67. Karal'nik S. M., Nesenyuk A. P. and Dobrovol'sky V. D., Ukr. Fiz. Zh. 10(6), 668-71 (1965).

68. Graham L. J. and Chang R., J. Appl. Phys. 36(10), 2983-6 (1965).

69. Harrison D. E., J. Chem. Phys. 41(3), 844 (1964).

70. Fugisaki H., Westmore J. R. and Tickner A. W., Can. J. Chem. 44(24), 3063-71 (1966).

71. Yamdagni R. and Porter R., J. Electrochem. Soc., 115(6), 601-4 (1968).

72. Costy M., Compt. Rend. 149, 674 (1909).

73. Mondain-Monval P., Bull. Soc. Chim. 54, 39, 1349 (1926).

74. Das Gupta K., Das S. R. and Ray B. B., Ind. J. Phys. 15, 389-99 (1941).

75. Muthmann W., "A Comprehensive Treatise on Inorganic Theoretical Chemistry," ed. Mellor J. W., 10, Longmans, London, 1940, p. 706.

76. Semiletov S. A., Trudy Inst. Krist., Akad. Nauk SSSR 1955(11), 115-20.

77. Asadov Yu. G., Dokl. Akad. Nauk SSSR 173(3), 570-2 (1967).

78. Abdullayev G. B., Asadov Yu. G. and Mamedov K. P., "The Physics of Selenium and Tellurium," ed. Cooper W. C., Pergamon, New York, 1969, p. 193.

79. Nekrasov B. V.,"Kurs Obshchei Khimii" (A Course in General Chemistry), Goskhimizdat, 1948, p. 326.

80. Melckerson M., Industr. Tekh. 88, 762 (1965).

81. Mondain-Monval P., Compt. Rend. 182, 1465-68 (1926).

82. Tanaka K., Mem. Coll. Sci. Kyoto Imp. Univ. A17, 59-78 (1934).

83. Prins J. A. and Dekeyser W., Physica 4, 900 (1937).

84. Isikawa H. and Sato H., Bull. Inst. Phys. Chem. Research 18, 143 (1939).

85. Morinaga T., Chihaya T., Shiota N. and Onozaki G., Nippon Kinzoku Gakkai-si 14B(3), 40 (1950).

86. Hirahara E., J. Appl. Phys. 20, 278 (1951).

87. Nasledov D. N., Dorin V. A. and Dikina J. M., Zhur. Tech. Fiz. 25, 29-38 (1955).

88. Hashimoto K., Yokoya S., Hirakawa K. and Okazaki A., Mem. Fac. Sci., Kyusyu Univ. Ser. B1, 151-6 (1955).

89. Dorabialska A., Jakuszewski B. and Kwapinski J., Zeszyty Nauk. Politech. Lodz. Chem. No. 6, 45-56 (1957).

90. Fourie D. J. and van der Walt C. M., Z. fur Physik 159(1), 63 (1960).

91. Abdullayev G. B., Aliev M. I., Bashshaliyev A. A. and Aliev G. M., Referativnii Zhur., Khimiya 1961(15), 29-30.

92. Goffe W. L. and Givens M. P., J. Opt. Soc. Am. 53(7), 804-6 (1963).

93. Mamedov K. P. and Nurieva Z. D., Izv. Akad. Nauk Azerb. SSR, Ser. Fiz.-Mat. i. Tekhn. Nauk 1962(2), 47-56.

94. Gattow G. and Heinrich G., Z. anorg. u. allg. Chem. 331, 256-74 (1964).

95. Mamedov K. P., Suleimanov Z. I. and Zeinalov V. Z., Azerb. Khim. Zh. 1965(4), 84-6.

96. Mamedov K. P. and Nurieva Z. D., Kristallografiya 12(4), 698-701 (1967).

97. Lanyon H. P. D., "The Physics of Selenium and Tellurium," ed. Cooper W. C., Pergamon, New York, 1969, p. 206-7.

98. Mamedov K. P., Kerimov G. I., Mekhtiev M. I. and Veliev M. I., Zh. Fiz. Khim. 40(12), 3086-9 (1966).

99. Gattow G. and Buss B., Z. anorg. u. allg. Chem. 363, 134-39 (1968).

100. Mondain-Monval P., Ann. Chim. 3, 5 (1935).

101. Orthmann H. J. and Ueberreiter K., Kolloid-Z. 147, 129-31 (1956).

102. Sekiguchi T., Sci. Papers Inst. Phys. Chem. Research (Tokyo) 55, 148-53 (1961).

103. Eisenberg A. and Tobolsky A. V., J. Polymer Sci. 61, 483 (1962).

104. Abdinov D. Sh. and Aliyev G. M., Ser. Fiz.-Tekh. i. Matemat. Nauk No.2, 109 (1964).

105. Chang R., Appl. Phys. Letters 6(12), 231-2 (1965).

106. Abdullayev G. B., Mekhtieva S. I., Abdinov D. Sh. and Aliev G. M., Phys. Letters 23(3), 215-6 (1966).

107. Chaudhari P., Beardmore P. and Bever M. B., Phys. and Chem. Glasses 7(5), 157-8 (1966).

108. Dzhalilov S. U. and Orudzheva Sh. O., Zh. Fiz. Khim. 40(9), 2130-2 (1966).

109. Dzhalilov S. U. and Rzaev K. I., Phys. Status Solid. 20(1), 261-6 (1967).

110. Gattow G. and Buss B., Naturwiss. 56(1), 37 (1969).

111. Andrievsky A. I., Nabitovich I. D. and Voloshchuk Ya. V., Kristallografiya 5, 369-74 (1960).

112. Cherkasov Yu. A. and Ionov L. N., Fiz. Tverd. Tela 9(3), 930-5 (1967).

113. Yamamori S., Nippon Kinzoku Gakkai-shi B15, 274-9 (1951).

114. Mondain-Monval P., Compt. Rend. 190, 120 (1930).

115. Gattow G. and Draeger M., Z. anorg. u. allg. Chem. 343(1,2), 55-7 (1966).

116. McAdie H., "Progress Towards Thermal Analysis Standards," Rept. No. 68-02 (Presented at Sec. Int. Conf. Thermal Anal.), App. 1, p. 5.

117. Garn P. D., "Thermoanalytical Methods of Investigation," Academic Press, New York, 1965, p. 20.

118. Smothers W. J. and Chiang Y., "Handbook of Differential Thermal Analysis," Chemical Publishing Co., New York, 1966, p. 101.

119. Moore W. J., "Physical Chemistry," 3'rd ed., Prentice-Hall, Englewood Cliffs, U. S. A., 1962, p. 109.

120. The Du Pont 900 DTA Instrument Manual, Wilmington, U. S. A., p. 2.15-2.16.

121. Billmeyer F. W., "Textbook of Polymer Science," Interscience Publishers, New York, 1965, p. 107.

122. Ke B., "Application of Differential Thermal Analysis to High Polymers," in "Organic Analysis," eds. Mitchell Jr., J., Kolthoff I. M., Proskauer E. S. and Weissberger A., 4, Interscience Publishers, New York, 1961, p. 361-92.

123. "Applications," Bull. 67-8A, Fisher Scientific Co., Instrument Div'n, Pittsburgh, U. S. A., p. 3.

124. The Perkin-Elmer DSC-1B Instrument Manual, Norwalk, Conn., U. S. A., 1966, Fig. 17, p. 60.

125. Wendlandt W. WM., "Thermal Methods of Analysis," Interscience Publishers, New York, 1964, p. 248.

126. Ke B. and Sisko A. W., J. Polymer Science 50, 87 (1961).

127. Lambert A., Polymer 10(5), 319-26 (1969).

128. Wunderlich B. and Bodily D. M., J. Polymer Science C6, 137 (1964).

129. Fyans R. L., Instrument News (Perkin-Elmer Corp., Norwalk, Conn., U. S. A.) 18(2), 12-13 (1967).

130. de Coninck W. Ö. and Raynaud E., Bull. Acad. Roy. Belg., Cl. Sci. 365 (1907).

131. The Perkin-Elmer DSC-1B Instrument Manual, Norwalk, Conn., U. S. A., 1966, p. 19-26.

132. McAdie H., "Progress Towards Thermal Analysis Standards," Rept. No. 68-02 (Presented at Sec. Int. Conf. Thermal Anal.), p. 10.

133. Stull D. R. and Prophet H., "The Calculation of Thermodynamic Properties over Wide Temperature Ranges," in "The Characterization of High-Temperature Vapors," ed. Margrave J. L., Wiley, New York, 1967, p. 371.

134. The Perkin-Elmer DSC-1B Instrument Manual, Norwalk, Conn., U. S. A., 1966, p. 26-27.

135. Fisher Scientific Co., Commercial literature.

136. McCullough J. P., Finke H. L., Messerly J. F., Kincheloe T. C., Todd S. S. and Waddington G., J. Phys. Chem. 61, 1105 (1957).

137. Goton R. and Whalley E., Can. J. Chem. 34, 1506-8 (1956).

138. McLaren E. H. and Murdock E. G., Can. J. Phys. 41, 95-112 (1963).

139. Sokolov V. A. and Schmidt N. E., Izv. Sek. Fiz.-Khim. Anal., Inst. Obshch. i Neorg. Khim., Akad. Nauk SSSR 27, 217-22 (1956).

140. Rastogi R. P., Nigam R. K., Sharma R. N. and Girdar H. L., J. Chem. Phys. 39(11), 3042 (1963).

141. van Hest J. A. M. and Diepen G. A. M., "Phys. Chem. High Pressures, Papers Symposium, London, 1962," (Published 1963), p. 10-18.

142. Dode M. and Hagege R., Compt. Rend. 248, 2339-41 (1959).

143. Hatcher W. H. and Skirrow F. W., J. Am. Chem. Soc. 39, 1939 (1917).

144. Driesbach R. R. (ed.), "Physical Properties of Chemical Compounds," Amer. Chem. Soc., Washington, 1955, p. 203.

145. Weast R. C. (ed.-in-chief), "Handbook of Chemistry and Physics," 50'th ed., The Chemical Rubber Co., Cleveland, 1969, p. C718.

146. Sklyankin A. A. and Strelkov P. G., Zhur. Priklad. Mekh. i Tekh. Fiz. 1960(2), 100-11.

147. Sekiguchi K., Yotsuyanagi T. and Mikami S., Chem. and Pharm. Bull. 12(9), 994 (1964).

148. Vassallo D. A. and Harden J. C., Anal. Chem. 34(11), 132 (1962).

149. Oelsen W., Oelsen O. and Thiel D., Z. Metallkunde 46(8), 555-60 (1955).

150. David D. J., Anal. Chem. 36(11), 2162-66 (1964).

151. Kelley K. K., "National Bureau of Standards Circular 500," Washington, 1952, p. 660.

152. Kubaschewski O., Z. Elektrochem. 54, 275 (1950).

153. Schneider A. and Hilmer O., Z. anorg. u. allg. Chem. 286, 97 (1956).

154. Roth W. A., Meyer I. and Zeuner H., Z. anorg. u. allg. Chem. 214, 309 (1933); 216, 303 (1934).

155. Weast R. C. (ed.-in-chief),"Handbook of Chemistry and Physics," 50'th ed., The Chemical Rubber Co., Cleveland, 1969, p. B260.

156. Kracek F. C., J. Phys. Chem. 34, 225 (1930).

157. Rao K. J. and Rao C. N. R., J. Mater. Sci. 1(3), 238 (1966).

158. Kelley K. K., "National Bureau of Standards Circular 500," Washington, 1952, p. 806.

159. "American Inst. of Physics Handbook," given as a reference in "Thermal Analysis Bulletin," Aug. 15, 1967, p. 4.

160. Ko H. C., Hu T., Spencer J. G., Huang C. Y. and Hepler L. G., J. Chem. Eng. Data 8(3), 364-66 (1963).

161. Kelley K. K., "U. S. Bureau of Mines Bulletin 393," 1936.

162. Kleppa O. J. and McCarty F. G., J. Chem. Eng. Data 8(3), 331-2 (1963).

163. Franzosini P. and Sinistri C., Ric. Sci., Rend. Sez. A 3(4), 411-8 (1963).

164. Doucet Y. and Vallet C., Compt. Rend. Acad. Sci. (Paris) 259(7), 1517 (1964).

165. Goodwin H. M. and Kalmus H. T., The Physical Review 28, 1 (1909).

166. The Du Pont 900 DTA Instrument Manual, Wilmington, U. S. A., Appendix.

167. Predel B., Z. Metallkunde 54, 206-12 (1963).

168. Barrall E. M., Porter R. S. and Johnson J. F., J. Phys. Chem. 71(5), 1224-28 (1967).

169. Smith M. R., "Stone Thermoscope," 1(2), March, 1968.

170. McAdie H., Report ICTA-66-01 (ORF 66-01) (Presented at Sec. Int. Conf. Thermal Anal.), p. 14.

171. The Du Pont 900 DTA Instrument Manual, Wilmington, U. S. A., p. 2.10.

172. Wendlandt W. WM., "Thermal Methods of Analysis," Interscience Publishers, New York, 1961, p. 162.

173. Krebs H., "The Physics of Selenium and Tellurium," ed. Cooper W. C., Pergamon, New York, 1969, p. 347.

174. Dorabialska A. and Swiatkowski W., Rocz. Chem. 43(10), 1869-76 (1969).

175. Moore W. J., "Physical Chemistry," 3'rd. ed., Prentice-Hall, Englewood Cliffs, U. S. A., 1962, p. 107.

176. Lovering E. G., Chem. in Can. 22(2), 13 (1970).

177. Markowitz M. M. and Boryta D. A., Anal. Chim. Acta 31, 397-99 (1964).

VITA

Kathryn G. Bennett was born on October 8, 1946 in Montreal, Canada. Her primary and secondary education were received in that city. From 1963 to 1967 she was enrolled at Marianopolis College, Montreal, and graduated with a Bachelor of Science degree in Honors Chemistry. She then entered the Graduate School of Sir George Williams University in the field of physical chemistry, under the supervision of Dr. R. A. Westbury. At present she is a candidate for the degree of Master of Science.